Aspects of the reactivity of coordinated ligands

Beddows, Claire J.

Award date:
1999

Awarding institution:
University of Bath

ASPECTS OF THE REACTIVITY OF COORDINATED LIGANDS

submitted by **CLAIRE J. BEDDOWS**

for the degree of Doctor of Philosophy

of the University of Bath

1999

ProQuest LLC
789 East Eisenhower Parkway
P.O. Box 1346
Ann Arbor, MI 48106-1346

"Doing creative science is a bit like playing jazz. One has to be disciplined but also open and ready to abandon an idea and pick up a new one when nature thrusts it upon one".

Berson, Creativity in Chemistry, Verlag Wiley, 1999.

MEMORANDUM

The work described in this thesis was carried out by the author between October 1995 and September 1998 within the Department of Chemistry at the University of Bath, under the supervision of Professor Michael Green. Unless otherwise indicated, the work is original and has not been submitted for any other degree.

ACKNOWLEDGEMENTS

First and foremost I would like to say a big thank you to my supervisor Professor Michael Green for his continued support and guidance throughout my Ph.D. It was great to have a supervisor who was always enthusiastic, encouraging and a good friend. Thanks also go to the support I received from post doctoral assistants Dr. Nick Carr and in particular Dr. Jason Lynam, who was a great inspiration in my final year of research and I am very grateful for his invaluable support and help.

Many thanks go to Proressor Neil Connelly and Dr. Tim Padget for running the EPRs and also to Dr. Cameron Jones and his group for accommodating me in their lab for 1 month which was good fun and also for the endless supply of phosphaalkyne. Thanks are also due to Dr. Mary Mahon for the crystallographic studies and Dr. Andy Burrows for his helpful advice and friendship. I would also like to thank all the technical staff within the department for always being there to help, especially Robert Stevens, Ahmed Sheibani, Alan Carver and Sheila Osborne.

I would also like to express my sincere thanks to the following people; my lab friends (Dr. Gareth Cairns, Mark Palmer, Chris Andrews and Ross Harrington) for all the fun and lively discussions, the boys in 2.10 for letting me use their glove box, Carol Fordham for always been supportive in every way and for always having a happy face, the EPSRC for my funding and to my good friends Phil Drake, Roger Jardine and Dr. Alan Walker for just being there.

Final thanks go firstly to my parents for all their love, support and encouragement and to Dr. Harish Patel for his friendship and support over the last 4 years and for all the time he has spent helping me put together this thesis, I do not think I would have done it without him, thank you.

SUMMARY

The work described in this thesis is divided into three separate results chapters. Chapter three is concerned with the synthesis and reactivity of keto-substituted π-allylic molybdenum complexes. This reports the synthesis of the *anti*-aldehyde substituted η^3-allylic complex [Mo{η^3-*exo-anti*-$CH_2CHCH(CHO)$}$(CO)_2$(L)] (where L = C_5H_5 or C_5Me_5). An investigation into its reactivity was also carried out, particularly with respect to nucleophiles. This chapter also looks at the reactivity of the η^3-γ-lactonyl complex [Mo(η^3-CHCHCH(O)$(CO)_2$(L)] (where L = C_5H_5 and C_5Me_5). This complex was found also to react with nucleophiles and a rationalisation of these observations was obtained through an examination of the charge and orbital contribution of both systems, both of which were obtained through Extended Hückel Molecular Orbital (EHMO) calculations.

Chapter four examines the reactivity of the η^2(3e)-vinyl complex [Mo{=C(Ph)CHPh}$\{P(OMe)_3\}_2$(η-C_5H_5)] (8) towards one-electron oxidants. Unexpectedly, the Lewis acid $B(C_6F_5)_3$ was found to act as a one-electron oxidant as (8) readily underwent a one-electron oxidation reaction with $[Fe(\eta\text{-}C_5H_5)_2]^+$, $[Ph_3C]^+$ and $B(C_6F_5)_3$ to form a relatively stable 17 e^- species which was detected by EPR. There is a subsequent discussion concerning the reaction path of the 17 e^- cation after the one-electron oxidation has taken place and the nature of the anion. When (8) was treated with $B(C_6F_5)_3$ *in situ* with *t*BuC≡P, CO or $P(OMe)_3$, the following cations were generated; [Mo(η^2-*t*BuC≡P)$\{P(OMe)_3\}_2$(η-C_5H_5)]$^+$, [Mo$(CO)_2\{P(OMe)_3\}_2$(η-C_5H_5)]$^+$ and [Mo(η^2-PhC≡CPh)$\{P(OMe)_3\}_2$(η-C_5H_5)]$^+$.

Chapter five describes some preliminary experiments concerning the $\eta^2(2e)$-phosphaalkyne complex $[Pt(t\text{BuC}{\equiv}P)(PPh_3)_2]$ (86). Firstly, the reactivity of (86) towards the oxygen transfer reagent dimethyl dioxirane (DMD) affords a zwitterionic carbene-type complex due to a rearrangement of the phosphaalkyne. Secondly, the reactivity of (86) towards $B(C_6F_5)_3$ affords a cationic phosphaalkene complex. Both complexes were characterised by NMR.

ABBREVIATIONS

Me	methyl
Et	ethyl
Pr	propyl
Bu^s	secondary butyl
*t*Bu	tertiary butyl
Ac	acetyl
Ph	phenyl
M	metal atom
bu_2bpy	4,4-di-tert-butyl-2,2-bipyridine
dmpz	3,5-dimethylpyrazole
DMAC	$MeO_2CC_2CO_2Me$
DMD	dimethyldioxirane
dppf	bis(diphenylphosphino)ferrocene
Cp	η^5-cyclopentadienyl
Cp*	η^5-pentamethylcyclopentadienyl
In	indenyl
L	ligand
X	halide or counterion
thf	tetrahydrofuran
hr	hour
m	minute
IR	infrared

NMR	nuclear magnetic resonance

with respect to NMR:

J	coupling constant in Hertz
vt	virtual coupling constant $\lvert J + J^1 \rvert$ in Hertz
ppm	parts per million
at	apparent triplet
δ	chemical shift
Hz	Hertz
s	singlet
d	doublet
t	triplet
m	multiplet

with respect to EPR:

q	quintet
d	doublet
G	Gauss
g	zeeman splitting constant for a free electron
A	hyperfine splitting constant

with respect to IR:

ν_{CO}	wavenumber of carbonyl band (cm^{-1})
v	very

s	strong
m	medium
w	weak
br	broad

with respect to mass spectral data:

FAB	fast atom bombardment
NBA	*m*-nitrobenzyl alcohol

CONTENTS

CHAPTER SEVEN: *References*

APPENDICES

CHAPTER ONE

THE CHEMISTRY OF CO-ORDINATED LIGANDS: ALKYNES, VINYLS AND BUTADIENYLS

1.1 Introduction

This chapter aims at giving a small insight into the reactivity of complexes containing ligands which donate electron density through versatile multiple metal-carbon bonds, a topic which has been extensively explored by organo-transition metal chemists over the last four decades. The enormity of this area makes it impossible to condense, however, this review attempts to outline some of the studies which have made major contributions to this highly fertile area.

The discussion begins with the establishment of the first reported $4e^-$ donor alkyne [η^2(4e)-alkyne], a turning point upon our understanding of the versatile nature of complexes which contain multiple metal-carbon bonds. This is followed by the reactivity of complexes which contain $4e^-$ donor alkynes which led to the development of the $3e^-$ donor vinyl species [η^2(3e)-vinyl]. More recently, significant progress has been made on the synthesis and reactivity of the $5e^-$ donor butadienyl species [η^4(5e)-butadienyl].

The progress which has been made upon the structural understanding of each of these species has allowed us to identify that the electron donor possesses the ability to change its bonding mode to compensate for changes in electron density on the metal, whether induced through reactivity or intramolecular stabilisation. It is also clear to see that there is a strong inter-relationship which exists between each of these ligands, as studies show the presence of these ligands found as intermediates to other related co-ordinated ligands.

1.2 Alkynes In Transition Metal Chemistry

Throughout the 1960-70's there was a lot of interest in the role of alkynes in transition metal chemistry. It was well established that they could function as $2e^-$ donors, but the rationale that they could act as $4e^-$ donors also, through utilisation of both sets of π-orbitals ($\pi_{\|}$ and $\pi_{\perp}$), was yet to be proved. However, this did address the question to the nature of the bonding in complexes which contained side-on co-ordinated alkynes as it had been assumed that they functioned in the same manner as $2e^-$ donor alkenes, regarded in the Dewar-Chatt-Duncanson model[1,2] as σ-donation from the olefin π-orbital and π-back donation from the metal into the π*-orbital. The suggestion that alkynes could act as $4e^-$ donors through both sets of π-orbitals was therefore recognition of the fact that alkynes present four orbitals of π-symmetry on complexation to a metal and not two, represented in Figure 1.1.

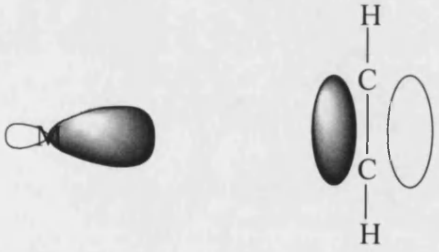

(i) $\Pi_{\|} \longrightarrow M(\sigma)$
σ dative

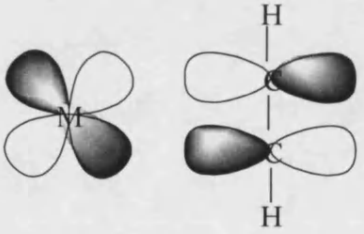

(ii) $M(d\pi) \longrightarrow \Pi_{\|}^*$
π retrodative

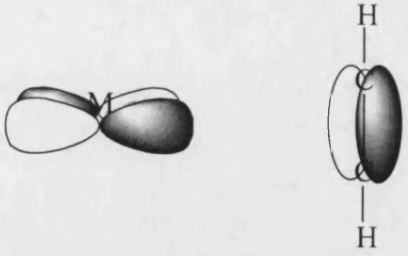

(iii) $\Pi_{\perp} \longrightarrow M(d\pi)$
π dative

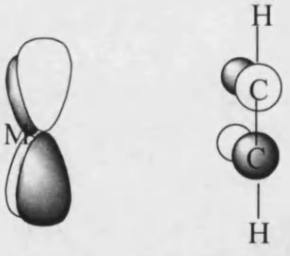

(iv) $M(d\delta) \longrightarrow \Pi_{\perp}^*$
δ retrodative

Figure 1.1

Figure 1.1 illustrates how each of the four alkyne orbitals are energetically favourable for bonding with a metal orbital [(i)-(iv)], however, the strength of these interactions differ and this is dependent upon the constraints imposed by the metal *i.e.* oxidation state and steric bulk. Molecular orbital calculations carried out in order to determine the overlap value for each orbital interaction concluded that the strongest interaction is the σ dative donation (i), followed by the π-retrodative interaction (ii). As these are the two strongest interactions, they are the most significant in bonding and are analogous to the orbitals represented in the Dewar-Chatt-Duncanson model[1,2] for metal-olefin bonding. However, $4e^-$ donation is accessible through the availability of the additional filled alkyne $\pi_\perp$-orbital which also donates significant electron density to the empty dπ-orbital (iii). Unlike the relatively strong synergic interaction (ii), the metal can only sustain a very weak δ-retrodative interaction with $\pi_\parallel$*-orbital (iv), consequently, the metal facilitates very little or no backbonding which enables $4e^-$ donor alkynes to be net electron donors.[3]

In 1963, Tate and Augl[4,5] reported for the first time, evidence to support this theory that an alkyne could function as a $4e^-$ donor and the complex in question was $[W(CO)(\eta^2\text{-}EtC_2Et)_3]$ (1). Counting each alkyne ligand as a $2e^-$ donor in d^6 metal (0) would only give a metal electron count of 14, which would not be expected to be stable. Interestingly, spectroscopic data proposed that the alkynes were chemically equivalent even though the ends of the alkynes were situated in different environments. The suggestion was that the complex had adopted a *pseudo*-tetrahedral structure where two of the three alkyne ligands were acting as $4e^-$ donors generating a stable metal electron count of 18.[6] To confirm this suggestion, King[7] subsequently carried out a detailed study of the molecular-orbital contributions and concluded that

each alkyne was rapidly switching its bonding mode between η^2(2e) and η^2(4e), at the same time the overall structure was geometrically consistent with one $2e^-$ donor alkyne and two $4e^-$ donor alkynes. Therefore, each alkyne is effectively donating 3 $1/3e^-$. The significance of this led King[7] to discover that it was impossible for all three alkynes to co-exist as $4e^-$ donors due to no available metal orbital of correct symmetry which would accommodate a third $4e^-$ alkyne, therefore establishing that [W(η^2-$EtC_2Et)_3$] cannot exist as a stable $18e^-$ complex.

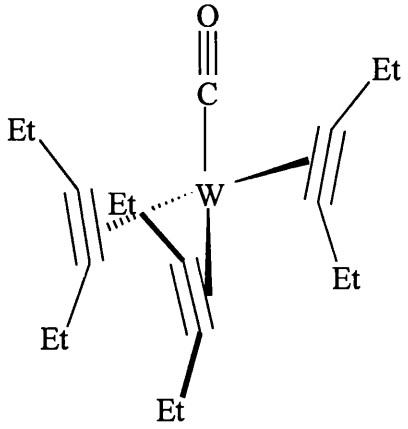

(1)

Figure 1.2

Since that point significant progress has been made on the synthesis and establishment of a wide range of complexes that contain $4e^-$ donor alkynes. This has confirmed the idea that there are many metal-alkyne systems which contain alkynes donating a greater number of electrons than two. Nevertheless, like the tris-alkyne system, the true nature of the alkyne bonding can often be misleading. For example, the bis-alkyne systems operate in a similar manner to those of the tris-alkyne systems,

where the two alkynes rapidly alternate between $2e^-$ and $4e^-$ donors, each alkyne effectively donating $3e^-$ (Figure 1.3).

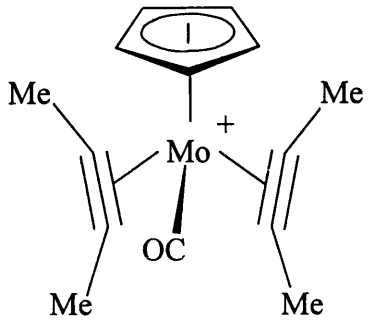

(2)

Figure 1.3

To identify the number of electrons an alkyne is formally donating to a metal, NMR has become a very effective tool, in particular ^{13}C-$\{^1H\}$ NMR. Templeton and Ward[8] first reported on the direct relationship which exists between the contact carbon chemical shift of the alkyne and the formal number of electrons donated for a series of Mo(II) and W(II) complexes. This systematic relationship can be illustrated by plotting the contact carbon chemical shift against the number of electrons donated per alkyne (Figure 1.4). There is a tendency for the chemical shifts to be more low field, the more electron density is donated to the metal *i.e.* $2e^- \rightarrow$ 100-130 ppm, $4e^- \rightarrow$ 175-230 ppm.[8]

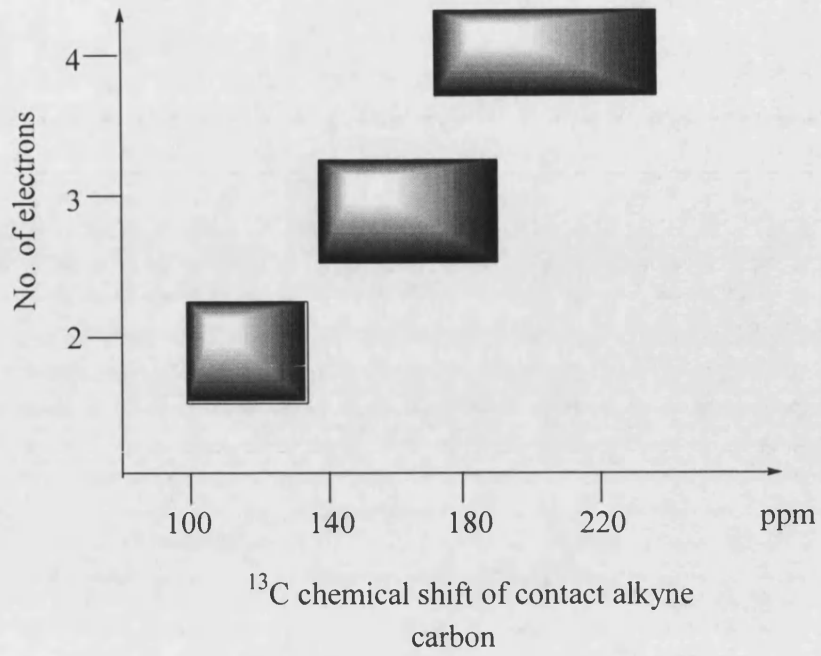

Figure 1.4

Other trends have also been identified on how spectroscopic methods can give information about the nature of the metal-alkyne bond. These include low field shifts in the ^{1}H NMR spectrum for terminal alkyne protons[9] and low alkyne absorptions within IR spectroscopy for a range of complexes containing the $MeO_2CC_2CO_2Me$ (DMAC) ligand.[10] Although the diester absorptions tend to be weak, they are consistent with the trend that the greater number of electrons donated to the metal weakens the C≡C bond and lowers the alkyne absorption υ(C≡C).

X-ray crystallography is also a useful tool as bond lengths and bond order are an excellent indication of the nature of the alkyne. On side-on co-ordination to a metal, alkyne ligands act in a similar manner to alkenes, with a reduction in bond order and an increase in bond length. Subject to exception, this can be a good indication upon the number of electrons donated to the metal. For example, 90 % of the four electron donor alkyne ligands in Mo(II) and W(II) monomers exhibit metal-

carbon bond lengths in the range of 2.03 ± 0.03 Å.[11] These are just a few examples of the many notable ways that the formal number of electrons donated to the metal from the alkyne can be identified. There are many more techniques that can be used to identify the nature of the metal-alkyne bond and these include trends within *intra*-ligand bond lengths,[12] bond angles[13] and ligand orientations of the alkyne.[14]

1.3 Synthesis and Reactivity of η^2-Vinyl Ligands

The fact that alkynes can act as $4e^-$ donors has inspired researchers to investigate their chemistry and in doing so to determine the similarities and differences from the analogous $2e^-$ donors. After all, the realisation that these species have the potential to stabilise intermediates with lower formal valence electron counts has presented the opportunity to generate a novel and exciting area of chemistry. Evidence that a novel chemistry exists for these species has been provided by many researchers, in particular by Green[15-17] and Davidson,[18-20] who have extensively studied the reactivity of $4e^-$ donor alkynes towards nucleophilic attack.

The rationale behind these investigations was to determine whether a parallel chemistry existed for $4e^-$ donor alkynes compared to $2e^-$ donor alkynes when reacted with nucleophiles. Reger[21] has reported on how η^1-vinyl complexes can be accessed through the nucleophilic attack (H^-) on an alkyne complex, in which the alkyne is acting as a $2e^-$ donor (Scheme 1.1).

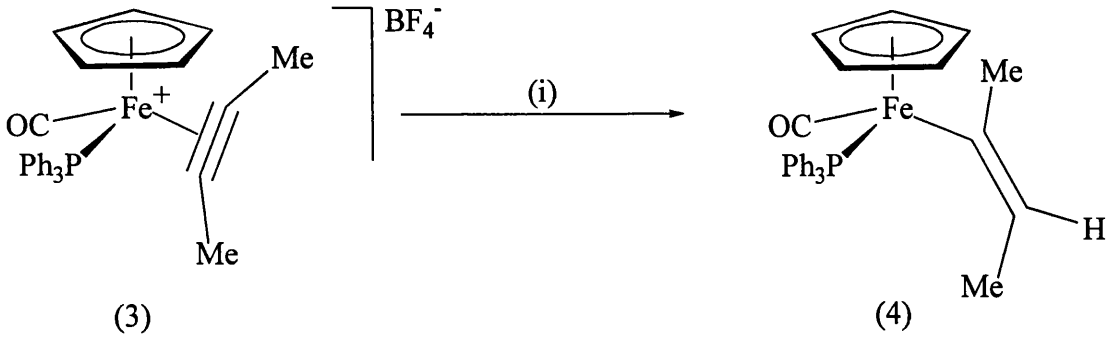

(3) (4)

Scheme 1.1 *(i) NaH.*

These co-ordinatively saturated η^1(1e) vinyl complexes such as (4) are stable products, however it was anticipated that due to the configuration around the metal, a 16e$^-$ η^1-vinyl complex would not be the stable product when a 4e$^-$ donor alkyne complex undergoes nucleophilic attack.

This theory was proved correct in two different ways; firstly, reaction of the 4e$^-$ alkyne complex $[Mo(\eta^2\text{-}t\text{BuC}_2\text{H})\{P(OMe)_3\}_2(\eta^5\text{-}C_9H_7)][BF_4]$ (5) with $NaBH_4$ in the presence of $P(OMe)_3$ results in the formation of the stable 18e$^-$ η^1(1e)-vinyl complex $[Mo(\sigma\text{-}CH{=}CHt\text{Bu})\{P(OMe)_3\}_3(\eta^5\text{-}C_9H_7)]$ (6) (Scheme 1.2).[22] As expected, the 16e$^-$ η^1-vinyl species requires additional electron density from the 2e$^-$ donor phosphite ligand to maintain stability.

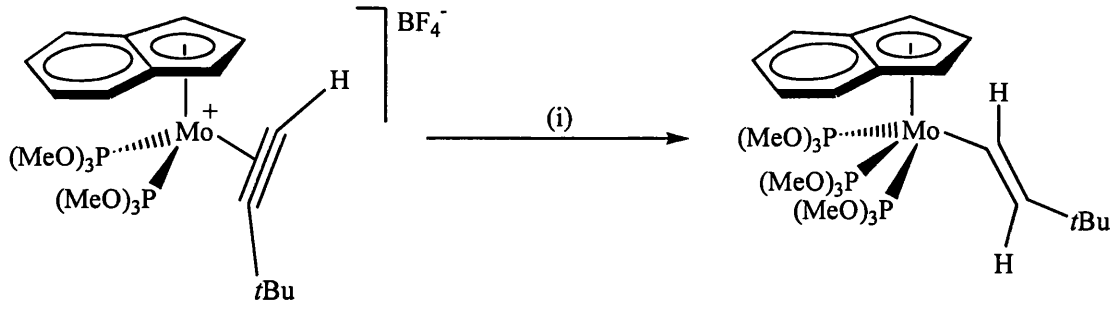

(5) (6)

Scheme 1.2 *(i) $NaBH_4$, $P(OMe)_3$.*

Secondly, it was found that the reaction between the 4e⁻ alkyne complex $[Mo(\eta^2\text{-}PhC_2Ph)\{P(OMe)_3\}_2(\eta\text{-}C_5H_5)][BF_4]$ (7) and $K[HBBu^s_3]$ (a source of H^-), yields the stable product $[Mo\{=CPhCH(Ph)\}\{P(OMe)_3\}_2(\eta\text{-}C_5H_5)]$ (8) (Scheme 1.3).[15,16]

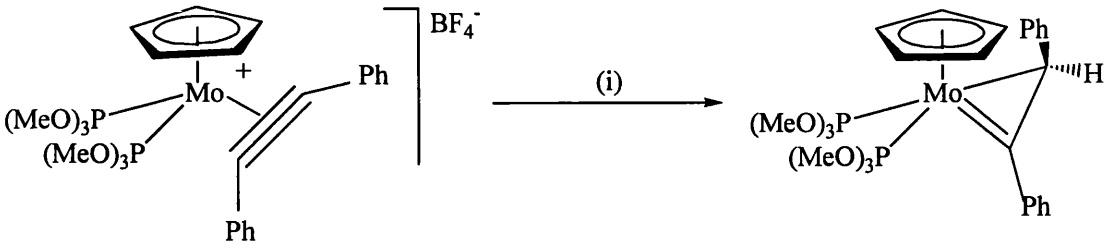

(7) (8)

Scheme 1.3 *(i) K[HBBu$^s_3$].*

Complex (8), a neutral complex, contains a CPhCHPh fragment and was therefore assigned as a η^2(3e)-vinyl in view of its metallacyclopropene structure where both carbons are bonded to the metal centre in the formation of a constrained three membered ring. More interesting was the observation that a strong relationship exists between the two modes of vinylic bonding and that the vinyl group can interchange between η^1(1e) and η^2(3e) when required. Slippage from η^1(1e) $\rightarrow$ η^2(3e) can occur to accommodate unsaturation through the co-ordinated $CPhCHPh^-$ fragment and slippage from η^2(3e)$\rightarrow$ η^1(1e) can provide an associative reaction path in which an 18 e⁻ configuration can be maintained (Scheme 1.4).

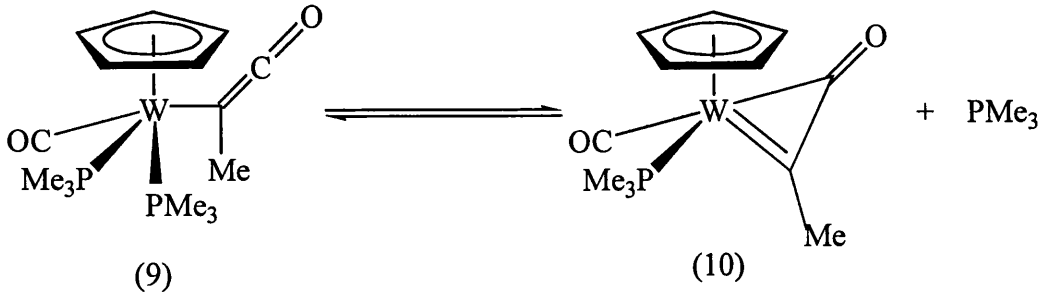

Scheme 1.4 *Inter-relationship between the two modes of vinylic bonding.*[23]

Complexes containing η^2(3e)-vinyl ligands are now well established and the bulk of this work has focused on accessing these complexes through the external attack of nucleophiles (hydrides,[15,16] isonitriles[18] and phosphorus reagents[24]) on co-ordinated 4e$^-$ donor alkyne ligands. However, an investigation of carbon-fluorine bond functionalisation has seen a novel synthetic approach to the synthesis of η^2(3e)-vinyl ligands.

Richmond[25] and co-workers have found that alkyne insertion into a perfluoroaryl-metal bond (Scheme 1.5) yields two products; a η^2(3e)-vinyl complex (12) being the major product and an unstable 4e$^-$ alkyne complex (13) as the minor complex. Further studies into the formation of (12) and (13) revealed that both products are probably formed *via* the same intermediate, an η^2(2e)-alkyne complex. However, it was also found that the two products were not inter-convertible moieties, which suggests that neither product is an intermediate to the other. Therefore, both products are formed through a competitive reaction path, where the η^2(2e)-alkyne complex can facilitate the formation of both products.

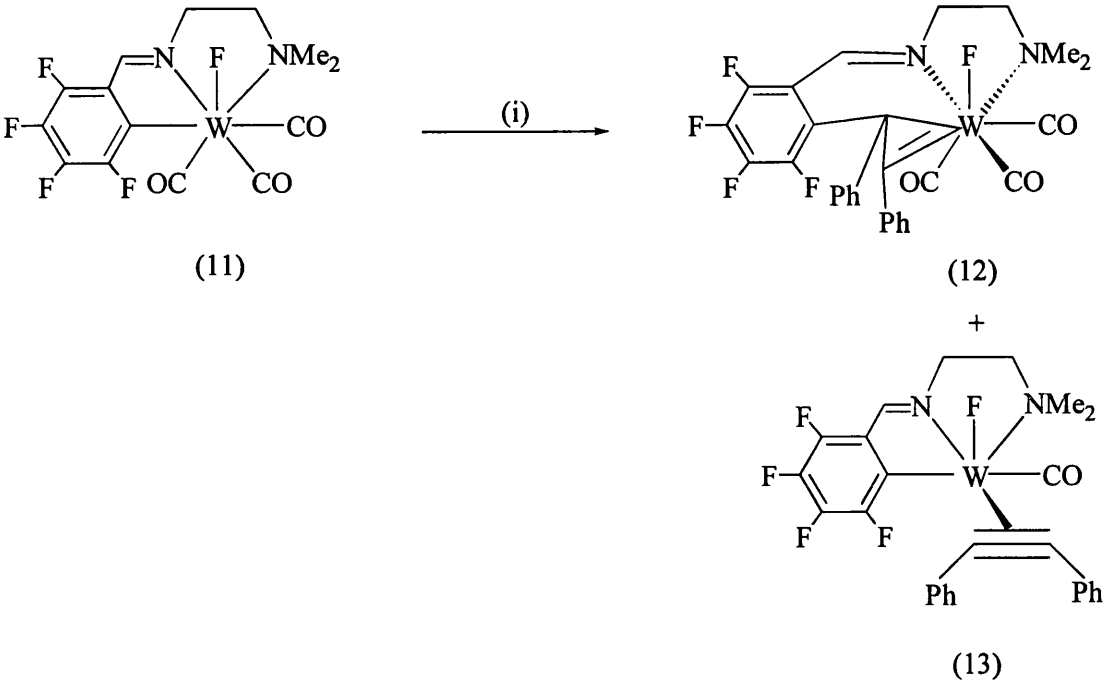

(11) (12) + (13)

Scheme 1.5 *(i) PhC_2Ph, 60 ^oC.*

In view of these observations it was thought that alkyne insertion into a non-fluorinated aryl carbon-tungsten-(II) bond would also result in the formation of η^2(3e)-vinyls. Surprisingly, this appeared to have a big effect on reactivity as reaction of (11) with a series of electron-rich alkynes resulted in the decomposition of the starting materials. However, reaction of (11) with a series of internal electron-deficient alkynes resulted in the exclusive formation of η^2(3e)-vinyls.

Since the formation of η^2(3e)-vinyls attracts considerable attention, in particular with regards to catalytic chemistry,[26] novel synthetic approaches to their formation are clearly desirable as it provides more information on their reactivity. This latest work is interesting as it probes the idea of synthesising η^2-vinyls in conjunction with exploring carbon-fluorine bond activation,[27] which is an essential step into the formation of the reaction precursor (11).

A common feature exhibited by the η^2-vinyl systems prepared by Green[16] and Davidson[19] is the fluxionality of the η^2-vinyl ligand, commonly known as the classical windscreen wiper motion (Figure 1.5). This is also a common feature exhibited by alkyne complexes. However, the η^2-vinyl complex (12) does not exhibit this dynamic feature due to the steric bulk of the rigid tridentate η^3-[C,N,N*] chelate ligand.

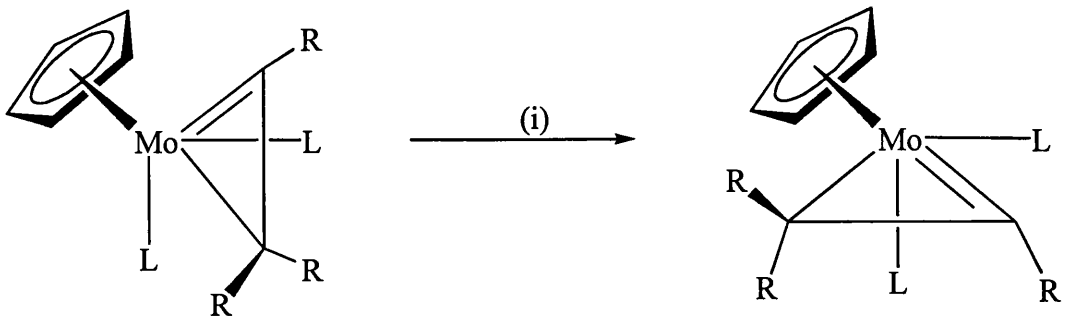

Figure 1.5 *(i) 90 ^{O} rotation.*

Further similarities between η^2-vinyl ligands and alkyne ligands were also found to lie within their frontier orbitals. Summarised by Green,[16] the major difference between the alkyne and $C_2H_3^-$ frontier orbitals lies in the energy and spatial nature of the $\pi_\perp$-orbital. This was derived from a fragment molecular orbital analysis, in which the frontier orbitals of the $[ML_2(\eta\text{-}C_5H_5)]^+$, HC_2H and $CHCH_2^-$ moities were calculated and compared (Figure 1.6) Although the frontier orbitals are similar, the $\pi_\perp$-orbital of the vinyl ligand is essentially pure $C_\alpha(P)$ in character and is therefore both asymmetric with respect to the two contact carbons and at higher energy than the $\pi_\perp$-orbital of the alkyne. Therefore, on energetic grounds this orbital enhances the donor ability of the vinyl fragment with respect to that of the alkyne.

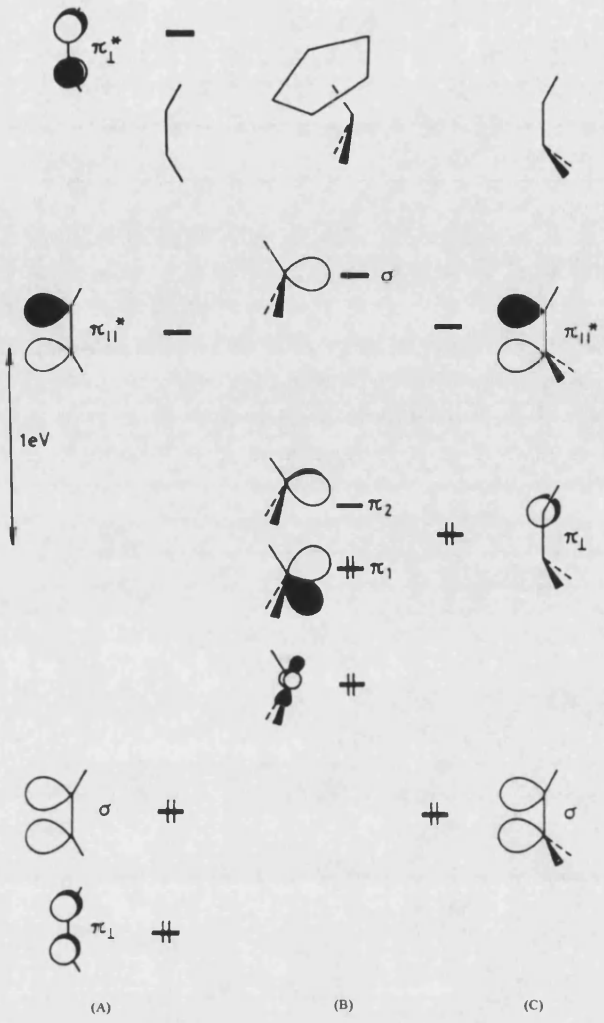

Figure 1.6 *Frontier molecular orbitals of the fragments (a) HC_2H, (b) $[Mo\{P(OH)_3\}_2(\eta\text{-}C_5H_5)]$ and (c) $HC_2H_2^{\cdot}$.*[16]

Whilst investigating the synthesis of a wide range of η^2(3e)-vinyl complexes by using a variety of nucleophiles and alkynes, it was found that there were certain disparities with the stability of these complexes. For example, the η^2-vinyl complex $[Mo\{=C(Ph)CMePh\}\{P(OMe)_3\}_2(\eta\text{-}C_5H_5)]$ (14) has a thermal bias to arrange into the η^3-allyl complex $[Mo\{\eta^3\text{-}CH_2C(Ph)CH(Ph)\}\{P(OMe)_3\}_2(\eta\text{-}C_5H_5)]$ (15) (Scheme 1.6)[28]. The rearrangement of the co-ordinated η^2-vinyl ligand into a η^3-allyl is facilitated by an $\eta^2 \rightarrow \eta^1$ change in bonding mode of the vinyl ligand (A), which is

followed by γ-hydrogen abstraction to form the intermediate hydrido η^2(2e)-vinylalkylidene complex (B). Hydrogen migration takes place from the metal centre on to the alkylidene carbon (C),which then affords the η^3-allyl complex (15). This rearrangement process also occurs in the complexes $[Mo(\eta^2\text{-}RC_2R)\{P(OMe)_3\}_2(\eta\text{-}C_5H_5)][BF_4]$ (where R=R=Me or *p*-tolyl).

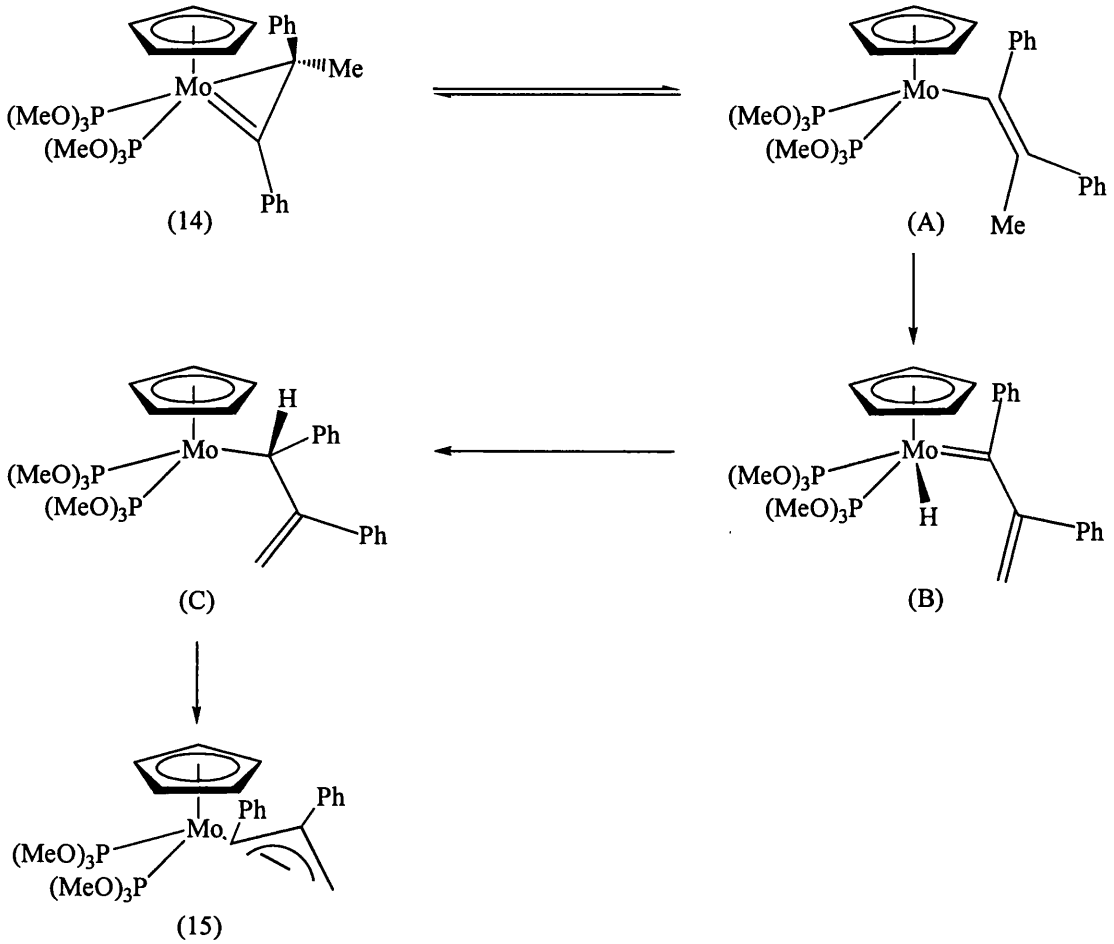

Scheme 1.6

Another molecular rearrangement of η^2-vinyl complexes was observed when the η^2-vinyl complex $[Mo\{=C(Ph)CHPh\}(CO)(PMe_2Ph)(\eta\text{-}C_5H_5)]$ (16) was reacted with iodosobenzene, with the intention of converting the co-ordinated CO into

uncoordinated CO_2 *via* oxygen transfer.[28] However, the result of the reaction was the surprising formation of the carbyne complex $[Mo\{\equiv CCHPh_2\}(CO)(PMe_2Ph)(\eta\text{-}C_5H_5)]$ (17) (Scheme 1.7). It appeared that the iodosobenzene could act as a one-electron oxidant and due to (16) being relatively electron-rich, a one-electron transfer reaction takes place generating a radical cation complex. This then rearranges *via* a 1,2-phenyl shift to form the carbyne complex (17).

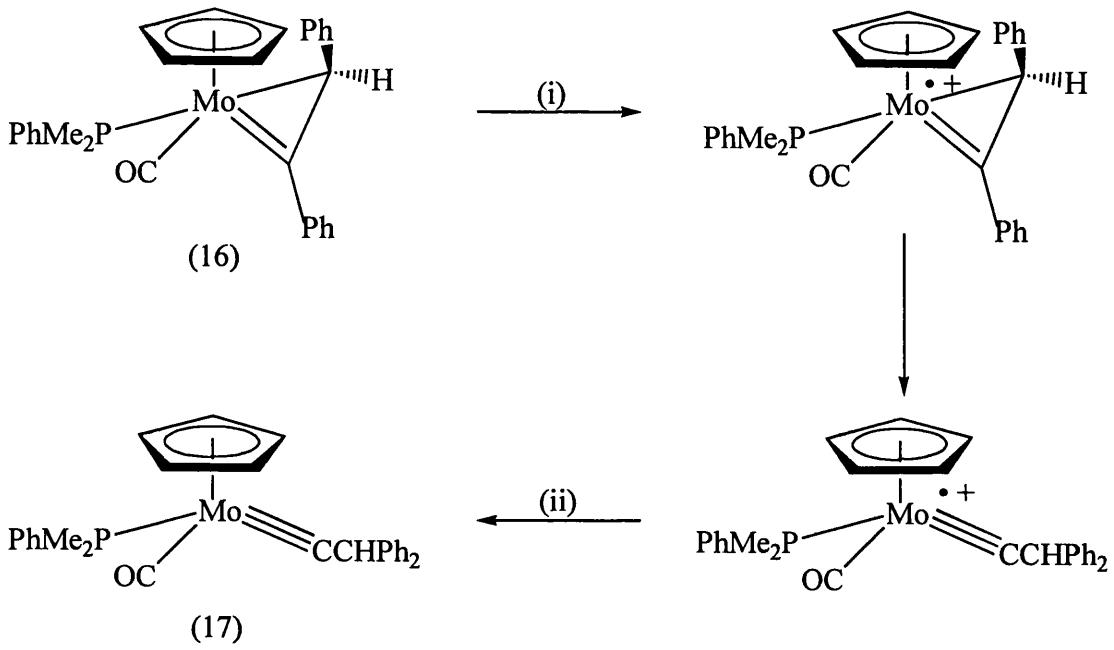

Scheme 1.7 *(i) +PhIO, -PhIO$^{\bullet+}$, (ii) +PhIO$^{\bullet+}$, -PhIO.*

Similar transformations have also been observed by Casey[29] for the rhenium alkyne complex $[Re(\eta^2\text{-}HC{\equiv}CCH_3)(CO)_2(\eta\text{-}C_5Me_5)]$ (18). When (18) was treated with $[Ph_3C]^+[PF_6]^-$ with the aim of obtaining a hydride abstraction reaction, the η^3-allyl complex $[Re(\eta^3\text{-}CH_3CHCPhCPh_2)(CO)_2(\eta\text{-}C_5Me_5)]^+[PF_6]^-$ (19) was afforded (Scheme 1.8). A study into the mechanism revealed that the initial stage of the reaction is the delivery of CPh_3 onto one of the alkyne contact carbons, forming the

cationic η^2(3e)-vinyl intermediate (A). A 1,2-hydrogen migration, to form the intermediate (B) is then followed by a 1,2-phenyl migration, which affords the cationic η^3-allyl complex (19) (Scheme 1.8).

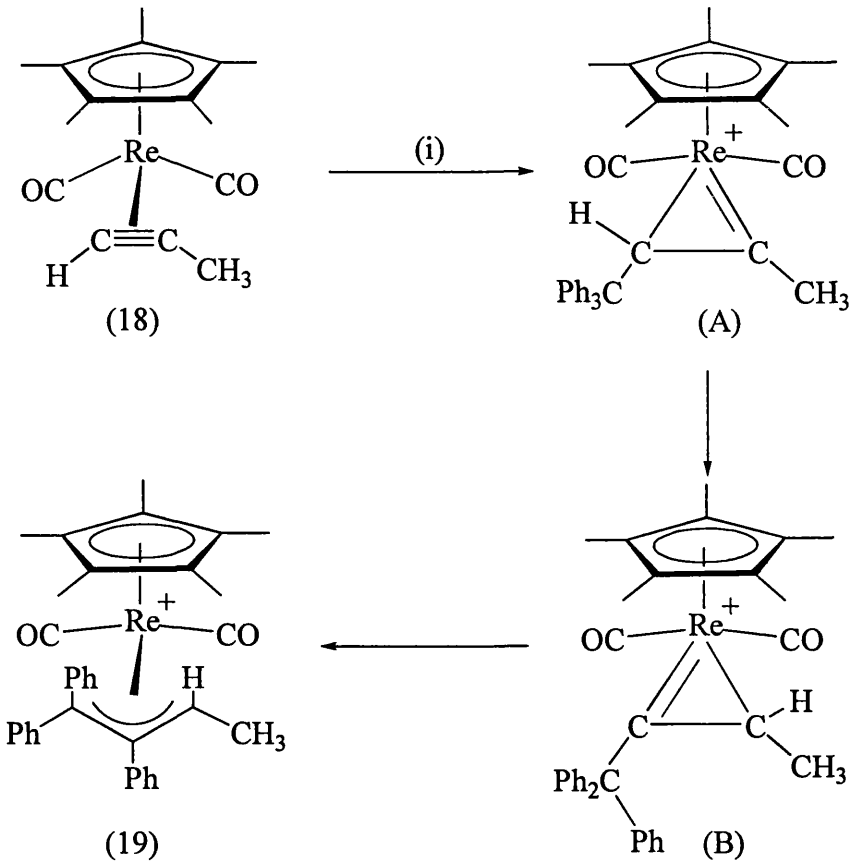

Scheme 1.8 *(i) $[Ph_3C]^+[PF_6]^-$.*

1.4 Synthesis and Reactivity of η^4(5e)-Butadienyls

A recent investigation by Green[30] and co-workers into the protonation of a series of halogenobis(alkyne) complexes (of general formula $[MoX(\eta^2\text{-alkyne})_2L]$, where X = Cl, Br or I and L = C_5H_5), has led to the formation and subsequent study of a range of η^4(5e)-butadienyl complexes of general formula $[Mo\{=C(R)\text{-}\eta^3\text{-}[C(R)C(R)CHR]\}X(OH_2)(\eta\text{-}C_5H_5)][BF_4]$. The study found that the reaction proceeds

via a η^2(3e)-vinyl-η^2(4e)-alkyne intermediate in which there is also the presence of co-ordinated H_2O.

The system used in the following example is $[MoCl(\eta^2\text{-}MeC_2Me)_2(\eta\text{-}C_5H_5)]$ (20) and this was found to react instantaneously towards $HBF_4.Et_2O$, generating the η^4(5e)-butadienyl complex $[Mo\{=C(Me)\text{-}\eta^3\text{-}[C(Me)C(Me)CHMe]\}Cl(OH_2)(\eta\text{-}C_5H_5)][BF_4]$ (21) in good yield. The first step of the reaction sequence was suggested to be the formation of an η^2(3e)-vinyl-η^2(4e)-alkyne intermediate (A), created by the delivery of a proton by $HBF_4.Et_2O$ onto one of the contact carbons of a co-ordinated alkyne (Scheme 1.9).

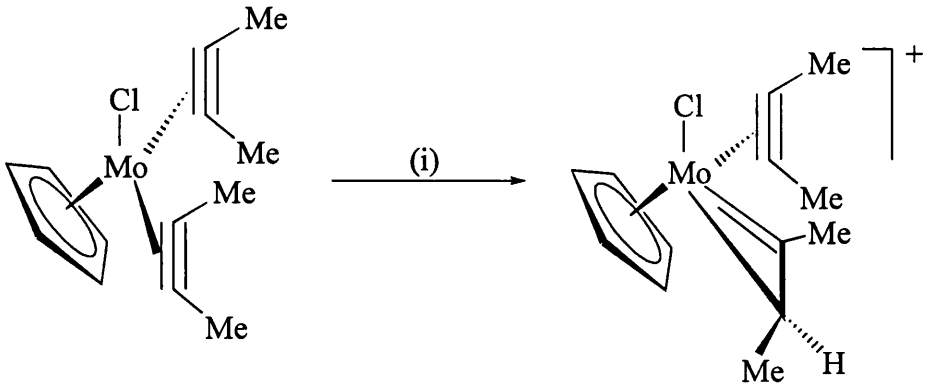

(20) (A)

Scheme 1.9 *(i) $HBF_4.Et_2O$.*

The next step of the reaction sequence is debatable as to whether attack by water occurs promoting the rotational opening of the η^2-vinyl to form a η^1(1e)-vinyl-η^2(4e)-alkyne intermediate (B) (Scheme 1.10). This would facilitate the migratory insertion of the η^1-vinyl onto the co-ordinated alkyne affording the $16e^-$ η^3(3e)-bonded

butadienyl intermediate (C). This then undergoes an electronic rearrangement to form the aqua cisoid η^4(5e)-butadienyl substituted cation (21) (Scheme 1.10).

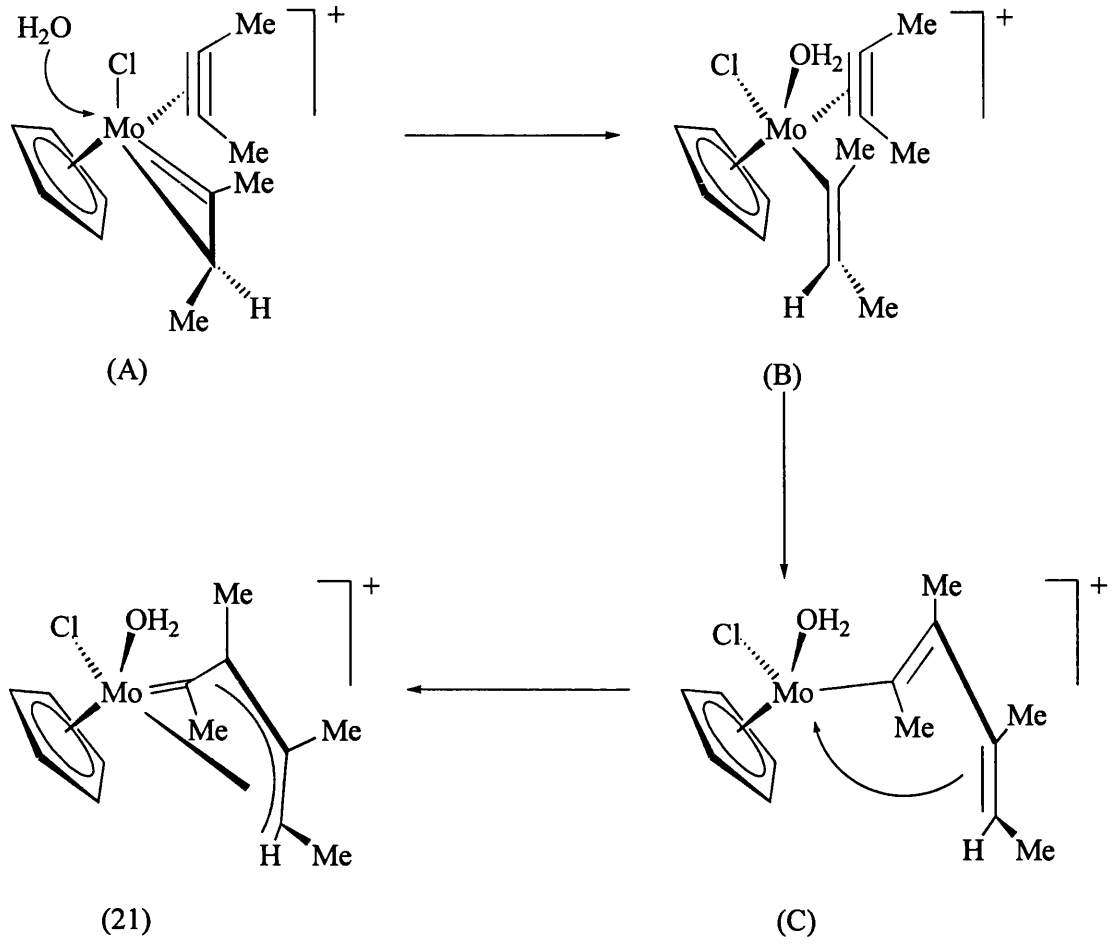

Scheme 1.10

The other alternative to the formation of (21) is by the direct coupling of the η^2-vinyl and η^2-alkyne ligands from the intermediate (A) which would directly afford (21). Both reaction paths are viable and it was not possible to decide which mechanism was occurring.

Subsequent studies were then undertaken to investigate the reactivity of the novel complex (21). It was found that reaction with acetonitrile quite easily displaced

the aqua ligand. From this observation, complex (21) was treated with a variety of reagents which would possibly displace the aqua ligand, including phosphines. It was found that the aqua ligand in (21) and the acetonitrile ligand in the analogous complex were both very labile and could be easily displaced by trimethylphosphine which is considered to be a poor π-acceptor.

Reactivity of the co-ordinated butadienyl ligand was also explored and an interesting reaction was discovered when the trimethylphosphite substituted complex $[Mo\{=C(Me)\text{-}\eta^3\text{-}[C(Me)C(Me)CHMe]\}Cl\{P(OMe)_3\}(\eta\text{-}C_5H_5)][BF_4]$ (22) was treated with the base $Li[N(SiMe_3)_2]$ (Scheme 1.11). A deprotonation reaction occurs affording the η^4-bonded vinylallene complex $[MoCl\{\eta^4\text{-}CH(Me)=C(Me)\text{-}C(Me)=C=CH_2\}\{P(OMe)_3\}(\eta\text{-}C_5H_5)]$ (23). In addition to this it was found that the reaction could be reversed by the protonation of (23) with $HBF_4.Et_2O$, thus establishing that an inter-relationship exists between η^4(5e)-butadienyl and η^4-vinylallene ligands.

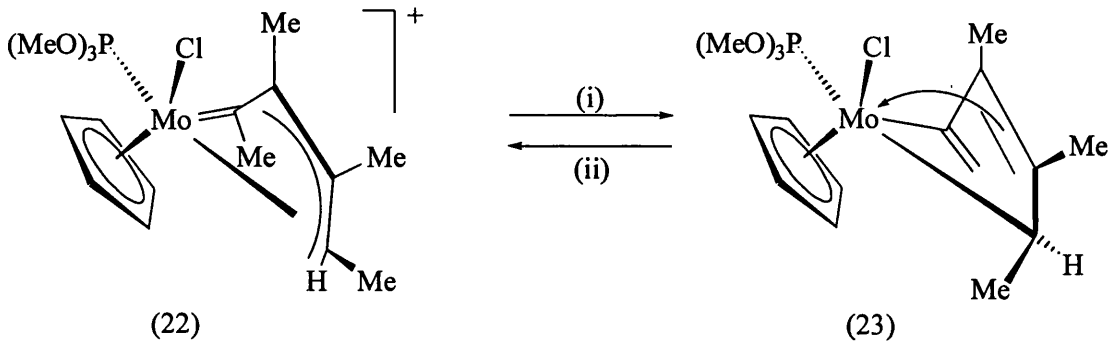

(22) (23)

Scheme 1.11 *(i) $Li[N(SiMe_3)_2]$, (ii) $HBF_4.Et_2O$.*

1.5 Conclusion

This introduction has given a brief synopsis of the chemistry of co-ordinated ligands. Most of the reactions mentioned have referred to the chemistry developed for molybdenum and tungsten monomers. However, recent work has tended to shift towards extending this chemistry towards other elements including platinum, tantalum and osmium. In summary, there still remains a continued driving force into investigating the chemistry of transition metal complexes containing co-ordinated ligands which exhibit multiple bond character.

CHAPTER TWO

THE CHEMISTRY OF PERFLUOROPHENYL SUBSTITUTED BORANES

2.1 Introduction

This chapter contains a discussion on how tris(pentafluorophenyl)borane $[B(C_6F_5)_3]$[31,32] (Figure 2.1) and other analogous perfluorophenyl substituted boranes have been introduced as co-catalysts within a variety of different catalytic processes for the homogeneous polymerisation of olefins. In analogy to traditional Ziegler-Natta catalysts, the active site homogeneity and the tailorability of this new generation of catalysts offers unprecedented control over the properties of the polymeric products.[33] The general reactivity of $B(C_6F_5)_3$ towards transition metals will also be reviewed along with the related compounds bis(pentafluorophenyl)borane $HB(C_6F_5)_2$,[34] the non-coordinating anion tetrakis(pentafluorophenyl)borate $[B(C_6F_5)_4]^-$ [35] and the novel bifunctional perfluoroaryl boranes $[(C_6F_5)_2B\text{-spacer-}B(C_6F_5)_2]$.[36]

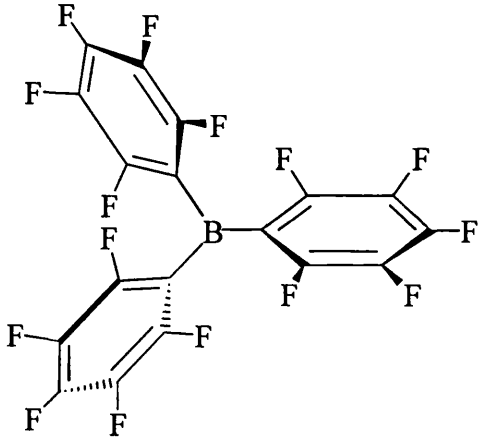

Figure 2.1 *Structure of tris(pentafluorophenyl)borane* $[B(C_6F_5)_3]$.[31]

2.2 Background of $B(C_6F_5)_3$ and Introduction to Catalysis

$B(C_6F_5)_3$ was first reported in 1964 by Massey and Park[31,37,38] who contributed in a series of papers titled '*Perfluorophenyl Derivatives of the Elements*'. However, it has only been within the last decade that there has been considerable interest in its reactivity. The reason behind this surge in interest is due to the recognition of its high Lewis acid strength and activity, hence its potential as a co-catalyst for group IV metallocene-based homogeneous olefin polymerisation reactions.

Currently, there is a great deal of interest in catalysis and polymer chemistry and it has been established that bent metallocenes[39-42] are highly active for the polymerisation of alkenic monomers to important commodity plastics.[43,44] It has been identified that cationic group IV metal alkyl complexes of the type $[Cp_2MR]^+$ (where M = Ti, Zr, Hf) are excellent active species in homogeneously Ziegler-type catalysed polymerisation reactions[39-42,45-47] and it is probable that they could develop into the next generation of Ziegler catalyst systems for industrial α-olefin polymer production.[39]

To form active catalysts, group IV metallocene systems require activator compounds, more frequently known as co-catalysts which activate[48-50] and stereoregulate[39,51,52] the metallocene alkyl species into forming the co-ordinatively unsaturated cationic metallocene alkyl species. Although it is presumed that the cationic species is responsible for olefin polymerisation, it has been established, though not fully understood, that the ion-ion interactions between the active cation and anion are a function of polymer activity. Hence, the weaker the ion-ion interactions, the better the polymer activity.

The mechanistics of the C-C coupling catalytic process are reasonably well understood (Scheme 2.1). Activator compounds react with $[Cp_2ZrR_2]$ to form the

reactive alkyl zirconocene cation (A) which is internally stabilised by a β-agostic interaction. The second step is the addition of the olefin to the cation to form the reactive intermediate (B). This is followed by the final step, the insertion reaction, where the sequence is repeated until a chain-transfer reaction takes place which is a highly exothermic process (C). The kinetic study carried out by Erker[53] concluded that it is not clear which of the two steps (B) or (C) is essential for stereocontrol of the C-C coupling reaction and whether the metallocene backbone is a function of activity.

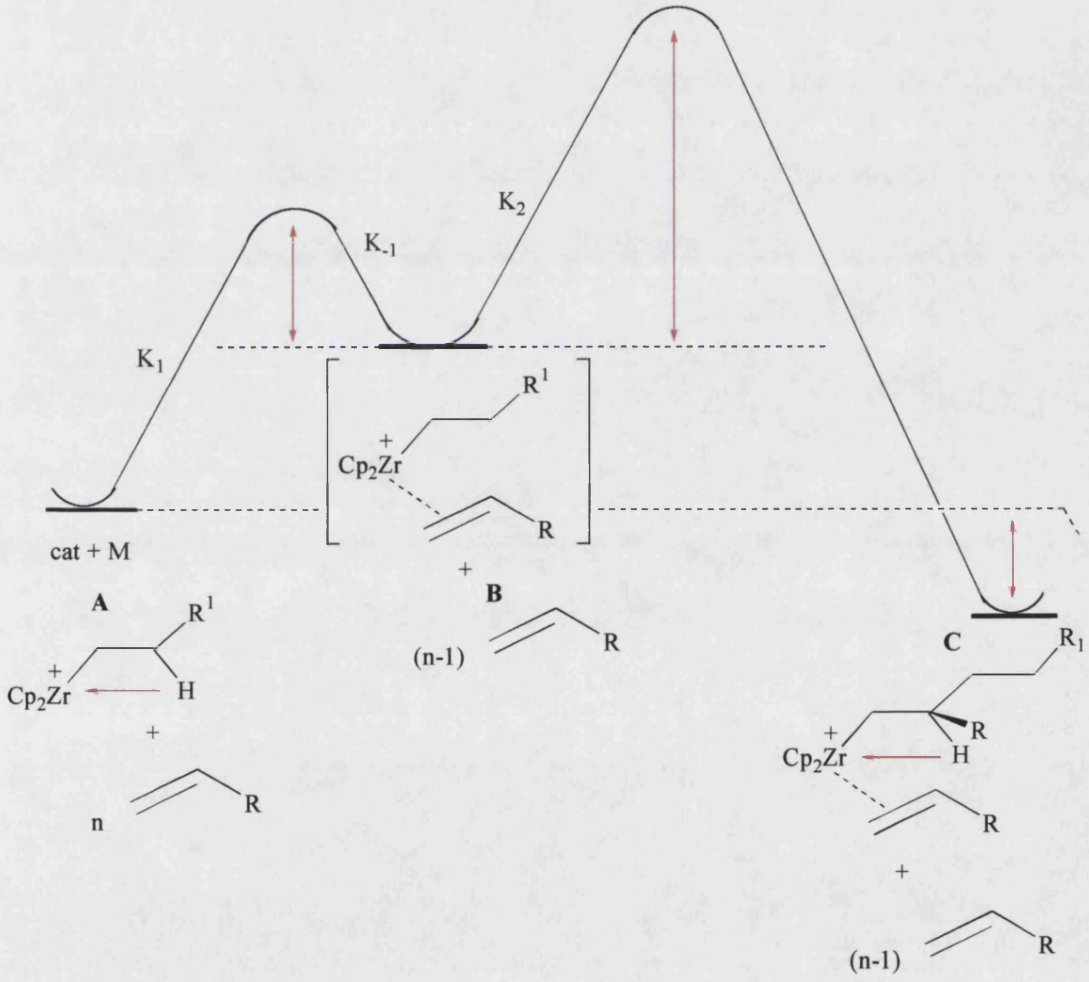

Scheme 2.1 *Mechanistic scheme showing C-C coupling catalytic process.*[53]

A traditional co-catalyst is methylaluminoxane (MAO)[39,40,45,54-56] and its role within this area of catalysis is to operate two main functions. Firstly, to serve as an alkylating agent and secondly, to act as a Lewis acid by abstracting a methyl group from the metal centre, therefore, creating an active cationic organometallic species responsible for olefin enchainment (Scheme 2.1).[32] However, although MAO has been successful within olefin polymerisation there are many disadvantages associated with its use. Firstly, it is difficult to isolate the active metallocene species and secondly, the process involves employing a large excess of MAO which has inspired researchers to investigate other, more efficient methods of activation for such C-C coupling catalysts.

Whilst investigating alternatives to MAO, Marks[57] and Ewen[58] independently introduced the theory that treatment of dimethyl zirconocene (*i.e.* a pre-alkylated catalyst precursor) with a Lewis acid more powerful than the resulting $[Cp_2ZrCH_3]^+$ cation would lead to highly active polymerisation catalysts. This idea prompted them to test an aluminium-free co-catalyst, $B(C_6F_5)_3$, due to its notable Lewis acid strength and stability which is somewhere between BF_3 and BCl_3 ($BCl_3 > B(C_6F_5)_3 > BF_3$). It also has the added advantage of being extremely soluble in non-polar and non-coordinating solvents and its three highly electronegative fluoro-substituted phenyl rings promote the borane to be chemically robust, a property which enables the borane to be resistant to electrophilic attack, which is effective for isolating the characterisable metallocene active species. For these reasons, it became important to establish a much safer method for the preparation of $B(C_6F_5)_3$. Its original synthesis was by treatment of pentafluorophenyllithium with BCl_3 at -78 °C[31], which has more recently been modified to refluxing $MgBr(C_6F_5)$ with BCl_3.[32]

2.3 Alkyl Abstraction Reactions with $B(C_6F_5)_3$

The theory proposed by Marks and Ewen[43] proved to be successful when a variety of dimethyl zirconocenes were treated with $B(C_6F_5)_3$, producing transition metal cations by direct electrophilic attack on the Zr-Me bond. Crystallographic studies on these cation-like compounds indicated that the ions were linked to one another *via* an unsymmetrical bridging methyl group most strongly associated with the boron atom (Scheme 2.2). However, variable temperature NMR studies indicated that two dynamic processes were occurring in solution which suggested that both Lewis acids $[Cp_2ZrCH_3]^+$ and $B(C_6F_5)_3$ were competing for the methanide group (Schemes 2.3 and 2.4).

$$Cp_2ZrMe(\mu\text{-}Me)B(C_6F_5)_3 \rightleftharpoons Cp_2ZrMe^+\ MeB(C_6F_5)_3^- \quad (24)$$

Scheme 2.2

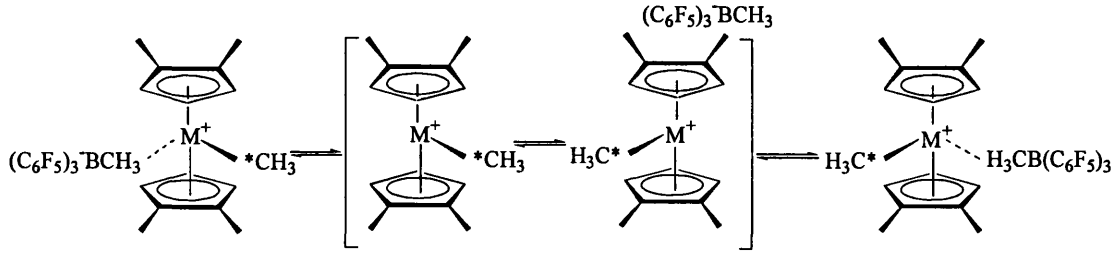

Scheme 2.3 *Process 1 involves separation of the anion from the cation, followed by a flipping over of the Zr-CH_3 group and reabstraction of the anion.*

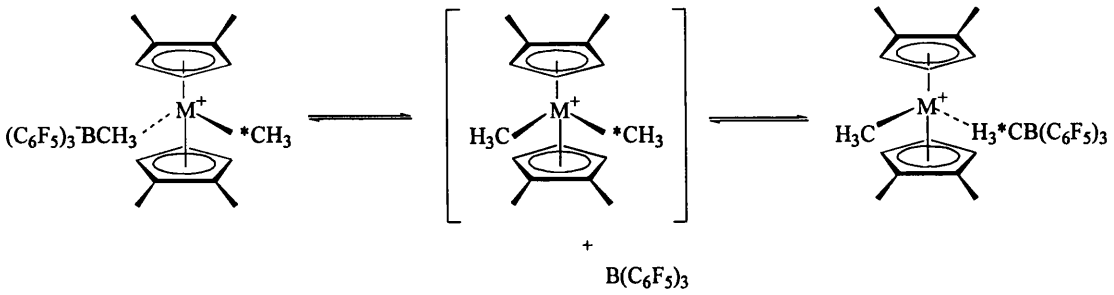

Scheme 2.4 *Process 2 involves dissociation of free borane, followed by abstraction of the other zirconocene methyl group by the borane.*

Interestingly, both process are influenced by the M-C bond strength, *i.e.* process 1 predominates when M = Zr and process 2 predominates when M = Hf due to the slightly stronger bond strength of Hf-C.

It is important to recognise that these preliminary studies by Marks[33] established the first quantitative data for ion pairing in a metallocene catalyst. Since these first studies, the idea that $B(C_6F_5)_3$ can act as a co-catalyst in homogeneous olefin polymerisation systems has become increasingly popular. Its application has now been acknowledged giving rise to numerous compounds of this type being synthesised. However, characterisation of these cation-like compounds has increased awareness of how tailoring these systems can lead to more efficient olefin polymerisation catalysts.

Other groups have shown that these abstraction reactions are not restricted to methyl groups or to the early transition metal systems. Bochmann[59] has illustrated that a benzyl ligand can be readily abstracted from $[Cp_2Zr(CH_2Ph)_2]$ (25) with $B(C_6F_5)_3$. The resulting cation (26) is stabilised by the other benzyl ligand. Interestingly, there is no detection of a bridging benzyl ligand (Scheme 2.5).

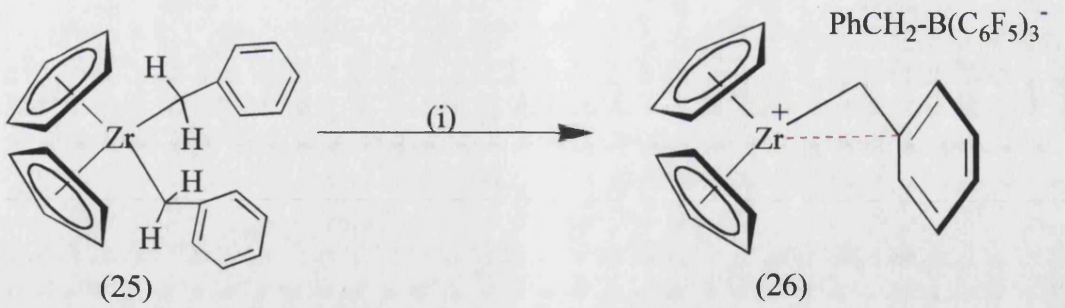

(25) (26)

Scheme 2.5 *(i) $B(C_6F_5)_3$.*

To prove that the methodology works in late transition metal systems, Puddephatt[60] has shown that under anhydrous conditions, $[PtMe_2(bu_2bpy)]$ (27) reacts with $B(C_6F_5)_3$ in the presence of a ligand L (where L = CO, C_2H_4 or PPh_3), to generate the ionic compound $[PtMe(L)(bu_2bpy)]^+[MeB(C_6F_5)_3]^-$ (28). Therefore, demonstrating that facile methyl ligand abstraction can occur in late transition metal systems, in this case facilitated through cation stabilisation by L (Scheme 2.6).

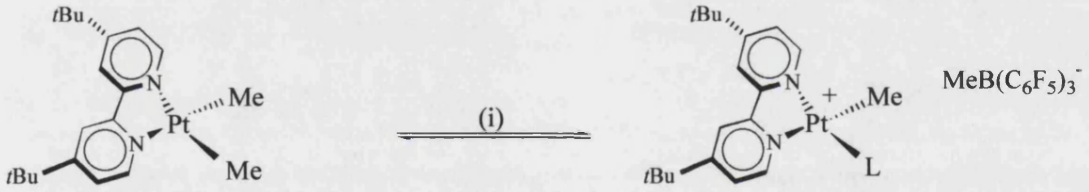

(27) (28)

Scheme 2.6 *(i) $B(C_6F_5)_3$, L (where L = CO, C_2H_4 or PPh_3).*

2.4 Synthesis and Reactivity of Zwitterionic Alkene Polymerisation Catalysts

Zwitterionic analogues of ionic metallocenes are at present being investigated extensively and major contributions of this chemistry have been provided by Erker[61-63] and Bochmann.[64,65] The interest towards zwitterionic systems has risen due to the fact they are neutral single components which do not require other co-catalysts,[32] which

gives them an advantage over prevailing metallocene systems. They are also much more soluble compared to non-zwitterionic catalysts and recent investigations have proved that catalytic activity can be suitably enhanced if the covalent nature between the active cation and anion is weakened. This process involves a 'covalent tethering'[66] of the anionic moiety to the metallocene ligand system whereby weakening the co-ordinating bridging ligand between the main group orbital and the metal centre induces an increase in catalytic activity.

There are two main types of zwitterionic metallocenes. Firstly, 'ring-type' zwitterions where the counter-anion is fixed to one of the Cp donors[62,64,67,68] and secondly 'girdle-type' zwitterions where the counter-anion is located on the alkyl group occupying the reactive wedge of the metallocene.[61,69-73] An important difference between these types of metallocenes is that the ring-type zwitterion maintains its zwitterionic structure throughout the polymerisation process whereas the girdle-type only retains its zwitterionic nature until the first termination step in the C-C coupling catalytic process.

An example of a ring-type zwitterion was reported by Erker[62] who found that reaction of the zirconocene complex 1,1-bis(cyclopentadienyl)-2,3,4,5-tetramethylzirconacyclopentadiene (29) with $B(C_6F_5)_3$ gave the zirconocene-betaine system (30) (Scheme 2.7). The reaction proceeds *via* an electrophilic aromatic substitution reaction and results in the functionalisation of one of the Cp ligands [η^5-$C_5H_4B(C_6F_5)_3$]. Interestingly, the vacant co-ordination site and the partial positive charge, both at the metal centre, are accommodated by an agostic interaction by one of the *ortho*-fluorine substituents of one of the C_6F_5 groups. This characteristic feature

has also been reported in other zwitterionic systems and is characterised by a significant high field shift in the ^{19}F NMR.

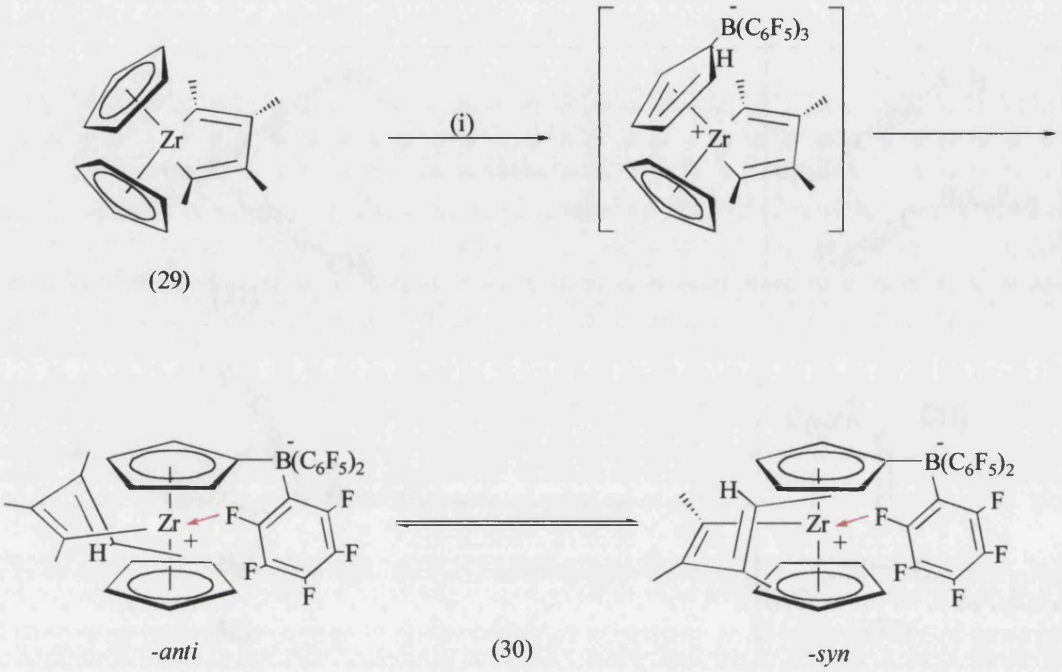

Scheme 2.7 *(i) $B(C_6F_5)_3$.*

Girdle-type zwitterions are by far the most reported of the zwitterionic systems and tend to be accessed through electrophilic attack on one of the hydrocarbyl (R) groups of $[Cp_2MR_2]$ by $B(C_6F_5)_3$. A novel system reported by Erker[70,74] indicated that an organometallic betaine could be accessed through the removal of an acetylide group from bis(propynyl)zirconocene (31) by $B(C_6F_5)_3$ (Scheme 2.8). Addition of the borane induces the transfer of a propynyl anion from the zirconium centre onto the boron. This is followed by the insertion of the boron-substituted alkyne into the zirconium-carbon bond of the 1,1-bis(cyclopentadienyl)zircona-propargyl cation intermediate, which results in the formation of the betaine (32). Interestingly, the novel betaine, where the electrophilic zirconium centre is stabilised through π-donation, is in endothermic equilibrium with its isomer, a methylenecyclopropene

has also been reported in other zwitterionic systems and is characterised by a significant high field shift in the ^{19}F NMR.

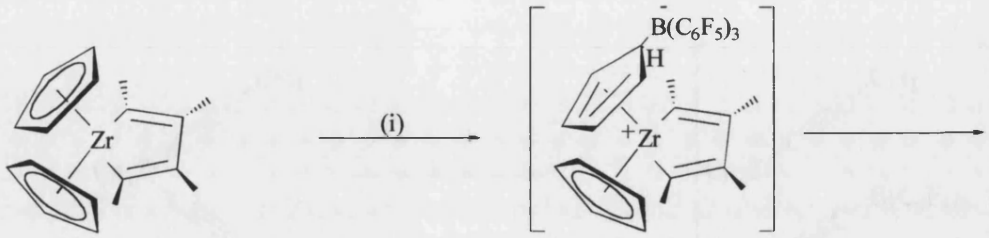

(29)

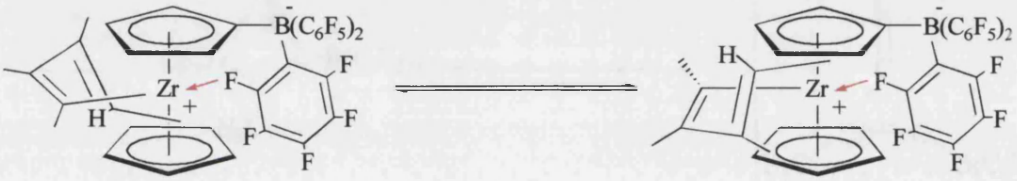

-anti (30) *-syn*

Scheme 2.7 *(i) $B(C_6F_5)_3$.*

Girdle-type zwitterions are by far the most reported of the zwitterionic systems and tend to be accessed through electrophilic attack on one of the hydrocarbyl (R) groups of $[Cp_2MR_2]$ by $B(C_6F_5)_3$. A novel system reported by Erker[70,74] indicated that an organometallic betaine could be accessed through the removal of an acetylide group from bis(propynyl)zirconocene (31) by $B(C_6F_5)_3$ (Scheme 2.8). Addition of the borane induces the transfer of a propynyl anion from the zirconium centre onto the boron. This is followed by the insertion of the boron-substituted alkyne into the zirconium-carbon bond of the 1,1-bis(cyclopentadienyl)zircona-propargyl cation intermediate, which results in the formation of the betaine (32). Interestingly, the novel betaine, where the electrophilic zirconium centre is stabilised through π-donation, is in endothermic equilibrium with its isomer, a methylenecyclopropene

strong β-CH agostic interaction. Due to the fact that low temperature NMR experiments failed to detect the *exo-* isomer, it could be argued that attack at the *endo-* carbon is preferred as it provides the zirconium centre with a much stronger agostic interaction through C_β-H and possibly through B-C_β.

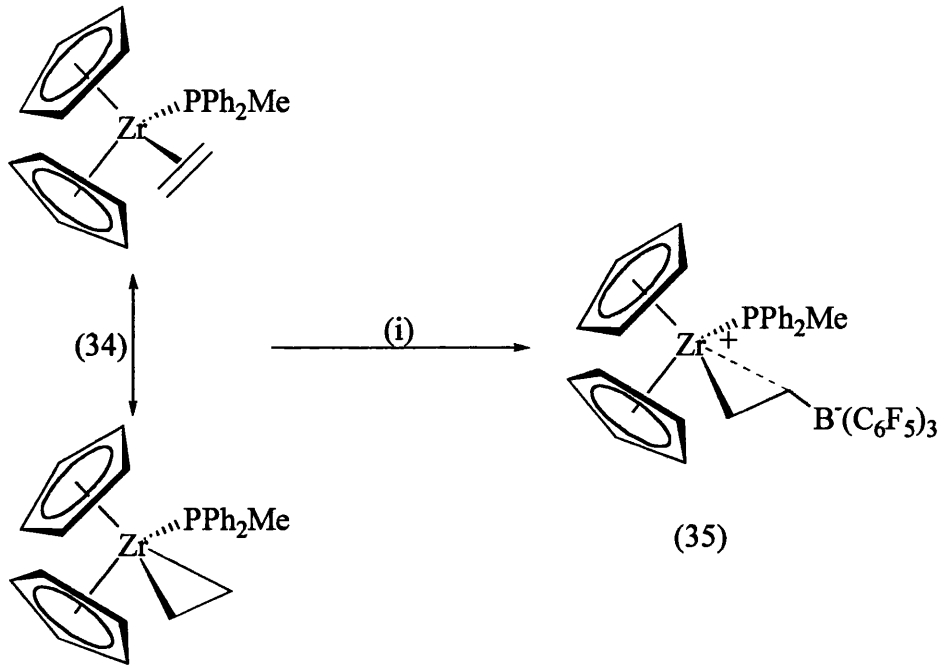

Scheme 2.9 *(i) $B(C_6F_5)_3$.*

Further investigations into girdle-type zwitterions led to the hypothesis that metallocene borate betaines which exhibit intramolecular stabilisation, can be tethered *i.e.* altering the geometric backbone to influence the intramolecular stabilisation of the electron deficient metal centre [M]. Erker[63] has demonstrated the systematic relationship between the π-allyl moiety being *E* or *Z* configurated and the intramolecular stabilisation of the electrophilic metal centre being either through an *ortho* F...[M] or an [M]...$CH_2B(C_6F_5)_3$ interaction.

Like the phosphine stabilised system, Erker[63] found that $B(C_6F_5)_3$ adds to the terminal CH_2 group of the conjugated diene ligand in $[Cp_2Zr(butadiene)]$ (36), to yield the metallocene borate betaine system (37) (Scheme 2.10).

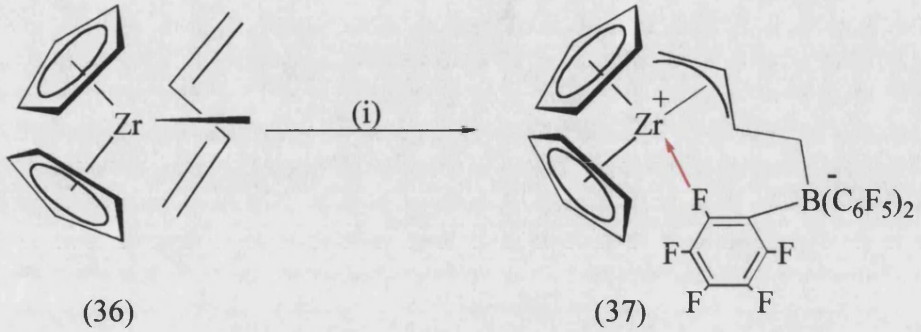

(36) (37)

Scheme 2.10 *(i) $B(C_6F_5)_3$.*

However, the electrophilic metal centre is stabilised through the co-ordination of an *ortho*-F atom from one of the C_6F_5 substituents from $B(C_6F_5)_3$ rather than a $[M]...CH_2B(C_6F_5)_3$ interaction. Therefore, the question arises as to why in some systems the intramolecular $[M]...CH_2B(C_6F_5)_3$ ion is favoured more than the [M]...F interaction and *vice versa*. For metallocene borate betaine systems an explanation for this differing behaviour has been established. It was suggested that intramolecular ion stabilisation is dependent upon whether the π-allyl moiety is *E* or *Z* configurated. When π-allyl systems are *E*-configurated only the *ortho*-F ion stabilisation occurs due to the geometrically prohibitive *E* position of the CH_2B substituent at the π-allyl ligand. Erker demonstrates that in cases such as (39) where the π-allyl moiety is *Z*-configurated, the system is stabilised through a $[Zr]...CH_2B(C_6F_5)_3$ (Scheme 2.11).

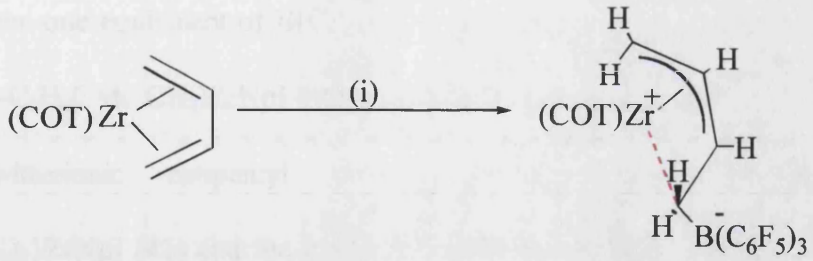

(38) (39)

Scheme 2.11 *(i) $B(C_6F_5)_3$ where COT = cyclooctatetrene.*

Unlike the systems that Marks[33] demonstrated, these ion pairs are intramolecular and are a result of tethering these earlier compounds to produce single, neutral components where it is possible to compensate for the electron deficient metal centre in different ways. In the example pictured above (Scheme 2.11), the CH_2 interaction forms an interesting five membered metallacycle.

Recently, a third type of zwitterion has been established and described as a 'tuck-in'[68] metallocene system. Structurally, these systems exhibit similar geometric features found in both ring-type and girdle-type systems due to the zirconocene precursor containing a Cp and one of the alkyl substituents being linked either directly or through a $(CH_2)_n$ spacer. This represents another example of how the anionic moiety in these systems is being covalently tethered with the aim of weakening the ion-ion interaction. Two recent examples are illustrated in Schemes 2.12[66] and 2.13,[68] where it is important to note that as the metallocene is adopting a more crowded geometry, there is a tendency for the kinetic product to be different from the thermodynamic product, an indication that, although the electronic properties of these complexes are comparable to the systems discussed previously, there is a greater steric requirement on the metallocene backbone as it tries to compensate for the electron deficient metal centre.

When one equivalent of $B(C_6F_5)_3$ is reacted with the cyclometallated complex $[Cp^*(\eta^5\eta^1\text{-}C_5H_4CMe_2CH_2)ZrNp]$ (40) (where $Cp^* = \eta\text{-}C_5Me_5$ and $Np = CH_2CMe_3$), a novel zwitterionic neopentyl complex is produced $[Cp^*\{\eta\text{-}C_5H_4CMe_2\text{-}CH_2B(C_6F_5)_3\}ZrNp]$ (41) and the anionic moiety is attached to one of the Cp ligands *via* a two carbon backbone (Scheme 2.12). As previously shown, (41) internally stabilises itself through the presence of an agostic interaction *via* the methylene carbon. However, the product was reported to be thermally unstable with respect to β-Me elimination.[76] Consequently, the borane migrates to the methyl group facilitating allylic C-H activation[76] where the product loses is zwitterionic nature. Interestingly, the thermodynamic product contains the well established $[MeB(C_6F_5)_3]^-$ anion. Regardless of the instability of (41), it was found to exhibit catalytic activity when exposed to olefins. The conclusion is that the zwitterion acts as a highly selective catalyst for the head-to-tail dimerisation of α-olefins, a process which tends to be favoured by the zwitterionic systems.

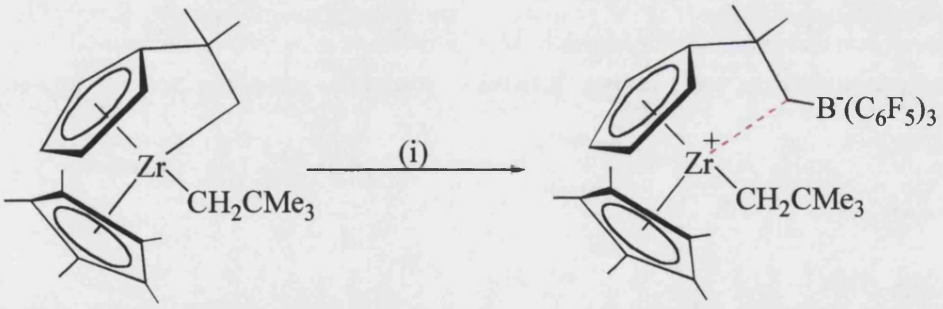

(40) (41)

Scheme 2.12 *(i) $B(C_6F_5)_3$.*

When one equivalent of $B(C_6F_5)_3$ is reacted with the tuck-in phenyl complex (42), electrophilic addition occurs at the carbon spacer CH_2 (Scheme 2.13). The kinetic product (43) is a zwitterion where the electrophilic metal centre is partially

stabilised by a weak *ortho*-fluorine interaction and an agostic C-H interaction from the phenyl group. However, the kinetic lability of the [M]...F interaction is compensated thermodynamically (44) with the interaction of the CH_2...[M] (methylene group) in addition to a much stronger C-H agostic interaction. Therefore, in this case there appears to be a thermodynamic bias for the BCH_2...[M] interaction over the [M]...F interaction. However, when (44) is reacted with hydrogen, benzene is eliminated to yield (45), where once again [M]...F stabilisation is retained. This clearly suggests that in this system, it is the steric bulk of the hydrocarbyl group, which is not co-ordinated to the borane, that determines how the metal centre is to be electronically compensated.

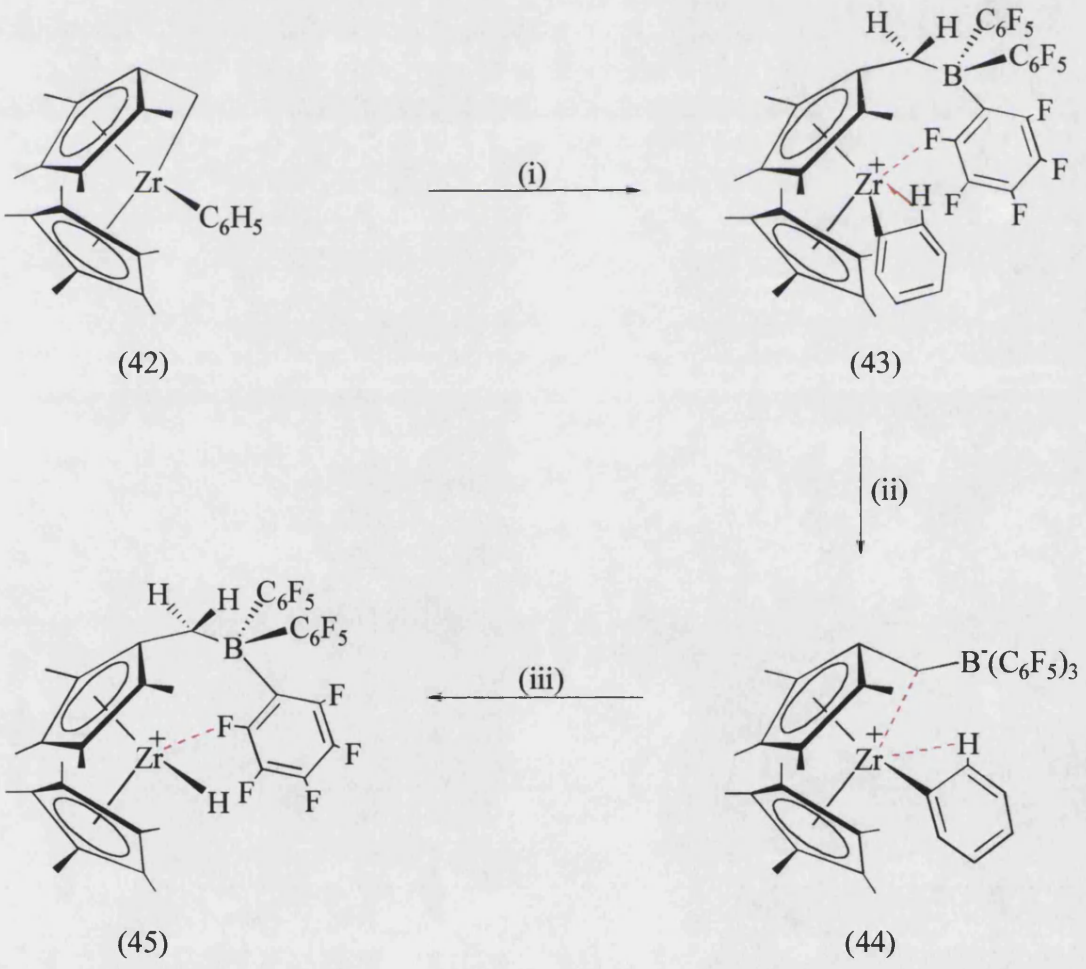

Scheme 2.13 *(i) $B(C_6F_5)_3$, (ii) 50 °C, (iii) H_2.*

2.5 Other Reactions of $B(C_6F_5)_3$

Despite the biggest application of $B(C_6F_5)_3$ being its crucial role as a co-catalyst for the homogeneous polymerisation of olefins, it does have a versatile chemistry. Among its citations are organic[77,78] as well as transition metal based reactions, where its diversity is an indication of its developing popularity. Recently, Tilley[79] reported the first direct detection of a 1,2-migration of hydrogen from silicon to a metal atom, a reaction made accessible by the reactive $B(C_6F_5)_3$. It was found that the remarkably inert (46) reacts instantaneously with $B(C_6F_5)_3$ to generate the silylene complex (47). The borane acts as a methyl abstractor and provides a vacant co-ordination site at the platinum metal, which allows the 1,2 migration of hydrogen to occur (Scheme 2.14).

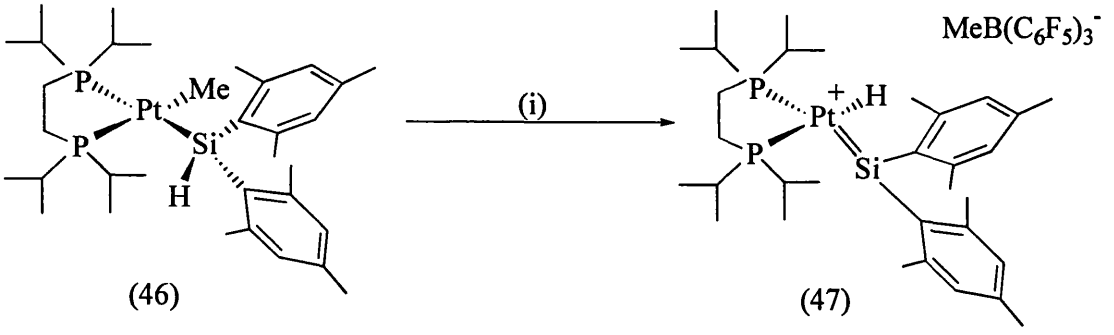

(46) (47)

Scheme 2.14 *(i) $B(C_6F_5)_3$.*

Another area of work connected with $B(C_6F_5)_3$ has been largely attributed to Green who has specialised in the reactivity of $B(C_6F_5)_3$ with transition metal complexes containing π-donor ligands *(e.g.* oxo,[80-82] alkoxide[81] and amide[83]), the aim of the research being to identify the nature of the interactions that co-exist within such frameworks. In view of the interest towards oxometal complexes it is not surprising that Green[84] has subsequently reported on the reactivity of $B(C_6F_5)_3$ towards H_2O.

Prior to Green's[84] investigation, there has been no in-depth study on the reactivity of $B(C_6F_5)_3$ towards H_2O. It is known that $B(C_6F_5)_3$ forms a trihydrate with water $[(H_2O)_2H_2O{\cdot}B(C_6F_5)_3]$,[85] however, the ability of the borane to form this adduct and its consequent reactivity does not appear to have been studied in great detail, though there have been reports which have hinted at the significance of the formation of this adduct.

Puddephat[60] reported on H_2O reacting with $B(C_6F_5)_3$ within the platinum system discussed previously (Section 2.3). This was proposed to have arisen from 'adventitious' H_2O entering the reaction vessel. It became evident that as H_2O forms an adduct with $B(C_6F_5)_3$, $H[HOB(C_6F_5)_3]$, a competitive reaction path is viable. It was suggested that the adduct can act as a strong acid which can protonate the Pt-Me bond, eliminating methane and forming the proposed intermediate $[PtMe(bu_2bpy)]^+$ $[HOB(C_6F_5)_3]^-$ (48). The structure of the anion was identified by X-ray crystallography and NMR studies indicated that in the absence of a ligand L, the anion co-ordinates to the platinum providing the first example of a transition metal complex containing a co-ordinated $[HOB(C_6F_5)_3]^-$ (Scheme 2.15).

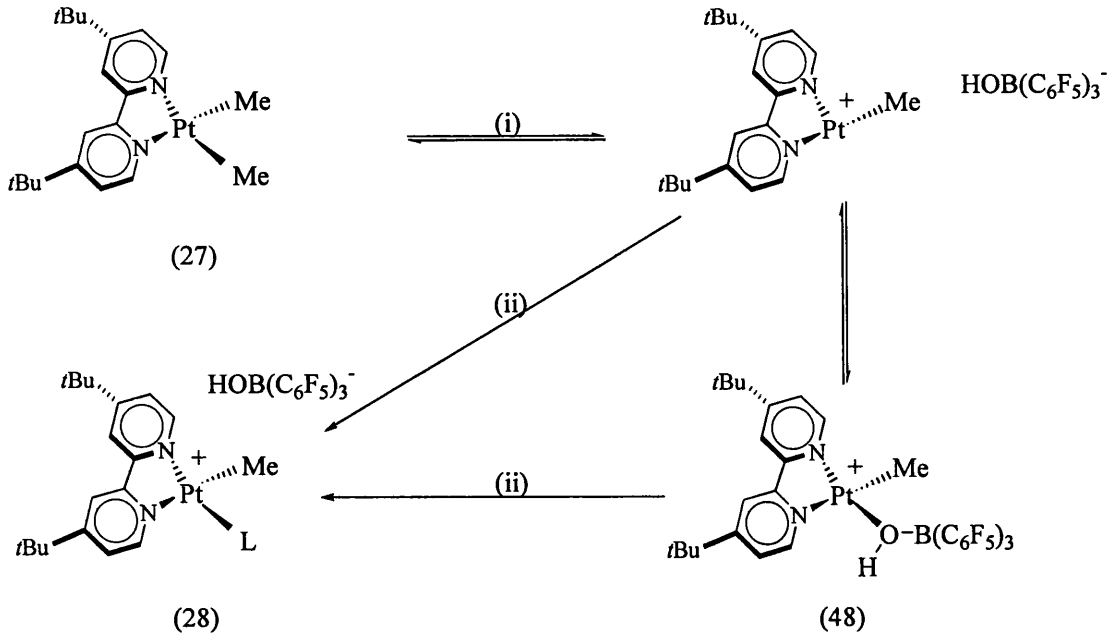

Scheme 2.15 *(i) $B(C_6F_5)_3 + H_2O \rightarrow H[HOB(C_6F_5)_3]$, $-CH_4$, (ii) L (where L=CO, C_2H_4 or PPh_3).*

In addition to this study, Siedle[85] has reported on the reactivity of the salt $[Et_3NH][(C_6F_5)_3BOH]$ made directly by reacting the adduct $[(H_2O)_2H_2O{\cdot}B(C_6F_5)_3]$ with Et_3N. Interestingly, the salt was shown to react with $[Cp_2ZrMe_2]$ (49) producing a catalyst capable of exhibiting polymerisation properties comparable to those produced by analogous perfluorinated boranes. In view of this, the chemistry of $B(C_6F_5)_3$ and H_2O is arguably an important study.

Preliminary investigations by Green[84] have shown that when $B(C_6F_5)_3$ reacts with H_2O in the presence of the metal base $[Ir(\eta\text{-}C_5H_5)(C_8H_{12})]$, a salt is formed containing the novel bi-nuclear anion $[(F_5C_6)_3B(\mu\text{-}OH)B(C_6F_5)_3]^-$. It was suggested that the bi-nuclear anion could be formed in two ways, firstly by the reaction of $B(C_6F_5)_3$ with $[HOB(C_6F_5)_3]^-$ or secondly by the reaction of $B(C_6F_5)_3$ with $H_2O{\cdot}B(C_6F_5)_3$ which undergoes ionisation (Scheme 2.16). However it is formed, it is

important to recognise that as the adduct can coexist with its conjugate base, the reactivity of these so called hydroxy-boranes could have significant relevance within catalytic applications and should therefore be explored further.

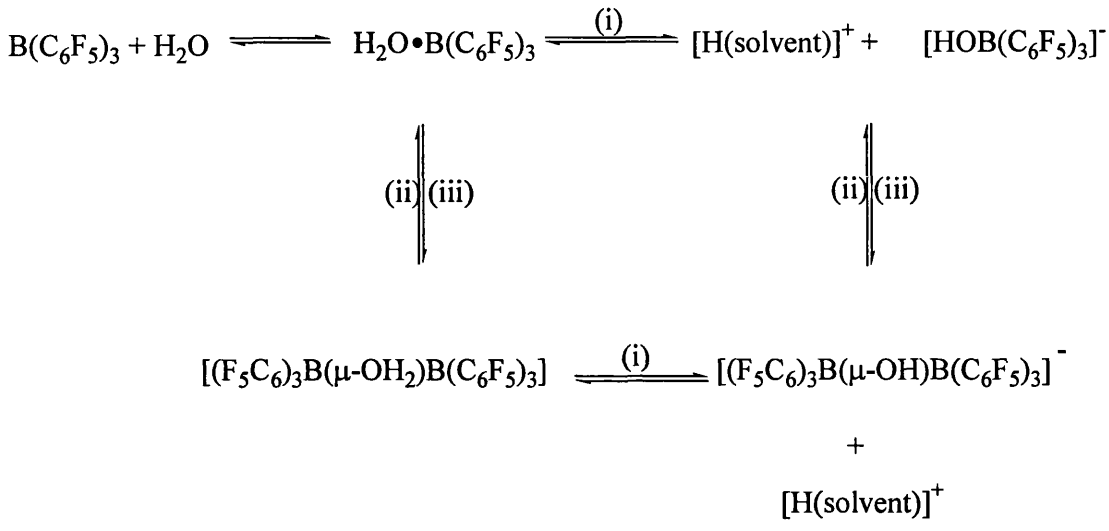

Scheme 2.16 *(i) solvent, (ii) -$B(C_6F_5)_3$, (iii) +$B(C_6F_5)_3$.*

2.6 Reactivity of Other Mono- and Bi-nuclear Perfluorophenyl Boranes

The significance of $B(C_6F_5)_3$ as a commercial co-catalyst has inspired researchers to synthesise other mono- and bi-nuclear perfluorophenyl boranes with the aim of adapting and applying their unique properties to other systems. Therefore, the synthesis of other fluorine substituted boranes, which at present are being extensively investigated, are vital to our understandings, not only within their role as commercial catalysts but also within selective anion-binding[86-89] and new materials.[90] The process of changing the number of electronegative boron substituents can be viewed as influencing the amount of electron density on the boron, hence, effectively altering the electrophilicity of the borane to suit its application.

Like $B(C_6F_5)_3$, the well established secondary borane bis(pentafluorophenyl)borane $[HB(C_6F_5)_2]$[91] has also been acknowledged to activate polymerisation when reacted with group IV metallocenes. However, unlike $B(C_6F_5)_3$, $HB(C_6F_5)_2$ is actually a dimer due to lack of π-bonding from the hydride ligand (Figure 2.2) and its main function is a hydroboration reagent, for example in the hydroboration of terminal alkynes (Scheme 2.17).

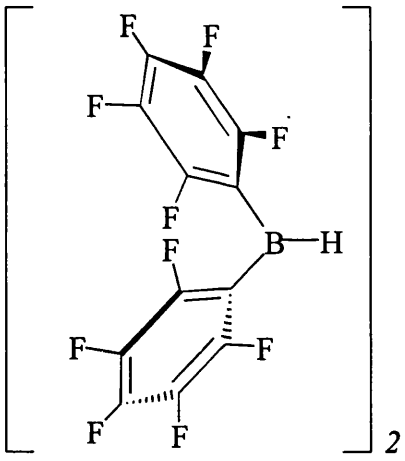

Figure 2.2 *Bis(pentafluorophenyl)borane.*

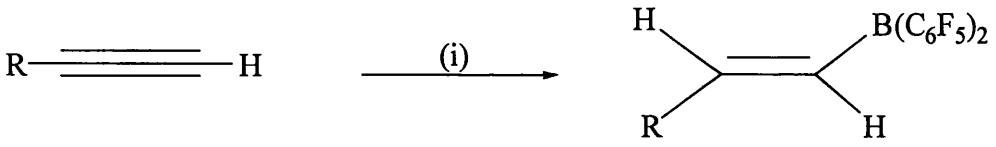

Scheme 2.17 *(i) $HB(C_6F_5)_2$.*

As discussed previously, one of the main reasons for investigating analogous compounds to $B(C_6F_5)_3$ is to identify their ability to function as co-catalysts. Therefore, the reactivity of $HB(C_6F_5)_2$ with simple group IV dialkyl metallocenes has been thoroughly investigated.[92,93] Interestingly, these studies have revealed that in the

course of these reactions a competing process occurs and the outcome of the reactions are solely dependent upon the reaction conditions *ie.* stoichiometry of $HB(C_6F_5)_2$ and solvent medium.

When the complex $[Cp_2ZrMe_2]$ (49) was reacted with $HB(C_6F_5)_2$ under a wide range of reaction conditions, the results were supportive of the theory that the reaction proceeds in two stages and that the first step is an alkyl/hydride exchange process (Scheme 2.18). It is the reactivity subsequent to this process that is dependent upon the reaction conditions. For example, when one equivalent of $HB(C_6F_5)_2$ is used in conjunction with toluene, a mixture of products is obtained. However, if four equivalents of $HB(C_6F_5)_2$ are used in the same solvent medium, one main product can be isolated. Mechanistic studies revealed that the alkyl/hydride exchange process is reversible and because there is an excess of $HB(C_6F_5)_2$ present, the Zr-H functions become trapped resulting in the formation of the bis-dihydridoborate complex $[Cp_2Zr\{(\mu\text{-}H)_2B(C_6F_5)_2\}_2]$ (50) (Scheme 2.18).

However, when one equivalent of $HB(C_6F_5)_2$ is used in conjunction with hexane, a clean reaction occurs resulting in the formation of the alkylidene complex $[Cp_2Zr(\mu\text{-}CH_2)(\mu\text{-}H)B(C_6F_5)_2]$ (51) and elimination of methane (Scheme 2.18). In this case, there is no excess of borane which allows the products of the alkyl/hydride exchange to react together with subsequent loss of alkane and incorporation of $HB(C_6F_5)_3$, to form the alkylidene complex.

Further reaction of (51) with $HB(C_6F_5)_2$ results in a mixture of products. One of the main products was identified to be the borate complex $[Cp_2Zr(\mu\text{-}H)_2\{CH_2(B(C_6F_5)_2)_2\}]$ (52). This is an intriguing complex as (51) has incorporated another equivalent of $HB(C_6F_5)_2$ facilitated by a penta-coordinated carbon. This is an

important study as it illustrates the dramatic influence reaction conditions can have. In this case it is the solvent medium which is the determining factor.

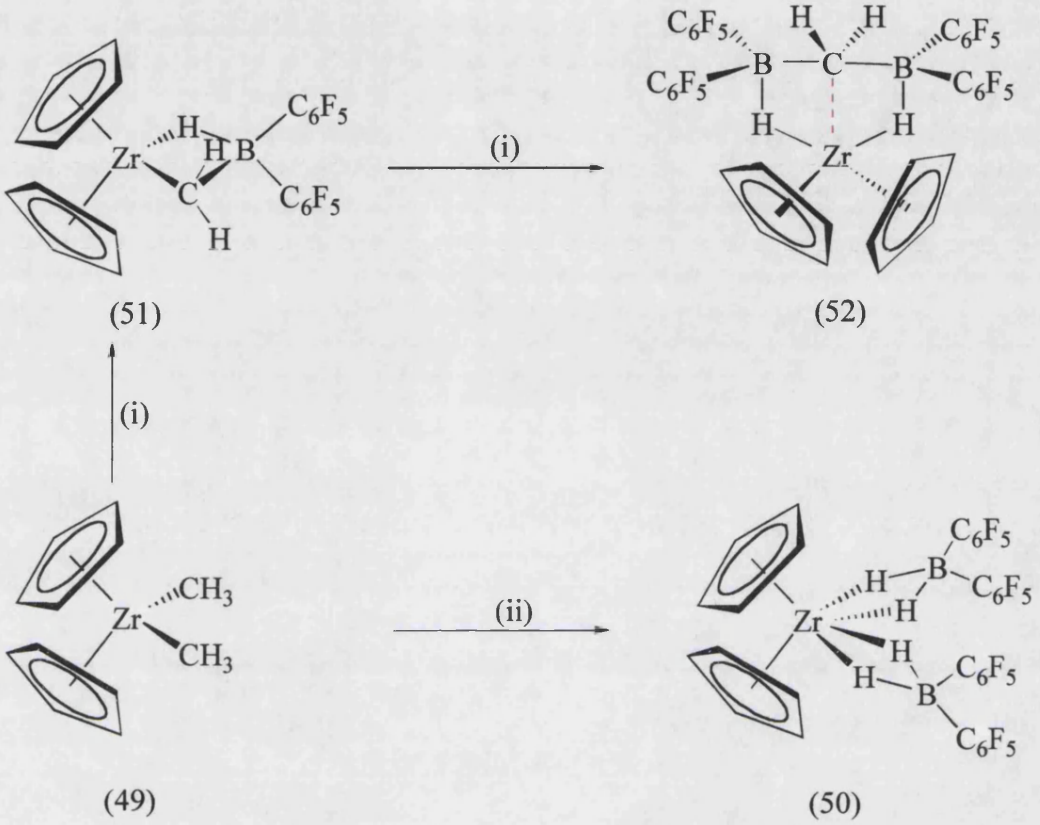

Scheme 2.18 *(i) $HB(C_6F_5)_2$, hexane, (ii) 4 $HB(C_6F_5)_2$, toluene, -2 $CH_3B(C_6F_5)_2$.*

Although major contributions to the catalytic applications have come from $B(C_6F_5)_3$ and even $HB(C_6F_5)_2$ there has been a steadily growing series of reports indicating that the non-coordinating anion tetrakis(pentafluorophenyl)borate $[B(C_6F_5)_4]^-$ [94] can also be effective within this area. It has generally been accepted that non-coordinating anions such as BPh_4^- do not behave as classical anions within Ziegler-Natta type catalysis due to the susceptibility of the phenyl groups to coordinate strongly to the electron deficient metal centre, promoting catalyst

deactivation. It is therefore surprising that the analogous $[B(C_6F_5)_4]^-$ anion is reported to show relatively weak or no noticeable interactions with electron deficient metal centres, enabling them to stabilise d^0 transition metal centres by acting as 'innocent' anions. The ability of $[B(C_6F_5)_4]^-$ to act so differently from its *proto* analogue is due to the fluoro substituents which induce basicity to the borane, effectively rendering any metal-aryl interactions and maintaining cation-anion interactions at a minimum.

Triphenylcarbenium tetrakis(pentafluorophenyl)borate $[Ph_3C]^+$ $[B(C_6F_5)_4]^-$ has been successfully reported to act as an alkyl abstractor when reacted with group IV metallocenes. The reaction proceeds with the trityl abstracting the methyl group so to generate the reactive species $[Cp_2ZrCH_3]^+$ $[B(C_6F_5)_4]^-$ (53), where there is no direct cation-anion interaction (Scheme 2.19). Therefore, it is clearly obvious that when $[B(C_6F_5)_4]^-$ is used in conjunction with cationic alkyl complexes they have the potential to co-activate olefin polymerisation, another system which is presently receiving growing attention.

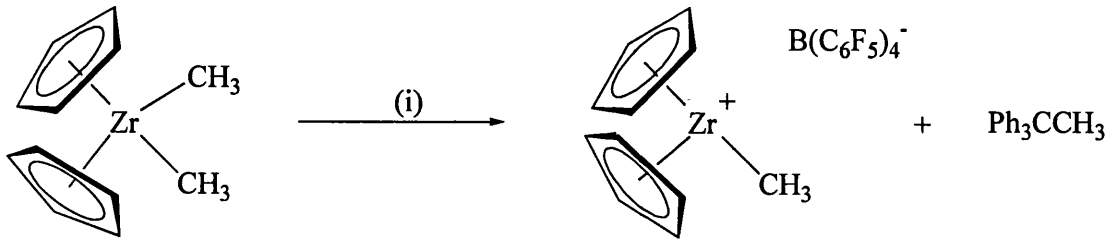

(49) (53)

Scheme 2.19 *(i) $[Ph_3C]^+[B(C_6F_5)_4]^-$.*

Like the boranes mentioned previously, the versatility of these species allows their adaptable properties to be applied to other systems. Lambert[95] is now exploring the potential of $[B(C_6F_5)_4]^-$ as a non-coordinating anion to assist in the generation of

the planar, three co-ordinate silylium cation, $[R_3Si]^+$. This species is known to exist in the gas phase but has not been stable in the liquid phase. It is thought that the use of an innocent anion such as $[B(C_6F_5)_4]^-$ will suitably enhance stability of the cation.

The latest development towards creating boranes as co-catalysts has engaged upon the rationale of synthesising bifunctional perfluoroaryl boranes of the general formula $(C_6F_5)_2B$-spacer-$B(C_6F_5)_2$. The term bifunctional proposes that such species will operate a dual role by providing counteranions much weaker than even non-coordinating anions such as $[B(C_6F_5)_4]^-$ at the same time, generating very reactive cationic species $[Cp_2MR]^+$, facilitated by dispersing the anion negative charge[96,97] through the hydrocarbon spacers. Diborane analogues of $B(C_6F_5)_3$ and $[B(C_6F_5)_4]^-$ have both been established[97] and their ability to activate metallocenes towards catalytic applications is at present being investigated.

Initially, these boranes were designed with bridging hydrides and then progressed towards hydrocarbon spacers[87,97] (A) (Figure 2.3). The latest advance is a bis(pentafluorophenyl)boryl tethered by a two-carbon perfluoro *ortho*-phenylene bridge (B) (Figure 2.3),[36] the idea being that a fully fluorinated backbone would enable the borane to be more resistant to proteolysis[84,85] and $-C_6F_5$ transfer.[98] Although the synthesis of such anions has proved very challenging, their properties have demonstrated that they can be clearly used within polymerisation applications and initial investigations claim that these diboranes can rival or even exceed the $B(C_6F_5)_3$ derived analogues.[97]

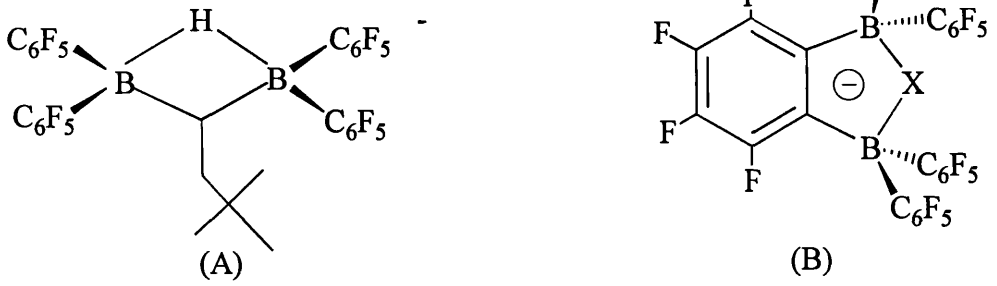

Figure 2.3

2.7 Conclusion

To summarise, the chemistry of perfluorophenyl substituted boranes is a highly abundant area of research covering many interesting applications. However, as this revival of interest towards these compounds has only taken place within the last decade, it is exciting to think what the future holds for such versatile compounds. Throughout this introduction it is clear that it is within the homogeneous polymerisation of olefins that the fundamental application of these boranes lies. Nevertheless, it is suggested that their unique properties can be adapted for a number of developing systems.

The ability of these boranes to stabilise electron deficient metal centres in a variety of different ways is a highly desirable property. As discussed in this chapter, the boranes can utilise a fluorine atom lone pair, a methyl bridge, a three centre two-electron μ-hydride and even the π-system from one of the rings. The attractive feature concerning their adaptability is the manner in which they can switch between bonding modes, facilitating a wide range of intermediates and kinetic/thermodynamic products.

Piers and Chivers[32] quoted in their review how the emergence of $B(C_6F_5)_3$ has now progressed from 'obscurity to applications'. These applications are now

increasing with the emphasis of unravelling and exploiting these obscurities. It is rewarding to know that the chemistry reported in this thesis (Chapter Four) has also unravelled one of the obscurities of $B(C_6F_5)_3$, a small but significant contribution to the ongoing investigations into perfluorophenyl substituted boranes.

CHAPTER THREE

SYNTHESIS AND REACTIVITY OF KETO-SUBSTITUTED π-ALLYLIC MOLYBDENUM COMPLEXES

3.1 Introduction

This chapter is concerned with the chemistry of molybdenum complexes which contain keto-substituted π-allylic fragments. Two systems have been investigated, the *anti*-aldehyde substituted η^3-allylic complex [Mo{η^3-$CH_2CHCH(CHO)$}$(CO)_2$(L)] [where L = η-C_5H_5 (54) or η-C_5Me_5 (55)] and the η^3-γ-lactonyl complex [Mo{η^3-CHCHCH(O)CO}$(CO)_2$(L)] [where L = η-C_5H_5 (56), η-C_5Me_5 (57) or η^5-C_9H_7 (58)] (Figure 3.1). Both systems undergo reactions when treated with nucleophiles and a rationalisation of these observations has been obtained through an examination of the charge and orbital contribution of both systems, both of which were obtained through Extended Hückel Molecular Orbital[99] (EHMO) calculations.

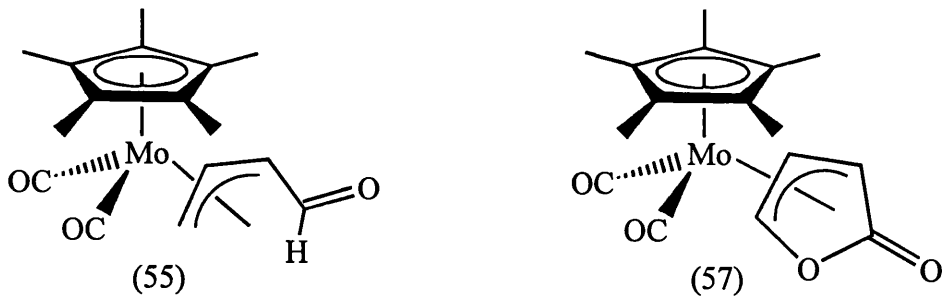

Figure 3.1

3.2 Synthesis and Reactivity of the *anti*-Aldehyde Complex [Mo{η^3-$CH_2CHCH(CHO)$}$(CO)_2$(L)] [where L = (η-C_5H_5) or (η-C_5Me_5)]

Due to continued interest in the use of transition metal fragments to control and direct chemical transformations at co-ordinated organic centres, much progress has been made with reactions based on the [Mo(η^3-allyl)$(CO)_2$(η-C_5H_5)] system.[100-102] Most of these studies were concerned with alicyclic molecules with the exception of

Liu[103,104] and co-workers, who investigated the reactivity of *syn*-substituted functional groups, *e.g.* [Mo{η^3-*syn*-$CH_2CHCH(CHO)$}$(CO)_2(\eta$-$C_5H_5)$]. Therefore, our first objective was to devise a selective pathway to the related *anti*-aldehyde substituted systems and then to explore their reactivity.

A possible selective pathway to the *anti*-aldehyde complexes had already been identified by Benyunes[105] whilst studying the protonation of *syn*- and *anti*-4-oxo-functionalised allyls, prepared from 1-trimethylsilyloxy-1,3-dienes (Scheme 3.1). This study indicated that protonation of the *syn*-4-oxo functionalised π-allyl [Mo{η^3-$CH_2CHCH(CHO)$}$(CO)_2(\eta$-$C_5H_5)$] (59a and 59b) with $HBF_4{\cdot}OEt_2$, could generate under kinetic control, a 1-hydroxy-substituted η^4-*s-trans*-1,3-diene (60a and 60b). At room temperature, (60a and 60b) isomerise into the corresponding 1-hydroxy-substituted η^4-*s-cis*-1,3-diene complex (61a and 61b), which when deprotonated with triethylamine, affords selectively the *anti*-aldehyde substituted system (54a and 54b). However, a disadvantage with this method is that the combined yields of the *syn*- and *anti*-aldehyde complexes are relatively low. Therefore, it was decided that an alternative procedure needed to be developed for the selective synthesis of the *anti*-aldehyde system.

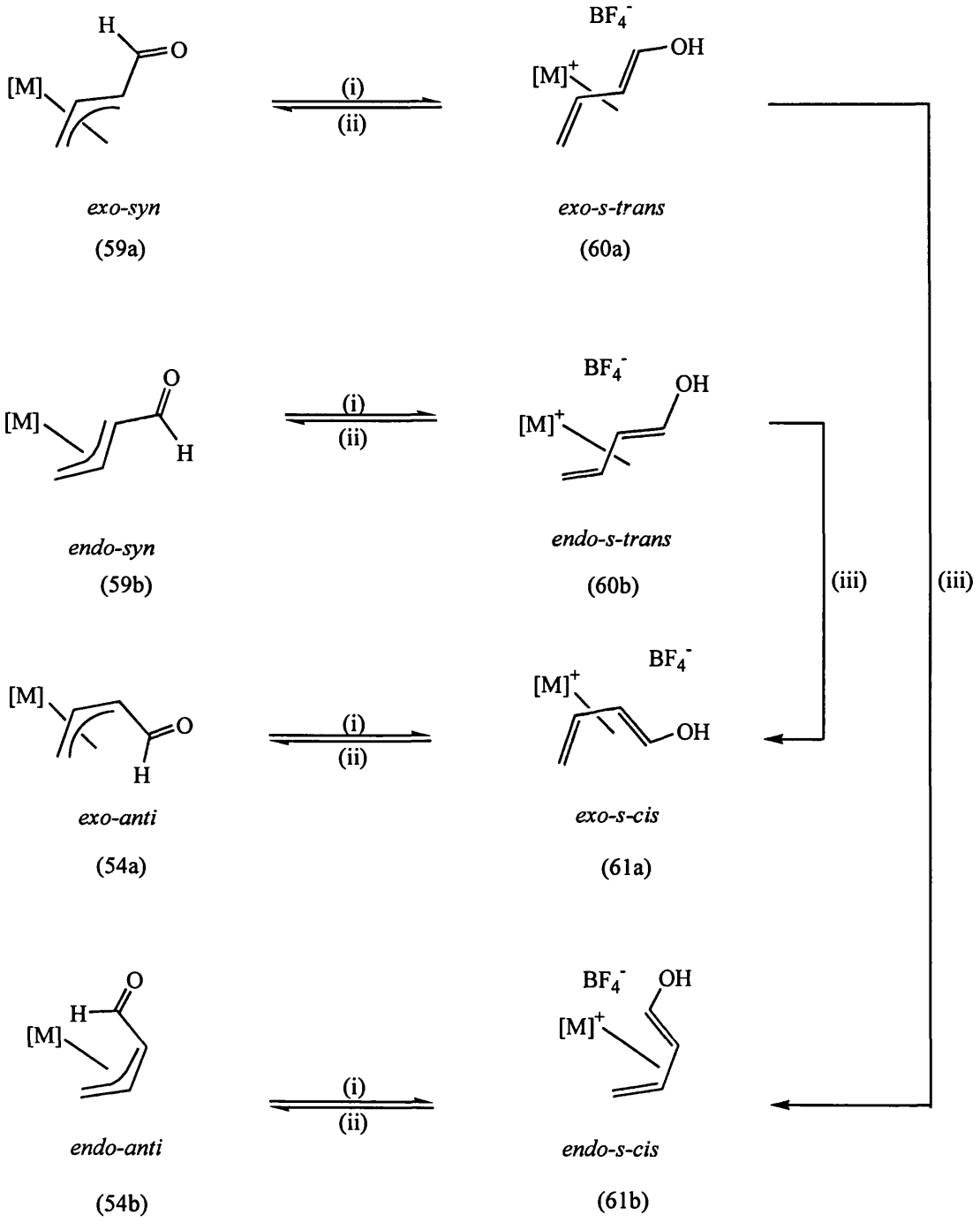

Scheme 3.1 *(i) $HBF_4{\cdot}OEt_2$, (ii) Et_3N, (iii) room temperature (where [M] = $Mo(CO)_2L$, and L = η-C_5H_5 or η-C_5Me_5).*

The idea for the new synthetic approach was based upon the assumption that if the kinetic product of the reaction of 1-trimethylsilyloxybuta-1,3-diene with a cationic bis(acetonitrile) complex is a η^4-*s-trans*-1,3-diene complex, the *syn*-aldehyde substituted η^3-allyl must be formed by a rapid desilylation reaction (Scheme 3.2). However, it was realised that the formation of the *anti*-aldeyhde substituted complex required a change in the bonding mode of the 1,3-diene from η^4-*s-trans* to η^4-*s-cis*, which needed to compete with the desilylation of the η^4-*s-trans*-trimethylsilyloxy-1,3-diene cation. Therefore, it was thought that by using an oxy-substituent on the 1,3-diene, which was less labile then the Me_3SiO system, there might be more time for complete *trans*- to *cis*-isomerisation to occur which would allow the *anti*-aldehyde substituted η^3-allyl complex to be formed selectively.

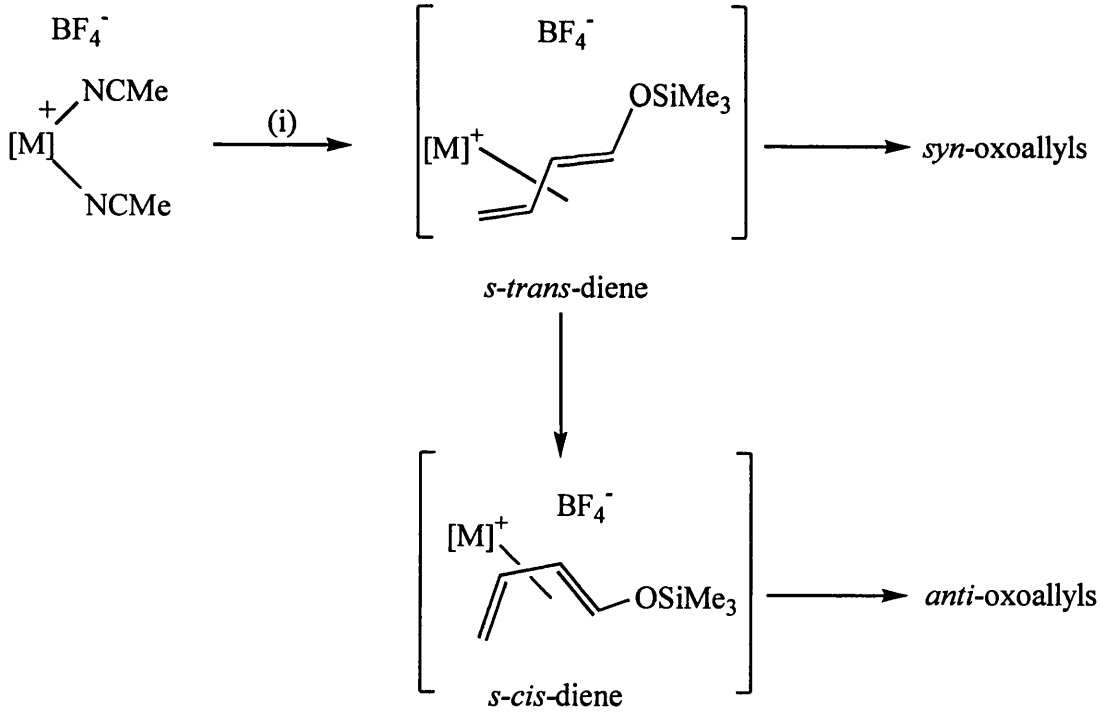

Scheme 3.2 *(i) 1-trimethylsilyloxybuta-1,3-diene (where [M] = $Mo(CO)_2L$, and L = η-C_5H_5 or η-C_5Me_5).*

Preliminary experiments by Butters[106] suggested that the problem might be solved by replacing the $OSiMe_3$ group with an $CH_3C(O)O$ substituent. Therefore, the starting point for this investigation was to extend these observations. Specifically, an excess of 1-acetoxybuta-1,3-diene was added to a solution of $[Mo(NCMe)_2(CO)_2(\eta\text{-}C_5H_5)][BF_4]$ (62) and the mixture was stirred at room temperature for 4 days, at which point the formation of a new product and the consumption of the starting material was observed by IR spectroscopy. The resulting reaction mixture was filtered *via* cannula and the solid washed with pentane. Removal of the solvent *in vacuo* afforded a yellow powder in good yield (85 %) which was identified by NMR spectroscopy and microanalysis as *s-cis*-$[Mo(\eta^4\text{-}CH_2CHCHCHOAc)(CO)_2(\eta\text{-}C_5H_5)][BF_4]$ (63) (Scheme 3.3).

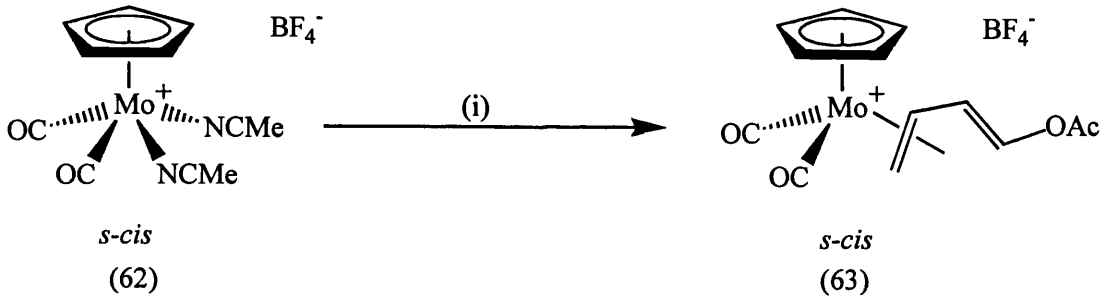

s-cis (62) *s-cis* (63)

Scheme 3.3 *(i) 1-acetoxy-1,3-butadiene.*

An aqueous solution of $NaHCO_3$ was then added to the cationic complex (63) which was stirred vigorously at room temperature for 0.5 hr. The organic layer was then separated from the mixture and dried. The organic extract was purified by chromatography and recrystallisation, which afforded selectively, the *anti*-aldehyde complex *exo-anti*-$[Mo\{\eta^3\text{-}CH_2CHCH(CHO)\}(CO)_2(\eta\text{-}C_5H_5)]$ (54) in good yield (87 %) (Scheme 3.4). This was identified by micro analysis, IR and NMR spectroscopy.

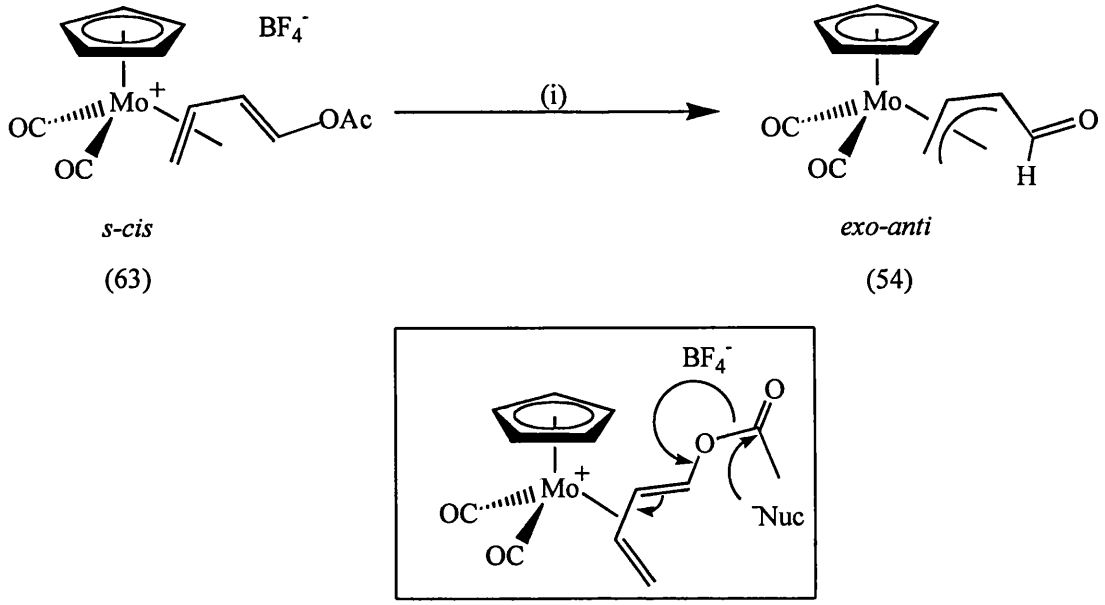

Scheme 3.4 *(i) $NaHCO_3$ (aq.), pH = 8.5.*

Preparation of the η^5-pentamethylcyclopentadienyl analogue followed a similar procedure, however, conversion to the cationic acetoxy-substituted η^4-diene appeared comparably slower to the cyclopentadienyl system. As expected, the reaction of $NaHCO_3$ with *s-cis*-[Mo(η^4-$CH_2CHCHCHOAc$)$(CO)_2$(η-C_5Me_5)][BF_4] (64) afforded *exo-anti*-[Mo(η^3-$CH_2CHCHCHO$)$(CO)_2$(η-C_5Me_5)] (55) in good yield (81 %). The molecular structure was determined by X-ray crystallography (Figure 3.2).

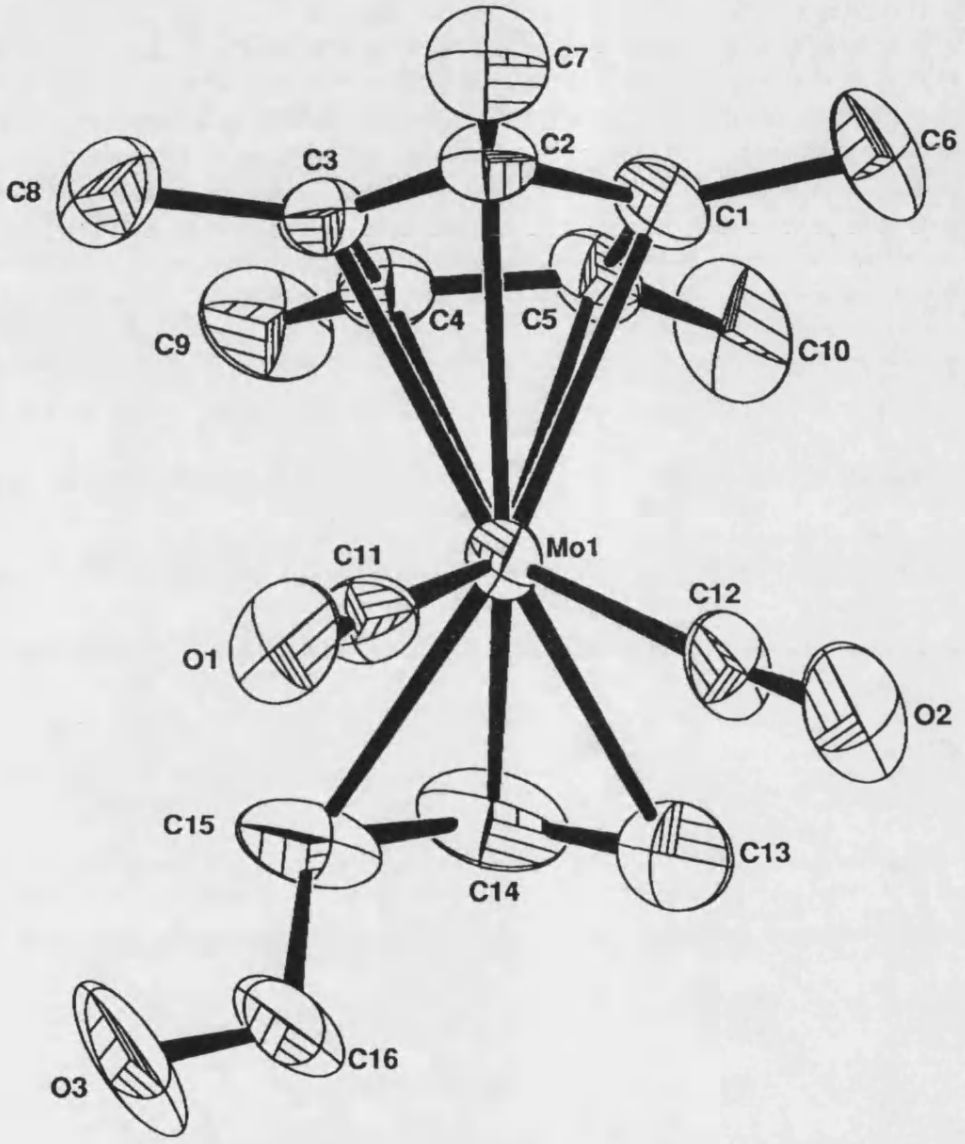

Figure 3.2 *X-ray crystal structure of the complex exo-anti-[Mo{η³-$CH_2CHCH(CHO)$}$(CO)_2$(η-C_5Me_5)] (55).*

Mo-C(1)	2.339(10)	Mo-C(2)	2.319(11)
Mo-C(3)	2.322(10)	Mo-C(4)	2.366(10)
Mo-C(5)	2.373(10)	Mo-C(11)	1.915(17)
Mo-C(12)	1.971(16)	Mo-C13)	2.303(14)
Mo-C(14)	2.176(13)	Mo-C(15)	2.297(13)
C(11)-O(1)	1.153(17)	C(12)-O(2)	1.126(15)
C(13)-C(14)	1.401(18)	C(14)-C(15)	1.439(20)
C(15)-C(16)	1.555(21)	C(16)-O(3)	1.246(23)
Mo-C(11)-O(1)	174.7(13)	Mo-C(12)-O(2)	174.7(16)
C(11)-Mo-C(12)	80.4(7)	C(13)-C(14)-C(15)	123.5(12)
C(14)-C(15)-C(16)	121.7(14)	C(15)-C(16)-O(3)	125.4(16)

Table 3.1 *Selected bond lengths (Å) and angles (°) for complex (55) with estimated standard deviations (e.s.d.s) in parentheses.*

Having established an efficient method for the preparation of these complexes, the reactivity of the aldehydic functionality towards nucleophiles was studied. Complex (54) was treated with an excess of $NaBH_4$ in MeOH and the reaction monitored by IR spectroscopy. After 0.5 hr there was an indication of complete consumption of the starting material. After chromatographic work-up a yellow crystalline solid was isolated. NMR spectroscopy and micro analysis indicated that a reduction of the aldehydic functionality had occurred, giving the hydroxyallyl complex *exo-anti*-[Mo(η^3-$CH_2CHCHCH_2OH$)$(CO)_2$(η-C_5H_5)] (65) in good yield (65 %). The reaction proceeds *via* nucleophilic attack by the nucleophile, H^-, on the *exo*-face of the oxoallyl, which is followed by rotation of the C-C bond to give the less sterically demanding product (Scheme 3.5).

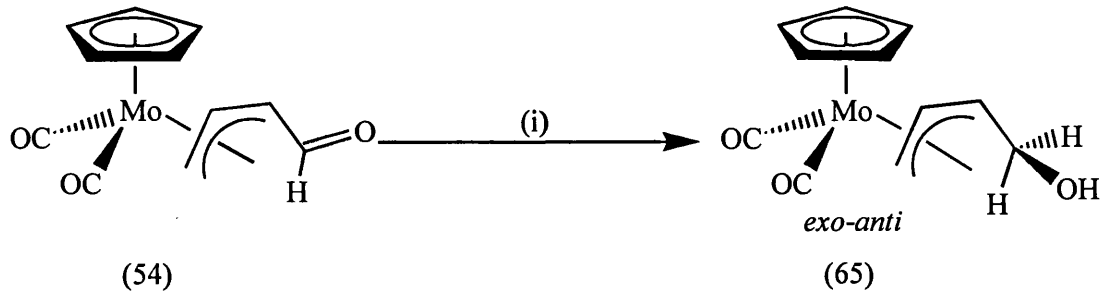

(54) (65)

Scheme 3.5 *(i) $NaBH_4$, MeOH, 0.5 hr.*

Butters[106] found that on stirring (54) and $NaBH_4$ in MeOH for a prolonged period of time after the initial 0.5 hr, the gradual formation of an additional product could be identified by TLC. After 30 hr, total consumption of (65) had occurred and a new product was identified by NMR spectroscopy and X-ray crystallography to be the methoxyallyl complex *exo-anti*-[Mo(η^3-$CH_2CHCHCH_2OMe$)$(CO)_2$(η-C_5H_5)], (66) (Scheme 3.6).

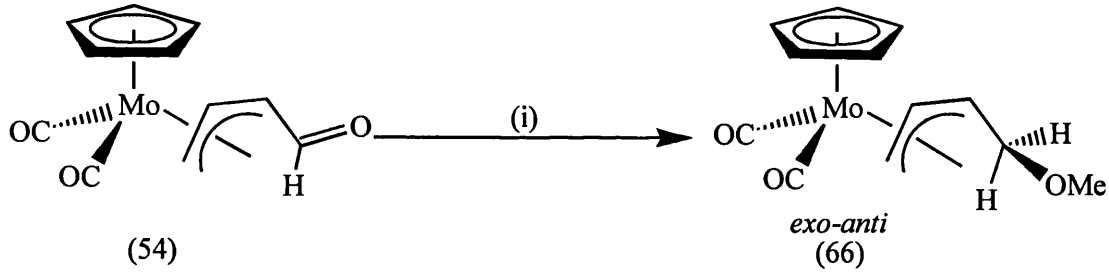

(54) (66)

Scheme 3.6 *(i) $NaBH_4$, MeOH, 30 hr.*

An explanation for these observations (Scheme 3.7) is that the newly formed hydroxyallyl complex (65) is susceptible to electrophilic attack by BH_3, which has been generated *in-situ* from $NaBH_4$. Therefore, electrophilic attack occurs at the oxygen atom of the hydroxyl moiety, which results in the rapid elimination of $[HOBH_3]^-$ and the formation of the η^4-diene cation (67). This cation readily reacts

with nucleophiles, hence, in the presence of $[MeO]^-$, nucleophilic addition takes place at the terminus of the 1,3-diene which leads to the formation of the methoxyallyl product (66). These reactions were also carried out by Butters[106] on the η^5-pentamethylcyclopentadienyl system and the products were also afforded in good yield.

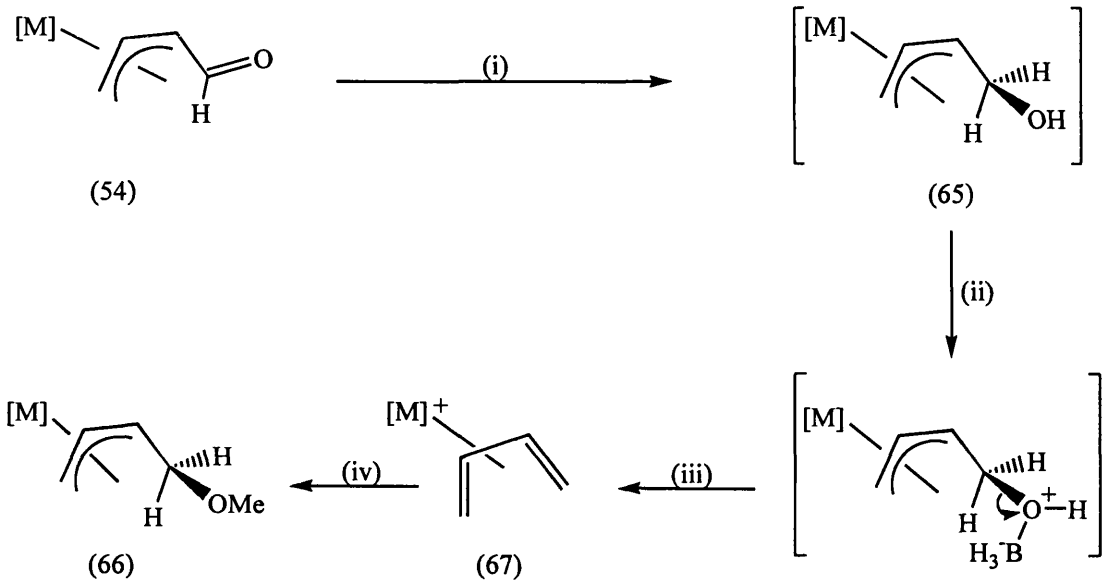

Scheme 3.7 *(i) $NaBH_4$, MeOH, 30 hr, (ii) BH_3, (iii) -$HOBH_3^-$ (iv) ^-OMe (where [M] = $Mo(CO)_2(\eta\text{-}C_5H_5)$).*

Referring to the reaction for the formation of the primary product (65) and the analogue *exo-anti*-$[Mo(\eta^3\text{-}CH_2CHCHCH_2OH)(CO)_2(\eta\text{-}C_5Me_5)]$ (68), these results can be rationalised by using the bond parameters derived from the X-ray crystal structure of complex (55) (Figure 3.2) for an EHMO calculation. As shown in Figure 3.3 and Table 3.1, this established the composition of the lowest unoccupied molecular orbital (LUMO), suggesting that if the reaction proceeds under frontier molecular orbital (FMO) control then the reaction would occur at C(16).

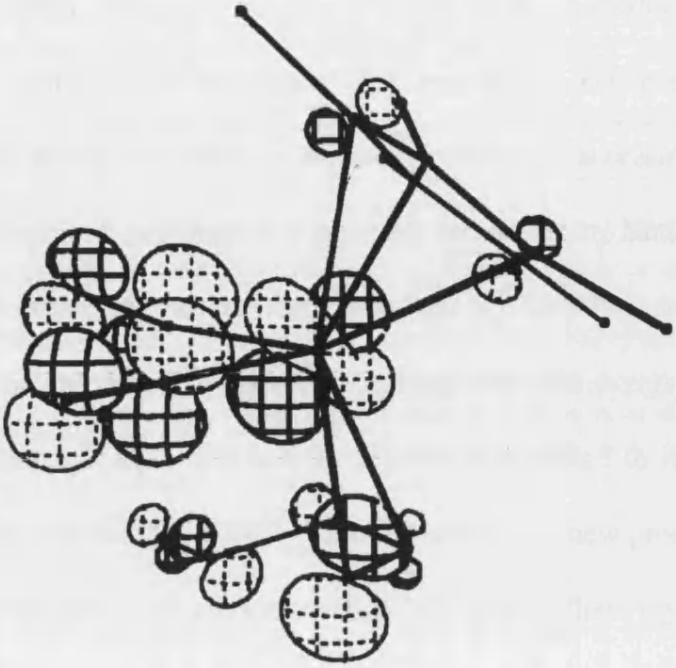

HOMO

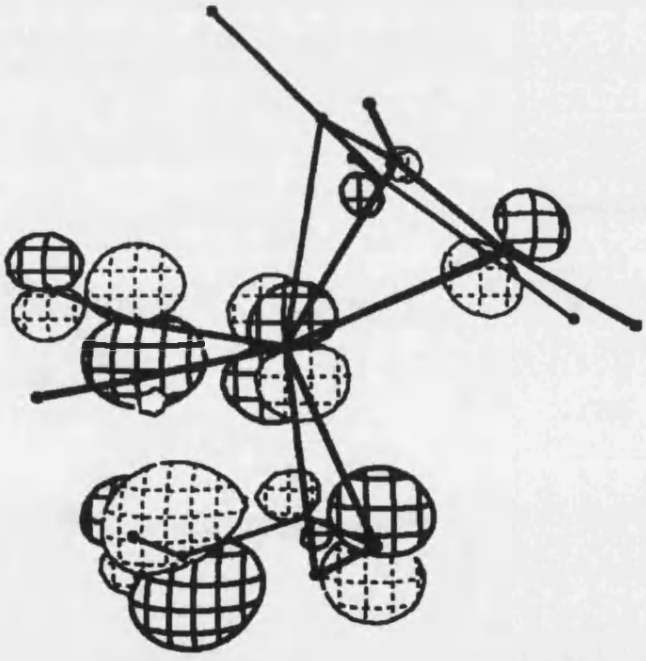

LUMO

Figure 3.3 *Representations of the theoretical HOMO and LUMO orbitals for* $[Mo\{\eta^3\text{-}HC(O)CHCHCH_2\}(CO)_2(\eta\text{-}C_5Me_5)]$ *(55).*

The reaction discussed proved to be an efficient method of reducing the aldehyde functionality for complexes (54) and (55). However, we were also interested in reversing the reduction, with the intention of accessing keto-substituted η^3-allyl complexes. A preliminary experiment carried out by Butters[106] involved the attempted oxidation of (69) to the corresponding ketoallyl complex under the conditions of an Oppenauer[107] oxidation (Scheme 3.8). An excess of aluminium tri-isopropoxide was added to (69) and the mixture was heated to reflux for 5.5 hr at which point IR spectroscopy indicated the formation of a new product. The mixture was chromatographed and recrystallisation afforded yellow crystals which were identified by X-ray crystallography to be the *exo-anti*-η^3-pentadienyl complex *exo-anti*-[Mo(η^3-$CH_2CHCHCHCH_2$)$(CO)_2$(η-C_5H_5)] (70). Therefore, it was evident that the ketoallyl product could not be accessed *via* this oxidation method as the conditions allow a competing elimination reaction to predominate.

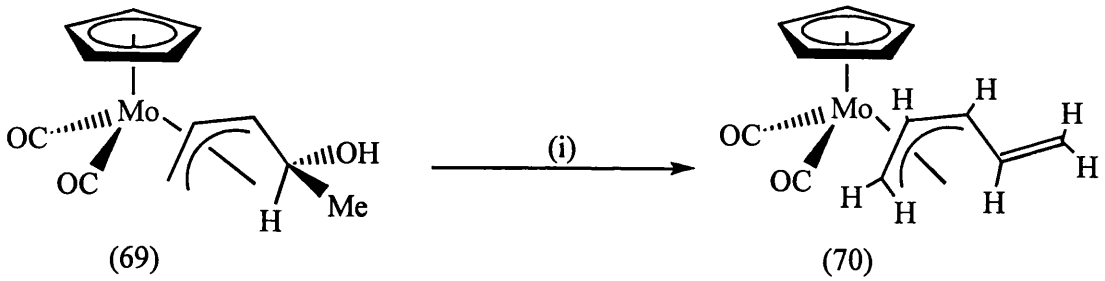

(69) (70)

Scheme 3.8 *(i) $Al(O^iPr)_3$, acetone, toluene, heat.*

This failure to convert (69) to the corresponding ketoallyl complex and the failure to convert (65) back to (54) with the Swern[108] oxidation procedure was very disappointing. Therefore, we were interested in using the Ley-Griffith[109] reagent, [tetra-n-butylammonium perruthenate (Bu^n_4N)(RuO_4)] which has been used as a mild

catalytic oxidant and has been used in conjunction with *N*-methylmorpholine *N*-oxide to convert alcohols to aldehydes and ketones. The ability of the reagent to avoid competitive side reactions, be selective and easy to use offered an attractive alternative to other methods previously tried.

This proved to be a successful approach. An excess of morpholine *N*-oxide was added to a solution of (65) at room temperature. After 10 minutes, a catalytic amount of the ruthenium reagent was added to the solution and the reaction was monitored by IR spectroscopy and allowed to stir for 10 hr. After this period of time the reaction mixture was diluted with CH_2Cl_2 and washed with a sodium sulphite solution. The organic layer was extracted and dried over Na_2SO_4. After the volatiles had been removed *in vacuo*, the residue was extracted with CH_2Cl_2 and filtered then chromatographed on alumina. A single yellow band was eluted and the reaction was successful as this was identified to be the *anti*-aldehyde complex (54) which was obtained in good yield (60 %) (Scheme 3.9). Therefore, the ruthenium reagent proved to be an efficient method of selectively oxidising an alcohol without destroying the relatively sensitive metal complex.

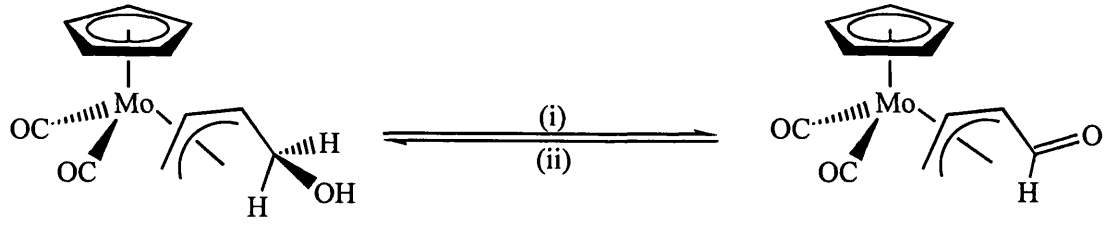

(65) (54)

Scheme 3.9 *(i) $NaBH_4$, MeOH, (ii) $[Bu^n_4N][RuO_4]$, morpholine-N-oxide, CH_2Cl_2.*

Preliminary experiments indicated that the Ley-Griffiths ruthenium reagent can also be used to oxidise alcohols such as [Mo{η^3-*exo-anti*-$CH_2CHCHCH(OH)Me$}$(CO)_2(\eta$-$C_5H_5)$] (69) to the corresponding *anti*-keto-substituted η^3-allyl complexes and this chemistry is presently being explored.

3.3 Reaction of the η^3-γ-Lactonyl Complex [Mo{η^3-OC(O)CHCHCH}$(CO)_2$(L)] (where L = η-C_5H_5, η-C_5Me_5 or η^5-C_9H_7) with Nucleophiles

The discovery of the novel η^3-γ-lactonyl complexes [Mo{η^3-OC(O)CHCHCH}$(CO)_2$(L)] [where L = η-C_5H_5 (56), η-C_5Me_5 (57) or η-C_9H_7) (58)] by Butters[110] had been the result of a study into establishing a series of furanyl-derived π-complexes of molybdenum. The initial approach had focused on the direct complexation of furan to a $[Mo(CO)_2(\eta$-$C_5H_5)]^+$ fragment and it had been expected that the reaction of *cis*-$[Mo(NCMe)_2(CO)_2(\eta$-$C_5H_5)][BF_4]$ (62) with an excess of furan would cause the replacement of the labile acetonitrile ligands and yield the desired η^4-furan complex. However, after several failed attempts including refluxing the mixture and attempting to access the furan-derived π-complex through protonation of the η^3-allyl complex $[Mo(\eta^3$-$C_3H_5)(CO)_2(\eta$-$C_5H_5)]$ (71), a solution to the problem was discovered.

It was found that in order to establish a facile ligand substitution reaction, a silyl-substituted furan appeared to be the key. Room temperature addition of an excess of 2-(trimethylsilyloxy)furan to a dichloromethane solution of *cis*-$[Mo(NCMe)_2(CO)_2(\eta$-$C_5Me_5)][BF_4]$ (72) resulted in the formation of the novel η^3-γ-lactonyl complex [Mo{η^3-OC(O)CHCHCH}$(CO)_2(\eta$-$C_5Me_5)$] (57) (Scheme 3.10),

which was structurally characterised by X-ray crystallography, the reaction proceeding *via* a fluoride-anion-induced desilylation mechanism.

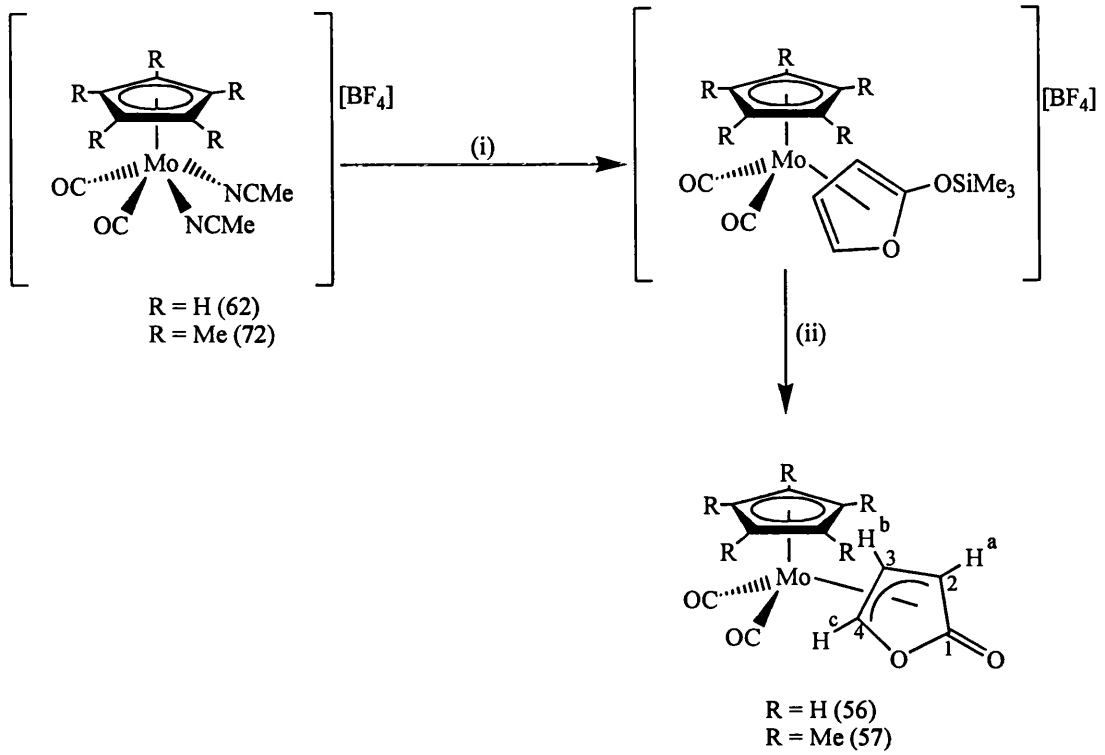

Scheme 3.10 *(i) 2-(trimethysilyloxy)furan, CH_2Cl_2, 25 °C, (ii) -Me_3SiF (where R = H, Me).*

In continuing our investigations into the chemistry of η^3-bonded allyl substituted complexes we were interested in exploring the reactivity of the novel η^3-γ-lactonyl complex (56). It was clearly important to establish whether a related chemistry could be developed to that of the *anti*-aldehyde complexes (54) and (55), since the structural identity of these complexes is fairly similar with the η^3-γ-lactonyl complexes containing a five-membered heterocyclic ring, which contains an oxygen atom instead of a hydrogen in position 5 of the bound organic fragment. This prompted us to treat the lactonyl complexes with nucleophilic reagents to investigate

whether overall addition of the nucleophile would be at the carbonyl carbon atom which was found for (54) and (55).

Butters[110] had carried out some preliminary reactions to study the reactivity of the lactone complexes towards nucleophilic addition, in which a series of amine nucleophiles as investigated (Schemes 3.11-3.13). Complex (57) and the analogous η^5-indenyl system (58) were reacted with 2 molar equivalents of benzylamine. The reaction afforded a bright yellow powder in good yield (85 %). NMR and micro analysis both indicated that the product (73) was a 1:1 adduct of benzylamine and (58). However, repeating the reaction by using only 1 molar equivalent of benzylamine led to a surprising decrease in yield (8 %). This observation was interesting as an X-ray structure carried out on (73) confirmed that the complex was zwitterionic and a 1:1 adduct. The structure also revealed that the course of the reaction was a lactone ring-opening reaction (Scheme 3.11). Further studies indicated that varying the amine allowed the reaction to proceed in a similar fashion (Schemes 3.12 - 3.13).

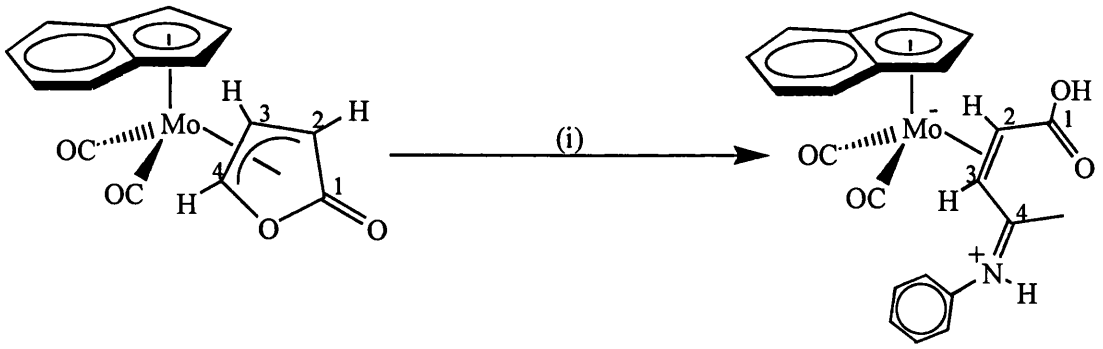

(58) (73)

Scheme 3.11 *(i) 2 equivalents benzylamine, CH_2Cl_2, 25 °C.*

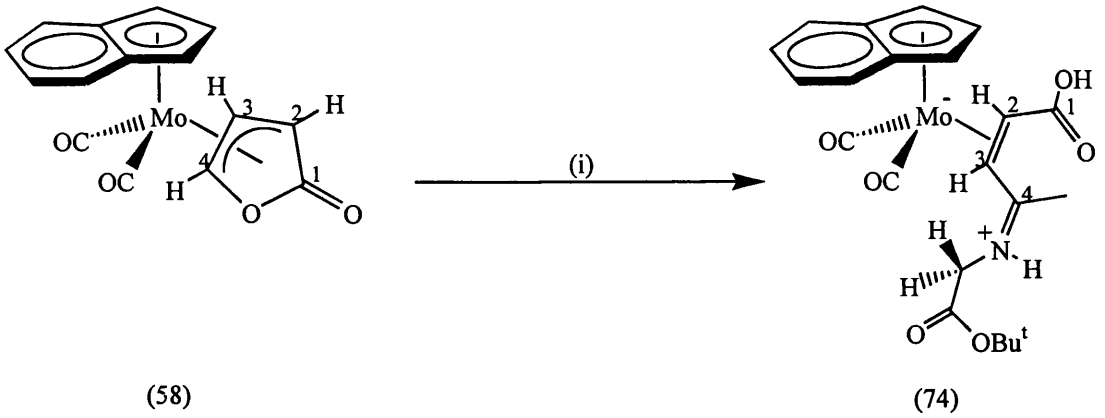

Scheme 3.12 *(i) glycine tert-butyl ester hydrochloride, NEt_3, CH_2Cl_2, 25 °C.*

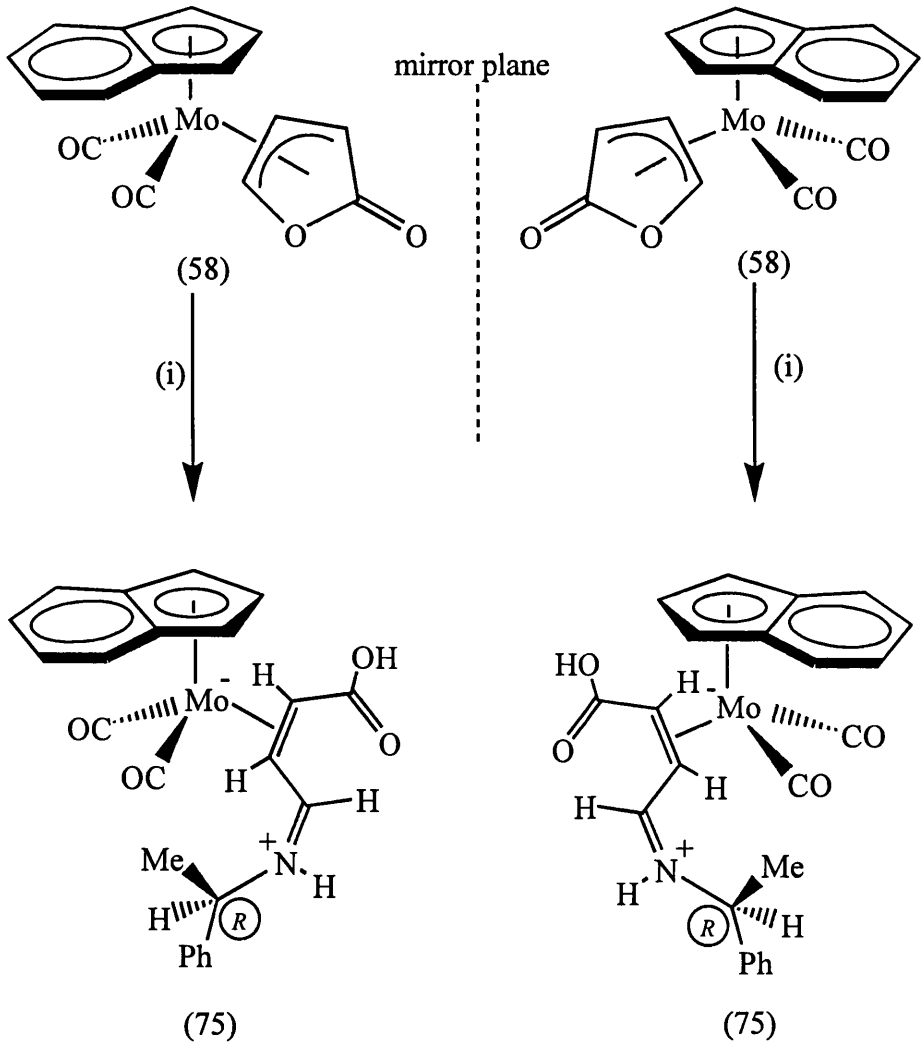

Scheme 3.13 *(i) (R)-α-methylbenzylamine, CH_2Cl_2, 25 °C. 1:1 mixture of the (R,R/S) and (R,S/R) diastereomers due to the lactone complex being chiral at the metal centre.*

Therefore, the initial study of the reactions of these η^3-γ-lactonyl complexes with nucleophiles had generated 1:1 adducts which were the result of a lactone ring opening process. However, the mechanistic pathway to these adducts proved interesting for two reasons. Firstly, the reaction appeared to afford a better yield using 2 molar equivalents of amine. Secondly, it was predicted that nucleophilic attack would occur on the lactone carbonyl carbon but the adducts didn't appear to have the structure expected on the basis of this assumption. Therefore it was suggested that an Extended Hückel Molecular Orbital (EHMO) calculation[99] (Figure 3.5) using the bond parameters that were established by X-ray crystallography for complex (57) may provide an insight into the mechanism. Representations of the theoretical Highest Occupied Molecular Orbital (HOMO) and LUMO were also obtained (Figure 3.4).

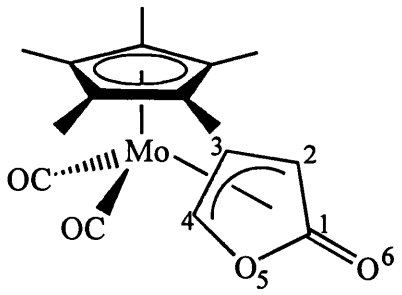

(57)

C^1	+1.180	O^5	-0.753
C^2	-0.107	O^6	-1.131
C^3	-0.078	Mo	+1.106
C^4	+0.404		

Figure 3.4 *Relative charge distribution for compound (57).*

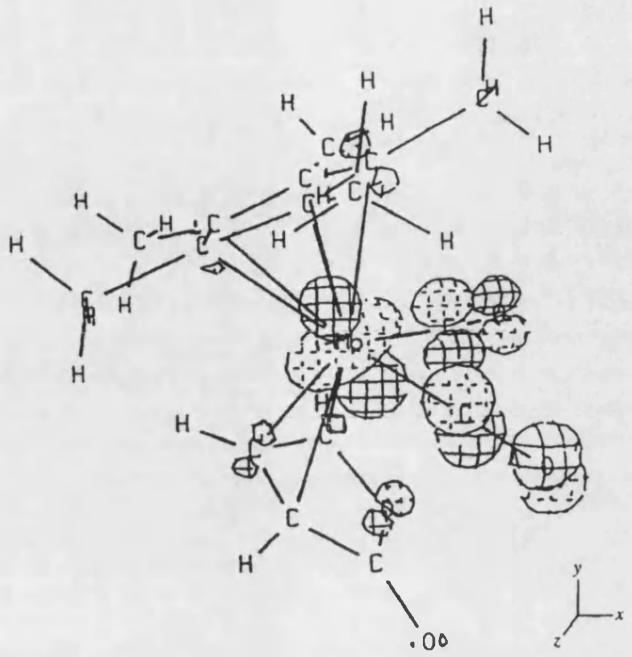

HOMO

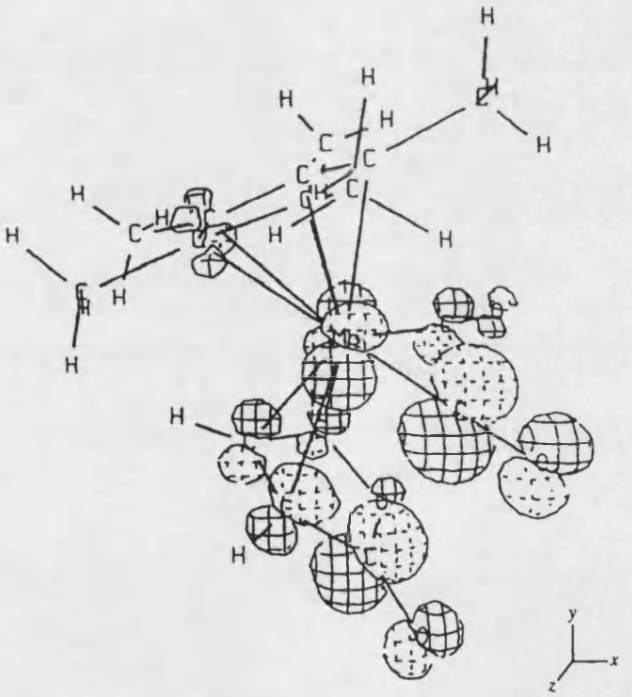

LUMO

Figure 3.5 *Representations of the theoretical HOMO and LUMO orbitals for* $[Mo\{\eta^3\text{-}OC(O)CHCHCH\}(CO)_2(\eta\text{-}C_5Me_5)]$ *(57).*

The EHMO calculations indicated that there are two areas which display a high degree of localised positive charge: Firstly, the lactone carbonyl carbon which has a localised charge of +1.18 and secondly the molybdenum metal centre which has a charge of +1.10. Consequently, there was good reason to believe that nucleophilic addition could also be FMO controlled.. Therefore, it was suggested that initial attack by the amine nucleophiles was taking place at the molybdenum metal centre rather than the carbonyl carbon and this is facilitated by the high positive charge and by the availability of the suitable LUMO.

Thus, the first stage of the reaction path involves attack at the molybdenum metal centre by the nucleophile which then causes a slippage of the bonding mode of the lactone from η^3 to η^1. The co-ordinated amine is then deprotonated by a second molecule of amine resulting in the formation of an anionic species, which rapidly forms an anionic η^2-alkene-substituted intermediate *via* reductive elimination and transfer of the amido moiety on to C^4. The final stage of the mechanism is initiated by an electron redistribution facilitated by the nitrogen lone pair which results in cleavage of the ring followed by proton transfer from $[NH_3R]^+$ to the carbonyl oxygen resulting in the formation of the zwitterionic η^2-olefinic complex (73) (Scheme 3.14).

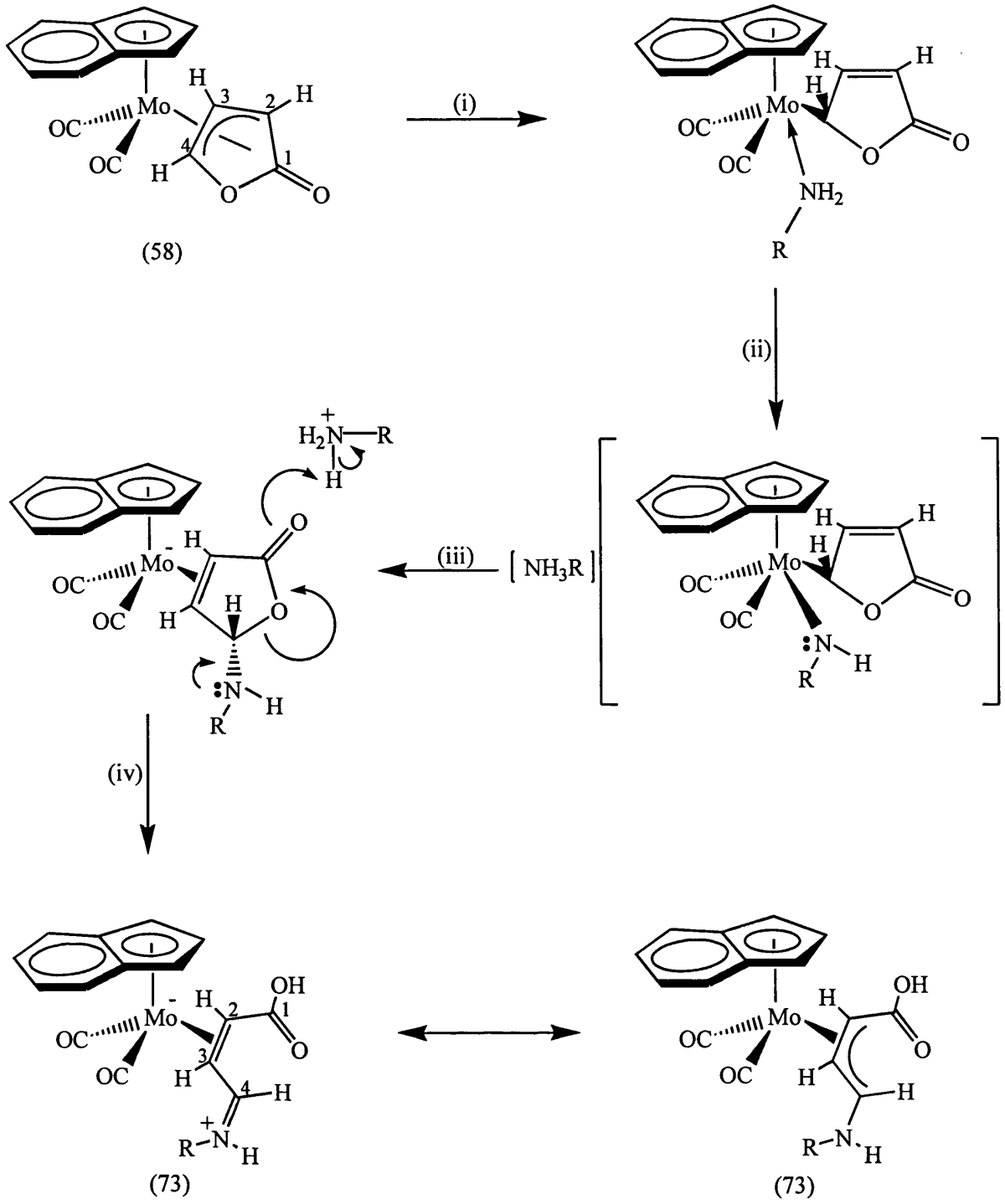

Scheme 3.14 *(i) $+NH_2R$, (ii) $+NH_2R$, $-[NH_3R]^+$, (iii) reductive elimination, (iv) $+[NH_3R]^+$, $-NH_2R$.*

We decided to continue these investigations into the reactivity of η^3-γ-lactonyl complexes of molybdenum with other nucleophiles. We were interested to investigate whether similar reactivity would also occur with non-amine nucleophiles and therefore [Mo{η^3-OC(O)CHCHCH}$(CO)_2(\eta$-$C_5H_5)$] (56) was treated with an organo-lithium reagent to establish whether the reaction was of a similar nature to those already discussed. Two molar equivalents of phenyllithium were added to a dichloromethane solution of (56) at -78 °C. The reaction mixture was then allowed to warm to room temperature and left to stir for one hour before the addition of two molar equivalents of water. Work-up of the reaction mixture followed by recrystallisation from dichloromethane and hexane afforded an orange/yellow powder in good yield (72 %). ^{1}H NMR spectroscopy indicated the formation of one product which contained two phenyl rings. This observation was supported by micro-analysis and mass spectroscopy which confirmed that the product was not a 1:1 adduct of phenyllithium and (56). In order to establish the nature of the novel complex (76), an X-ray diffraction study was undertaken (Figure 3.6) and the complex was identified as *exo-anti*-[Mo(η^3-CHPhCHCHCPhO)$(CO)_2(\eta$-$C_5H_5)$] (76).

The structure was very interesting as the compound crystallised in the *exo*-conformation and displayed a 'piano-stool' arrangement, in which the central molybdenum atom is bonded to two terminal carbonyl ligands, a η^5-cyclopentadienyl ring and an organic fragment. The organic fragment is bonded to the molybdenum in an η^3 fashion *via* a di-substituted η^3-allyl group. The substituents are a phenyl group and a ketone group. The ketone group is a phenyl ketone and faces away from the metal, such that both phenyls twist away from each other lying in different planes. It is also interesting to note that the inner carbon of the allyl moiety is closer to the metal

[Mo-C(9) 2.224(9) Å] than both the outer carbons [Mo-C(8) 2.463(8) Å and Mo-C(10) 2.321(8) Å].[111,112] Furthermore H(9) and H(10) of the allylic group lie underneath the cyclopentadienyl ligand, whereas H(8) faces towards the oxygen of the ketone group where there is possibly a slight hydrogen bond interaction.

Therefore, it became evident that the reaction sequence using this nucleophile follows a completely different mechanism from the ones already discussed (Scheme 3.15). For this system, the observations suggested that initial attack by the first mole of phenyllithium is at C^1 *(i.e.* the carbonyl carbon) of the η^3-γ-lactonyl complex, which causes cleavage of the lactonyl ring. The intermediate can be represented in two canonical forms where the organic fragment contains an aldehyde and a ketone moiety. This is once again susceptible to nucleophilic attack by the second mole of phenyllithium and this time the interesting fact is that the nucleophile is selective to the carbonyl of the aldehyde moiety rather than that of the ketone, which affords intermediate (A).

Work up with water yields a two step reaction where the first mole of water protonates the intermediate (A), which transforms it to the intermediate (B). This is followed by the reaction of the second mole of water which delivers a proton to the molybdenum metal centre forming the hydride intermediate (C). There are then two possible reaction paths available to the intermediate (C). The first is a hydride migration from the metal centre onto the organic fragment at C^3 which produces the intermediate (D), a η^1 sigma bonded organic ligand. This then leads to the formation of the η^3-allyl complex (76) through the elimination of water. The second reaction path is the reversible hydride migration from the metal centre onto the organic fragment at C^2 forming the intermediate (E), also a η^1-sigma bonded organic ligand.

However, as the reaction path between (C) and (E) is reversible, this all pushes through to the formation of (D) where dehydration occurs affording the η^3-allyl complex (76). It was not possible to determine whether the reaction path proceeds *via* step (E) and further studies would be required to determine this.

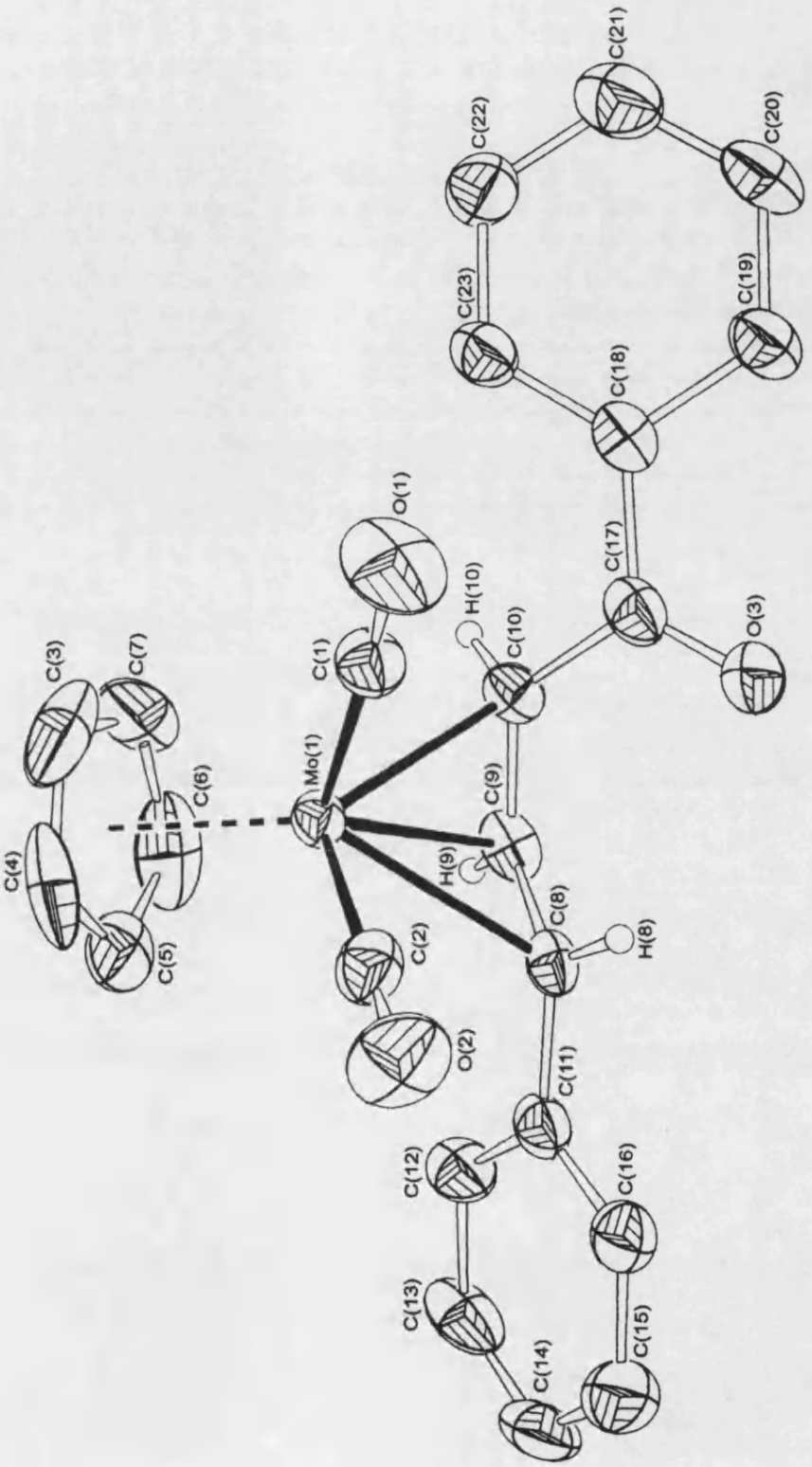

Figure 3.6 *X-ray structure of exo-anti-[Mo(η^3-CHPhCHCHCPhO)(CO)$_2$(η-C_5H_5)] (76).*

Mo-C(1)	1.950(7)	Mo-C(2)	1.963(9)
Mo-C(3)	2.292(12)	Mo-C(4)	2.303(9)
Mo-C(5)	2.343(9)	Mo-C(6)	2.328(10)
Mo-C(7)	2.300(11)	Mo-C(8)	2.436(8)
Mo-C(9)	2.224(9)	Mo-C(10)	2.321(8)
C(1)-O(1)	1.134(9)	C(2)-O(2)	1.135(9)
C(8)-C(9)	1.391(12)	C(9)-C(10)	1.401(11)
C(10)-C(17)	1.464(11)	C(17)-O(3)	1.221(10)
C(8)-C(11)	1.470(11)	C(17)-C(18)	1.483(12)
Mo-C(1)-O(1)	175.2(8)	Mo-C(2)-O(2)	177.7(8)
C(1)-Mo-C(2)	76.8(3)	C(8)-C(9)-C(10)	124.7(9)
C(9)-C(10)-C(17)	125.2(8)	C(9)-C(8)-C(11)	126.8(9)
C(10)-C(17)-C(18)	117.6(7)	C(10-C(17)-O(3)	122.7(8)
C(18)-C(17)-C(3)	119.6(8)		

Table 3.2 *Selected bond lengths (Å) and angles (°) for complex (76) with estimated standard deviations (e.s.d.s) in parentheses.*

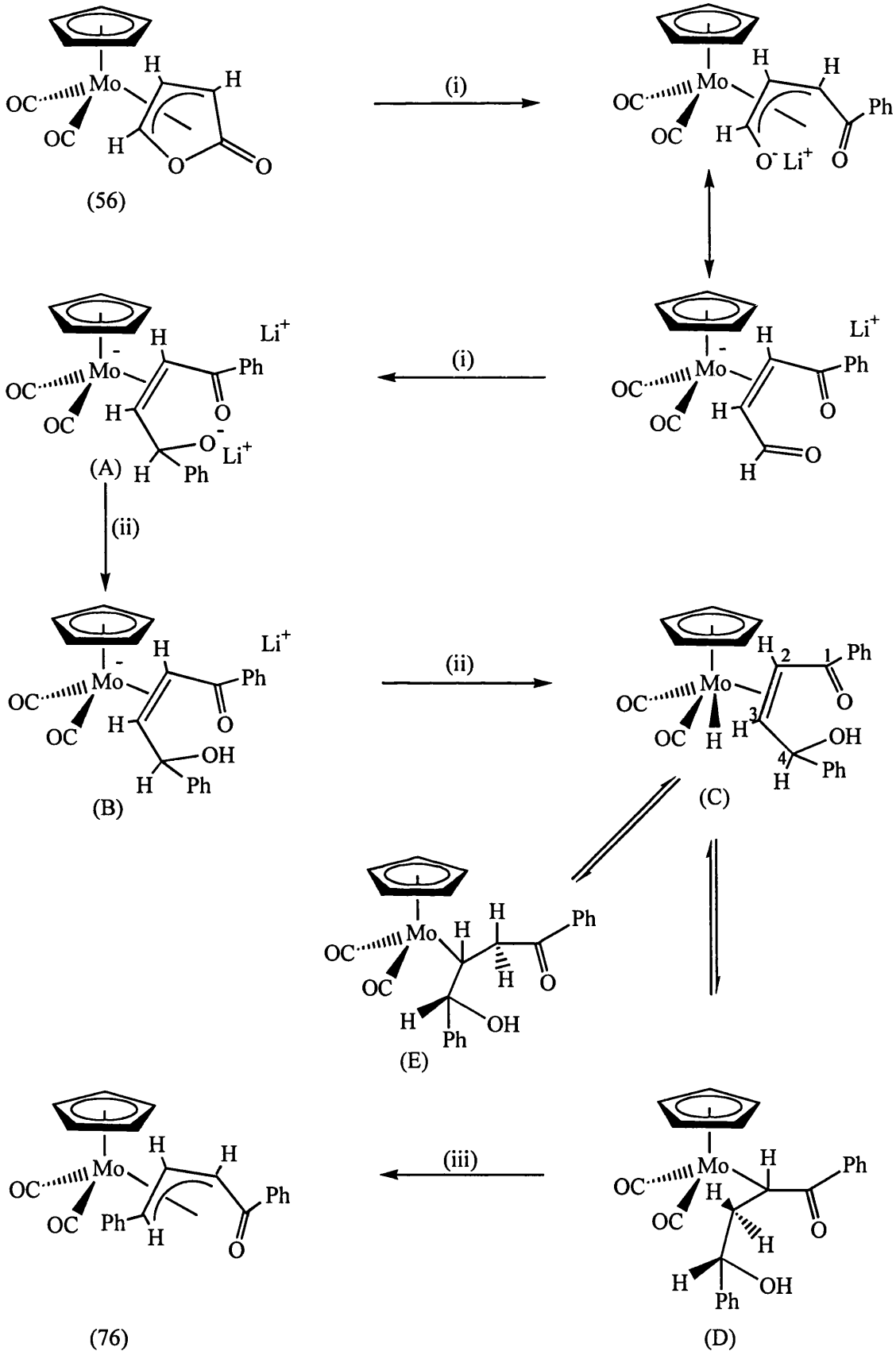

Scheme 3.15 *(i) PhLi, (ii) H_2O, (iii) -H_2O.*

The mechanism in this case is very interesting and poses a number of questions. For example, why when using the nucleophile phenyllithium does initial nucleophilic attack on the lactonyl complex target a different electrophilic site in comparison to the cases previously studied with other nucleophiles? Secondly, when the second molecule of phenyllithium reacts, why does it selectively attack the carbonyl moiety of the aldehyde instead of that of the ketone, and thirdly, why is the dehydration step selective towards the formation of the allyl? To provide answers to these questions it is important to refer back to the EHMO calculations and the HOMO and LUMO representations carried out on complex (57). From this, the conclusion was that there are two potential areas of attack from nucleophiles, both of which are facilitated by a high positive charge and available LUMO. We have identified these as being the molybdenum metal centre and the carbon of the lactonyl carbonyl functionality and we have shown by example that using different groups of nucleophiles causes the nucleophilic attack to selectively target either one of these sites and therefore, it is the choice of nucleophile which determines the regioselectivity.

The reactivity of a nucleophile towards any reagent is dependent upon a number of factors. In the case we have investigated, the lactonyl complex demonstrates that nucleophilic attack is regioselective. To understand this it is important to understand the properties of these nucleophiles and how this affects their reactivity. Firstly, the structure of the nucleophile should be considered. It is possible that in the case we have examined, regioselectivity is a result of steric hindrance and that the phenyllithium could be too big to actually attack the metal centre and is

forced to attack at the carbonyl functionality. However, the amine-based nucleophiles are much smaller and are able to attack the metal centre.

Hardness and softness is also a very important property of nucleophiles and electrophiles and this is a factor independent of strength. Hard and soft can be easily explained in terms of the HOMO and LUMO energies and their separation. Soft-soft interactions tend to be formed between nucleophiles with high-energy HOMOs and electrophiles with low-energy LUMOs. This means that the HOMOs and LUMOs are close in energy and will have a greater interaction, forming a more stable bond. Hard-hard interactions are the opposite to this and tend to be formed between nucleophiles which contain low-energy HOMOs and electrophiles with high-energy LUMOs. The energy separation between the HOMOs and LUMOs is often very large meaning there is very little covalent interaction. Therefore, it is usually the electrostatic attraction of opposite charges which constitutes the hard-hard interaction.

Applying this theory to our study and including what we know from the EHMO calculations, we can explain the regioselectivity of the reactions of the lactone complex with varying nucleophiles from a HOMO-LUMO perspective. When the lactone complex reacts with a nucleophile such as benzylamine, initial attack is at the metal centre. The reason for this is that the nucleophile contains a low-energy HOMO and attacks the molybdenum metal centre as it has the availability of a suitable LUMO. This reaction illustrates a hard-hard interaction where we have direct co-ordination of NH_2R *via* N to the metal centre. However, when the nucleophile is phenyllithium, initial attack on the lactone is now at the carbon of the carbonyl functionality. This is explained by the phenyllithium having a high-energy HOMO which is facilitated by the carbon atom having a low-energy LUMO. In this case

there is the formation of a more stable bond. Therefore, although the charge separations for the lactone complex suggest that the molybdenum metal centre and the carbon of the carbonyl functionality exhibit a balance in electron density, we have displayed that varying the nucleophile can determine the regioselectivity of attack. We have identified that each nucleophile requires a suitable LUMO and therefore complexes such as the lactone which display a division in electron density will be more susceptible to differing behaviour by nucleophiles.

In view of these observations it is important to establish why when the second molar equivalent of phenyllithium reacts, it attacks the aldehyde moiety rather than the ketone. The main reason for this is steric hindrance which also plays a large part in effecting nucleophilicity. Aldehydes have more reactive carbonyl groups than ketones and are therefore more electrophilic. The reason for this is that aldehydes are sterically less hindered than ketones making them more susceptible to attack.

Thirdly, it is important to understand why the dehydration step is selective towards formation of the allyl. In ionic elimination reactions, especially bimolecular ones, the stereoelectronic requirement is that the groups to be eliminated be conformationally anti and not gauche or eclipsed.[113] This allows the bond orbitals of the leaving groups to be in the same plane, which becomes the plane of the π- bond.

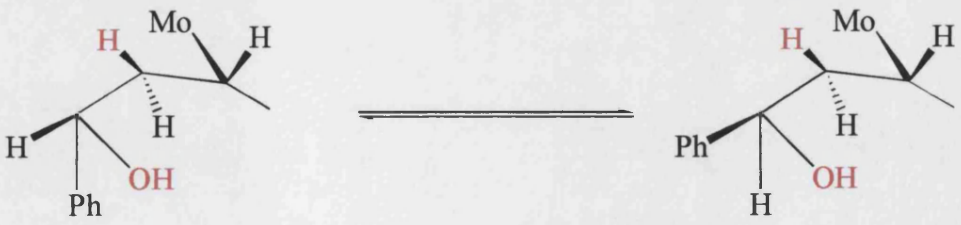

gauche *Anti*

Figure 3.7

In this case the sterically favoured transition state involves rotation of the carbon bond, so that the elimination reaction can proceed when the groups to be eliminated are *anti*.

One brief investigation into the reactivity of this novel η^3-allylic complex (76) focused on the possibility that it would lose carbon monoxide when heated to give a new co-ordinated organic fragment. The idea is taken from earlier work where a similar reaction occurred on a manganese fragment.[114] When 3-benzoyl-1-methyl-π-allyltetracarbonyl-manganese (77) is heated just above its melting point, evolution of carbon monoxide occurs. Sublimation yields a novel yellow crystalline complex identified as 5-methyl-2-phenyl-π-1-oxapentadienyltricarbonyl-manganese (78). The thermal reaction involves a loss of carbon monoxide and a change in the proton environment of the terminal proton H(1) in (78). The reaction was found to be reversible so when (78) was heated under a pressure of carbon monoxide (77) was reformed (Scheme 3.16).

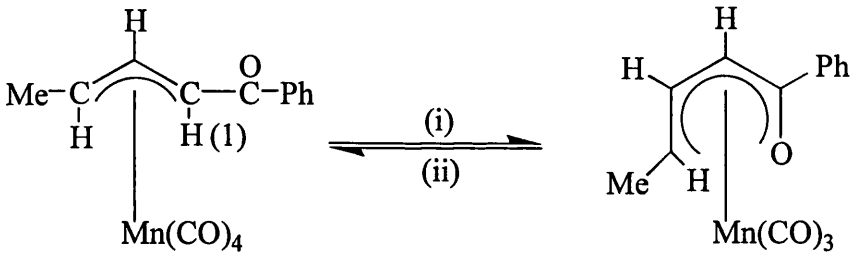

(77) (78)

Scheme 3.16 *(i) heat, (ii) CO.*

In view of the fact that the novel molybdenum complex (76) contained a similar organic fragment to that of the manganese complex (77), it seemed attractive to consider that they would act in the same manner. However, on heating (76) to just

above its melting point, there was no evidence of the evolution of carbon monoxide and the complex was recovered unchanged.

3.4 Conclusion

To summarise, we have demonstrated that in the systems (54)-(58), general reactivity with regard to nucleophiles is dictated by the nature of the LUMO and the available charge. An examination of complexes (54) and (55) by an EHMO study observed that the reactions were FMO controlled and this was reinforced by observing that the majority of the LUMO contribution is situated at the carbon of the carbonyl functionality which is where nucleophilic attack is also concentrated. However, complexes (56)-(58) differ in that both the metal and the carbon of the lactonyl functionality have a suitable LUMO contribution and available charge and it was found that as the metal and the carbonyl functionality had a similar charge the reactivity of (56)-(58) towards nucleophiles was dictated by the nature of the nucleophile.

CHAPTER FOUR

PATHWAYS TO η^2(4e)-PHOSPHAALKYNE TRANSITION METAL COMPLEXES

4.1 Introduction

The synthesis of *tert*-butylphosphaalkyne in 1981 led to the development of low-coordinate phosphorus compounds and a rapid development in the chemistry of main group compounds which contain multiple bonds. The reactivity of phosphaalkynes within inorganic and organic chemistry is now a highly studied area in which their behavioural characteristics bear many similarities to those of alkynes. This is particularly reflected in transition metal chemistry where the synthesis of phosphorus analogues of popular unsaturated hydrocarbon π-complexes has been adopted.

The P≡C bond in for example *t*BuC≡P includes two orthogonal π-systems creating the potential for the phosphaalkyne to be either a $2e^-$ or a $4e^-$ donor ligand upon complexation to a metal. Phosphaalkynes can also adopt various co-ordination modes ranging from mono-nuclear to poly-nuclear complexes with side-on, end-on and bridging co-ordination modes, in analogy to their alkyne counterparts. However, one of the disparities between phosphaalkynes and alkynes is the ability of the phosphaalkyne to be a potential $6e^-$ donor ligand. This enhanced ligating property is facilitated by the availability of the lone pair of electrons on the phosphorus, which in addition to the P≡C π-system, can interact with an additional metal centre.

Reaction paths (a-k) (Scheme 4.1) illustrate how phosphaalkynes have become valuable and versatile building blocks in organic, inorganic and organometallic chemistry. Reactions (a-d) demonstrate the ability of the phosphaalkyne to adopt a variety of bonding modes on complexation to a metal: (a) shows the phosphaalkyne adopting a side-on bonded η^2(2e) bonding mode in a mono-nuclear complex,[115] (b) demonstrates the less preferred end-on η^1-ligating mode of the phosphaalkyne

facilitated by the complex containing a suitable pocket in which only a linear phosphaalkyne can co-ordinate[116] and (c) shows the ability of the phosphaalkyne to bridge between two metal centres, forming an η^2(4e) donor phosphaalkyne,[117,118] where each metal atom effectively receives $2e^-$. The phosphorus lone pair can offer additional co-ordination potential[119] (d) which effectively renders the phosphaalkyne as a $6e^-$ donor.

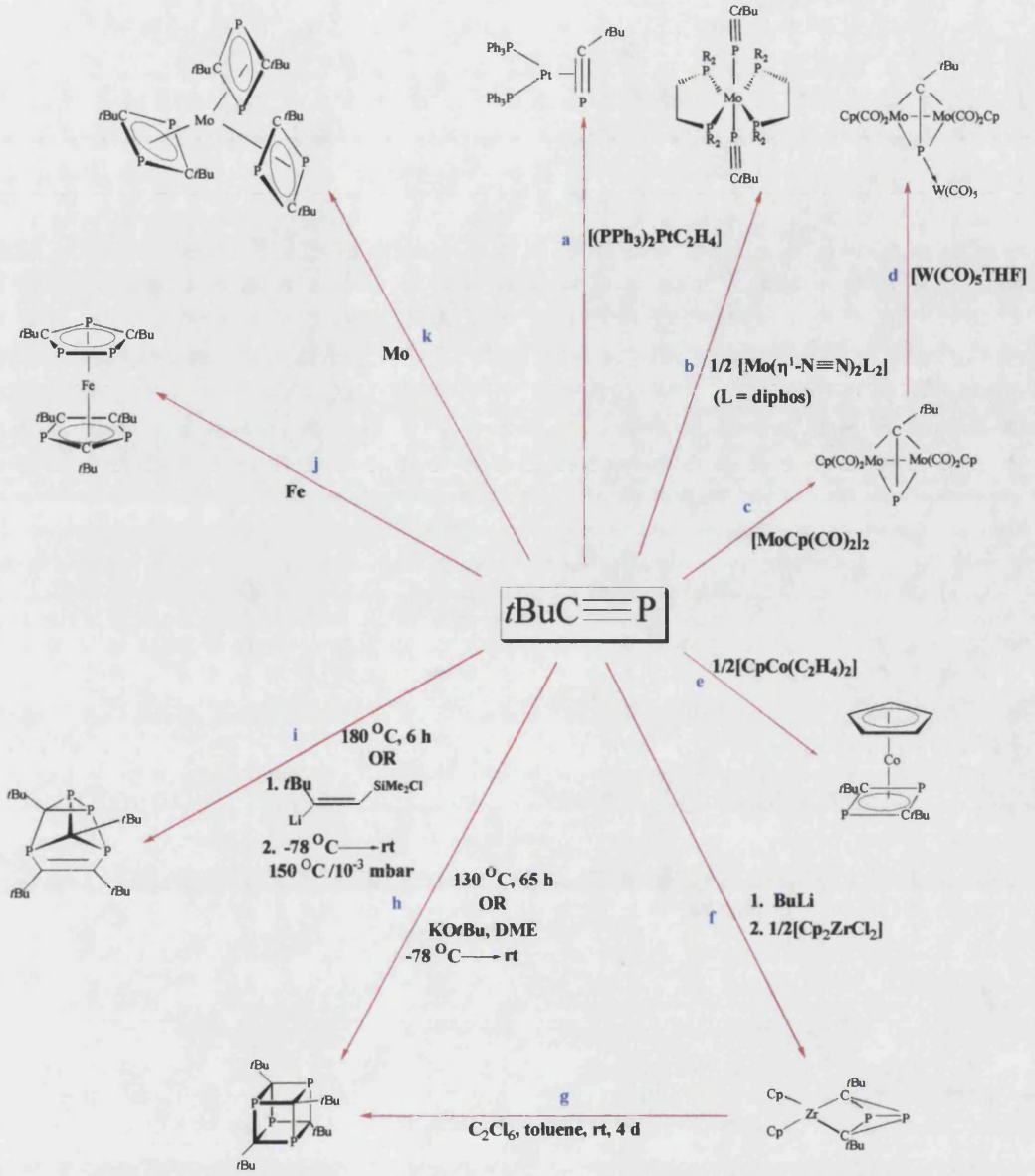

Scheme 4.1

Cyclodimerisation of phosphaalkynes in the co-ordination sphere of a metal atom (e-f) has also been well reported and it is the role of the metal in these reactions which dictates the nature of the dimerisation process. For example, when two phosphaalkynes are oxidatively coupled at an electron rich transition metal centre such as cobalt, a 1,3-diphosphacyclobutadiene complex is obtained (e).[120-122] However, the process differs in the presence of electron poor transition metals such as

zirconium and hafnium as 1,3-diphosphabicyclobutanediyl complexes are obtained (f).[123]

Interestingly, these organophosphorus ligands can be released from the metal by oxidation with hexachloroethane as demonstrated in (g).[124] In this example, after oxidation, the organophosphorus ligand follows a sequence of [4+2] and [2+2] cycloadditions, which provides easy access to the tetraphosphacubane cage. Phosphaalkynes can also undergo thermal[125,126] or base induced[127,128] reactions to form predominantly tetramers. The structure of the tetramer is solely dependent upon the temperature of the reaction and on the strength of the base and it is interesting to see how small changes in these conditions can be crucial to the structure of the cage (h and i). In contrast, when phosphaalkynes undergo transition metal mediated reactions, the products tend to be a mixture of *di-* and *tri-*merised phosphaalkynes as opposed to tetramers.

Reactions (j) and (k)[129-130] illustrate how the co-condensation of metal atoms, generated by metal vapour synthesis techniques, with *t*BuC≡P can lead to a variety of sandwich or homoleptic complexes where the phosphaalkyne can form a range of pentaphosphametallocenes, phosphacyclobutadienes and even 3-membered phosphirenyl ring systems, hence demonstrating the potential phosphaalkynes can provide in both organic and transition metal chemistry.

4.2 Synthesis of η^2-(4e) Mononuclear Phosphaalkyne Complexes

The aim of this project was to further develop one of the research areas of the group involving the synthesis and chemistry of stable mononuclear complexes containing η^2(4e)-phosphaalkyne ligands. Surprisingly, the existence of stable

mononuclear 4e⁻ phosphaalkynes has shown to be fairly uncommon which is interesting because the 'alkyne-like' behaviour of phosphaalkynes supposedly dominates their rich co-ordination chemistry.[131]

The first evidence to suggest that they existed came from Binger[132] who reported that the metallocene complex (79), which contains an η^2(2e)-bonded phosphaalkyne, reacts with BEt_3 to remove PMe_3, forcing the phosphaalkyne to compensate for the electronic loss by adopting a switch in bonding mode from η^2(2e) → η^2(4e). However, this was found to exist only in equilibrium with the corresponding phosphorus-bridged dimer (81), which was the only species that could be isolated (Scheme 4.2).

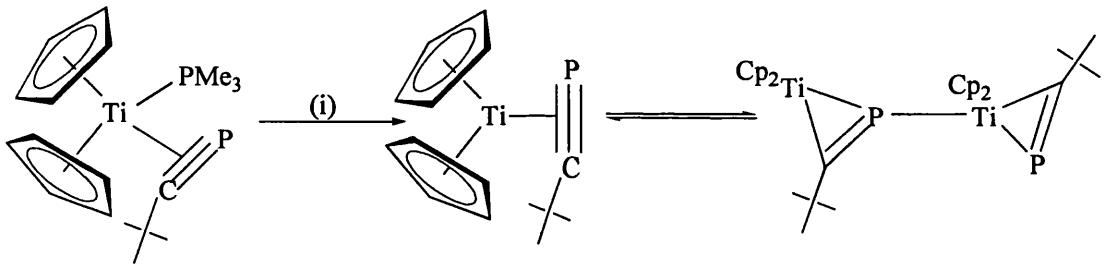

(79) (80) (81)

Scheme 4.2 *(i) BEt_3, -Me_3PBEt_3.*

Following this, Bauers[133] working in our group demonstrated the synthesis of the first stable mononuclear η^2(4e)-bonded phosphaalkyne complex. It was found that when the zwitterionic η^2-vinyl complex (82) was treated with one equivalent of $HBF_4.Et_2O$ in the presence of PhC_2Ph, the *trans*-stilbene complex (83) was generated *in situ*, followed by the regeneration of the η^2(4e)-bonded alkyne complex (84), the reaction proceeding *via* a stilbene displacement reaction (Scheme 4.3). It was therefore thought that *t*BuC≡P would also displace stilbene to generate the 4e⁻

phosphaalkyne complex. This suggestion proved correct as on cooling the stilbene complex to -78 ^{o}C and adding one equivalent of *t*BuC≡P, an instantaneous reaction took place. The result of this reaction was the formation of the highly air sensitive, zwitterionic η^2(4e) phosphaalkyne complex [Mo{η^2-P(OMe)$_2$OBF$_2$OP(OMe)$_2$}(η^2-P≡C*t*Bu)(η-C$_5$H$_5$)] (85).

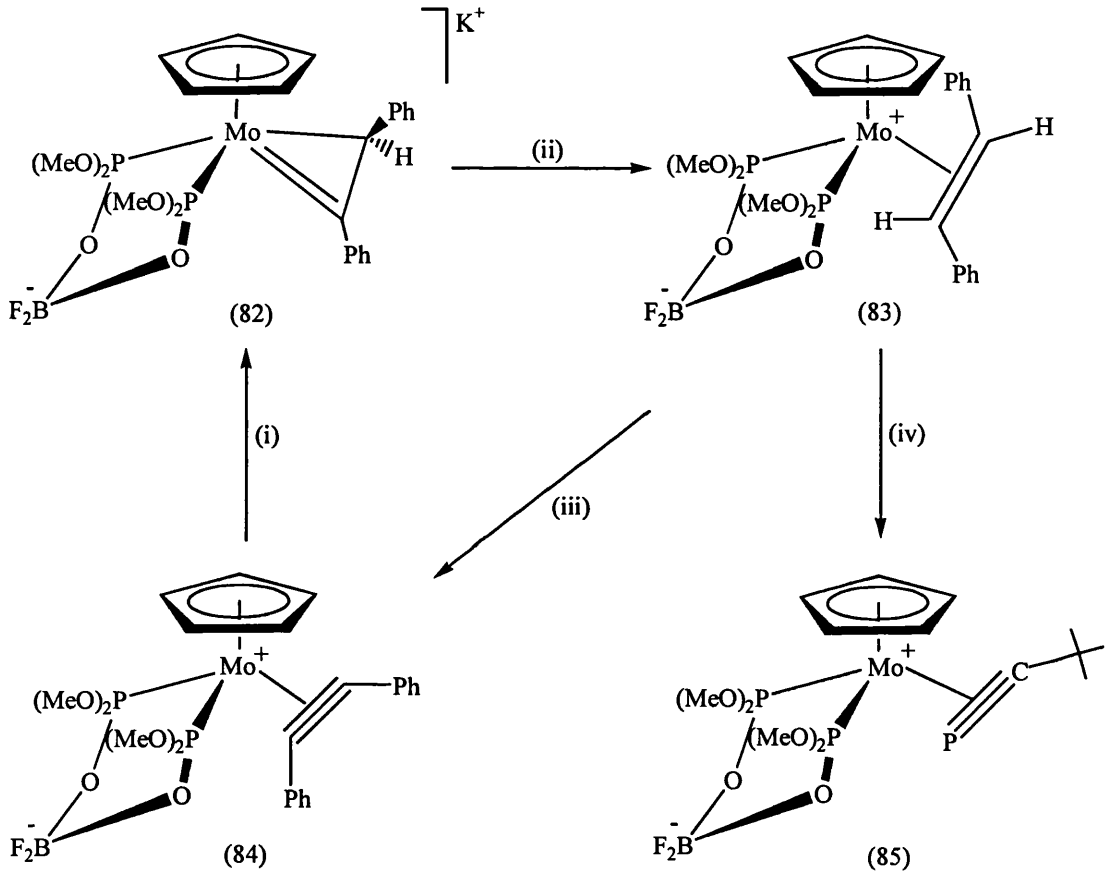

Scheme 4.3 *(i) K[BHBu$^s_3$], thf, -78 → 25 ^{o}C, (ii) HBF$_4$.Et$_2$O, thf, -78 → 25 ^{o}C, (iii) PhC$_2$Ph, CH$_2$Cl$_2$, -trans-stilbene, (iv) tBuC≡P, thf, -78 → 25 ^{o}C, -trans-stilbene.*

The protonation of η^2(3e)-vinyls has been studied extensively and has been shown to have a diverse chemistry. Templeton[134] and co-workers reported that the η^2(3e)-vinyl [W{=C(Ph)C(H)Me}$(CO)_2${HB(dmpz)$_3$}] is protonated on the β-carbon of the η^2(3e)-vinyl, generating the β-agostic stabilised cation [W{=C(Ph)CH_2Me}$(CO)_2${HB(dmpz)$_3$}][BF_4]. Therefore, it was thought that protonation of (82) by $HBF_4.Et_2O$ to generate the co-ordinatively unsaturated cationic *trans*-stilbene substituted complex (83), which can then react with PhC_2Ph or *t*BuC≡P to give *trans*-stilbene and (84) or (85) respectively, could be explained in two ways (Scheme 4.4).[135] Firstly, protonation can proceed by charge-controlled attack of H^+, delivered by $HBF_4.Et_2O$ on the C_α of the η^2(3e)-vinyl ligand, generating (83). Alternatively, protonation can occur by attack on the C_β of the η^2(3e)-vinyl ligand to give (A), a carbene complex which is stabilised by a C_β agostic Mo(μ-H)C interaction. This species can then rearrange into (83) either by route (A) → (B) → (83) or (A)→ (C) → (83) (Scheme 4.4).

However, EHMO studies [16,136] of known 18e, d^4, η^2(3e)-vinyl complexes have shown that the LUMO arises from the M-Cα π*-interaction. Also, the C_α carbon is shown to have a significant build up of negative charge in contrast to the C_β carbon (net charges in typical example by Mulliken population analysis of EHMO orbital: C_α, 0.5 e; C_β, 0.15 e). This suggests that if protonation is assumed to proceed *via* charge controlled attack, it is the direct reaction path (82) → (83) which is preferred (Scheme 4.4).

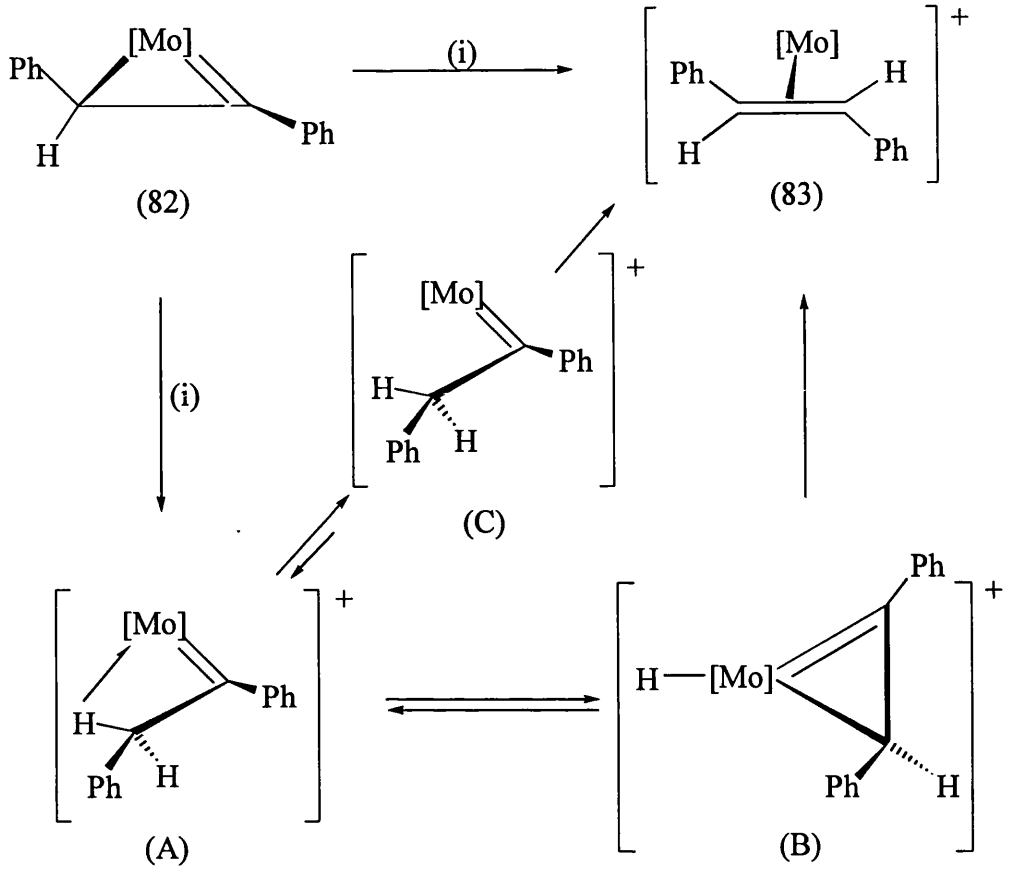

Scheme 4.4 *(i) $HBF_4.OEt_2$ (where [Mo] = $CpMo\{\eta^2\text{-}P(OMe)_2OBF_2OP(OMe)_2\}$.*

Complex (85), which was fully characterised by analytical and spectroscopic data, displayed a low field ^{31}P NMR signal at 467.8 ppm, which was assigned to the phosphorus of the η^2(4e)-bonded *t*BuC≡P. This low field ^{31}P NMR resonance can be taken as a signature of 4e⁻ donor phosphaalkynes as it reflects significant deshielding compared to those of η^2(2e)-bonded *t*BuC≡P ligands *i.e.* $[Pt(\eta^2\text{-}P{\equiv}C\textit{t}Bu)(PPh_3)_2]$ (86) (84.1 ppm).[115]

Support for this rationale was provided by the work of Regitz[137] who reported the generation of phosphorus analogues of cyclopropenium ions 'phosphirenylium cations'. On generating the cation (B) from the salt (A) (Scheme 4.5), there is a

massive downfield shift in the $^{31}P-\{^{1}H\}$ NMR (-3.02 ppm → 309.7 ppm), indicative of deshielding at the phosphorus centre due to aromaticity of the ring.

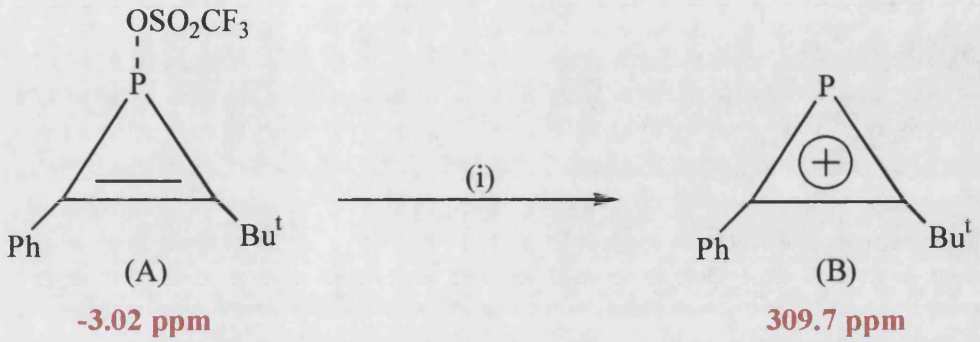

Scheme 4.5 *(i) $B(OSO_2CF_3)_3$, SO_2 liquid, -78 ^{O}C, ^{31}P NMR data.*

This is also reflected in the $^{13}C-\{^{1}H\}$ and ^{1}H NMR for which there is a downfield shift for both the two diagnostic ring carbons and the *t*Bu and Ph protons. Therefore, in view of the isolobal relationship which exists between $MoL_2(\eta-C_5H_5)$ and CR (Figure 4.1), one would expect a low field resonance in the $^{31}P-\{^{1}H\}$ NMR to occur on formation of an η^2(4e)-bonded phosphaalkyne.

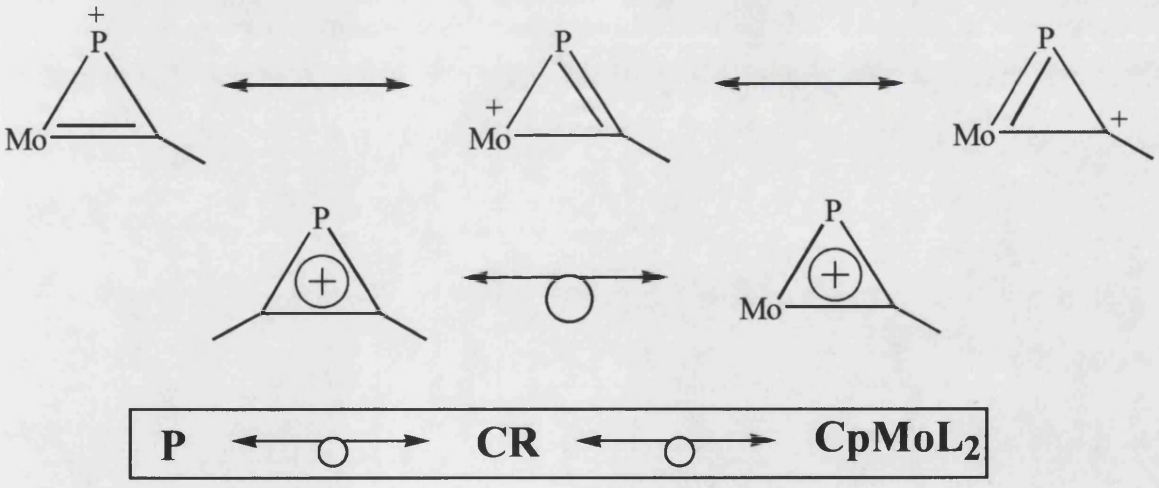

Figure 4.1

As expected, the ^{13}C-{^{1}H} NMR spectrum is supportive of the phosphaalkyne adopting a η^2(4e)-bonding mode: the contact ^{13}C chemical shift of the phosphaalkyne is at 328.5 ppm. It is well documented that 4e$^-$ donor alkynes exhibit low field ^{13}C chemical shifts, therefore, it is assumed that the correlation between ^{13}C NMR and formal number of electrons donated (see Chapter One, Section 1.1) is also reflected in phosphaalkyne chemistry.

This trend is also consistent with the findings of Binger[132] with the 4e$^-$ phosphaalkyne species (80). A NMR study carried out on the equilibrium mixture of (80) and (81) contained low field resonances in both the ^{31}P and ^{13}C-{^{1}H} NMR (431.6 and 298.6 ppm respectively) which were assigned to (80). This indicated that 4e$^-$ donor phosphaalkynes could be observed by low field resonances in both ^{13}C-{^{1}H} NMR and ^{31}P NMR spectroscopy.

The aim of this project was to extend this preliminary investigation by looking to access other 4e$^-$ phosphaalkyne systems by using η^2-vinyls as precursors. In the case of the formation of (85), the cation contains the anionic chair-shaped bidentate phosphite ligand which renders the complex zwitterionic. We decided that the starting point for our investigation would be the η^2(3e)-vinyl [Mo{=C(Ph)CHPh}{P(OMe)$_3$}$_2$(η-C$_5$H$_5$)] (8) obtained in good yield by addition of KHBu$^s_3$ to a solution of [Mo{η^2(4e)-PhC$_2$Ph}{P(OMe)$_3$}$_2$(η-C$_5$H$_5$)][BF$_4$] (7) in thf (Chapter 1 Scheme 1.3).[16] The purpose of the present work was to prepare the novel cation [Mo{η^2-(4e)-P≡C*t*Bu}{P(OMe)$_3$}$_2$(η-C$_5$H$_5$)]$^+$ (87)$^+$ and in doing so, open the way to the exploration of its reactivity. Furthermore, it was hoped to establish whether a related chemistry existed to that of the cationic 4e$^-$ alkyne species [Mo{η^2-(4e)-RC≡CR}{P(OMe)$_3$}$_2$(η-C$_5$H$_5$)]$^+$. It was envisaged that the 4e$^-$ phosphaalkyne

cation $(87)^+$ would differ from the zwitterionic complex (85) with respect to crystallinity, opening the way to further structural knowledge of 4e⁻ phosphaalkyne complexes through X-ray crystallography.

In accordance with the work of Bauers,[133] the idea that the η^2(3e)-vinyl fragment can undergo protonation, generating a labile stilbene complex which can be easily displaced by *t*BuC≡P, provides a good synthetic route to the 4e⁻ phosphaalkyne cation. However, as an alternative to the generation of a labile stilbene complex by protonation, it was decided to explore the possibility of reacting (8) with tris(pentafluorophenyl)borane [$B(C_6F_5)_3$]. This idea was stimulated by the report by Erker[63] that $B(C_6F_5)_3$ reacts with (36), by electrophilic addition onto the terminal butadiene carbon atom, forming the (π-allyl) zirconocene complex (37) (Scheme 4.6).

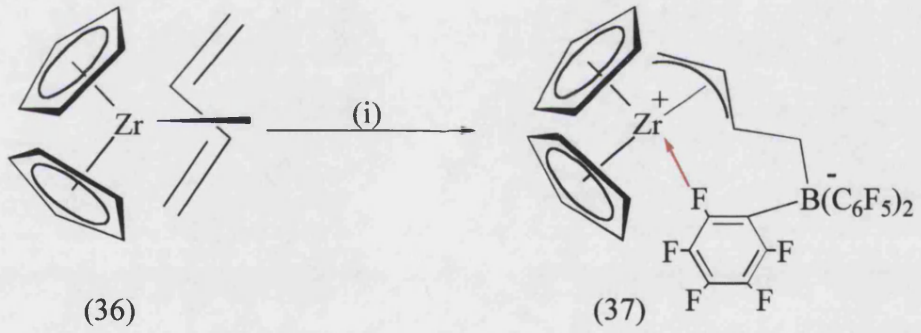

(36) (37)

Scheme 4.6 *(i) $B(C_6F_5)_3$.*

With this insight, we decided to develop the idea that $B(C_6F_5)_3$ would react with the η^2-vinyl complex (8) by electrophilic addition onto the carbene carbon C_α. This would produce an intermediate containing a borane-substituted alkene, which could then be displaced by *t*BuC≡P, providing access to the 4e⁻ phosphaalkyne cation and borane-substituted anion (Scheme 4.7).

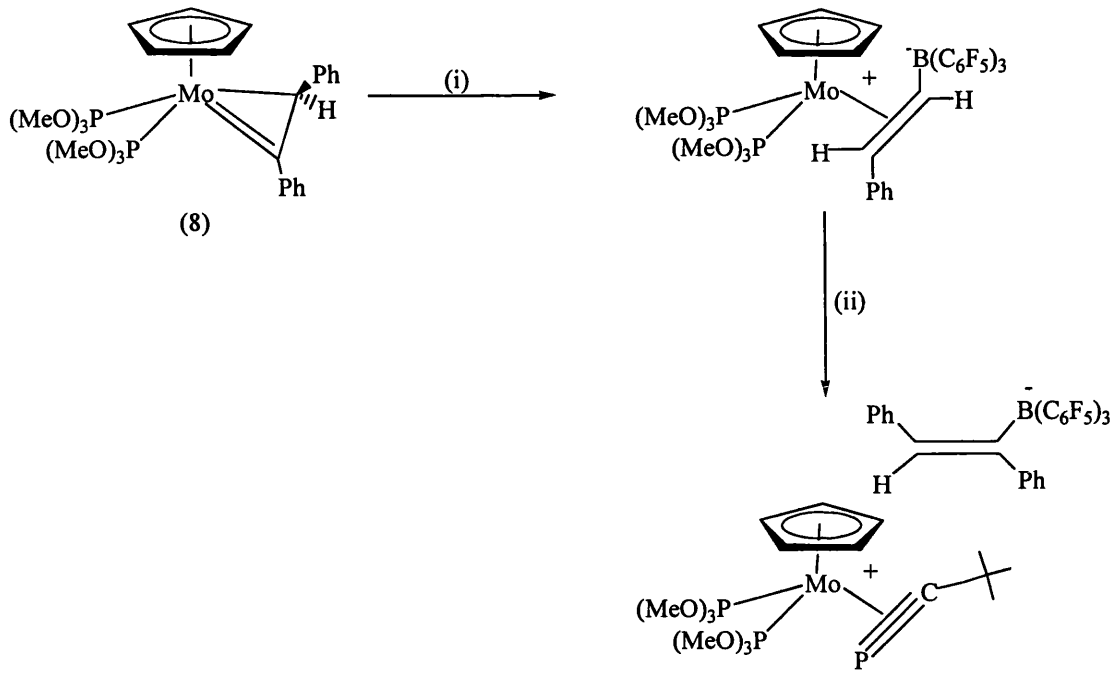

Scheme 4.7 *(i) $B(C_6F_5)_3$, (ii) tBuC≡P, CH_2Cl_2, -78 °C → rt.*

Before we carried out the reaction, we felt it was important to determine whether $B(C_6F_5)_3$ would react with *t*BuC≡P. The purpose of this was firstly to establish whether the reaction (shown in Scheme 4.7) could be carried *in situ* or whether the borane intermediate would have to be isolated before addition of *t*BuC≡P. Secondly, a report by Regitz[137] established that *t*BuC≡P reacts with the Lewis acid aluminium trichloride resulting in a spirocyclotrimerization of the phosphaalkyne. It was, therefore, important to examine whether the Lewis acid $B(C_6F_5)_3$ would react in a similar manner. Surprisingly, however, we did not observe any reaction between $B(C_6F_5)_3$ and *t*BuC≡P and after 3 d of stirring at room temperature in a CH_2Cl_2 solution, both reagents were found to be unreacted.

The reaction was carried out by addition of one equivalent of *t*BuC≡P to the η^2-vinyl complex (8) in CH_2Cl_2 at -78 °C. One equivalent of $B(C_6F_5)_3$ in CH_2Cl_2 was then added to the mixture *via* cannula, and the solution allowed to warm to room

temperature. Over 2 hrs, a progressive colour change took place (green → red → blue). Work up by removal of the solvent in *vacuo* afforded a deep green/blue oil.

The product was characterised by NMR spectroscopy. The spectra exhibited the features expected for the 4e⁻ cation $[Mo(\eta^2\text{-}P{\equiv}C\textit{t}Bu)\{P(OMe)_3\}_2(\eta\text{-}C_5H_5)]^+$ $(87)^+$. The ^1H NMR spectrum displayed a singlet at 5.52 ppm and a virtual triplet at 3.38 ppm [J(PH) = 11.3 Hz] which can be assigned to the cyclopentadienyl ligand and the two phosphite ligands respectively. A singlet at 1.48 ppm was assigned to the *tert*-butyl group, which, when integrated also revealed that there was only one phosphaalkyne molecule incorporated. The $^{31}P\text{-}\{^1H\}$ NMR displayed two resonances (Figure 4.2), a low field triplet at 492.3 ppm [J(PP) = 30.1 Hz] which can be assigned to the phosphorus of the phosphaalkyne [(85) = 467.8 ppm] and a doublet at 175.1 [J(PP) = 30.1 Hz] which corresponds to the two phosphite ligands (Figure 4.2).

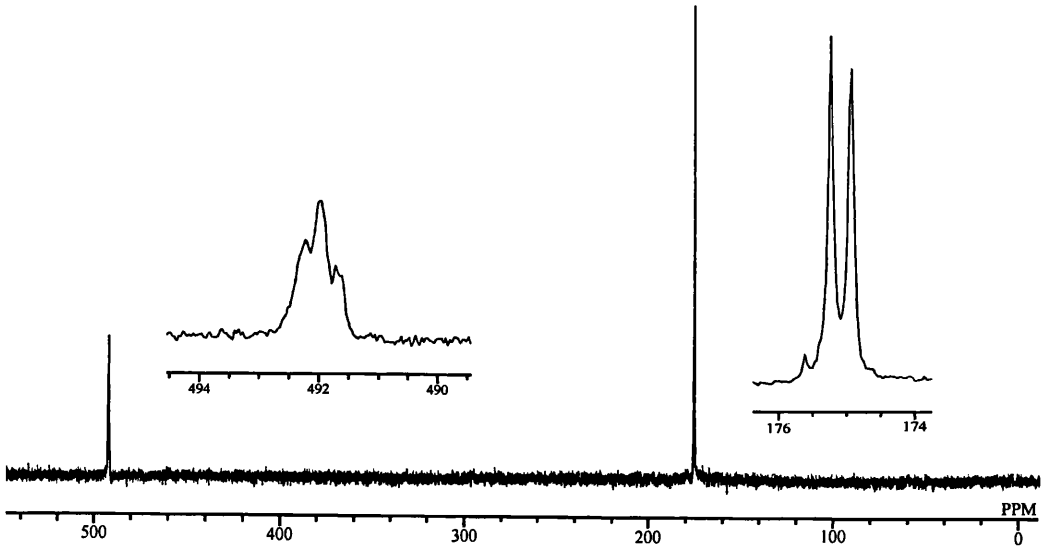

Figure 4.2 *^{31}P NMR of $[Mo(\eta^2\text{-}P{\equiv}CtBu)\{P(OMe)_3\}_2(\eta\text{-}C_5H_5)]^+$ $(87)^+$.*

As was observed in (85), there is only one resonance exhibited for the two phosphite ligands. This can be attributed to the rapid windscreen wiper motion of the phosphaalkyne ligand, a feature also observed with alkyne ligands in solution on the NMR timescale.[16] By analogy with the structure of the analogous alkyne complex $[Mo(\eta^2\text{-}t\text{BuC}_2\text{H})\{P(OMe)_3\}_2(\eta\text{-}C_5H_5)][BF_4]$, it is assumed that the bulky *t*Bu group of the *t*BuC≡P is oriented as shown in Scheme 4.8.

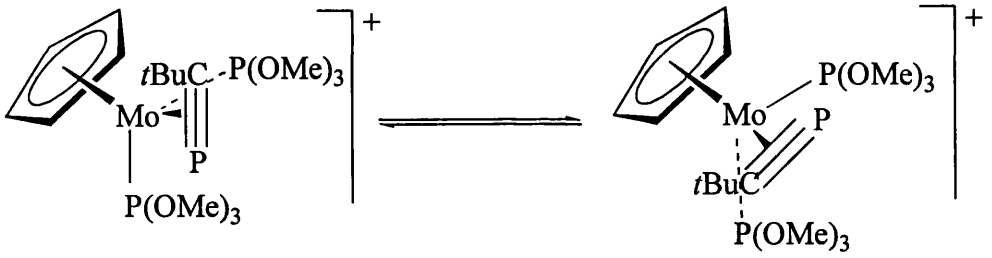

Scheme 4.8

In addition to this, the $^{13}C\text{-}\{^1H\}$ NMR exhibits a low field doublet of triplets for the contact carbon of the phosphaalkyne at 334.6 ppm [*J*(CP) = 113.9 Hz, *J*(CP) = 8.6 Hz] [(85) = 328.5 ppm {*J*(CP) = 114.4 Hz, *J*(CP) = 6.6 Hz}]. Therefore, both the ^{31}P and $^{13}C\text{-}\{^1H\}$ NMR data provide convincing evidence that the cation contains a $4e^-$ phosphaalkyne ligand.

Surprisingly, there were two broad peaks in the ^{11}B NMR at -4.4 and - 5.6 ppm and for this reason we became uncertain about the true nature of the anion and whether it was a borane-substituted alkene as first assumed. In an attempt to establish the identity of the reaction intermediate and structure of the anion, it was decided to carry out the reaction of the η^2-vinyl (8) with $B(C_6F_5)_3$ only and monitor the reaction by observing the NMR spectra as the temperature varied. This experiment showed that attack by $B(C_6F_5)_3$ on the η^2-vinyl might not be selective and indicated that the initial kinetic product isomerised to a thermodynamic controlled product. This is

illustrated by the ^{31}P-{^{1}H} and ^{19}F NMR spectra shown in Figure 4.3 and 4.4. Figure 4.3 shows an AB doublet pattern which appeared at -78 °C, and when warmed to -50 °C began to disappear and be replaced by a second AB doublet pattern. The conversion from one to the other becomes more evident as the temperature is warmed to room temperature.

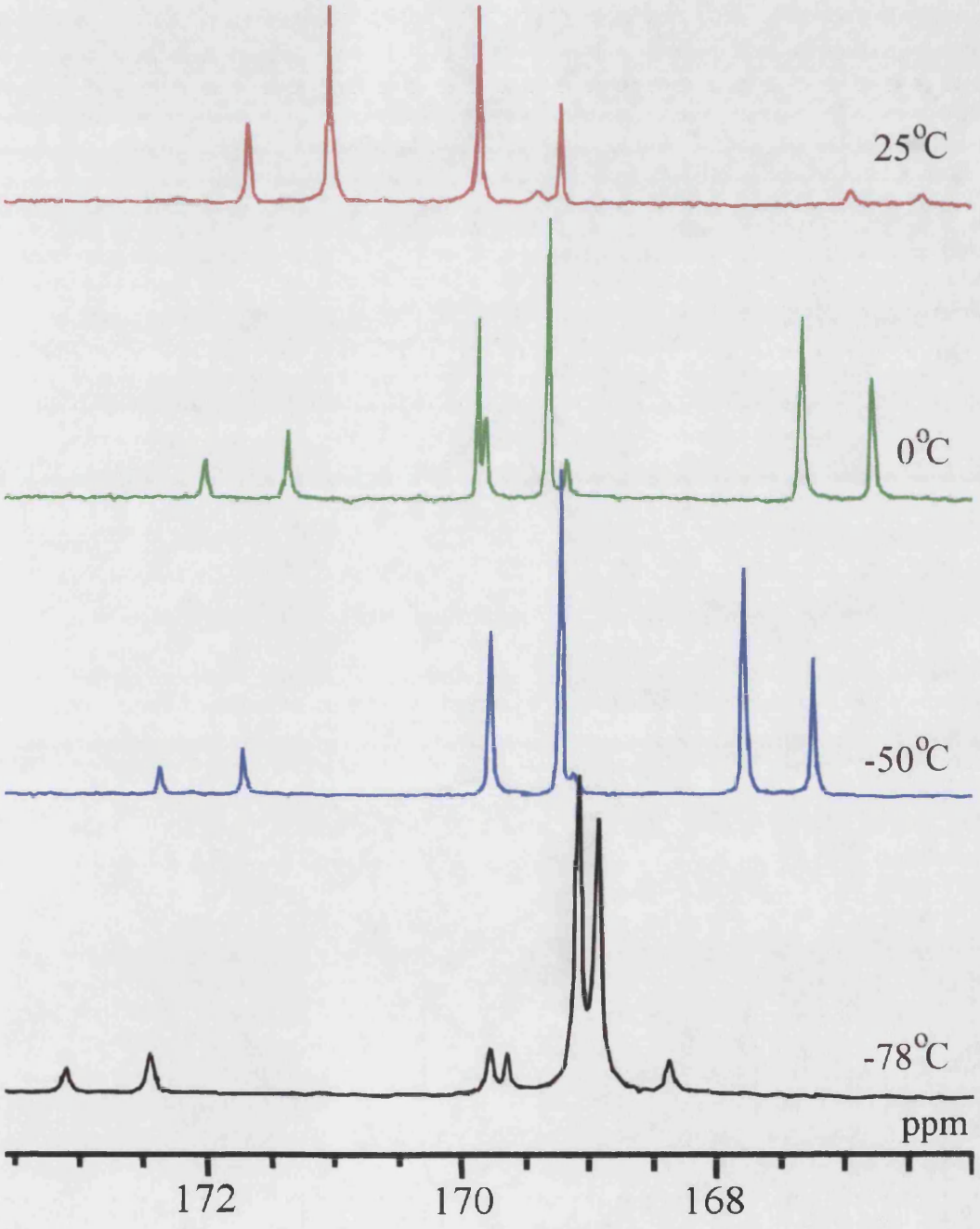

Figure 4.3 *^{31}P-{^{1}H} NMR for (8) + $B(C_6F_5)_3$, -78 °C → rt.*

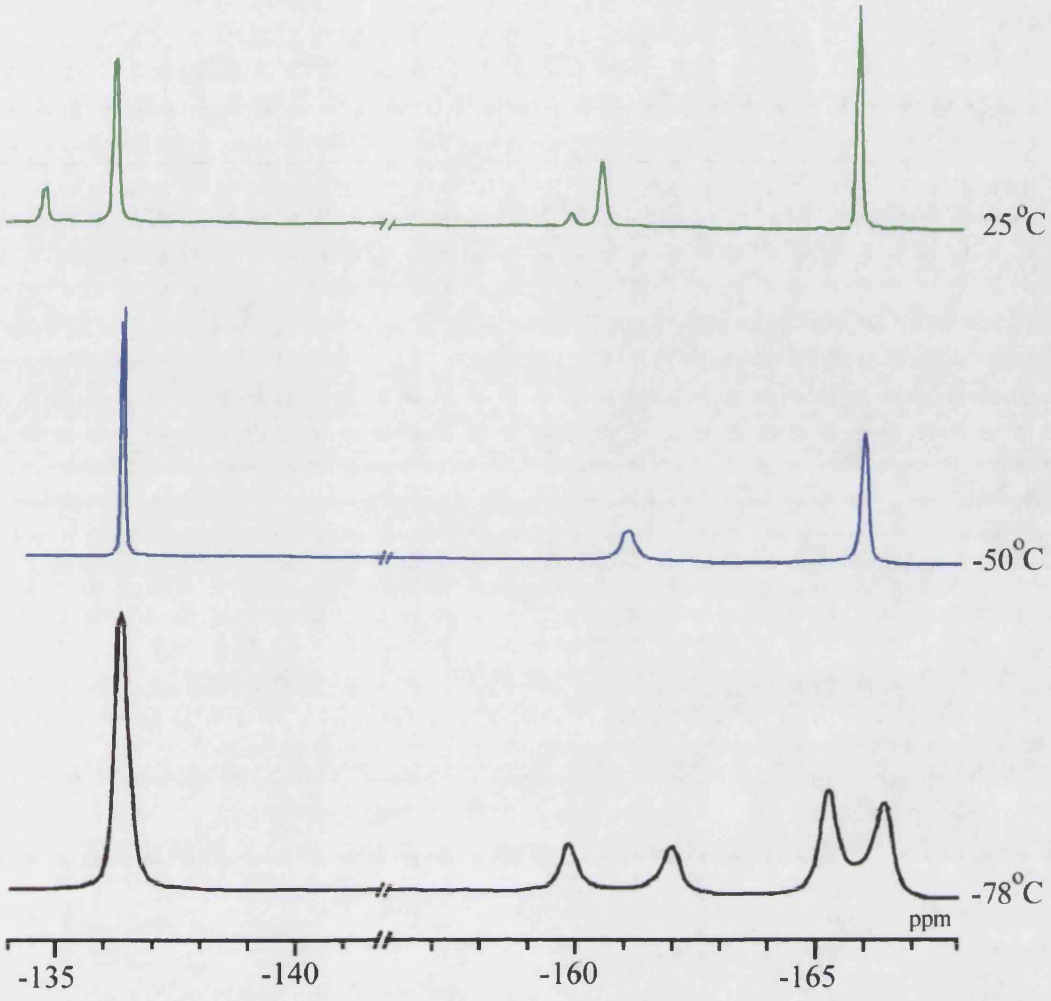

Figure 4.4 *^{19}F NMR for (8) + $B(C_6F_5)_3$, -78 °C → rt.*

Our initial explanation for this observation was that the borane was selectively attacking the η^2-vinyl at one face only, hence the generation of a kinetic intermediate. However, this species is unstable towards borane lability and the borane reversibly dissociates thus allowing attack on the other face of the η^2-vinyl, generating the more stable thermodynamic product. It was assumed that when this reaction was carried out in the presence of *t*BuC≡P, both the kinetic and thermodynamic borane substituted alkenes were displaced, thus giving two isomeric vinyl borane anions. The rate at which this capture occurs appeared to be temperature dependent, thus allowing for

approx 60 % of isomerisation to occur prior to the displacement reaction. Hence, *t*BuC≡P traps the intermediates which then generate two anions, *cis* and *trans*-borane substituted alkenes (Scheme 4.9).

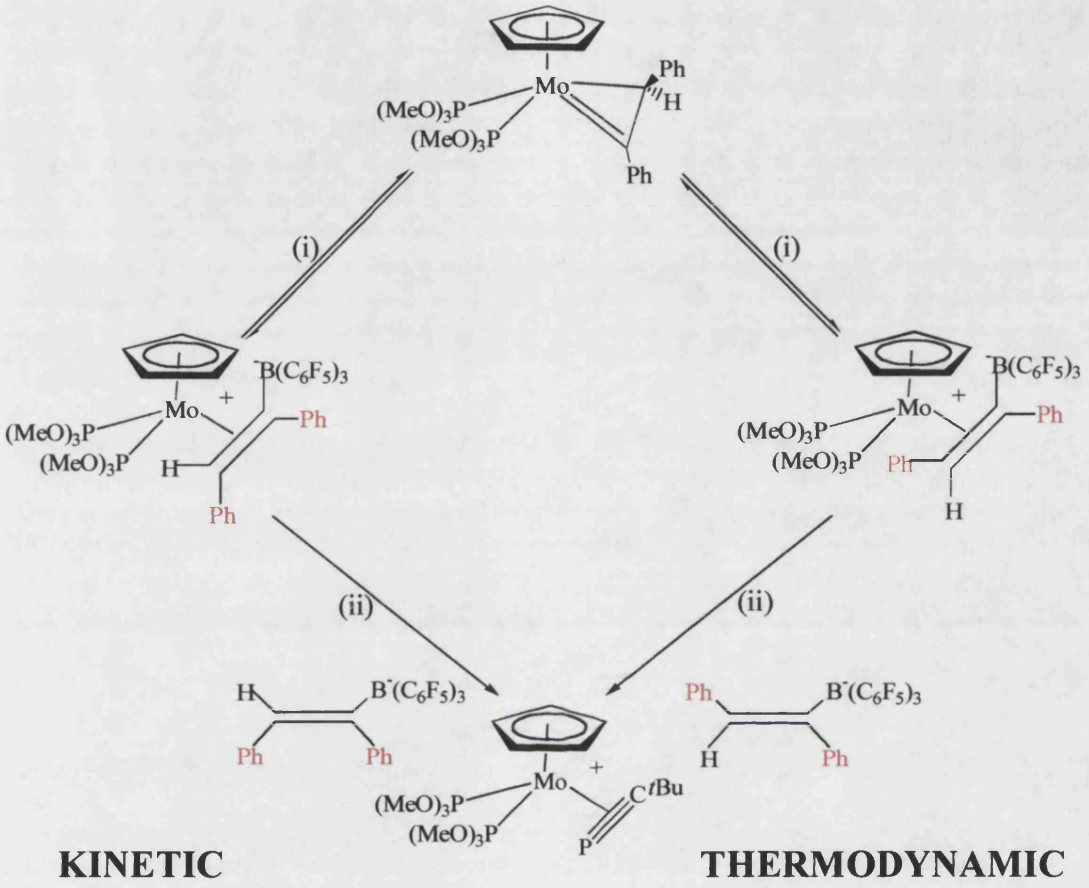

Scheme 4.9 *(i) $B(C_6F_5)_3$, (ii) tBuC≡P.*

In order to establish a better understanding of this process, we decided to continue the reactions by quenching the intermediate with other reagents. Firstly, an investigation of the reactivity of (8) with $B(C_6F_5)_3$ in the presence of CO was carried out. One equivalent of $B(C_6F_5)_3$ was added to (8) at -78 ^{O}C resulting in an immediate colour change (green → red). Carbon monoxide was then bubbled through the solution and as the temperature began to increase to room temperature there was a progressive colour change (red → orange).

Monitoring the reaction by IR spectroscopy indicated the presence of two metal bound carbonyl ligands identified by two strong infra red absorption bands at 1998 and 1927 cm^{-1}. The ^{31}P-{^{1}H}NMR spectrum of the reaction mixture revealed one singlet at 170.3 ppm, which was consistent with the cation being the *cis*-carbonyl cation $[Mo(CO)_2\{P(OMe)_3\}_2(\eta\text{-}C_5H_5)]^+$ $(88)^+$. The ^{11}B NMR exhibited two broad peaks at -4.4 and -5.6 ppm, which are analogous to those seen in the phosphaalkyne complex. However, the relative intensities of the two boron signals differed to those seen in (87). A plausible interpretation of these observations was that CO is a much better ligand than *t*BuC≡P and reacts at a much faster rate with the kinetic/themodynamic borane-substituted alkene intermediates, thus enabling the formation of the kinetic-based anion in excess of its thermodynamic counterpart.

In analogy with Bauers[139], who had prepared the *tetra*-substituted phosphite complex $[Mo\{P(OMe)_3\}_4(\eta\text{-}C_5H_5)][BF_4]$ (89) we decided to react (8) with $B(C_6F_5)_3$ in the presence of $P(OMe)_3$ with the intention of making the *tetra*-substituted phosphite cation and the unknown anion in the hope of being able to crystallise the complex, so to determine the structure of the anion. Prior to carrying out the reaction we felt it was important to react $B(C_6F_5)_3$ with neat $P(OMe)_3$ to determine if there was a reaction. As expected, $B(C_6F_5)_3$ reacted instantaneously with $P(OMe)_3$, and from a preliminary NMR study, it appeared that the reaction had generated an adduct.

With this knowledge, we still felt that the reaction should be carried out like the phosphaalkyne reaction, where the trapping reagent is added to the reaction mixture before the addition of $B(C_6F_5)_3$. Hence, the reaction was carried out by cooling (8) to -78 ^{o}C and adding two molar equivalents of $P(OMe)_3$, followed by one equivalent of $B(C_6F_5)_3$. On warming to room temperature there was a colour change

(green → brown) and after one hour at ambient temperature the solvent was removed in *vacuo*, leaving a brown oily residue.

After examining the ^{31}P-{^{1}H}NMR spectra of the reaction mixture, we were surprised to see two singlet resonances of equal intensity. The first resonance at 188.9 ppm was assigned to the *tetra*-substituted phosphite cation $(90)^+$, identical to $(89)^+$ (δ = 190.9 ppm), which reflects the equivalence of the phosphite moieties by a singlet in the ^{31}P-{^{1}H}NMR. However, we were uncertain of the nature of the second product which will be referred to as (91) and this was seen as a singlet at 175.6 ppm. On purification of the oil, carried out by washing with pentane, the oil began to solidify into a highly air sensitive red/brown powder. A further NMR study on the powder provided more information, as the singlet at 188.9 ppm completely disappeared leaving the singlet at 175.6 ppm.

Further information provided by NMR spectroscopy was even more surprising, in particular the ^{13}C-{^{1}H} spectrum which showed a low field triplet at 223.6 ppm [J(CP) = 13.5 Hz]. In addition to this was the ^{1}H NMR spectrum which exhibited a virtual triplet at 3.52 ppm [{J(HP) + J(HP')} = 10.99 Hz]. After much deliberation, it became apparent that the *tetra*-substituted phosphite cation $(90)^+$ was highly air sensitive and rapidly decomposed, however, it was uncertain why the remaining complex contained a low field resonance in the ^{13}C-{^{1}H} NMR which is consistent with the presence of a metal-carbon multiple bond. It soon became apparent, however, that the data for this unknown species (91) were remarkably similar to those of another species we were investigating in a parallel study.

As mentioned in Chapter One, there has been considerable interest within our group towards the reactivity of η^2(3e)-vinyl complexes. One of the investigations

related to the synthesis of a series of carbyne complexes and in particular, the findings that the η^2-vinyl complex [Mo{=C(Ph)CHPh}(CO)(PMe_2Ph)(η-C_5H_5)] (16) reacts with iodosobenzene to generate the carbyne complex [Mo($\equiv$CCHPh_2)(CO)(PMe_2Ph)(η-C_5H_5)] (17).[28] It was suggested that on initial reaction with PhIO, (16) generates a radical cation, which stabilises itself by rearranging into a carbyne complex, facilitated *via* a 1,2-phenyl shift (Scheme 4.10). This suggested that electron-rich η^2-vinyl complexes might readily undergo one-electron transfer reactions.

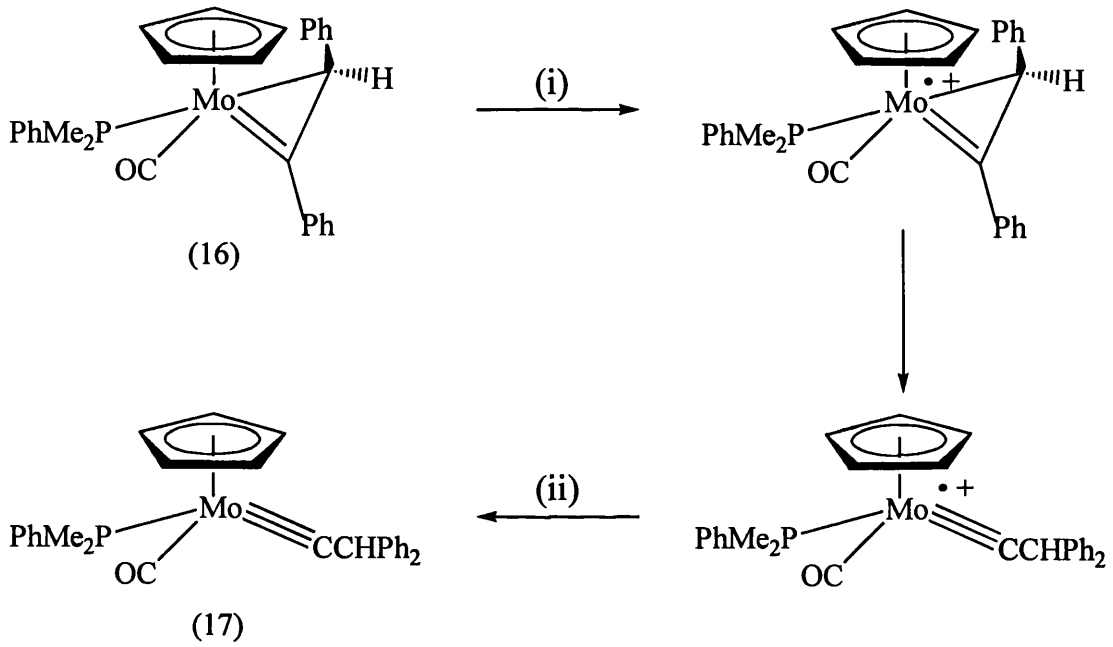

Scheme 4.10 *(i) +PhIO, -PhIO$^{\bullet+}$, (ii) +PhIO$^{\bullet+}$, -PhIO.*

In seeking to explore this idea we examined whether complex (8) would also undergo a one electron oxidation when reacted with the ferrocenium cation [Fe(η-C_5H_5)$_2$][PF_6]. The reaction could, as with other η^2(3e)-vinyls, lead to the generation of a radical cation followed by rearrangement to a 17e$^-$ carbyne. Our intention was to then investigate whether we could access the neutral carbyne

$[Mo\{\equiv CCHPh_2\}\{P(OMe)_3\}_2(\eta\text{-}C_5H_5)]$ through reduction of the $17e^-$ carbyne with reagents such as cobaltocene (Scheme 4.11).

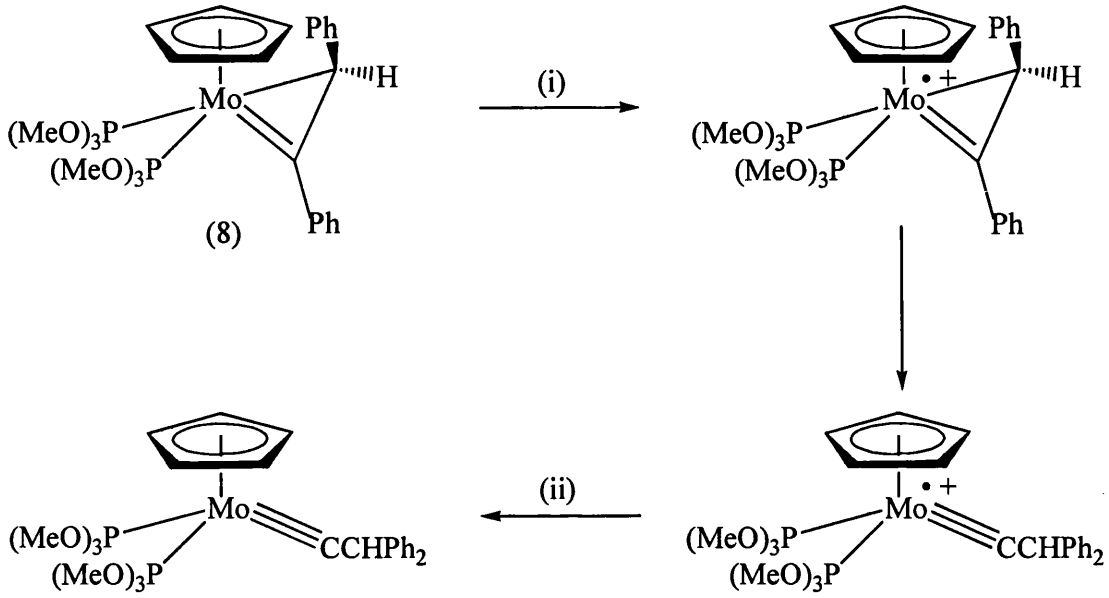

Scheme 4.11 *(i) $[Fe(\eta\text{-}C_5H_5)_2][PF_6]$, -$[Fe(\eta\text{-}C_5H_5)_2]$, (ii) $[Co(\eta\text{-}C_5H_5)_2]$, -$[Co(\eta\text{-}C_5H_5)_2][PF_6]$.*

The reaction was carried out by addition of one equivalent of $[Fe(\eta\text{-}C_5H_5)_2][PF_6]$ to a solution of (8) in CH_2Cl_2 at -78 °C. As the solution began to warm to room temperature, there was a progressive colour change (green → red). At room temperature, the solvent was removed *in vacuo* and on washing with hexane, a yellow solution was obtained which was shown to contain ferrocene.

Before reacting the remaining species with cobaltocene, we decided to attempt to measure the NMR spectrum of this species, although we expected to see a very broad spectrum because the expected $17e^-$ carbyne complex would be paramagnetic. However, we were surprised to discover that the NMR study revealed a clean diamagnetic species. The $^{31}P\text{-}\{^1H\}$ NMR exhibited a singlet at 175.6 ppm and more interesting was the $^{13}C\text{-}\{^1H\}$ NMR which displayed a low field triplet at 223.2 ppm

[J(CP) = 12.4 Hz]. It was the existence of this resonance that led us to believe that this compound was the η^2(4e)-alkyne cation [Mo{η^2(4e)-PhC$_2$Ph}{P(OMe)$_3$}$_2$(η-C$_5$H$_5$)][PF$_6$] (7)$^+$. A plausible explanation for this result is that the η^2(3e)-vinyl complex (8) undergoes a one-electron oxidation with [Fe(η-C$_5$H$_5$)$_2$][PF$_6$], to form the 17e$^-$ species (8)$^{\bullet+}$ which can then lose a hydrogen atom[140,141] to form the cationic η^2(4e)-alkyne complex (7)$^+$ (Scheme 4.12).

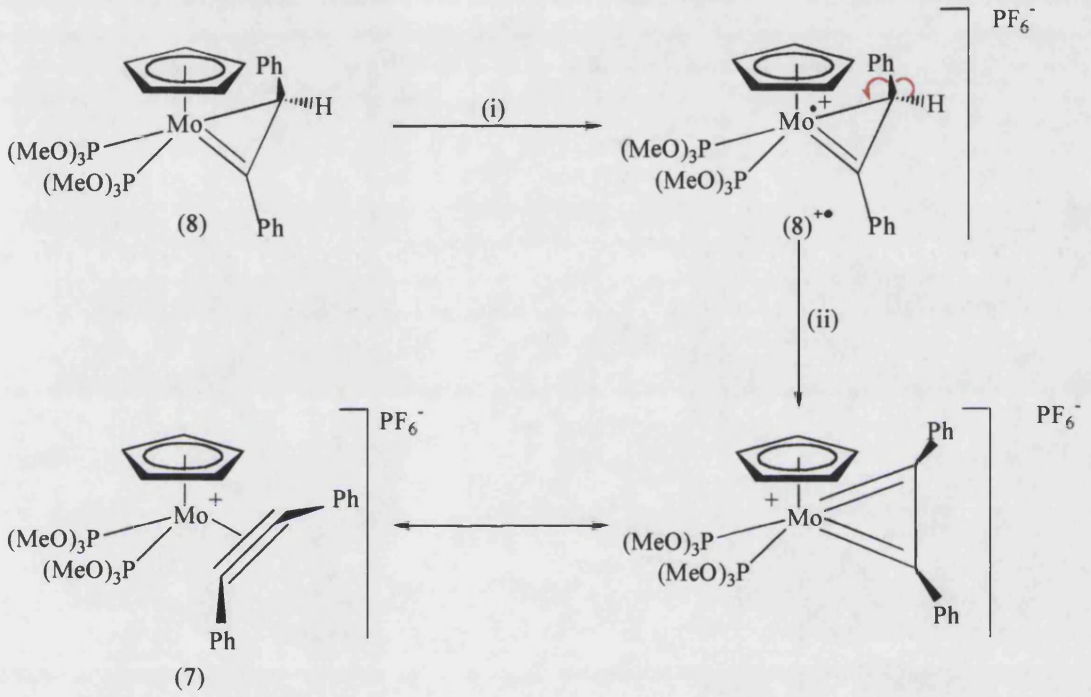

Scheme 4.12 *(i) + [Fe(η-C$_5$H$_5$)$_2$][PF$_6$], -[Fe(η-C$_5$H$_5$)$_2$], - H$^\bullet$.*

Consequently, it was the NMR data for the η^2(4e)-alkyne complex (7)$^+$ that appeared to be identical to the NMR spectra of the novel complex isolated when (8) is reacted with B(C$_6$F$_5$)$_3$ in the presence of P(OMe)$_3$, previously referred to as (91). The fact that the η^2(4e)-alkyne complex is formed in both reactions and the facility with which the d^4, η^2(3e)-vinyl complex (8) appeared to undergo a one-electron oxidation with [Fe(η-C$_5$H$_5$)$_2$][PF$_6$], suggested the interesting possibility that it might also

undergo electron transfer on treatment with $B(C_6F_5)_3$. This suggestion, if true began to pose many questions as to the nature of the reactions of $B(C_6F_5)_3$, was it possible that $B(C_6F_5)_3$ can act as a one electron oxidant? More importantly, why was it only in the presence of $P(OMe)_3$ that the η^2(4e)-alkyne cation $(91)^+$ [which is equivalent to $(7)^+$] is generated, whereas in the presence of *t*BuC≡P or CO, the cations $(87)^+$ and $(88)^+$ are generated respectively.

To clarify these questions, we began to reanalyse all our data. In doing so we were surprised to find that the NMR spectra indicated the presence of small traces of the η^2(4e)-alkyne species $(91)^+$ in addition to the main products of the reactions with *t*BuC≡P and CO. We were therefore initially confused as to how $B(C_6F_5)_3$, a well established strong Lewis acid, could bring about a one-electron oxidation.

An insight into the processes involved in these reactions was obtained by following these reactions by EPR spectroscopy. One equivalent of $[Fe(\eta\text{-}C_5H_5)_2][PF_6]$ was added to a solution of (8) in CH_2Cl_2/thf (1:2) at 195 K. As the reaction mixture was allowed to warm from 195 K to 260 K, a well resolved isotropic EPR spectrum was observed as a doublet of doublet of doublets with Mo satellites [$A(^1H)$ 8.0 G, $A(^{31}P^1)$ 23.7 G, $A(^{31}P^2)$ 37.8 G, $A(^{95,97}Mo)$ 17.0 G; g_{iso} = 2.011] (Figure 4.6). On warming to room temperature, the signal collapsed suggesting that the reaction involved an initial one-electron oxidation to form the 17e$^-$ radical cation $(8)^{\bullet+}$, which was stabilised by significant delocalisation of the spin onto the η^2-vinyl fragment. It was therefore conceivable that the η^2(4e)-alkyne cation $(7)^+$ was generated by H$^\bullet$ loss from the β-carbon of the η^2-vinyl radical cation $(8)^{\bullet+}$.

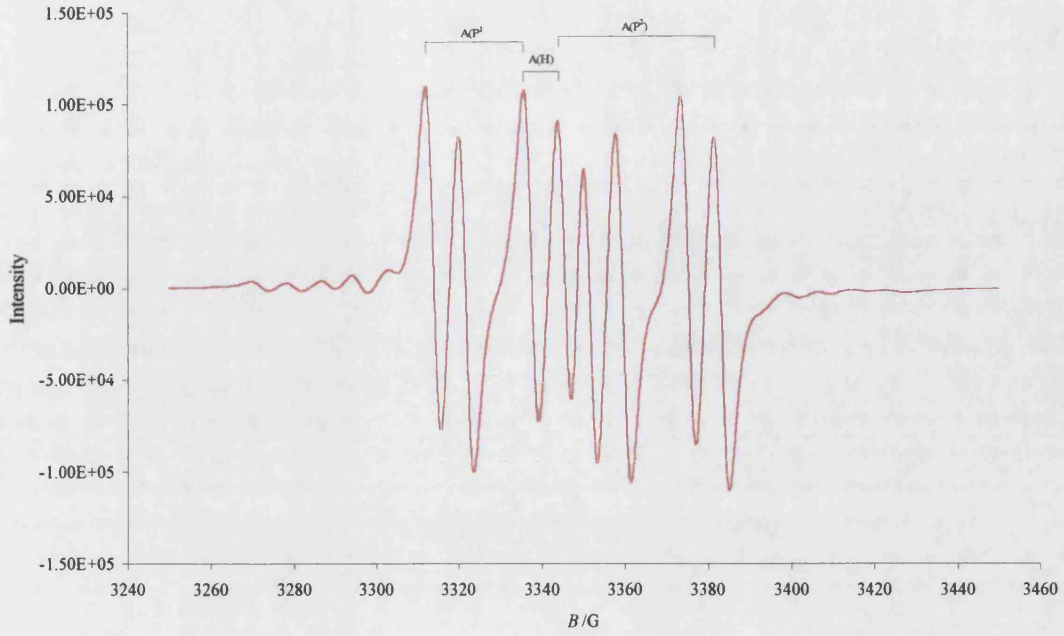

Figure 4.6 *EPR Spectrum of (8) + $[Fe(\eta\text{-}C_5H_5)_2][PF_6]$.*

When this reaction was repeated with the deuterated η^2(3e)-vinyl complex $[Mo\{=C(Ph)CDPh\}\{P(OMe)_3\}_2(\eta\text{-}C_5H_5)]$ (8D) at 260 K in CH_2Cl_2, the corresponding EPR signal was observed (Figure 4.7) as a doublet of doublets with Mo satellites [$A(P^1)$ 23.8 G, $A(P^2)$ 37.9 G, A(Mo) 16.9 G; g_{iso} = 2.011]. Thus, the EPR data for (8) and (8D) fully support the rationale shown in Scheme 4.11.

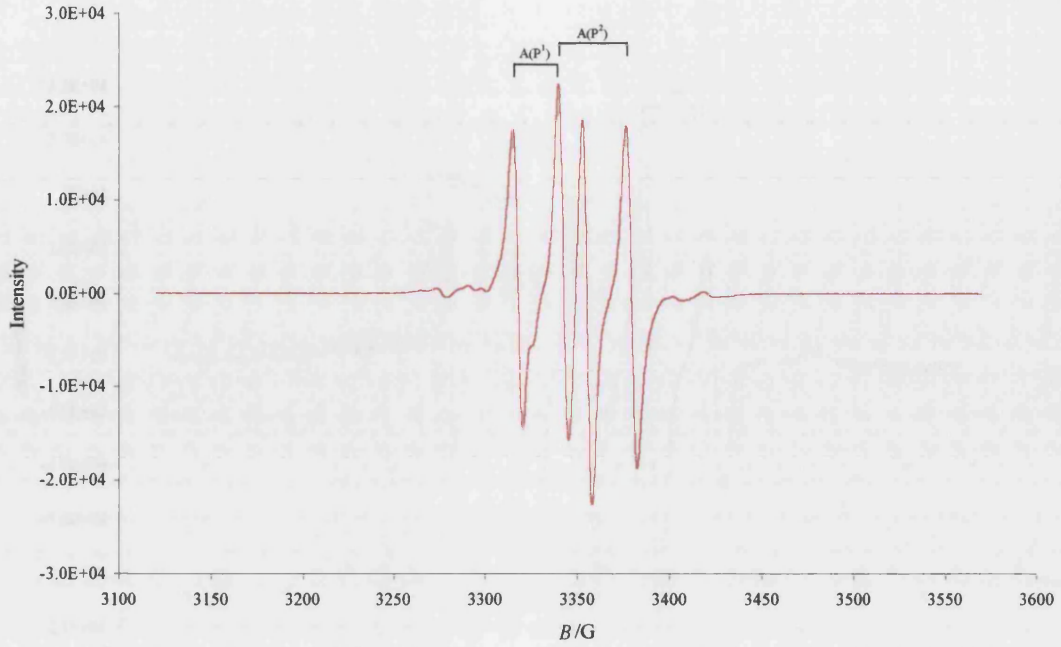

Figure 4.7 *EPR Spectrum of (8D) + [Fe(η-C_5H_5)$_2$][PF_6].*

Interestingly, when $B(C_6F_5)_3$ was added to a solution of (8) in CH_2Cl_2/dichloroethane at 195 K and the reaction mixture was allowed to warm to 260 K, the EPR spectrum was identical to that observed when [Fe(η-C_5H_5)$_2$][PF_6] was added to a solution of (8) (Figure 4.8). In addition to this was a minor unidentified molybdenum centred radical species, thus implying that $B(C_6F_5)_3$ was acting as a one-electron oxidant. Significantly, there was no evidence for the formation of a boron centred radical species. When $B(C_6F_5)_3$ was reacted with the deuterated complex (8D) in CH_2Cl_2, the EPR signal for $(8D)^{\bullet+}$ appeared as expected and was stable at 260 K. This also contained the same minor molybdenum radical species present in $(8)^{\bullet+}$, which appears as a triplet in the EPR and has a g value of 1.975 (Figure 4.9).

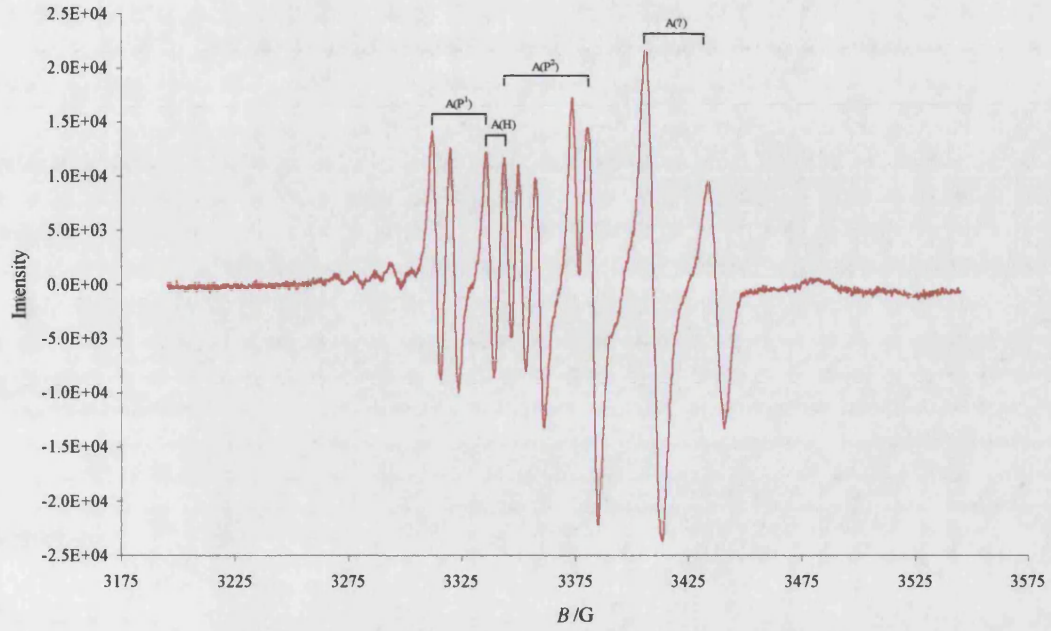

Figure 4.8 *EPR spectrum of (8) + $B(C_6F_5)_3$.*

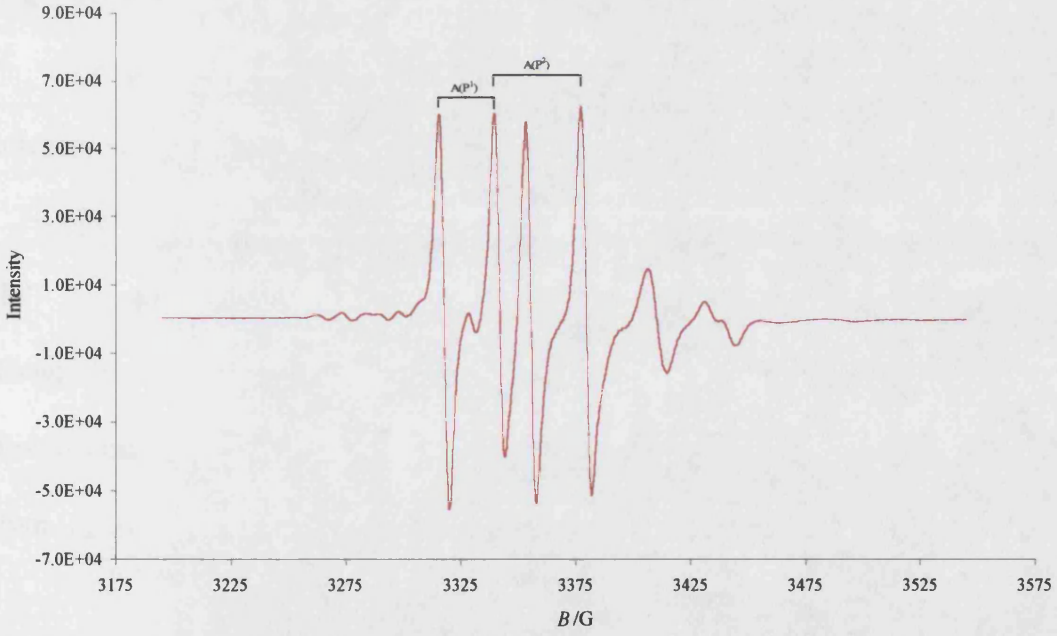

Figure 4.9 *EPR spectrum of (8D) + $B(C_6F_5)_3$.*

These observations were very surprising as they implied that the corresponding radical cation $(8)^{\bullet+}$ could be efficiently generated by using $[Fe(\eta\text{-}C_5H_5)_2][PF_6]$ or $B(C_6F_5)_3$. From the evidence presented for both systems, the most probable explanation indicated that $B(C_6F_5)_3$, like $[Fe(\eta\text{-}C_5H_5)_2][PF_6]$ can also act as a one-electron oxidant. This result was unexpected as, to the best of our knowledge, there were no reports of $B(C_6F_5)_3$ acting as a one-electron oxidant, moreover, this possibility did not seem to have been considered.

In fact, when it is remembered that $B(C_6F_5)_3$ is isoelectronic to the well-known one-electron oxidant $[CPh_3]^+$, it becomes a very plausible suggestion that $B(C_6F_5)_3$ should also have the potential to be a one-electron oxidant. In making a further analogy, η^2(3e)-vinyls can be viewed as metallacyclopropenes and because of the isolobal relationship which exists between $CH\leftrightarrow MoL_2(\eta\text{-}C_5H_5)$, it can be expected that they would show reactivity patterns similar to those found with cyclopropenes.

This was confirmed when it was observed that addition of $[Ph_3C][BF_4]$ to a solution of (8) exhibited the same signal as was observed when adding $[Fe(\eta\text{-}C_5H_5)_2][PF_6]$ and $B(C_6F_5)_3$. In addition to the signal attributed to the radical cation $(8)^{\bullet+}$ was the characteristic signal of the $Ph_3C^{\bullet}$ radical[142] (Figure 4.11). Both signals disappeared on warming to room temperature and it was interesting that the rate of disappearance of $(8)^{\bullet+}$ was faster than was observed when this species was generated from (8) and $[Fe(\eta\text{-}C_5H_5)_2][PF_6]$ or $B(C_6F_5)_3$.

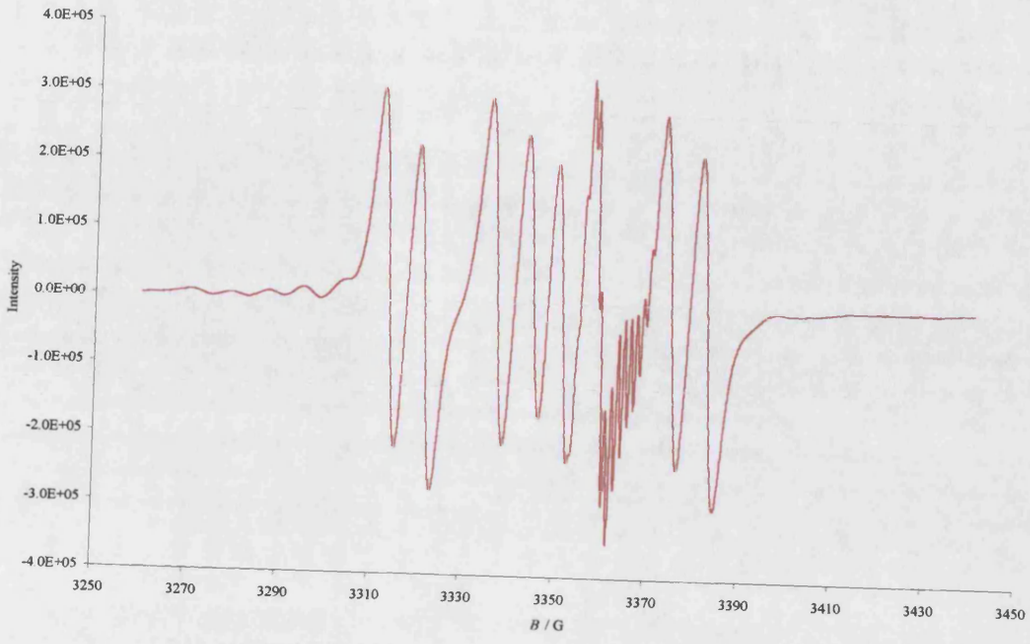

Figure 4.10 *EPR spectrum of (8) + $[Ph_3C][BF_4]$.*

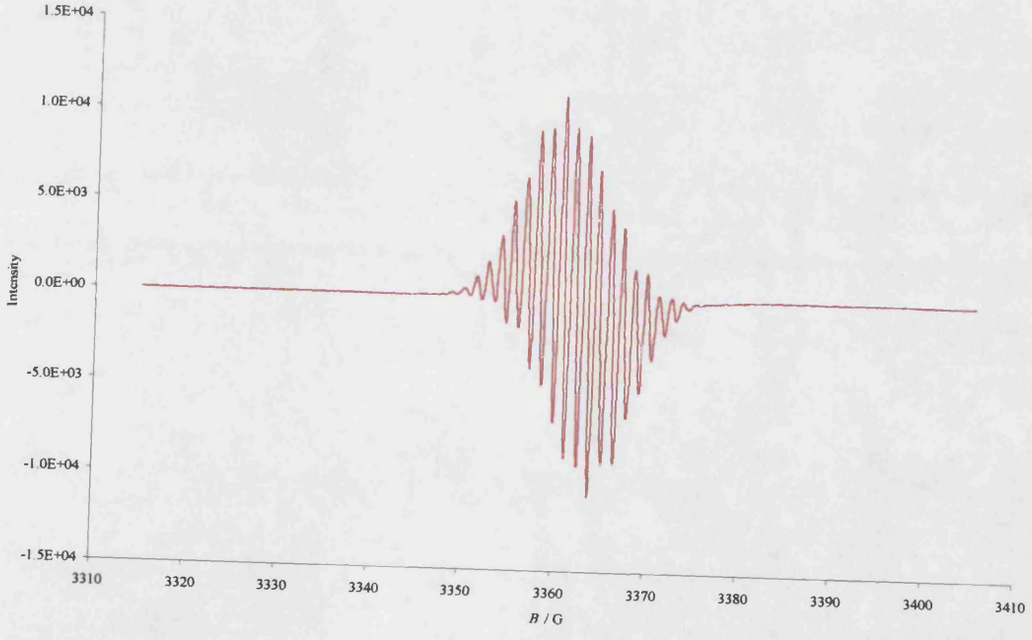

Figure 4.11 *EPR spectrum of $Ph_3C^{\bullet}$, subtracted from $(8)^{\bullet+}$ (Figure 4.6).*

Further support for these suggestions came from both an EHMO calculation and a Cyclic Voltammogram. An EHMO calculation based on the established bond parameters for (8), indicated the presence of a metal centred HOMO (32 % d_z^2, 42 % d_{xy}, 2% d_{xz}, 4% d_{yz}) from which an electron could be easily removed (Figure 4.12).

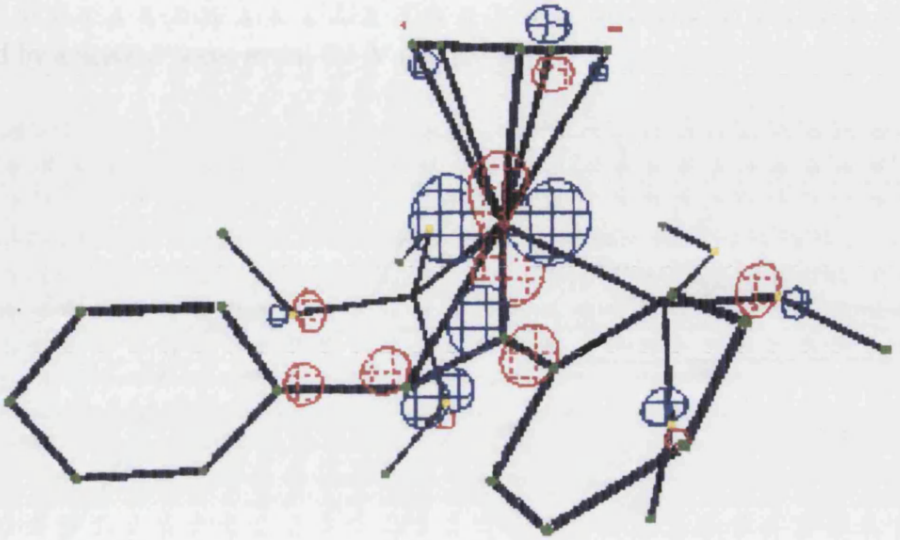

HOMO

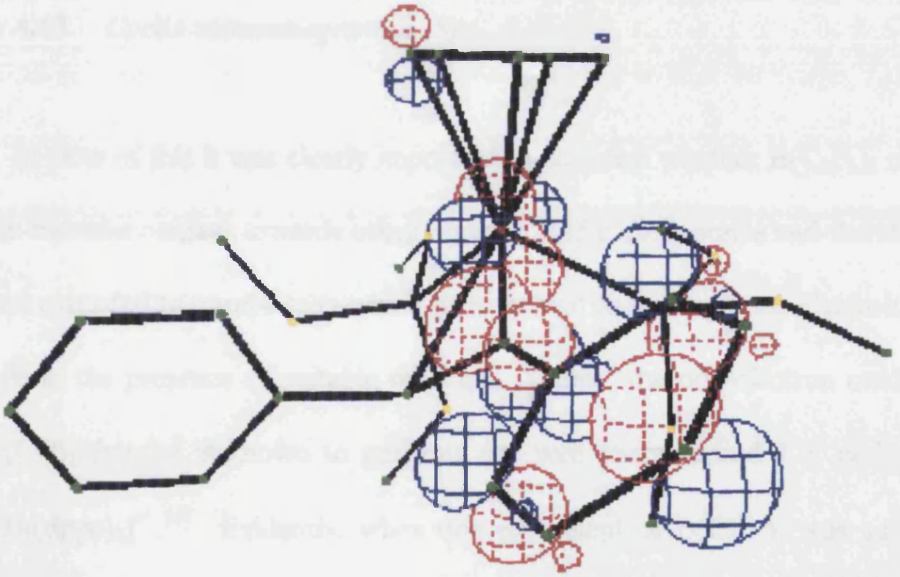

LUMO

Figure 4.12 *Representations of the theoretical HOMO and LUMO orbitals for* $[Mo\{=C(Ph)CHPh\}\{P(OMe)_3\}_2(\eta\text{-}C_5H_5)]$ *(8).*

The cyclic voltammogram (CV) of (8) in CH_2Cl_2 at a platinum electrode shows a reversible oxidation wave at *ca.* -0.11 V, implying the ready formation of $(8)^{\bullet+}$, followed by a second wave at *ca.* 0.1 V (Figure 4.13).

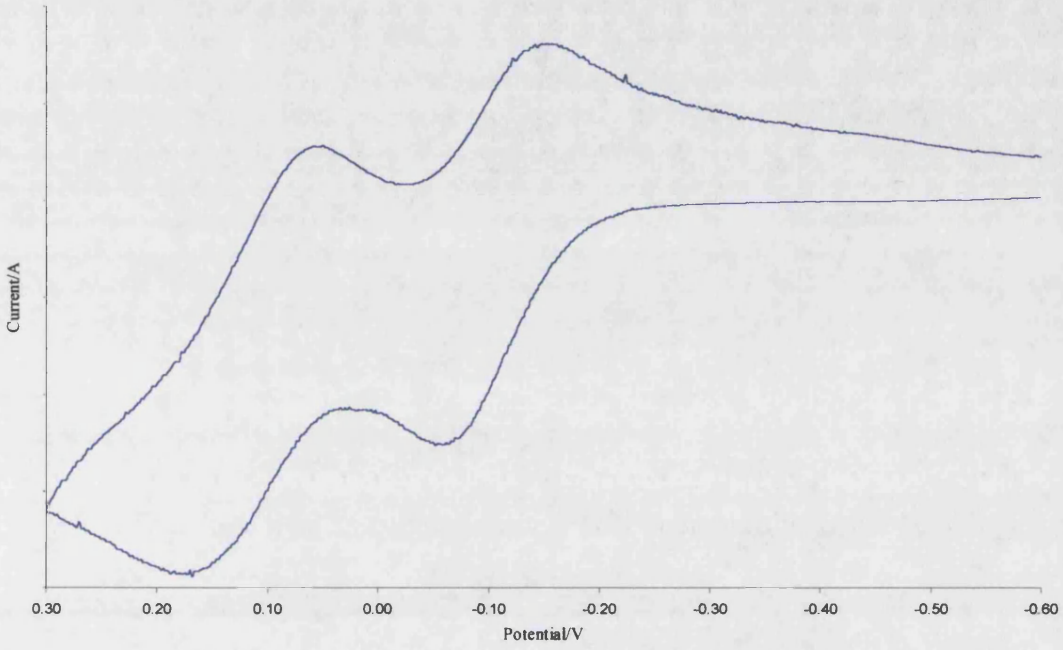

Figure 4.13 *Cyclic voltammogram of (8).*

In view of this it was clearly important to establish whether $B(C_6F_5)_3$ could act as a one-electron oxidant towards other organometallic compounds and the study was therefore extended to compounds which were known to undergo one electron transfer reactions in the presence of suitable oxidants. Hence, the one-electron oxidation of *cis*-$[Cr(CO)_2(dppe)_2]$ is known to generate the well characterised 17e$^-$ cation *trans*-$[Cr(CO)_2(dppe)_2]^{\bullet+}$.[143] Evidently, when one equivalent of $B(C_6F_5)_3$ was added to a solution of the d^6-complex *cis*-$[Cr(CO)_2(dppe)_2]$ in toluene at 195 K, a rapid reaction occurred. On monitoring this reaction by EPR spectroscopy, a well resolved signal appeared at 260 K in CH_2Cl_2. This signal was a 1:4:6:4:1 quintet, [A(^{31}P), 28.5 G, g value 2.012] which was consistent with literature data [A(^{31}P) 28.6 G, g value

2.012][143] for *trans*-$[Cr(CO)_2(dppe)_2]^{\bullet+}$ (Figure 4.14), thus providing further support that $B(C_6F_5)_3$ can act as a one-electron oxidant.

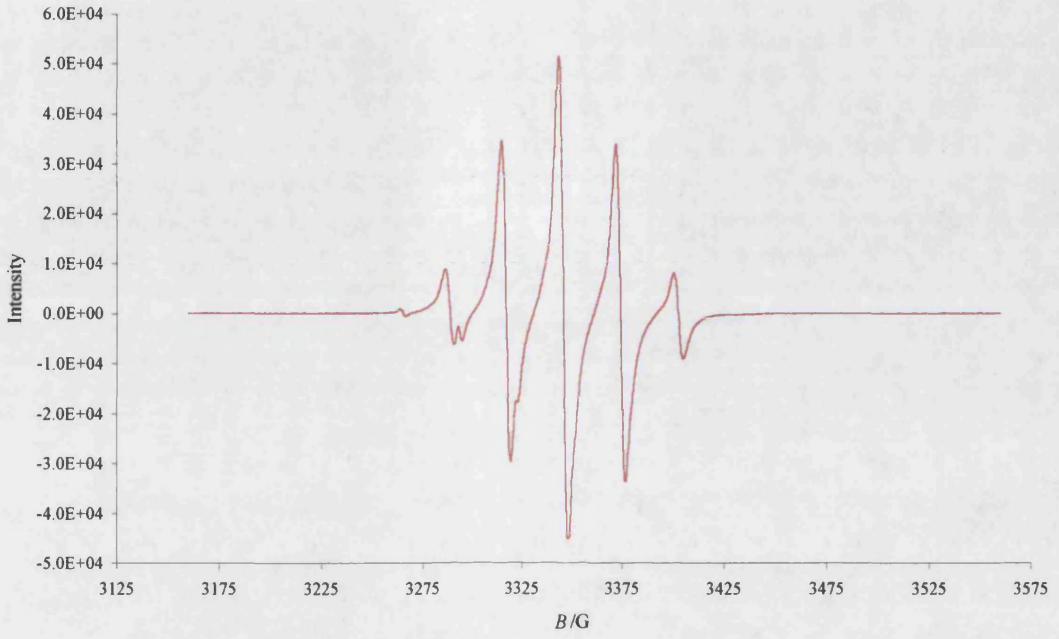

Figure 4.14 *EPR spectrum of cis-$[Cr(CO)_2(dppe)_2]$ + $B(C_6F_5)_3$.*

Although the evidence to support the suggestion that $B(C_6F_5)_3$ can act as a one-electron oxidant appeared clear, there were still questions that needed to be answered with respect to the nature of the borane radical once the one-electron transfer reaction has taken place. In contrast to the reactivity of (8) with $[Ph_3C][BF_4]$, in which the generated trityl radical was seen in the EPR, there was no evidence for a boron centred radical in the EPR of (8) with $B(C_6F_5)_3$. However, it was felt that the conditions for stabilising such a reactive radical species were not possible and that it was probable that the highly reactive species $[B(C_6F_5)_3]^{\bullet-}$ scavenges traces of water from the solvent, generating the known counter anion $[HOB(C_6F_5)_3]^-$ and $H^\bullet$ (Scheme 4.13).

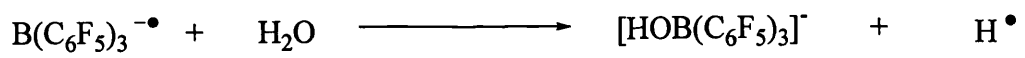

Scheme 4.13

This assumption was consistent with all the reactions which have been reported for $B(C_6F_5)_3$ in which the borane anions were still unidentified. The anion $[HOB(C_6F_5)_3]^-$ has been characterised previously and is shown to have a ^{11}B NMR resonance at -4.2 ppm.[85] As mentioned previously, the reactions of (8) with $B(C_6F_5)_3$ in the presence of either *t*BuC≡P or CO, both contain two ^{11}B NMR resonances that we were unable to formally identify. However, it is highly likely that the peak at -4.3 ppm can be attributed to $[HOB(C_6F_5)_3]^-$ and that at -5.6 ppm to $[(C_6F_5)_3B(\mu\text{-}OH)B(C_6F_5)_3]^-$, which is generated by further reaction of $[HOB(C_6F_5)_3]^-$ with $B(C_6F_5)_3$ (previously discussed in Chapter Two, Section 2.5).

Thus, it is suggested that the reaction can take two main reaction paths (Scheme 4.14). As already discussed, the evidence suggests that step one is a one electron oxidation process generating the radical cation $(8)^{\bullet+}$ and the radical anion $B(C_6F_5)_3^{\bullet-}$. It is at this stage when there are two reaction paths, the reason being because of the highly reactive anion. The radical anion scavenges water, probably from the solvent, generating the hydroxy anion $^-HOB(C_6F_5)_3$ and H$^\bullet$. Simultaneous to this process, the radical cation is undergoing two processes, the first being a H$^\bullet$ loss to generate the 4e$^-$ alkyne as seen with $[Fe(\eta\text{-}C_5H_5)_2][PF_6]$ and $[Ph_3C][BF_4]$. The second however, is a radical-radical combination reaction, with the radical cation $(8)^{\bullet+}$ reacting with H$^\bullet$ (generated from $^{\bullet-}B(C_6F_5)_3$ + H_2O) to generate the *trans*-stilbene complex (92) (Scheme 4.14).

This rationale explains why in the reactions of (8) with $B(C_6F_5)_3$ in the presence of CO or *t*BuC≡P, the alkyne complex is generated in addition to (88) or (87). The 4e⁻ phosphaalkyne complex and the *cis*-carbonyl complex are both generated by a stilbene displacement reaction. Therefore, in the case of *t*BuC≡P and CO, H• addition to $(8)^{\bullet+}$ is much faster than H• loss thus giving rise to the co-ordinated *trans*-stilbene complex (92). Thus, stilbene displacement reactions predominate over the formation of the η^2(4e)-alkyne complex (91).

Surprisingly, although the reaction of (8) with $B(C_6F_5)_3$ in the presence of $P(OMe)_3$ generated the *tetrakis* phosphite complex (90) and the η^2(4e)-alkyne complex (91), only (91) was stable. The formation of (91) can be explained by the initial one-electron oxidation taking place, however, as the radical cation is produced, the radical anion reacts with $P(OMe)_3$ in preference to traces of water. This means that the radical anion forms $[MeOB(C_6F_5)_3]^-$ rather than $[HOB(C_6F_5)_3]^-$ and in doing so, hinders the generation of H•. Because there is little or no H• formed, the radical-radical combination reaction between H• and the radical cation $(8)^{\bullet+}$, and thus, the formation of the *trans*-stilbene complex (92), is curtailed. Consequently, there is very little or no competing process between H• loss and H• addition and the radical cation is forced to lose H•, generating the η^2(4e)-alkyne complex (91) almost exclusively.

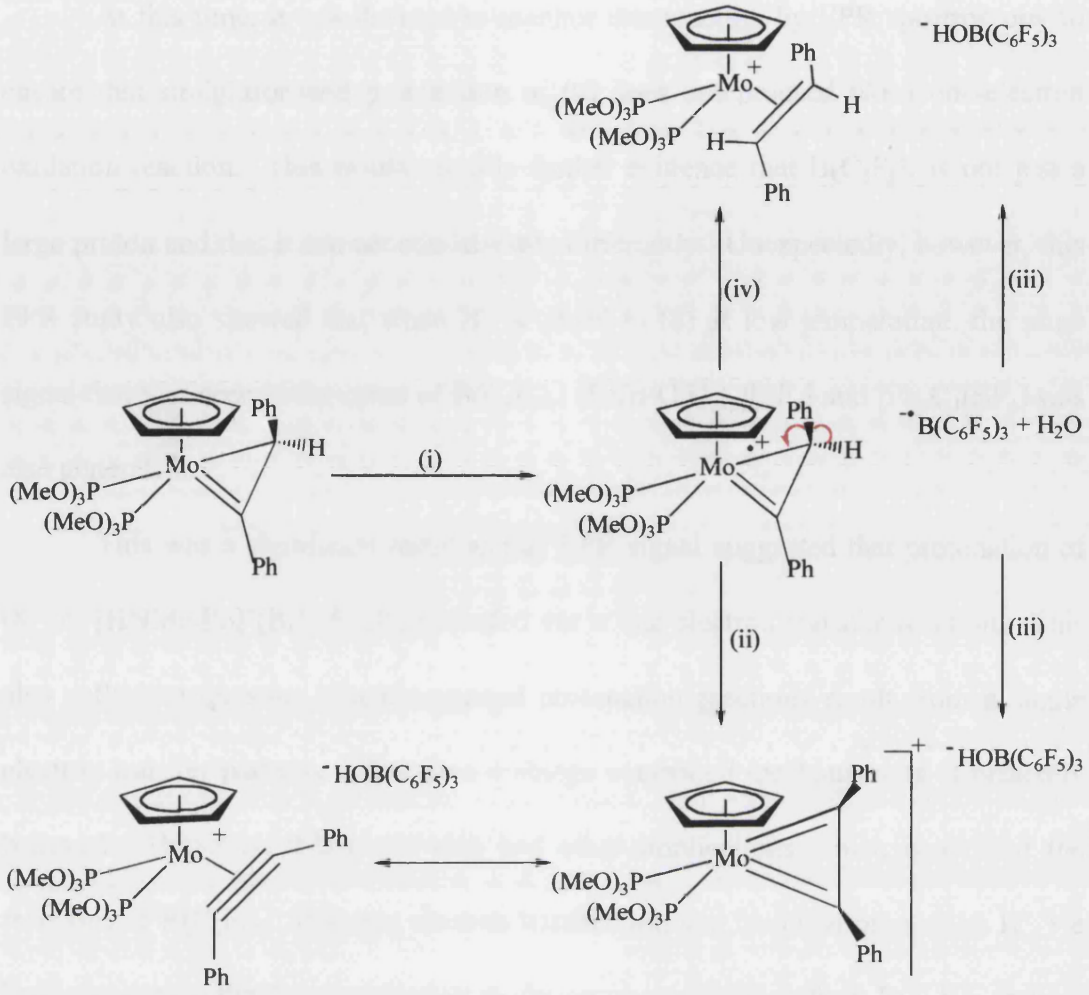

Scheme 4.14 *(i) $B(C_6F_5)_3$, (ii) $-H^{\bullet}$, (iii) $-H^{\bullet}$, (iv) $+H^{\bullet}$.*

It was obviously desirable to try and obtain a crystal structure of an η^2(4e)-bonded phosphaalkyne complex and as (85) and (87) were oils the aim was to investigate the protonation of (8) in the presence of phosphaalkyne using other protonation sources, with the aim of promoting access to a more crystalline complex. Therefore, $[HNMe_2Ph]^+[B(C_6F_5)_4]^-$, a source of H^+ proved effective in this aim. The reaction of (8) with $[HNMe_2Ph]^+[B(C_6F_5)_4]^-$ in the presence of *t*BuC≡P was carried out by Lynam[144] and was found to generate $[Mo(\eta^2\text{-}P{\equiv}C\textit{t}Bu)\{P(OMe)_3\}_2(\eta\text{-}C_5H_5)]^+[B(C_6F_5)_4]^-$ in quantitative yield.

At this time, it was decided to monitor this reaction by EPR spectroscopy to ensure that straightforward protonation of (8) does not proceed *via* a one-electron oxidation reaction. This would provide further evidence that $B(C_6F_5)_3$ is not just a large proton and that it can act considerably differently. Unexpectedly, however, this EPR study also showed that when H^+ is added to (8) at low temperature, the same signal that was seen in the cases of $B(C_6F_5)_3$, $[Fe(\eta\text{-}C_5H_5)_2][PF_6]$ and $[Ph_3C][BF_4]$ was also generated.

This was a significant result as this EPR signal suggested that protonation of (8) by $[HNMe_2Ph]^+[B(C_6F_5)_4]^-$ proceeded *via* a one-electron transfer reaction. This also calls into question whether general protonation reactions result from a single electron transfer pathway rather than a charge controlled mechanism as is presently believed. However, this result also had other implications which concerned the reactions of $B(C_6F_5)_3$. If single electron transfer was the favoured process by H^+, we had to be certain that the one electron oxidation was originating from $B(C_6F_5)_3$ and not from its hydrolysed counterpart, $H[HOB(C_6F_5)_3]$, which is also a source of H^+.

Further efforts were therefore made to solve this problem by a more detailed analytical study on all of the data. The presence of a signal at +52 ppm in the ^{11}B NMR in the reaction between (8) and $B(C_6F_5)_3$ in the presence of phosphaalkyne gave the primary evidence that there remained unreacted $B(C_6F_5)_3$ in this reaction which was still intact, *i.e.* not hydrolysed. Secondly, we began to realise that it was only in the cases where $B(C_6F_5)_3$ had been employed as the oxidant towards (8) that we had the emergence of two products, the η^2(4e)-alkyne complex (91) and the stilbene complex (92). In contrast, the reactions that used $[Fe(\eta\text{-}C_5H_5)_2]$ or $[Ph_3C][BF_4]$

generated (91) only and from the experiment using $[HNMe_2Ph]^+[B(C_6F_5)_4]^-$ and (8), only the *trans*-stilbene complex (92) was obtained.

Therefore, this evidence suggested that the formation of the two products derived from a competitive reaction path, *i.e.* (91) is not an intermediate to the formation of (92) and *vice versa*. However, the interesting observation that $B(C_6F_5)_3$ demonstrates a duality with respect to the other one-electron oxidants gave us an insight to the problem. In order to propose a plausible explanation, a mechanism has been depicted in Scheme 4.15 which suggests a stepwise pathway for the formation of both (91) and (92) and therefore complexes (87), (88) and (90).

Scheme 4.15 depicts three possible routes: route 1 = (i) → (iii), route 2 = (i) → (iv) and route 3 = (i) or (ii) → (v). Interestingly, the common factor through out each reaction path is that they all generate the radical cation fragment $(8)^{\bullet+}$ as the initial step. The reaction paths are then dependent upon two conditions: firstly, whether we are using $B(C_6F_5)_3$ or its hydrolysed counterpart $H[HOB(C_6F_5)_3]$ and secondly, whether the reaction conditions *e.g.* solvents are totally anhydrous or contaminated with traces of H_2O.

Route 1 can only be followed by using $B(C_6F_5)_3$ in conjunction with $P(OMe)_3$. The η^2(4e)-alkyne complex (91) is generated by the one-electron oxidation of (8) by $B(C_6F_5)_3$, followed by the reaction of the radical anion $^{\bullet-}B(C_6F_5)_3$ with $P(OMe)_3$. The radical cation is forced to stabilise itself by losing $H^\bullet$ as the radical anion combines with $P(OMe)_3$ to form $[MeOB(C_6F_5)_3]^-$.

The mechanistic pathway of route 2 can only be obtained by using $B(C_6F_5)_3$ under completely anhydrous reaction conditions. In an earlier discussion we pointed out the isoelectronic relationship between $[CPh_3]^+$ and $B(C_6F_5)_3$. Theoretically, this

could imply that under the right reaction conditions, $^{\bullet-}B(C_6F_5)_3$ could also abstract $H^{\bullet}$ from the radical cation $(8)^{\bullet+}$, generating the η^2(4e)-alkyne cation $(91)^{+}$ and $[HB(C_6F_5)_3]^{-}$.

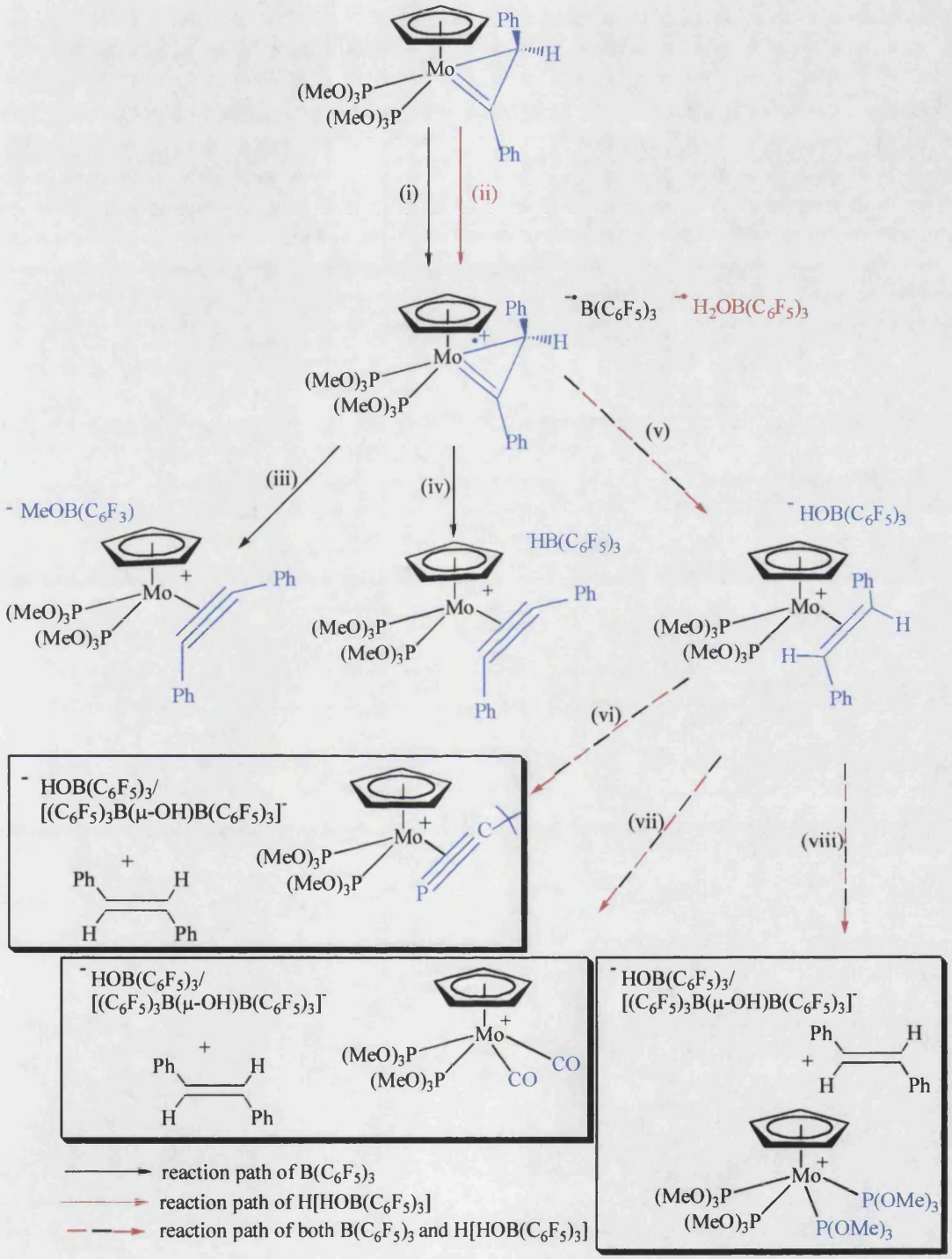

Scheme 4.15 *(i) $B(C_6F_5)_3$, (ii) $H[HOB(C_6F_5)_3]$, (iii) $P(OMe)_3$, (iv) anhydrous conditions, (v) traces of H_2O, (vi) tBuC≡P, (vii) CO, (viii) $P(OMe)_3$.*

Experimentally, $[HB(C_6F_5)_3]^-$ has never been identified as the major counter-anion in any of the experiments where $B(C_6F_5)_3$ has been used, however, a minor peak in the ^{11}B-$\{^1H\}$ NMR at -17.4 ppm (in the reaction between (8) and $B(C_6F_5)_3$ in the presence of CO) correlates to the generation of $[HB(C_6F_5)_3]^-$ in small yield. Therefore, it can be suggested that under ideal reaction conditions, the reaction between (8) and $B(C_6F_5)_3$ would generate $(91)^+$ and $[HB(C_6F_5)_3]^-$ in quantitative yield.

Route 3 can be followed by using either $B(C_6F_5)_3$ or $H[HOB(C_6F_5)_3]$. Initially, this is true as the EPR data imply that both reagents can act as one-electron oxidants. However, to generate the co-ordinated *trans*-stilbene complex involves either the radical anion $^{\bullet-}B(C_6F_5)_3$ reacting with H_2O, generating a source of $H^\bullet$ which combines with $(8)^{\bullet+}$ to form the stilbene complex (92) or the radical anion $^{\bullet-}H[HOB(C_6F_5)_3]$ which reacts with $(8)^{\bullet+}$ to also form (92). In the presence of reagents such as *t*BuC≡P, CO and $P(OMe)_3$, stilbene can be displaced creating the complexes (87), (88) and (90) [Scheme 4.15 (vi)-(viii)].

Therefore, we suggest that the reason why (91) and (92) can both be generated is due to a combination of routes 1-3. In particular, the reactions that were carried out in the presence of CO and *t*BuC≡P clearly established by NMR studies that the counter-anions $[HB(C_6F_5)_3]^-$, $[HOB(C_6F_5)_3]^-$ and $[(C_6F_5)_3B(\mu\text{-}OH)B(C_6F_5)_3]^-$ were all produced in varying yields. This is a subtle indication that the formation of these anions are co-dependent upon the reaction conditions as the hydrolysis of $B(C_6F_5)_3$ to $H[HOB(C_6F_5)_3]$ and the amount of trace H_2O in the solvent or glassware will vary significantly in each reaction. We conclude that these are the reasons why we suggest that $B(C_6F_5)_3$ can act as a one-electron oxidant and why, with respect to other established one-electron oxidants, $B(C_6F_5)_3$ can display a duality.

The only experiment that we are uncertain about is the low temperature NMR study concerning the addition of $B(C_6F_5)_3$ to (8) at -78 ^oC. The NMR spectra (Figures 4.3 and 4.4) appear to be dynamic and upon raising the temperature from -78 ^oC to room temperature there is evidence to suggest the formation of kinetic and thermodynamic isomers, which we had previously explained in terms of *cis*- and *trans*-isomers of $(F_5C_6)_3BCPh{=}CPhH$, the essential feature being that the kinetic isomer is unstable. Our original thoughts on this study was that $H^{\bullet}$ reacts with $(8)^{\bullet}$ to initially form co-ordinated *cis*-stilbene. One could argue that this dynamic process could be caused by one end of the co-ordinated *cis*-stilbene turning through an angle of 180 ^{o}, generating the *trans*-stilbene complex (92) (Scheme 4.16). This process is energetically favourable when it is considered that the co-ordinated alkene can slip from $\eta^2 \rightarrow \eta^1$ which facilitates the isomerisation process.[145]

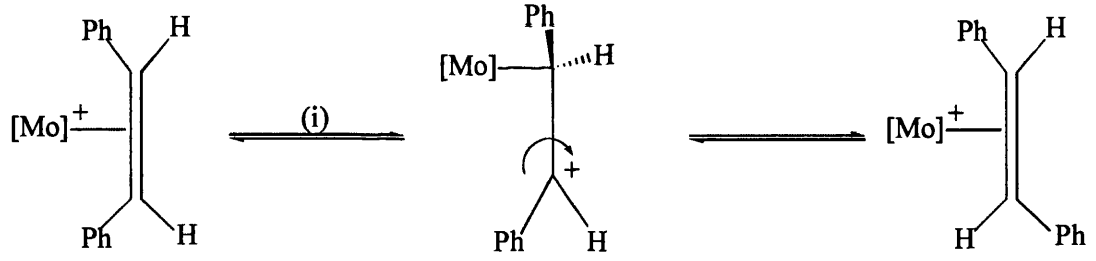

Scheme 4.16 *(i) -78 $^oC \rightarrow +25\,^oC$ (where [Mo] = $[Mo\{P(OMe)_3\}_2(\eta\text{-}C_5H_5)]$).*

However, we have found that all six *o*-fluorines, all six *m*-fluorines and all three *p*-fluorines present in the $B(C_6F_5)_3$ residue also undergo the mutual interconversion (Figure 4.4) This could indicate that the $[HOB(C_6F_5)_3]^-$ does not act as an innocent anion and as the *cis/trans*-stilbene complexes are co-ordinatively unsaturated, there is a

vacant co-ordination site available at the metal to which the anion could co-ordinate (Scheme 4.17). This would be in analogy to the work of Puddephat[60] who reported that $[HOB(C_6F_5)_3]^-$ co-ordinates to $[PtMe(bu_2bpy)]^+$ through the oxygen atom (Chapter 2 Scheme 2.15).

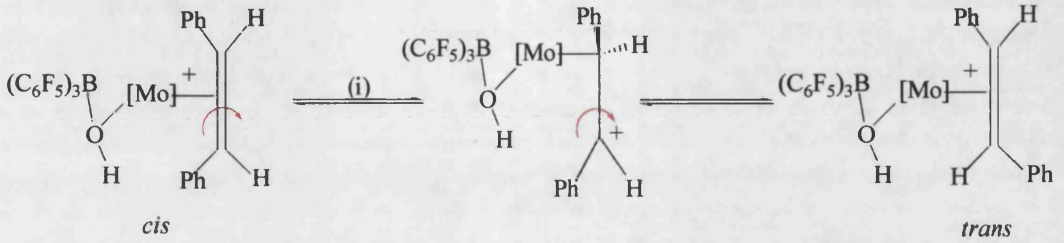

Scheme 4.17 *(i) -78 $^{O}C \rightarrow +25\,^{O}C$ (where [Mo] = [Mo{P(OMe)$_3$}$_2$(η-C_5H_5)]).*

A third explanation for this dynamic process is that $H^{\bullet}$ reacts with the molybdenum metal centre rather than the vinyl ligand, hence generating the metal hydride complex $[Mo\{=C(Ph)CHPh\}H\{P(OMe)_3\}_2(\eta\text{-}C_5H_5)]^+[HOB(C_6F_5)_3]^-$. This can then rearrange to the *trans*-stilbene complex by migration of the hydrogen from the metal onto the α-carbon of the η^2(3e)-vinyl ligand (Scheme 4.18).

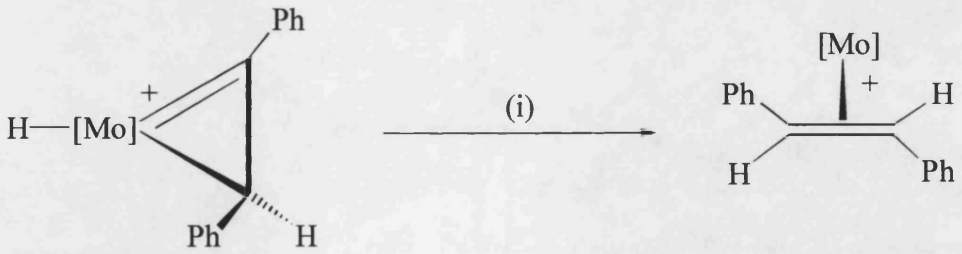

Scheme 4.18 *(i) -78 $^{O}C \rightarrow +25\,^{O}C$ (where [Mo] = [Mo{P(OMe)$_3$}$_2$(η-C_5H_5)]).*

This kinetic/thermodynamic transformation is currently being investigated as more information is required to determine whether the kinetic isomer is the *cis*-

stilbene complex or the hydride complex. This may potentially lead to a better understanding of the sequence of steps followed by the reactivity of $H^{\bullet}$ and H^{+} towards η^2(3e)-vinyl complexes.

4.3 Coupling Reactions of Phosphaalkynes and Alkynes in the Co-ordination Sphere of a Metal

Complexes containing η^2-bonded phosphaalkyne ligands, in particular $2e^-$ donor ligands, are now well established. However, studies dealing with the coupling reactivity of these species towards *t*BuC≡P and alkynes have lead to a variety of different products. These reactions range from dimerisations (head to head and head to tail) of phosphaalkynes in the co-ordination sphere of a transition metal to the coupling of phosphaalkynes and alkynes to generate a wide range of metallacyclopentadienes and mono-phosphacyclobutadienes. The most noteworthy feature of these products has been the investigation into their formation in which it has proven extremely difficult to provide clear cut evidence for the mechanisms involved.

Bauers[133] found that when one equivalent of *t*BuC≡P was added to (85) and stirred for 3 days, the 1,3-diphosphacyclobutadiene complex (93) was obtained in 48 % yield. The proposed mechanism for this was that (85) undergoes a switch in bonding mode of the co-ordinated *t*BuC≡P [η^2(4e)→η^2(2e)] so as to accommodate a second η^2(2e)-bonded phosphaalkyne. Head to tail coupling of the η^2(2e)-bonded phosphaalkynes takes place to form the metallacyclopentadienes which is followed by reductive elimination to generate the 1,3-diphosphacyclobutadiene ring (Scheme 4.19). This mechanism has been reported to account for a large majority of the 1,3-diphosphacyclobutadiene ring systems as it has the analogy with the reaction

sequence for the oxidative coupling of two alkynes in the formation of cyclobutadiene.[146,147]

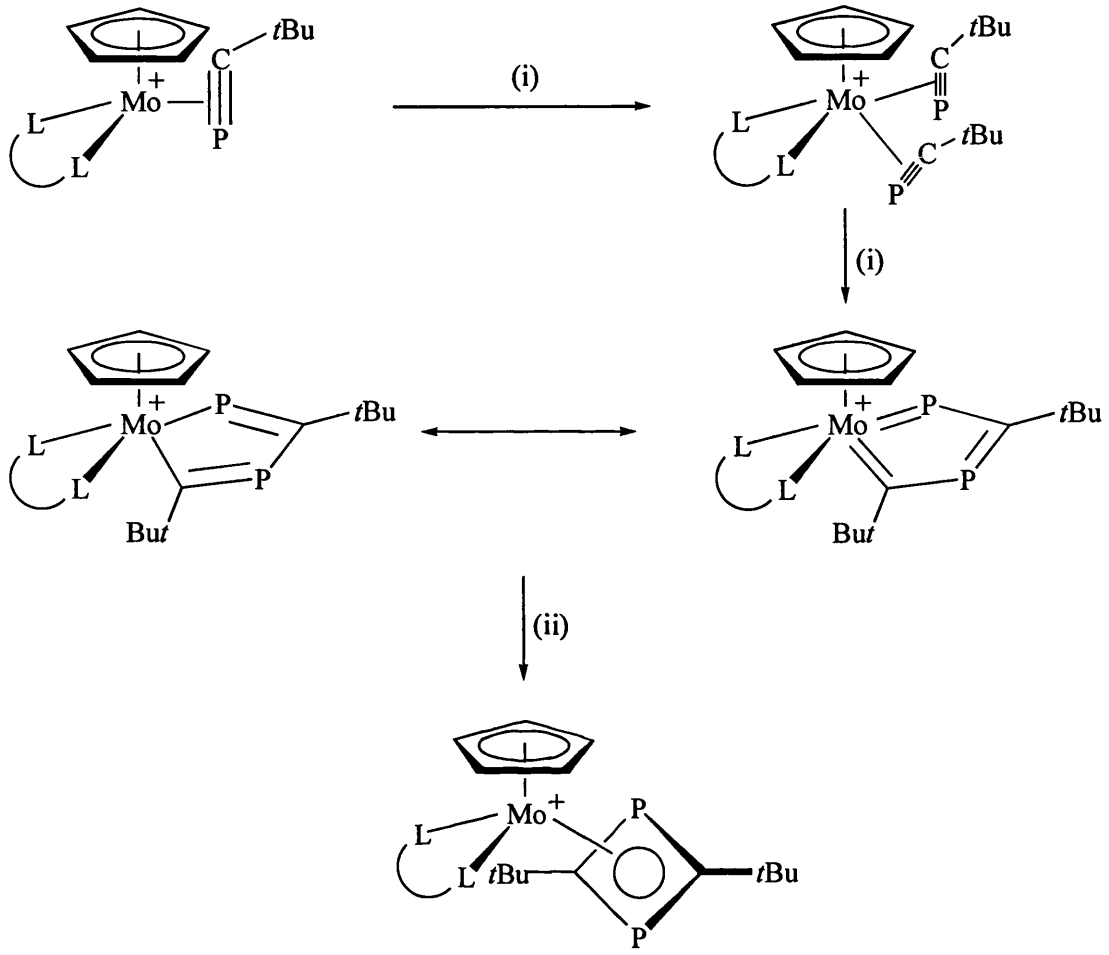

Scheme 4.19 *(i) tBuC≡P, toluene, 25 °C, 3 d, (ii) reductive elimination (where L^L = [(MeO)$_2$POBF$_2$OP(OMe)$_2$]).*

The introduction to this chapter remarked on how the electron density of the transition metal had a considerable effect on the metal mediated coupling of two phosphaalkyne ligands. A recent paper by Creve[148] and co-workers has addressed the puzzling issue about the formation of phosphaalkyne dimers by using density functional theory calculations. Surprisingly, their findings shed new light upon the

reaction pathway of diphosphacyclobutadienes and introduces the theory that other, novel reaction intermediates could be involved.

The study revealed that there are several possible routes which can lead from the bis(π-phosphaalkyne) to the diphosphacyclobutadiene complexes. The computational study was carried out on free diphosphacyclobutadiene species and then on various representative metal complexes. As expected, it was found that in some metal complexes such as $[Ti\{\eta^4\text{-}P_2C_2(t\text{Bu})_2\}COT]$, the diphosphacyclopentadiene complex is the most probable reaction intermediate. However, by changing the metal complex to $[Co\{\eta^4\text{-}P_2C_2(t\text{Bu})_2\}(\eta\text{-}C_5H_5)]$, the complex 1-cobaltadiphosphacyclopentadiene has a relatively high energy content which means it is highly unlikely that it acts as a reaction intermediate. In contrast to experimental observations, an unknown species described as a tilted 1,3-diphosphabicyclobutanediyl ligand, is energetically more favourable.

These results postulate that the oxidative coupling of two phosphaalkynes in the co-ordination sphere of a metal is influenced by both the electron density and the regiochemistry of the metal complex. Therefore, this paper gives more insight as to why some diphosphacyclobutadienes are formed *via* head-to-head coupling and others head-to-tail and also, that it is not possible to generalise on the mechanistic pathway of the formation of diphosphacyclobutadienes.

Although we had planned to investigate the reactivity of (87) towards tBuC≡P so as to generate $[Mo\{\eta^4\text{-}P_2C_2(t\text{Bu})_2\}\{P(OMe)_3\}_2(\eta\text{-}C_5H_5)]^+$, we found that the η^2(3e)-vinyl complex $[Mo\{=C(Ph)CHMe\}\{P(OMe)_3\}_2(\eta^5\text{-}C_9H_7)]$ (94) reacts with $B(C_6F_5)_3$ in the presence of one equivalent of tBuC≡P to generate the 1,3-diphosphacyclobutadiene complex $[Mo\{\eta^4\text{-}P_2C_2(t\text{Bu})_2\}\{P(OMe)_3\}_2(\eta^5\text{-}C_9H_7)]^+$ $(95)^+$

in 42 % yield. Although this was surprising, indenyl complexes are known to react much faster than their cyclopentadienyl analogues,[149] which would therefore promote access to the η^4-diphosphacyclobutadiene complex rather than the η^2(4e)-phosphaalkyne complex (Scheme 4.20).

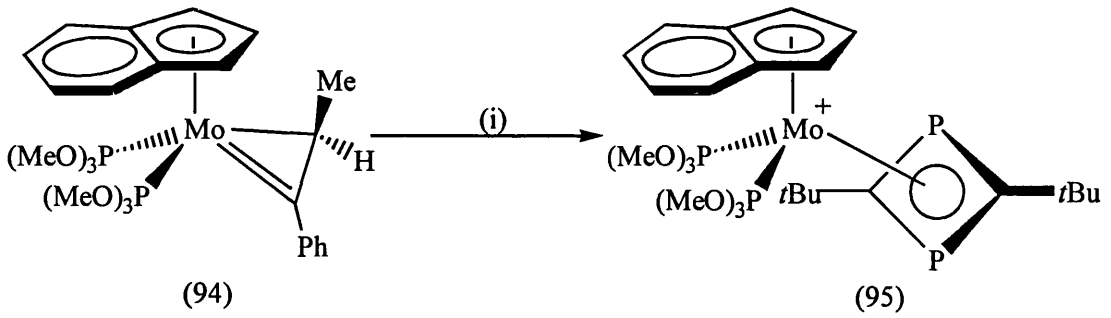

(94) (95)

Scheme 4.20 *(i) $B(C_6F_5)_3$, tBuC≡P.*

The characterisation of (95) was accomplished by NMR spectroscopy and the resonances were similar to those found for the diphosphacyclobutadiene complex (93). The ^{31}P-{^1H} NMR spectrum shows two singlets for the diphosphacyclobutadiene ligand at 67.1 and 65.7 ppm [(93) = 56.5 and 51.1 ppm] and a singlet for the two phosphite ligands at 160.0 ppm [(93) = 151.7 ppm]. In analogy to (93), the *tert*-butyl protons are chemically equivalent but the ring exhibits two different resonances for the phosphorus atoms suggesting that the ring is not rotating but spanning a plane of symmetry. The ^{13}C-{^1H} resonance of the diphosphacyclobutadiene carbon atoms was observed as an apparent triplet at 97.7 ppm [J(CP) = 54.3 Hz]. The signals for the ring carbons are expected to be split into an apparent triplet due to coupling with the two inequivalent phosphorus atoms as was also reported for the system [Co(η^4-P_2C_2(*t*Bu)$_2$)(η^5-C_9H_7)] at 109.6 ppm [J(CP) 54.4 = Hz].[150]

Unlike the well reported dimerization of phosphaalkynes in the co-ordination sphere of transition metal complexes to produce diphosphacyclobutadienes, reports of cooligomerizations between phosphaalkynes and other unsaturated systems such as alkynes, however, are very rare. A report by Binger[151] found that the rhodium η^4-monophosphacyclobutadiene complex (97) can be afforded in high yield when one molecule of *t*BuC≡P is refluxed with (96) in thf (Scheme 4.21).

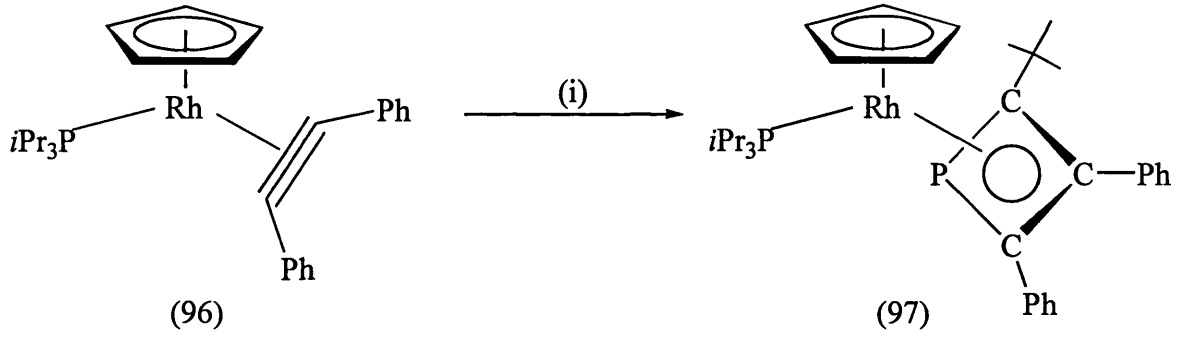

(96) (97)

Scheme 4.21 *(i) tBuC≡P.*

As is shown in Scheme 4.21, the phosphaalkyne and alkyne ligands couple to form the monophosphacyclobutadiene ring. It therefore, seemed feasible that the η^2(4e)-phosphaalkyne complex (87) could react with an alkyne to also form a η^4-monophosphacyclobutadiene complex. Therefore, complex (87) was treated with an excess of but-2-yne and left in an NMR tube at room temperature. Over a period of two weeks there was a progressive colour change (blue → red) and a dramatic change in the ^{31}P-{^{1}H) NMR spectrum as the features characteristic for the metal complex (87) slowly disappeared and were replaced by a new set of resonances, indicative of the formation of a novel product.

The characterisation of this novel compound (98) was accomplished by NMR spectroscopy, which revealed that the compound possibly contained a 1-metalla-3-monophosphacyclopentatrienyl unit, which must have been formed by a P-C coupling of the diphenylacetylene and phosphaalkyne ligands (Scheme 4.22). The appearance in the ^{13}C-{^{1}H} NMR of two low field resonances at 224.6 and 175.3 ppm suggested that two carbons were bound to the molybdenum metal centre. The other carbon signal attributed to the cyclopentatrienyl unit was found as a doublet of doublets at 143.0 ppm [J(CP) = 67.9 Hz, J(CP) = 20.4 Hz]. It was suggested that the large coupling is attributed to the phosphorus atom directly bonded through the P-C double bond and the smaller coupling to the phosphorus of the $P(OMe)_3$ ligand lying *trans* to the P-C bond. Consistent with this structure was the ^{31}P-{^{1}H} spectrum where three singlets of equal intensity were detected at 181.0, 159.8 and 134.8 ppm. Due to the fact that the phosphite ligands are inequivalent it is impossible to assign which phosphorus resonance is that of the cyclopentatrienyl unit, especially since chemical shifts attributed to both phosphite and phosphaalkene moities can typically fall within this range.

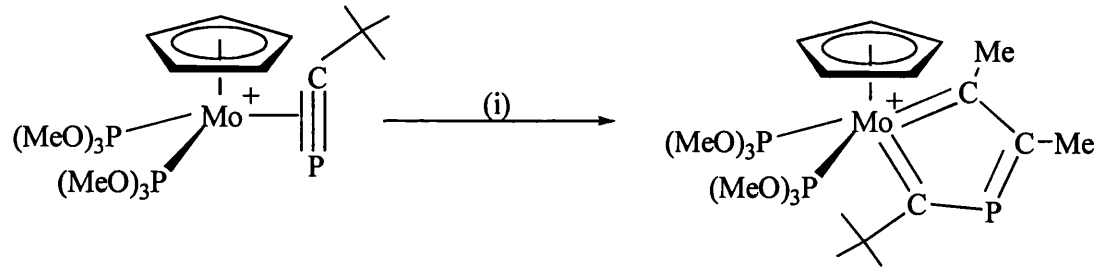

(87) (98)

Scheme 4.22 *(i) MeC_2Me, rt, 2 weeks.*

As the time taken for this transformation to take place was two weeks, it is possible that complex (98) is an intermediate for the η^4-monophosphacyclobutadiene complex and that over a longer period of time reductive elimination could occur to facilitate this. Unfortunately, complex (98) could not be studied by an X-ray diffraction study and further work is currently being undertaken to obtain structural evidence for the proposed complex. However, detailed analysis of the NMR spectra provided good evidence for the structure of the 1-metalla-3-monophosphacyclopentatrienyl unit, the most interesting feature being how it is the carbon of the phosphaalkyne that is co-ordinated to the molybdenum and not the phosphorus.

4.4 Conclusion

In summary, the work discussed in this chapter has further developed the idea that η^2(4e)-phosphaalkyne complexes can be accessed by using η^2(3e)-vinyl complexes as precursors. In accordance with other η^2-bound phosphaalkyne ligands, preliminary studies revealed that (87) readily couples with unsaturated ligands affording diphosphacyclobutadienyl and monophosphacyclopentatrienyl type ligands.

More importantly, we have shown that the reactivity of the η^2(3e)-vinyl complex (8) towards one-electron oxidants is a rich source for further investigation, in particular, by the finding that $B(C_6F_5)_3$ can act as a one-electron oxidant. At the onset of these findings, there was no other evidence to suggest that $B(C_6F_5)_3$ has ever been considered as a one-electron oxidant. However, a recent report by Norton[152] has carried out similar work, which suggests that $B(C_6F_5)_3$ is a possible one-electron oxidant.

We believe, therefore, that it is clearly possible that other organometallic species can undergo one-electron oxidation on treatment with $B(C_6F_5)_3$ and also, we have shown, probably contrary to what most chemists think, that single electron transfer reactions could also be the driving force behind many other established reactions. Hence, the possibility that H^+ can also effect single electron transfer must also be considered.

CHAPTER FIVE

REACTIVITY OF η^2(2e)-PHOSPHAALKYNE COMPLEXES OF PLATINUM

5.1 Introduction

The first transition metal phosphaalkyne complex to be reported was $[Pt(PPh_3)_2(tBuC{\equiv}P)]$ (86) back in 1981.[115] Since then there has been a vast expansion into the synthesis and reactivity of phosphaalkyne complexes and the reactivity of (86) with complexes such as $Pd(PPh_3)_4$ to form the unusual pentametallic cluster $[Pd_2Pt_3(PPh_3)_5(tBuC{\equiv}P)_3]$, is a good example of both the phosphaalkyne P≡C bond and the phosphorus lone pair electrons being used in bonding. [153]

This chapter reports on the investigation of the behaviour of (86) and the analogous novel complex [Pt(dppf)(*t*BuC≡P)] (99) towards electrophilic attack. The first approach involved reacting (86) or (99) with dimethyl dioxirane (DMD), a valuable reagent in organometallic chemistry for performing oxidative transformations. Secondly, with the insight gained from Chapter Four on $B(C_6F_5)_3$, the aim was to extend this work to complex (86). This chapter extends current work with phosphaalkyne systems and describes synthetic and reactivity studies.

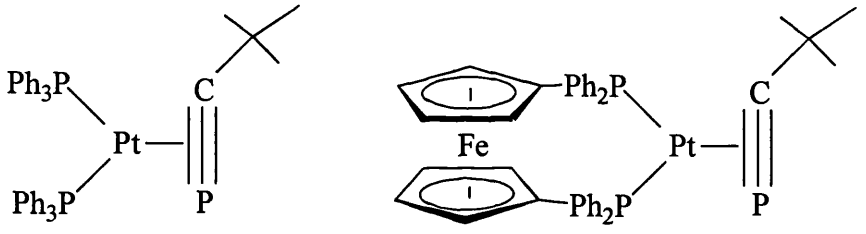

(86) (99)

Figure 5.1

5.2 Reactivity of [Pt(η^2-*t*BuC≡P)$(L)_2$] [where L = $(PPh_3)_2$, $(PMe_3)_2$ or (dppf)] towards DMD

The idea for this research was initiated by recent work carried out within the group. Following the work of Bauers[133] into the synthesis of η^2(4e)-phosphaalkyne complexes it was hoped that these investigations could be extended to rhenium chemistry. Protonation of the η^2(3e)-vinyl complex [Re{=C(Ph)CHPh}Br$(PPh_3)(\eta$-$C_5H_5)$] (100) by $HBF_4.Et_2O$ in the presence of diphenylacetylene was carried out by Carr[154,155] and was shown to afford *trans*-stilbene and a cationic complex which was identified as being [Re(η^2(4e)-PhC_2Ph)Br$(PPh_3)(\eta$-$C_5H_5)$][BF_4] (101) (Scheme 5.1). However, there was evidence to suggest that there were trace amounts of another product which was identified by X-ray crystallography as being the dicationic, oxygen bridged species $[Re_2Br_2(PPh_3)_2(\mu$-$O)(\eta$-$C_5H_5)_2][BF_4]_2$ (102) (Scheme 5.1).

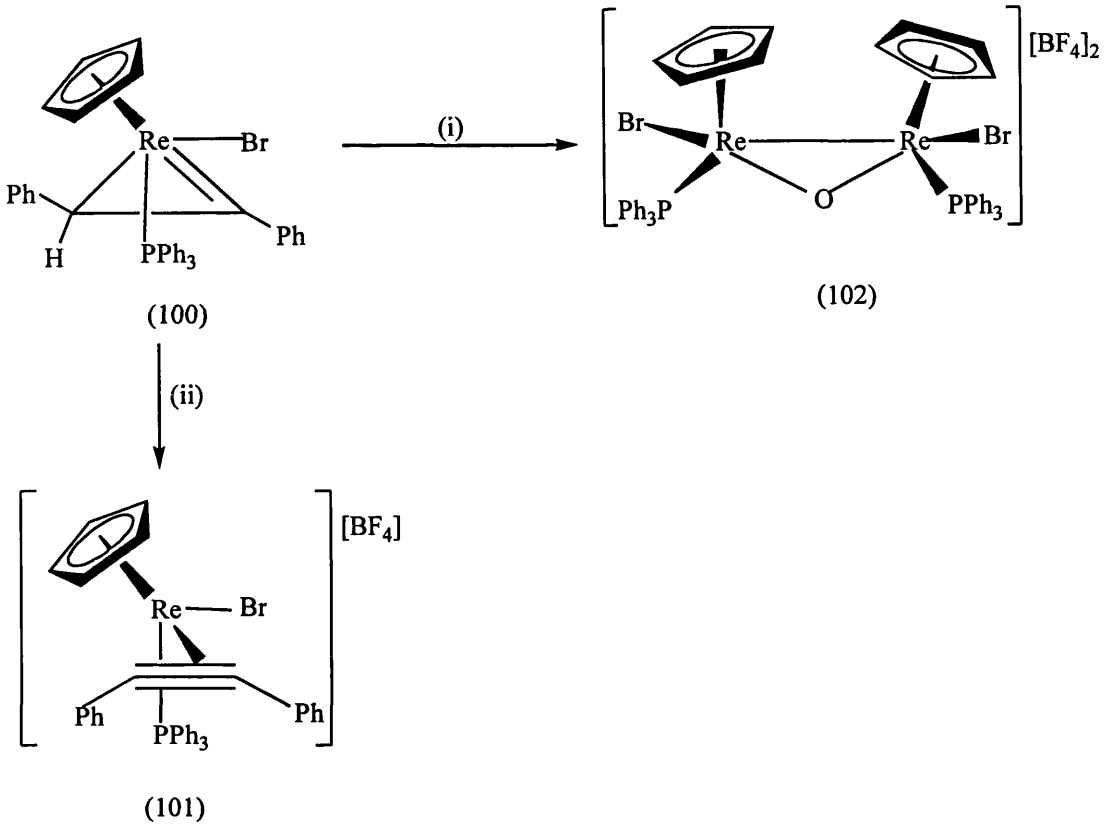

Scheme 5.1 *(i) $HBF_4.Et_2O$, - trans-stilbene, (ii) $HBF_4.Et_2O$ + PhC_2Ph, - trans stilbene.*

Further insight into the formation of (102) was provided when (100) was treated with $HBF_4.Et_2O$, in the absence of diphenylacetylene, as the oxygen-bridged species was formed, in a yield of 68 % and was the only rhenium-containing species isolated from the reaction. These results led to the suggestion that protonation of (100) by $HBF_4.Et_2O$ initially generates co-ordinated *trans*-stilbene to give a thermally unstable $16e^-$ complex. In the presence of diphenylacetylene, *trans*-stilbene is displaced to afford the mononuclear complex (101), however, it appeared that in the absence of diphenylacetylene, *trans*-stilbene is displaced by a source of O^{2-} to afford the dinuclear complex (102). The source of O^{2-} possibly originates from traces of water in the solvent or the $HBF_4.Et_2O$.

It was anticipated, therefore, that when (100) is treated with $HBF_4.Et_2O$ in the presence of *t*BuC≡P, the η^2(4e)-phosphaalkyne complex [Re(*t*BuC≡P)Br(PPh_3)(η-C_5H_5)][BF_4] would be formed as *t*BuC≡P would be able to displace the co-ordinated stilbene. Surprisingly, the product of the reaction was a green neutral solid and although spectroscopic data from NMR indicated that the η^2(3e)-vinyl group had disappeared there was no indication that the product contained the η^2(4e)-bonded phosphaalkyne ligand. An X-ray diffraction study indicated that the phosphaalkyne was bound to the rhenium in a phospha-η^2(3e)-vinyl group fashion and the phosphorus was also co-ordinated to a proton and a F_3B^-O ligand. Of particular interest was the P-C bond length which was significantly shorter than a typical P-C single bond which suggested that there was multiple bond contribution from the canonical form, which contains the η^2(4e)-bonded λ^5-phosphaalkyne $(F_3B)^-$-OP(H)≡C*t*Bu (103) (Scheme 5.2).

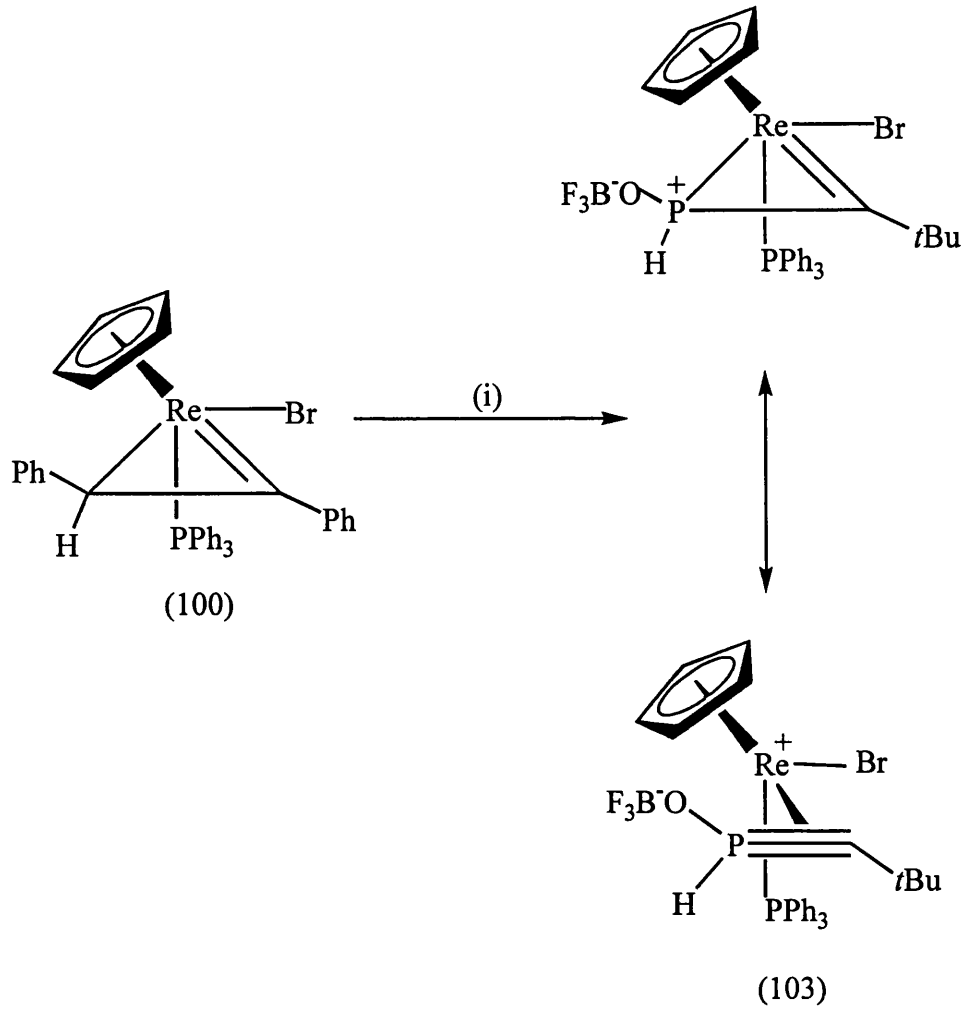

Scheme 5.2 *(i) $HBF_4.Et_2O$ + tBuC≡P.*

The fact that the oxidation state of the phosphorus had been promoted from P(III) to P(V) was very unexpected, especially since this included the co-ordination of BF_3O^-. From the experiments shown in Scheme 5.1 it was possible to rationalise these results. Firstly, protonation of (100) in the absence of added substrates generates the co-ordinated *trans*-stilbene complex which is rapidly oxidised to an unsaturated rhenium-oxo compound which, in the case of (102) can be captured by the stilbene complex. However, in the presence of *t*BuC≡P, the unsaturated rhenium-oxo compound undergoes a reaction through transfer of the oxygen from the rhenium metal centre onto the phosphorus. The subsequent bonding of the BF_3 and hydrogen

atom originate from the $HBF_4.Et_2O$ and it is therefore possible that this is the source of the oxygen.

In an effort to extend this work, our objective was to elaborate on this idea of functionalisation by accessing the chemistry of λ^5-phosphaalkynes through the transfer of oxygen onto the phosphorus centre of an η^2-bound phosphaalkyne complex. As shown in Chapter 4 Scheme 4.1, the phosphorus lone pair within co-ordinated phosphaalkyne complexes is easily utilised for co-ordination with other metal centres, so it was interesting to determine how facile co-ordination with oxygen would be.

It was decided as a preliminary investigation to examine the reactivity of (86) towards a suitable oxidising agent. The η^2(2e)-phosphaalkyne platinum complex is readily available from the reaction of $[Pt(\eta^2\text{-}C_2H_4)(PPh_3)_2]$ with tBuC≡P[115], however, choosing an appropriate oxidising agent was very important. The main concern was in finding a relatively sensitive oxidising reagent that would work under mild conditions and would not fragment the platinum complex (86).

The idea of using DMD as a possible oxidant was adopted after a report by Schenk[155] who described DMD as having the ability to act as a mild electrophilic oxygen transfer reagent. This report identified how DMD had contributed in a novel stereoselective synthesis of chiral sulfoxides *via* oxidation of Ru-coordinated thioethers. DMD proved successful as it generated better yields and enantioselectivity compared to other previous attempts.

The oxidation of metal-coordinated thioethers with DMD occurs in three stages (Scheme 5.3): firstly, the co-ordination of a prochiral thioether to an enantiomerically pure transition metal complex which is, secondly, followed by the

oxidation of the metal co-ordinated thioether by DMD. Finally, subsequent decomplexation of the sulfoxides is obtained by reaction of the metal complex with NaI.

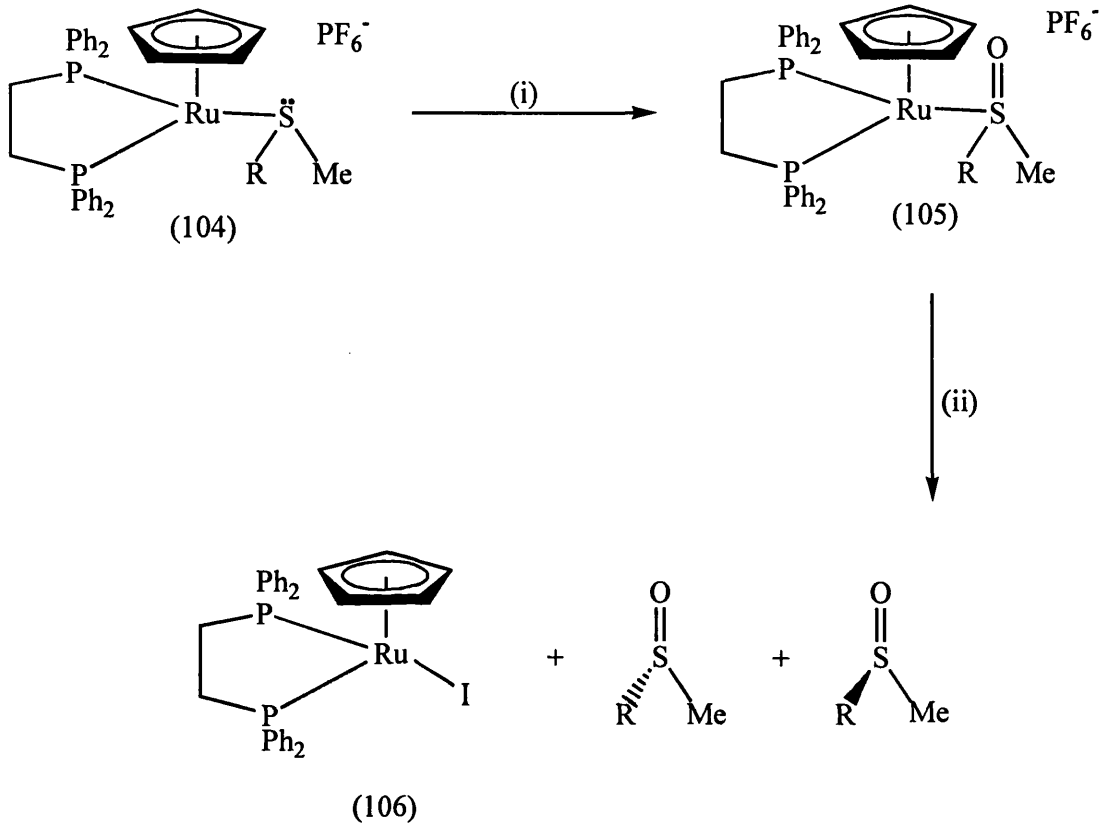

Scheme 5.3 *(i) DMD, (ii) NaI.*

The reason why the enantiomeric purity of these sulphoxides significantly improved by using DMD is due to the high diastereoselectivity of the oxygen transfer. When the sulphoxides are diastereoisomers, they exist as three rotamers. The energetically favourable rotamer occurs when the two sulphur substituents are oriented towards the cyclopentadienyl ring, allowing the sulphur lone pair to be protected by the chelating phosphine.[157-159] This suggests that it is one of the two high

energy rotamers that the oxygen atom preferentially transfers onto. Therefore, the diastereoselectivity of the oxidation is dependent upon the difference in energy of the two remaining rotamers.

The only problem encountered with using DMD was that it had the capability to release ligands present in transition metal complexes. For example, it had been reported that addition of DMD under mild conditions to arene tricarbonylchromium(0) compounds resulted in the liberation of the organic ligand (Scheme 5.4).[160] Therefore, it was uncertain whether DMD would be an effective oxygen transfer reagent towards complex (86) as it was possible that it could result in fragmentation.

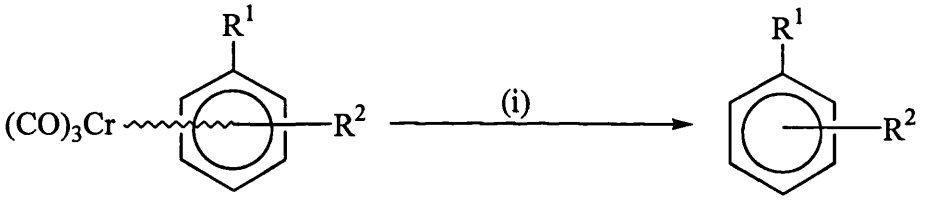

Scheme 5.4 *(i) DMD.*

The reaction was carried out by slowly adding a freshly prepared solution of DMD to a suspension of (86) in acetone at -78 °C. As the mixture was allowed to warm to room temperature there was a noticeable progressive colour change. At room temperature, the volatiles were removed *in vacuo* and the solid was extracted with CH_2Cl_2 and filtered through a Celite pad. Recrystallisation from CH_2Cl_2 and hexane resulted in the precipitation of a fine yellow powder (107).

Characterisation of the powder by IR revealed that the spectra exhibited a band at 1090 cm^{-1} which is typical of a P=O stretch. The ^{31}P-{^{1}H} NMR spectrum exhibited three phosphorus signals, the first was observed at 38.8 ppm [J(PtP) = 322 Hz], the second at 22.9 ppm [J(PP) = 13.4 Hz, J(PtP) = 1998.7 Hz] and the third at 14.0 ppm [J(PP) = 13.3 Hz, J(PP) = 6.7 Hz, J(PtP) = 4748.7 Hz] (Figure 5.2).

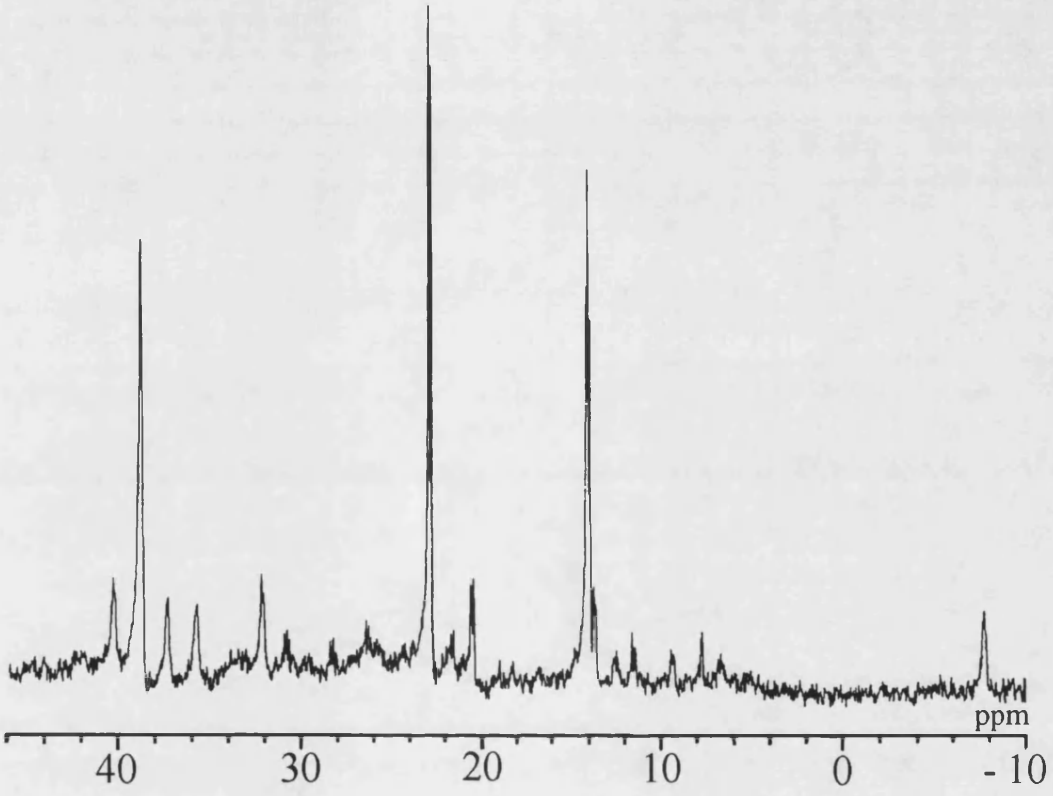

Figure 5.2 *^{31}P-{^{1}H} NMR of (107).*

It was interesting to compare the magnitude of the J(PtP) coupling constants and particularly significant in this sense was the J(PtP) value of 4748.7 Hz which suggested that there was nothing directly bonded to the platinum *trans* to P^{1}.[161] Therefore, our initial thoughts on the structure of the complex derived from NMR and IR spectroscopy was that the complex adopted a carbene-type structure with a double

bond between the platinum and the carbon. The phosphorus was bound to a single oxygen atom *via* a double bond (Figure 5.3).

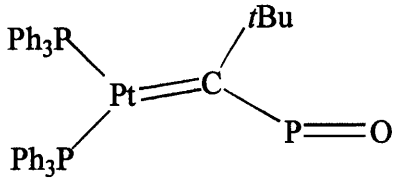

(A)

Figure 5.3

However, after further characterisation through high-resolution mass spectroscopy, the m/z at 869 suggested that the complex may have incorporated more than one oxygen atom. A second structure was proposed which was consistent with the data obtained from NMR, IR and mass spectroscopy. The structure was now proposed to exhibit a zwitterionic carbene-type structure where the phosphorus of the phosphaalkyne is pentavalent (107).

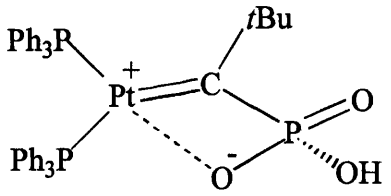

(107)

Figure 5.4

After long consideration we believe that on addition of the DMD to the phosphaalkyne complex (86), there is an instantaneous reaction in which an oxygen atom is co-ordinated to the phosphorus atom *via* its lone pair (Scheme 5.5). There is a

possibility of two structures that the complex can adopt at this stage. However, it is more conceivable that the structure initially forms the penta-valent structure which then quickly rearranges to the tri-valent species in which the phosphorus regains its lone pair.

From the evidence supported by mass spectroscopy we know that the tri-valent structure is only an intermediate and we recognise that it is a highly reactive species due to its lone pair of electrons. It has been reported that oxophosphines, $\sigma^2\eta^3$-P (two co-ordinate) have been characterised with a high degree of reactivity and at this time no oxophosphine is known to be stable at room temperature.[162] However, from various spectroscopic techniques it is certain that these two co-ordinate compounds do exist. For example, a number of reactions are suspected to involve elimination of an oxophosphine, but this has not yet been proved with trapping reactions. It is assumed that they are so reactive, traces of water found in the solvent would be more than adequate to transform them into a stable species. The species H-P=O has been generated by flash photolysis, but other species such as HOO-P=O were also detected which gave reason to believe that the oxophosphine was very reactive towards water.[163]

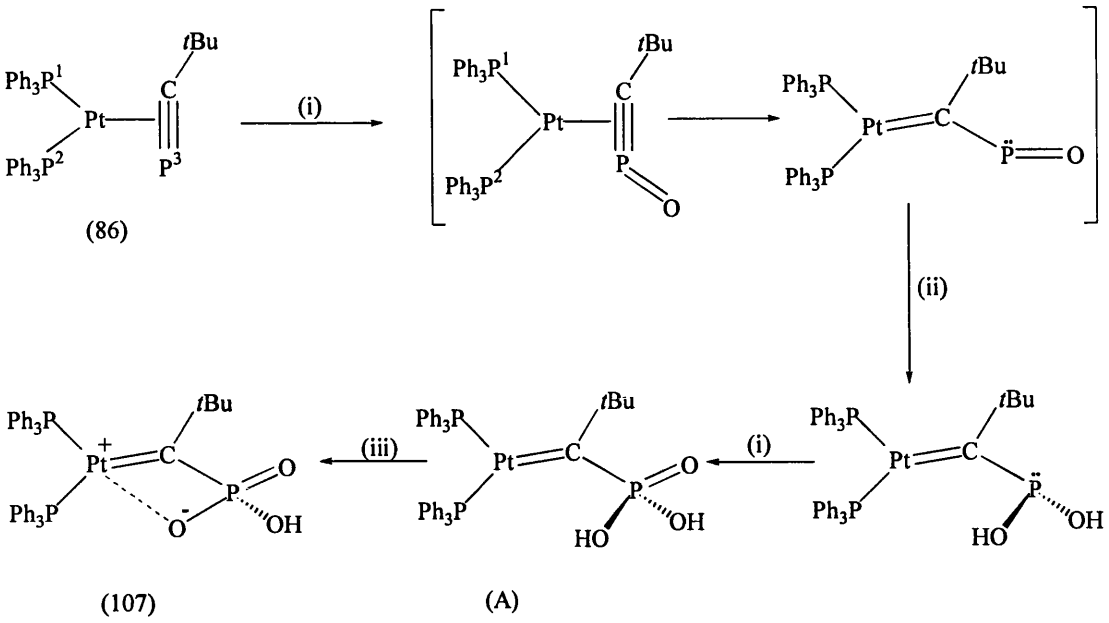

Scheme 5.5 *(i) DMD, (ii) H_2O, (iii) –H.*

Therefore, instantaneously the oxophosphine picks up a molecule of water. The origin of the water is most probably from the DMD as its synthesis requires water and although it is dried before use over molecular sieves, the oxophosphine only requires a trace amount to react. It is then possible that as a tri-valent phosphorus complex, it is still susceptible to oxidation *via* the lone pair of electrons on the phosphorus. The final steps of the reaction are that another molecule of DMD reacts with the intermediate $[Pt\{=C(t\text{Bu})P(OH)_2\}(PPh_3)_2]$ by transfer of an oxygen atom onto the phosphorus to generate the intermediate $[Pt\{=C(t\text{Bu})P(OH)_2{=}O\}(PPh_3)_2]$ (A) which loses H to generate the zwitterionic metal carbene $[Pt{=}C(t\text{Bu})P(OH)(O){=}O(PPh_3)_2]$ (107).

However, an alternative structure to the zwitterion is the structure shown below in Figure 5.5. In this case, the carbon of the phosphaalkyne is not a carbene which is more consistent with the $^{13}C\text{-}\{^1H\}$ NMR data. Both structures are possible and this area of work requires further study to determine the structure.

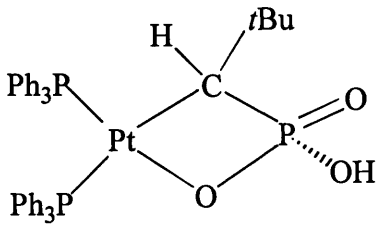

(107)

Figure 5.5

Unfortunately, although the complex is crystalline, crystals grown of the complex have not been good enough to diffract. So although we have been unsuccessful in identifying the structure crystallographically we feel that the spectroscopic evidence fully supports the proposed mechanism. The end result also accords with our aim, with the oxidation state of the phosphorus increasing from P(III) to P(V). To conclude, in the case we have reported, oxidation has triggered a remarkable new reaction.

To extend this investigation, we decided to look at analogous platinum phosphaalkyne complexes, in particular those which contained chelated phosphines. Firstly, addition of one molar equivalent of *t*BuC≡P to a solution of [Pt(η^2-C_2H_4)(dppf)] in CH_2Cl_2 at room temperature resulted in the formation of a bright yellow solution. After one hour the volatiles were removed *in vacuo* which afforded a good yield of a bright yellow powder which was identified as [Pt(η^2-*t*BuC≡P)(dppf)] (99).

Complex (99) was characterised by NMR and mass spectroscopy and was identified by means of the ^{31}P resonance at 80.1 ppm characteristic of other [Pt(η^2-

*t*BuC≡P)(PR_3)$_2$] complexes. An interesting feature concerning the ^{31}P NMR spectrum for complex (99) was that unlike complex (86) where the signals attributed to the phosphine moieties resonate as two sets of doublet of doublets, the phosphine moieties resonated as an apparent triplet at 23.1 ppm. However, this resonance exhibited two sets of platinum satellites which indicated that the triplet was actually two apparent triplets that were coincident with each other 23.1 ppm [*J*(PP) = 26.9 Hz, *J*(PtP) = 3642.0 Hz] and 23.1 ppm [*J*(PP) = 16.8 Hz, *J*(PtP), 3192.6 Hz].

A freshly prepared solution of DMD was added to (99) in CH_2Cl_2 at -78 ^{o}C. On reaching ambient temperature, the volatiles were removed in *vacuo* and the solid was extracted with CH_2Cl_2 and filtered through Celite. Recrystallisation from CH_2Cl_2 and hexane resulted in the precipitation of a bright yellow powder which was characterised as being the zwitterionic carbene complex [Pt{=C(*t*Bu)P(OH)(O)=O}(dppf)] (108). The ^{31}P NMR signals were analogous to those exhibited for complex (107) *i.e* 39.6 ppm [*J*(PtP) = 311.9 Hz], 21.0 ppm [*J*(PP) = 16.8 Hz, *J*(PtP) = 2107.7 Hz] and 12.5 ppm [*J*(PP) = 16.7 Hz, *J*(PP) = 6.7 Hz, *J*(PtP) = 4732.7 Hz].

However, when the reaction is carried out with the PMe_3 system [Pt(η^2-*t*BuC≡P)(PMe_3)$_2$] the reaction does not work and we assume that the DMD fragmented the complex. This can be explained in terms of steric and electronic effects of the complexed phosphines. It is generally accepted that the structural characteristic of a phosphine in a complex is its cone angle which can influence the structure and reactivity of the complexes.[164] Generally, the bigger the cone angle of the phosphine, the bigger the steric bulk of the co-ordinated phosphine. Therefore, when these complexes are reacted with reagents like DMD, the steric bulk of the

phosphine can offer a degree of stability which can protect the metal and hence the molecule from fragmentation.

Measured cone angles have calculated the value for PMe_3 to be 123° and for PPh_3 to be 150°, [165] a significant larger cone angle in the case of triphenylphosphine. Therefore, we can put forward the assumption that in the systems which contain the phosphines PPh_3 and dppf, the directed approach of the DMD to the P^3 is aided by the steric bulk of the phosphine ligands. In the case of the system containing PMe_3, the steric bulk of the phosphine is much smaller and is not enough to sterically guide the DMD to the P^3, driving the reaction pathway to the fragmentation of complex.

5.3 Reactivity of [Pt(η^2-*t*BuC≡P)(PPh_3)$_2$] (86) towards $B(C_6F_5)_3$

Our interest in the chemistry of $B(C_6F_5)_3$ led us to investigate its reactivity towards the platinum complex (86). We wondered whether the $B(C_6F_5)_3$ would interact with the phosphorus lone pair causing the phosphaalkyne ligand to rearrange. The reaction was carried out by adding a dropwise solution of $B(C_6F_5)_3$ in CH_2Cl_2 to (86) at -78 °C. An instantaneous colour change in the reaction mixture indicated that a reaction had taken place, and as the solution was allowed to warm to room temperature, there was a further progressive colour change of the solution. After 2 hr at ambient temperature, the solvents were removed *in vacuo*, leaving a purple oily residue.

The ^{31}P-{^1H} NMR spectrum of the oil was messy, however, it was possible to identify two main resonances, the first being an apparent triplet at 185.7 ppm [*J*(PP) =19.9 Hz, *J*(PtP) 135.9 Hz]. The second resonance appeared to be a triplet at 20.7 ppm [*J*(PP) =35.6 Hz]. However, it was obvious due to the sharp ^{31}P resonances that

there was no phosphorus-boron interaction and the ^{11} B NMR spectrum exhibited one broad peak at -4.4 ppm which from previous knowledge, indicated that the $B(C_6F_5)_3$ could have hydrolysed.

It was decided to carry out the reaction and monitor it by NMR as the temperature was increased from -78 ^{o}C $\rightarrow$ 20 ^{o}C. Examination of the ^{31}P-{^{1}H} NMR spectrum at -78 ^{o}C exhibited a broad resonance at 130 ppm, characteristic of a phosphorus-boron interaction. As the temperature was elevated to -50 ^{o}C, there appeared more resonances including signals at 185.7 and 168.3 ppm, both of which appeared to have splitting although it was not possible to resolve it. There was also the appearance of a multiple set of resonances between 21.0 and 17.3 ppm. At -25 ^{o}C, it became evident that the signals at 168.3 and 130.0 ppm had disappeared and it was possible to detect that the resonance at 185.7 ppm was a doublet of doublets. It was also possible to detect that the multiplet signals between 21.0 and 17.3 ppm were two sets of apparent triplets. When the temperature was raised to room temperature, the spectrum exhibited a doublet of doublets at 185.7 ppm [J(PP) = 24.1 Hz, J(PP) = 13.9 Hz and J(PtP) = 134.8 Hz], and two sets of apparent triplets at 22.8 ppm [J(PP) = 16.5 Hz] and 22.5 ppm [J(PP) = 20.3 Hz].

It appeared that the low temperature NMR study was important as it revealed that on initial reaction with (86), $B(C_6F_5)_3$ reacted to form a P-$B(C_6F_5)_3$ interaction, which means that initially the borane was not hydrolysed. However, it becomes evident that as the temperature was raised, this interaction breaks down. Also, another interesting feature was at -25 ^{o}C where there are two similar resonances at 168.3 and 185.7 ppm, which it seems could indicate the presence of kinetic and thermodynamic

isomers as the disappearance of the peak at 168.3 ppm is in conjuction with the increase in intensity of the peak at 185.7 ppm.

In trying to determine the structure of this novel compound it was interesting that the low value of *J*(PtP) resembled that of the starting material [Pt(η^2-*t*BuC≡P)(PPh_3)$_2$], in which the phosphorus of the η^2-*t*BuC≡P is found at 81.2 ppm [*J*(PtP) = 62.0 Hz].

From these NMR studies we propose that the first step of the reaction is an interaction between $B(C_6F_5)_3$ and (86) *via* a phosphorus dative bond (Scheme 5.6). This can then rearrange into the phosphaalkene type structure (A). Due to the final product containing a single resonance in the ^{11}B NMR spectrum at -4.4, we believe that the $B(C_6F_5)_3$ slowly begins to react with traces of water, resulting in the displacement of the $B(C_6F_5)_3$ from the phosphorus by H^+ to form (109), which is stabilised by the anion $[HOB(C_6F_5)_3]^-$. As (109) is a 14 e^- species it is possible that there is electronic stability facilitated by the phosphorus lone pair within (E)-(109) and from a β-agostic interaction within (Z)-(109).

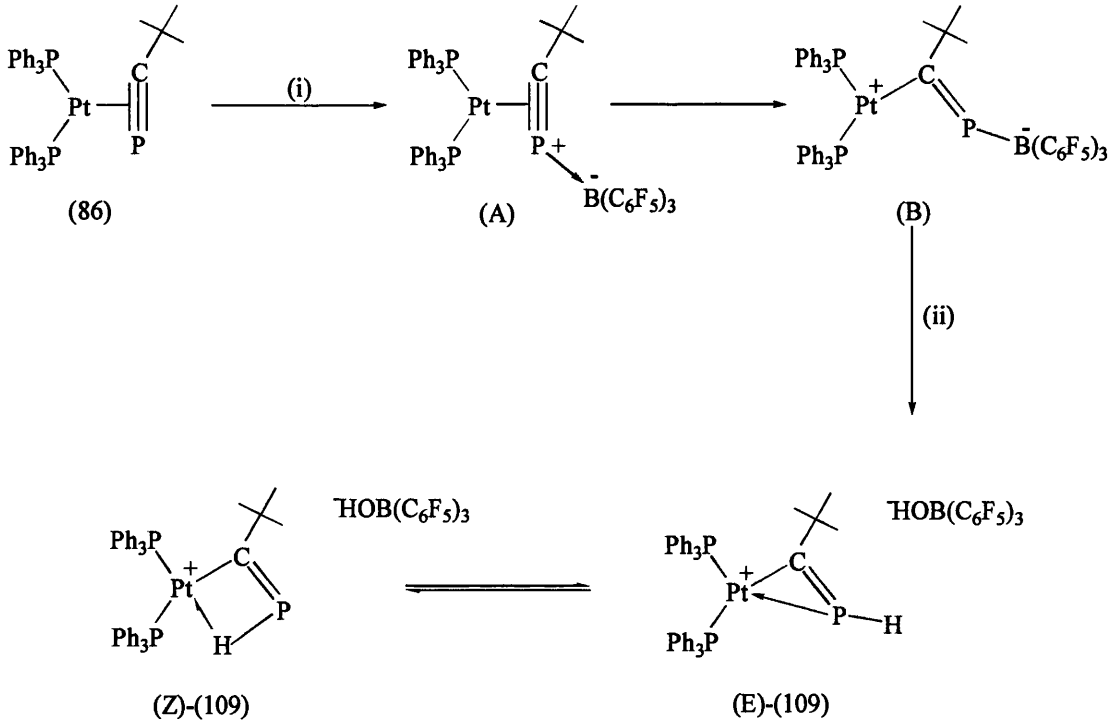

Scheme 5.6 *(i) $B(C_6F_5)_3$, (ii) H_2O.*

The final product is interesting as it contains a phosphaalkene. Recent work by Weber[165] has reported on the synthesis of various phosphaalkenyl complexes, some of which are similar to our proposed structure where it is the carbon of the phosphaalkene which is co-ordinated to the metal. Scheme 5.7 illustrates the synthesis of a phosphaalkenylrhenium complex which was synthesised by the nucleophilic addition of a phosphide to a CO ligand at low temperature.[166] Interestingly, when the reaction mixture was warmed to –40 ^{o}C, a 1,3-$Si(CH_3)_3$ shift takes place which affords the kinetic isomer (*E*)-(112). At temperatures above -40 ^{o}C, the kinetic isomer rapidly isomerises to the thermodynamic isomer *(Z)*-(112).

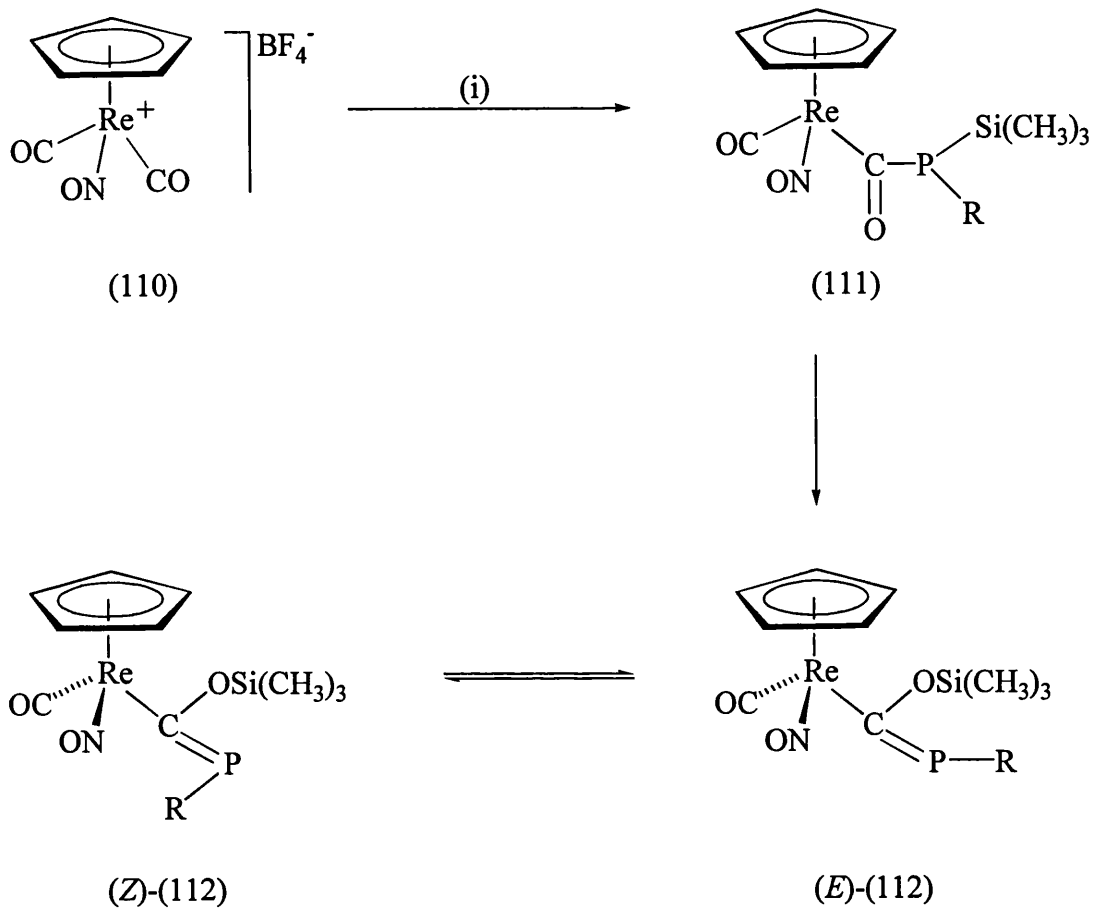

(110) (111)

(*Z*)-(112) (*E*)-(112)

Scheme 5.7 *(i) + LiPR(Si(CH$_3$)$_3$), - LiBF$_4$ (where R = tBu, (CH$_3$)$_3$Si, Ph).*

Interestingly, the ^{31}P data for the phosphaalkene complex (112) indicates that the stronger the electron donor ability of the R substituent, the more low field the corresponding phosphaalkenyl shift becomes *i.e.* [where R = *t*Bu δ = 272.8, R = $(CH_3)_3Si$ δ = 212.4, R = Ph δ = 194.4]. Therefore, the resonance at 185.5 ppm, exhibited for complex (109) would be consistent with the presence of a phosphaalkenyl unit with a hydrogen substituent on the phosphorus. Also consistent with the rhenium system is the generation of kinetic and thermodynamic isomers.

Therefore, the product identified at 168.3 ppm is most probably the kinetic (*E*)-isomer (109) which isomerises between -50 °C and 20 °C to generate the thermodynamic (*Z*)-isomer (109).

5.4 Conclusion

To summarise, the results discussed in this chapter report the reactivity of the η^2(2e)-phosphaalkyne complexes of platinum towards electrophilic reagents. The interesting features found in this study was the readiness of the phosphaalkyne ligand to rearrange into carbene and phosphaalkene-type structures to accommodate substituents on the phosphorus atom.

In comparing the reactivity of (86) towards both DMD and $B(C_6F_5)_3$ it is interesting to note the direction of the phosphorus shift of the phosphaalkyne, *i.e.* (107) exhibited an upfield shift in the ^{31}P NMR from 81.2 to 38.8 ppm, whereas (109) exhibited a large downfield shift in the ^{31}P NMR from 81.2 to 185.7 ppm, both reflecting the change in electron density and oxidation state of the novel complexes.

Unfortunately, due to a lack of time, a more detailed investigation of these reactions is still required and further work is currently been carried out with regards to determining structural evidence for the proposed carbene and phosphaalkene-type complexes.

CHAPTER SIX

EXPERIMENTAL PROCEDURE

6.1 General Experimental Procedures

All reactions were carried out under an atmosphere of dry, oxygen-free dinitrogen, using standard Schlenk techniques, unless otherwise stated. All solvents were freshly distilled over an appropriate drying agent and further degassed before use where necessary. Reagents were obtained from commercial sources and were used as received, unless otherwise indicated. Chromatography columns used BDH alumina (Brockman activity II) as solid support.

NMR spectra were recorded on JEOL JNM GX270 (270 MHz) or JEOL EX400 (400 MHz) Fourier transform spectrometers at the temperatures indicated. NMR spectra were referenced to the following standards: ^{1}H, Me_4Si; ^{13}C, Me_4Si; ^{31}P, 85% H_3PO_4; ^{11}B, BF_3Et_2O; ^{19}F, $CFCl_3$.

Infrared spectra were recorded on a Nicolet 510P FT-IR spectrometer. The samples were dissolved in the stated solvents and the absorption recorded using sodium chloride cells.

Microanalyses were determined in the Department of Chemistry and FAB mass spectra were determined in the Department of Materials, both within the University of Bath.

EPR studies were obtained courtesy of Dr T. Padget and Dr. N. Connelly, University of Bristol. X-band EPR spectra were recorded using a Bruker ESP-300E spectrometer with a Bruker variable temperature accessory and a Hewlett Packard 5350B microwave frequency counter. Radical species were generated *in-situ* at low temperature by allowing a frozen solution of one reactant topped with the second to melt. The field calibration was checked by measuring the resonance of the diphenylpicrylhydrazyl radical.

Crystal data was collected on a CAD4 automated four-circle diffractometer and was corrected for Lorentz, polarisation and X-ray absorption effects. The structures were solved by Patterson methods and refined using the SHELX suite of programs.[xx] This procedure was carried out by Dr. Mary Mahon of the University of Bath.

EHMO calculations were carried out by Dr. Mary Mahon and Dr. Jason Lynam of the University of Bath.

6.2 Preparation of Starting Materials

The following compounds were prepared according to the published literature procedures:

$[Mo(NCMe)_2(CO)_2(\eta\text{-}C_5Me_5)][BF_4]$[105]

$[Mo\{=C(Ph)CHPh\}\{P(OMe)_3\}_2(\eta\text{-}C_5H_5)]$[16]

$[Pt(\eta^2\text{-}P{\equiv}C\textit{t}Bu)(PPh_3)_2]$[115]

*t*BuC≡P was kindly donated by Dr C. A. Jones (University of Wales, Cardiff).

6.3 Preparation of *s-cis*-$[Mo(\eta^4\text{-}CH_2CHCHCHOAc)(CO)_2(\eta\text{-}C_5H_5)][BF_4]$ (63)

An excess of 1-acetoxy-1,3-butadiene (9.40 cm^3, 79.0 mmol) was added to a solution of the blood-red complex *cis*-$[Mo(NCMe)_2(CO)_2(\eta\text{-}C_5H_5)][BF_4]$ (62) (3.05 g, 7.90 mmol) in CH_2Cl_2 (55 cm^3). After stirring at ambient temperature for 2 d a bright yellow precipitate was observed. Stirring was continued for a further 2 d, resulting in the formation of more precipitate. The mixture was filtered *via* cannula and the yellow solid was washed with several portions of CH_2Cl_2 and then pentane. Removal

of the solvent followed by drying, first under nitrogen and then *in vacuo*, afforded *s-cis*-[Mo(η^4-$CH_2CHCHCHOAc$)$(CO)_2$(η^5-C_5H_5)][BF_4] (63) (2.80 g, 85 %) obtained as a pale yellow powder.

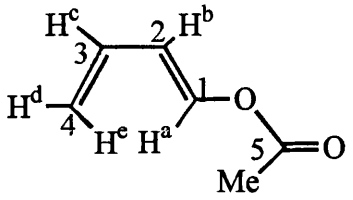

^1H NMR: [$(CD_3)_2CO$, 20°C]: δ 6.48 (br m, 1H, H^b), 6.29 (br m, 1H, H^c), 6.12 (s, 5H, C_5H_5), 6.07 [br d, 1H, H^a, $J(H^aH^b)$ = 6.8], 3.01 [ddd, 1H, H^d, $J(H^dH^c)$ = 7.8, $J(H^dH^e)$ = 2.0, $J(H^dH^b)$ = 1.4], 2.38 [br d, 1H, H^e, $J(H^eH^c)$ = 10.7], 2.06 (s, 3H, Me).

^{13}C-{^1H} NMR: [$(CD_3)_2CO$, 20°C]: δ 220.2 (CO), 219.2 (CO), 167.9 (C^5), 102.8 (C^1), 93.9 (C^2 or C^3), 91.6 (C_5H_5), 88.3 (C^2 or C^3), 50.0 (C^4) and (Me).

IR: ν_{CO}/cm^{-1} ($MeNO_2$) at 2068 (vs), 2020 (s) and 1759 (mw).

FAB Mass Spectrum: (+) FAB in NBA: 331, $[M]^+$; 303, $[M\text{-}CO]^+$; 275, $[M\text{-}2CO]^+$ and 232, $[M\text{-}2CO\text{-}Ac]^+$.

(-) FAB in NBA: 87, $[BF_4]^-$.

Microanalysis: $C_{13}H_{13}BF_4MoO_4$ requires: C = 37.5, H = 3.1 %

found: C = 37.0, H = 3.2 %

6.4 Preparation of *anti*-[Mo(η^3-$CH_2CHCHCHO$)$(CO)_2$(η-C_5H_5)] (54)

Sodium hydrogen carbonate (75 cm^3, 70 g of a 0.1 M aqueous solution, pH 8.5, ca, 7.50 mmol) was added to a solution of the yellow complex *s-cis*-[Mo(η^4-$CH_2CHCHCHOAc$)$(CO)_2$(η-C_5H_5)][BF_4] (63) (3.00 g, 7.21 mmol) in CH_2Cl_2 (60

cm^3). The two-phase system was vigorously stirred at room temperature for 0.5 hr. The aqueous layer was removed and extracted several times with CH_2Cl_2. The extracts and organic layer were combined and washed with several portions of water, before drying over magnesium sulphate. The mixture was filtered and the yellow filtrate was concentrated to a small volume under reduced pressure, before being chromatographed on alumina. Elution with CH_2Cl_2 afforded a bright yellow band which gave, after removal of solvent and recrystallisation from CH_2Cl_2/hexane, *anti*-[Mo(η^3-$CH_2CHCHCHO$)$(CO)_2$(η-C_5H_5)] (54) (1.80 g, 87 %) as a bright yellow powder.

NMR spectroscopy showed (54) to exist in solution at room temperature as a 10:1 mixture of the *exo* and *endo*. Low temperature NMR experiments were necessary for the determination of the coupling constants.

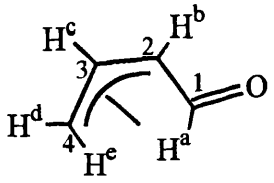

Exo-anti isomer (54) (major)

^1H NMR: (CD_2Cl_2, 20°C): δ 7.14 (br s, 1H, H^a), 5.40 (br s, 5H, C_5H_5), 4.76 (br s, 1H,H^c), 4.05 (br s, 1H, H^b), 3.03 (br s, 1H, H^d) and 1.77 (br s, 1H, H^e).

(CD_2Cl_2, -40 °C): δ 6.98 [d, 1H, H^a, $J(H^aH^b)$ = 7.9], 5.40 (s, 5H, C_5H_5), 4.78 [ddd, 1H, H^c, $J(H^cH^e)$ = 11.9, $J(H^cH^d)$ = 8.2, $J(H^cH^b)$ = 7.0], 4.00 [ddd, 1H, H^b, $J(H^bH^a)$ = 7.9, $J(H^bH^c)$ = 7.0, $J(H^bH^d)$ = 1.4], 3.02 [ddd, 1H, H^d, $J(H^dH^c)$ = 8.2, $J(H^dH^e)$ = 2.7, $J(H^dH^b)$ = 1.4], 1.68 [dd, 1H, H^e, $J(H^eH^c)$ = 11.9, $J(H^eH^d)$ = 2.7].

^{13}C-{^{1}H} NMR: (CD_2Cl_2, 20 °C): δ 234.7 (br s, CO), 234.3 (br s, CO), 186.7 (br s, C^1), 92.2 (br s, C_5H_5), 72.2 (br s, C^3), 59.5 (br s, C^2), 40.2 (br s, C^4).

(CD_2Cl_2, -50 °C): δ 234.7 (CO), 234.5 (CO), 186.1 (C^1), 92.0 (C_5H_5), 71.8 (C^3), 58.7 (C^2), 40.0 (C^4).

Endo-anti isomer (54)

^{1}H NMR: (CD_2Cl_2, 20°C): δ 7.84 (br s, 1H, H^a), 5.30 (br s, 5H, C_5H_5), 4.50 (br s, 1H, H^c), 4.19 (br s, 1H, H^b), 2.78 (br s, 1H, H^d), 2.65 (br s, 1H, H^e).

(CD_2Cl_2, -40 °C): δ 7.71 [d, 1H, H^a, $J(H^aH^b)$ = 7.9], 5.30 (s, 5H, C_5H_5), 4.46 [ddd, 1H, H^c, $J(H^cH^e)$ = 11.2, $J(H^cH^d)$ = 7.3, $J(H^cH^b)$ = 6.2], 4.28 [dd, 1H, H^b, $J(H^bH^a)$ = 7.9, $J(H^bH^c)$ = 6.2], 2.77 [d, 1H, H^d, $J(H^dH^c)$ = 7.3], 2.65 [d, 1H, H^e, $J(H^eH^c)$ = 11.2].

^{13}C-{^{1}H} NMR: (CD_2Cl_2, 20 °C): δ 234.7 (br s, CO), 234.3 (br s, CO), 186.7 (br, s, C^1), 92.2 (br s, C_5H_5), 72.2 (br s, C^3), 59.5 (br s, C^2), 40.2 (br s, C^4).

(CD_2Cl_2, -50 °C): δ 235.4 (CO), 235.1 (CO), 186.6 (C^1), 90.9 (C_5H_5), 86.4 (C^3), 61.0 (C^2), 34.2 (C^4).

IR: ν_{CO}/cm^{-1} (CH_2Cl_2) at 1973 (vs), 1896 (s) and 1649 (m).

FAB Mass Spectrum: (+) FAB in NBA: 288, $[M]^+$; 260, $[M\text{-}CO]^+$ and 232, $[M\text{-}2CO]^+$.

Microanalysis: $C_{11}H_{10}MoO_3$ requires C = 46.2, H = 3.5 %
found C = 46.3, H = 3.5 %

6.5 Preparation of *s-cis*-[Mo(η^4-$CH_2CHCHCHOAc$)$(CO)_2(\eta$-$C_5Me_5)$][BF_4] (64)

An excess of 1-acetoxy-1,3- butadiene (0.460 cm^3, 435 mg, 3.88 mmol) was added to a solution of the blood-red complex *cis*-[$Mo(NCMe)_2(CO)_2(\eta$-$C_5Me)_5$][BF_4] (72) (177 mg, 0.39 mmol) in CH_2Cl_2 (25 cm^3) and the mixture was stirred at room temperature for 4 d. Monitoring by infrared spectroscopy showed the gradual consumption of the starting material and the formation of a new product. The solvent was removed *in vacuo*, and the resulting green-brown residue was extracted with CH_2Cl_2 and filtered through Celite. The bottle-green filtrate was concentrated to a small volume under reduced pressure, following which addition of Et_2O precipitated a green solid. The supernatant liquid was removed *via* syringe and the solid washed with several portions of Et_2O and then pentane. A further purification was effected by recrystallisation from CH_2Cl_2/Et_2O to afford *s-cis*-[Mo(η^4-$CH_2CHCHCHOAc$)$(CO)_2(\eta$-$C_5Me_5)$][BF_4] (64) (133 mg, 71. %) as a green powder.

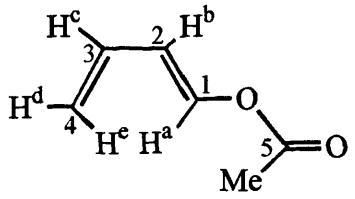

^1H NMR: (CD_2Cl_2, 20 °C): δ 6.08 (m, 1H, H^c), 5.97 (m, 1H, H^b), 4.58 [d, 1H, H^a, $J(H^aH^b)$ = 6.8], 2.57 [d, 1H, H^d, $J(H^dH^c)$ = 7.8], 2.03 (s, 3H, Me), 1.98 (s, 15H, C_5Me_5), 1.05 [d, 1H, H^e, $J(H^eH^c)$ = 10.7].

^{13}C-{^1H} NMR: (CD_2Cl_2, 20 °C): δ 221.6 (CO), 220.3 (CO), 169.3 (C^5), 106.1 (C_5Me_5), 100.1 (C^1), 95.3 (C^2 or C^3), 89.0 (C^2 or C^3), 59.5 (C^4), 20.5 (Me), 10.8 (C_5Me_5).

IR: ν_{CO}/cm^{-1} (CH_2Cl_2) at 2053 (vs), 2006 (s) and 1759 (mw).

FAB Mass Spectrum: (+) FAB in NBA: 401, $[M]^+$; 373, $[M-CO]^+$ and 345, $[M-2CO]^+$.

(-) FAB in NBA: 87, $[BF_4]^-$.

Microanalysis: $C_{18}H_{23}BF_4MoO_4$ requires C = 44.5, H = 4.8 %

found C = 45.0, H = 5.0 %

6.6 Preparation of *exo-anti*-[Mo(η^3-$CH_2CHCHCHO$)$(CO)_2$(η-C_5Me_5)] (55)

Sodium hydrogen carbonate (50 cm^3, 50 g of a 0.1 M aqueous solution, pH 8.5, *ca*, 5.0 mmol) was added to a solution of the green complex *s-cis*-[Mo(η^4-$CH_2CHCHCHOAc$)$(CO)_2$(η-C_5Me_5)][BF_4] (64) (1.94 g, 3.99 mmol) in CH_2Cl_2 (50 cm^3). The two-phase system was vigorously stirred at room temperature, causing the mixture to turn yellowish in colour. After 2 hr, the aqueous layer was removed and extracted several times with CH_2Cl_2. The extracts and organic layer were combined and washed with several portions of water, before drying over magnesium sulphate. The mixture was filtered and the yellow filtrate was concentrated to a small volume under reduced pressure, before being chromatographed on alumina. Elution with Et_2O afforded a single yellow fraction which gave, after removal of solvent and recrystallisation from Et_2O, *exo-anti*-[Mo(η^3-$CH_2CHCHCHO$)$(CO)_2$(η-C_5Me_5)] (55) (1.15 g, 81 %) as bright yellow crystals.

The molecular structure of (55) was determined by X-ray crystallography. X-ray quality crystals were obtained by CH_2Cl_2/Et_2O/hexane layer diffusion at room temperature.

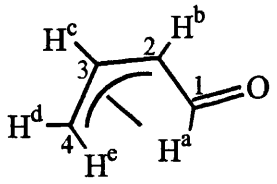

^1H NMR: (CD_2Cl_2, 20°C): δ 7.00 [d, 1H, H^a, $J(H^aH^b)$ = 7.8], 3.51 [ddd, 1H, H^c, $J(H^cH^e)$ = 11.6, $J(H^cH^d)$ = 8.4, $J(H^cH^b)$ = 7.1], 3.42 (m, 1H, H^b), 2.28 [ddd, 1H, H^d, $J(H^dH^c)$ = 8.4, $J(H^dH^e)$ = 2.8, $J(H^dH^b)$ = 1.4], 1.88 (s, 15H, C_5Me_5), 1.75 [dd, 1H, H^e, $J(H^eH^c)$ = 11.6, $J(H^eH^d)$ = 2.8].

^{13}C-{^1H} NMR: (CD_2Cl_2, 20°C): δ 237.5 (CO), 237.2 (CO), 184.8 (C^1), 104.9 (C_5Me_5), 80.1 (C^3), 65.0 (C^2), 42.4 (C^4), 10.4 (C_5Me_5).

IR: ν_{CO}/cm^{-1} (CH_2Cl_2) at 1960 (vs), 1883 (s) and 1664 (m).

FAB Mass Spectrum: (+) FAB in NBA: 359, $[M]^+$; 330, $[M\text{-}CO]^+$ and 302, $[M\text{-}2CO]^+$

Microanalysis: $C_{16}H_{20}MoO_3$ requires C = 53.9, H = 5.7 %
found C = 54.0, H = 5.7 %

6.7 Preparation of *exo-anti*-[Mo(η³-$CH_2CHCHCH_2OH$)(CO)₂(η-C_5H_5)] (65)

Sodium borohydride (20 mg, 0.53 mmol) was added to a solution of the yellow complex *anti*-[Mo(η³-$CH_2CHCHCHO$)(CO)₂(η-C_5H_5)] (54) (100 mg, 0.35 mmol) in methanol (10 cm^3) and the mixture was stirred at ambient temperature for 0.5 hr. Monitoring by infrared spectroscopy indicated the complete consumption of starting material and the formation of a new product. Water (0.5 cm^3) was added and the mixture was stirred for 0.5 hr before the solvents were removed *in vacuo*. The yellow residue was extracted with several portions of Et_2O which were concentrated to a small volume under reduced pressure and chromatographed on alumina. Elution with

Et_2O/hexane (1:1) afforded a yellow fraction which gave, after removal of solvents and recrystallisation from CH_2Cl_2/pentane, *exo-anti*-[Mo(η^3-$CH_2CHCHCH_2OH$)$(CO)_2$(η-C_5H_5)] (65) (65 mg, 65 %) as yellow crystals.

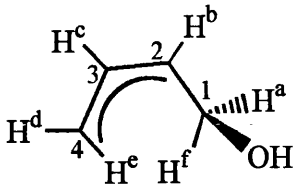

^1H NMR: ($CDCl_3$, 20 °C): δ 5.28 (s, 5H, C_5H_5), 4.12 [ddd, 1H, H^c, $J(H^cH^e)$ = 11.4, $J(H^cH^b)$ = 7.7, $J(H^cH^d)$ = 7.5], 3.93 (m, 1H, H^b), 3.78 (m, 1H, H^a), 2.94 [ddd, 1H, H^d, $J(H^dH^c)$ = 7.5, $J(H^dH^e)$ = 2.4, $J(H^dH^b)$ = 1.6], 2.14 [dd, 1H, H^f, $J(H^fH^b)$ = 11.0], 1.50 (br s, 1H, OH), 1.41 [dd, 1H, H^e, $J(H^eH^c)$ = 11.4, $J(H^eH^d)$ = 2.4].

^{13}C-{^1H} NMR: ($CDCl_3$, 20 °C): δ 236.8 (CO), 236.3 (CO), 91.6 (C_5H_5), 69.1 (C^1), 66.6 (C^3), 53.9 (C^2), 38.1 (C^4).

IR: ν_{CO}/cm^{-1} (CH_2Cl_2) at 1948 (vs) and 1865 (s).

FAB Mass Spectrum: (+) FAB in NBA: 273, $[M\text{-}OH]^+$; 245, $[M\text{-}OH\text{-}CO]^+$ and 217, $[M\text{-}OH\text{-}2CO]^+$.

Microanalysis $C_{11}H_{12}MoO_3$ requires: C = 45.9, H = 4.2 %
found: C = 46.0, H = 4.2 %

6.8 Preparation of *anti*-[Mo(η^3-$CH_2CHCHCHO$)$(CO)_2$(η-C_5H_5)] (54)

Morpholine N-oxide (274 mg, 2.34 mmol) was added to a solution of (65) (450 mg, 1.56 mmol) in CH_2Cl_2 (5 cm^3) which contained 4 Å molecular sieves. After stirring at room temperature for 10 m, [Bu_4N][RuO_4] (27 mg, 0.08 mmol) was added.

The reaction was monitored by IR spectroscopy and after 10 hr was complete. The reaction mixture was diluted with CH_2Cl_2 (50 cm^3) and washed with sodium sulphite solution (0.5 M, 10 cm^3), and NaCl (0.5 M, 10 cm^3). The organic layer was dried (Na_2SO_4) and the volatile material removed *in vacuo*. The residue was extracted with CH_2Cl_2 (10 cm^3) and filtered through a small pad of alumina, the volume reduced *in vacuo* to 3 cm^3 and chromatographed on alumina. Elution with CH_2Cl_2 gave a single yellow band, which on recrystallisation from CH_2Cl_2/hexane afforded the bright yellow powder (54) (268 mg, 60 %), identification reported in 6.4.

6.9 Preparation of *exo-anti*-[Mo(η^3-CHPhCHCHCPhO)(CO)$_2$(η-C_5H_5)] (76)

Phenyllithium (0.39 cm^3 of a 1.8 M solution in thf, 0.69 mmol) was added to a solution of the yellow complex [Mo{η^3-OC(O)CHCHCH}(CO)$_2$(η-C_5H_5)] (54) (100 mg, 0.35 mmol) in thf (15 cm^3) at -78 ^oC. The mixture was allowed to warm to ambient temperature and was then treated with H_2O (0.5 cm^3), stirring continued for 10 m, after which the solvents were removed *in vacuo*. The residue was extracted with CH_2Cl_2 and hexane (ratio 1:1) (10 cm^3), the volume reduced *in vacuo* to 3 cm^3 and the solution chromatographed on alumina. Elution with CH_2Cl_2 gave a single orange band, which on recrystallisation from CH_2Cl_2/pentane afforded bright orange crystals (111 mg, 72 %) of *exo-anti*-[Mo(η^3-CHPhCHCHCPhO)(CO)$_2$(η-C_5H_5)] (76).

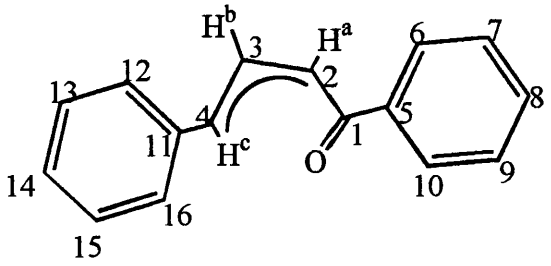

***Exo-anti* isomer**

^1H NMR: CD_2Cl_2, 20 ^oC): δ 7.96-7.81 (m, 2H, C_6H_5), 7.57-7.15 (m, 8H, C_6H_5), 6.0 [d, 1H, H^c, $J(H^cH^b)$ = 11.5], 5.42 [dd, 1H, H^b, $J(H^bH^c)$ = 11.5, $J(H^bH^a)$ = 7.1], 5.34 (s, 5H, C_5H_5), 4.59 [d, 1H, H^a, $J(H^aH^b)$ = 7.1].

^{13}C-{^1H} NMR: (CD_2Cl_2, 20 ^oC): δ 250.8 (br s, CO), 248.5 (br s, CO), 198.0 (br s, C^1), 141.2 (br s, C^5), 94.1 (br s, C_5H_5), 84.9 (br s, C^3), 73.7 (C^2), 65.6 (C^4) and 50.3.

***Endo-Anti* isomer**

^1H NMR: (CD_2Cl_2, 20 ^oC): δ 7.96-7.81 (m, 2H, C_6H_5), 7.57-7.15 (m, 8H, C_6H_5), 5.11 [dd, 1H, H^b, $J(H^bH^c)$ = 11.7, $J(H^bH^a)$ = 6.6], 5.03 (s, 5H, C_5H_5), 4.76 [d, 1H, H^a, $J(H^aH^b)$ = 6.2], 4.73 [d, 1H, H^c, $J(H^cH^b)$ = 10.5].

^{13}C-{^1H} NMR: (CD_2Cl_2, 20 ^oC): δ 250.8 (br s, CO), 248.5 (br s, CO), 198.0 (br s, C^1), 141.2 (br s, C^5), 93.5 (br s, C_5H_5), 84.9 (br s, C^3), 71.2 (C^2), 29.8 (C^4).

IR: ν_{CO}/cm^{-1} (CH_2Cl_2) at 1956 (vs), 1877 (s) and 1636 (m).

FAB Mass Spectrum: (+) FAB in NBA: 439, $[M]^+$; 412, $[M\text{-}CO]^+$ and 384, $[M\text{-}2CO]^+$

Microanalysis $C_{23}H_{18}MoO_3$ requires: C = 63.0, H = 4.1 %
found: C = 62.6, H = 4.1 %

6.10 Preparation of $[Mo(\eta^2\text{-}P{\equiv}C\textit{t}Bu)\{P(OMe)_3\}_2(\eta\text{-}C_5H_5)]^+[HOB(C_6F_5)_3]^-$/ $[(C_6F_5)_3B(\mu\text{-}OH)B(C_6F_5)_3]^-$ (87)

A solution of the η^2(3e)-vinyl complex $[Mo\{=C(Ph)CHPh\}\{P(OMe)_3\}_2(\eta\text{-}C_5H_5)]$ (8) (150 mg, 0.25 mmol) in CH_2Cl_2 (15 cm^3) was cooled to -78 °C and treated with *t*BuC≡P (42 μl, 1.25 mmol). $B(C_6F_5)_3$ (130 mg, 0.25 mmol) was then dissolved in CH_2Cl_2 (5 cm^3) and added to the mixture *via* cannula. The mixture was allowed to warm to ambient temperature and stirred for 1 hr. The solvent was removed *in vacuo* which afforded $[Mo(\eta^2\text{-}P{\equiv}C\textit{t}Bu)\{P(OMe)_3\}_2(\eta\text{-}C_5H_5)]^+[HOB(C_6F_5)_3]^-/[(C_6F_5)_3B(\mu\text{-}OH)B(C_6F_5)_3]^-$ (87) (201 mg 76 %) as a green/blue oil. Yield was calculated by assuming the $[HOB(C_6F_5)_3]^-$ anion was produced in 100 % yield.

Mixture of (87) and trans-stilbene

^1H NMR: (CD_2Cl_2, 20 °C): δ 7.41-7.01 (m, 12H, *trans*-stilbene), 5.53 (s, 5H, C_5H_5), 3.38 [vt, {*J*(HP) +*J*(HP')} = 11.32, 18H, PO*Me*], 2.95 (br s, 1H, B-O*H*), 1.49 (s, 9H, *t*Bu).

^{13}C-{^1H} NMR: (CD_2Cl_2, 20 °C): δ 334.6 [dt, *J*(CP) =113.9, *J*(CP) = 8.6, P≡*C*], 148.1 [d, *J*(CF) = 234.2, *o*-$B(C_6F_5)_3$], 138.8 [d, *J*(CF) = 242.8, *p*-$B(C_6F_5)_3$], 137.4 (s, *ipso*-Ph), 136.7 [d, *J*(CF) = 257.9, *m*-$B(C_6F_5)_3$], 128.8 (s, C_6H_5), 128.6 (s, C_6H_5), 128.3 (s, C_6H_5), 127.7 (s, C_6H_5), 126.5 (s, C_6H_5), 123.7 [s br, *ipso*-$B(C_6F_5)_3$], 94.4 (s, C_5H_5), 33.6 (s, C*Me*$_3$), 31.7 (s, *C*Me$_3$).

^{31}P-{^1H} NMR: (CD_2Cl_2, 20 °C): δ 492.4 [t, *J*(PP) = 30.1, *P*≡C], 175.1 [d, *J*(PP) = 30.1, $P(OMe)_3$].

^{11}B-{^1H} NMR: (CD_2Cl_2, 20 °C): δ -4.2 (s, 1B, HO*B*), -5.6 [s, 2B, *B*(μ-OH)*B*].

^{19}F NMR: (CD_2Cl_2, 20 °C): δ -134.6 [s, 6F, *o*-F, $HOB(C_6F_5)_3$], -136.0 [s, 12F, *o*-F, $[(C_6F_5)_3B(\mu\text{-}OH)B(C_6F_5)_3]$, -162.4 [s, 3F, *p*-F, $HOB(C_6F_5)_3$], -163.1 [s, 6F, *p*-F, $[(C_6F_5)_3B(\mu\text{-}OH)B(C_6F_5)_3]$, -166.7 [s, 6F, *m*-F, $[HOB(C_6F_5)_3]$, -167.2 [s, 12F, *m*-F, $[(C_6F_5)_3B(\mu\text{-}OH)B(C_6F_5)_3]$.

FAB Mass Spectrum: (+) FAB in NBA: 481, $[M\text{-}2CH_3]^+$; 391, $[M\text{-}t\text{BuC}{\equiv}\text{P-}CH_3]^+$ and 221, $[M\text{-}t\text{BuC}{\equiv}\text{P-P}(OMe)_3]^+$.

6.11 Preparation of $[Mo(CO)_2\{P(OMe)_3\}_2(\eta\text{-}C_5H_5)]^+[HOB(C_6F_5)_3]^-/[(C_6F_5)_3B(\mu\text{-}OH)B(C_6F_5)_3]^-$ (88)

A solution of the η^2(3e)-vinyl complex $[Mo\{{=}C(Ph)CHPh\}\{P(OMe)_3\}_2(\eta\text{-}C_5H_5)]$ (8) (100 mg, 0.17 mmol) in CH_2Cl_2 (15 cm^3) was cooled to -78 °C and treated with a solution of $B(C_6F_5)_3$ (87 mg, 0.17 mmol) in CH_2Cl_2 (5 cm^3). The mixture was bubbled with carbon monoxide and was allowed to warm to ambient temperature. Monitoring the reaction by infrared spectroscopy indicated the presence of two strong infrared absorption bands at 1998 and 1927 cm^{-1}. After 1 hr at ambient temperature the solvent was removed *in vacuo* which afforded $[Mo(CO)_2\{P(OMe)_3\}_2(\eta\text{-}C_5H_5)]^+[HOB(C_6F_5)_3]^-/[(C_6F_5)_3B(\mu\text{-}OH)B(C_6F_5)_3]^-$ (88) (114 mg 68 %) as a bright yellow oil. Yield was calculated by assuming the $[HOB(C_6F_5)_3]^-$ anion was produced in 100 % yield.

Mixture of (88) and trans-stilbene

^1H NMR: (CD_2Cl_2, 20 °C): δ 7.42-7.02 (m, 12H, *trans*-stilbene), 5.31 (s, 5H, C_5H_5), 3.64 [d, *J*(PH) = 11.6, 18H, PO*Me*], 2.93 (br s, 1H, B-O*H*).

$^{31}P\text{-}\{^1H\}$ NMR: (CD_2Cl_2, 20 °C): δ 170.3 [s, $POMe)_3$].

^{11}B-{^{1}H} NMR: (CD_2Cl_2, 20 °C): δ 17.4 [s, 1B, H*B*(C_6F_5)$_3$], -4.3 (s, 1B, HO*B*), -5.8 [s, 2B, *B*(μ-OH)*B*].

^{19}F NMR: (CD_2Cl_2, 20 °C): δ -134.8 [d, *J*(FF) = 21.2, 6F, *o*-F, HOB(C_6F_5)$_3$], -136.4 [d, *J*(FF) = 19.8, 12F, *o*-F, (C_6F_5)$_3$B(μ-OH)B(C_6F_5)$_3$], -161.4 [t, *J*(FF) = 21.2, 3F, *p*-F, HOB(C_6F_5)$_3$], -163.5 [t, *J*(FF) = 19.8, 6F, *p*-F, (C_6F_5)$_3$B(μ-OH)B(C_6F_5)$_3$], -167.2 [t, *J*(FF) = 18.4, 6F, *m*-F, HOB(C_6F_5)$_3$], -167.5 [t, *J*(FF) = 12F, 18.4, *m*-F, (C_6F_5)$_3$B(μ-OH)B(C_6F_5)$_3$].

IR: ν_{CO}/cm^{-1} (CH_2Cl_2) at 1998 (br), 1927 (br).

FAB Mass Spectrum: (+) FAB in NBA: 467, [M]$^+$; 439, [M-CO]$^+$ and 284, [M-2CO - 2OMe$_3$ - C_5H_5]$^+$.

6.12 Preparation of [Mo(η^2-PhC≡CPh){P(OMe)$_3$}$_2$(η-C_5H_5)]$^+$[MeOB(C_6F_5)$_3$]$^-$ (91)

A solution of the η^2(3e)-vinyl complex [Mo{=C(Ph)CHPh}{P(OMe)$_3$}$_2$(η-C_5H_5)] (8) (150 mg, 0.25 mmol) in CH_2Cl_2 (15 cm^3) was cooled to -78 °C and treated with P(OMe)$_3$ (60 μl, 0.50 mmol). B(C_6F_5)$_3$ (130 mg, 0.25 mmol) was then dissolved in CH_2Cl_2 (5 cm^3) and added to the mixture *via* cannula. The mixture was allowed to warm to ambient temperature and stirred for 1 hr. The solvent was removed *in vacuo* and the residue washed several times with hexane. The solvent was again removed *in vacuo* which afforded [Mo(η^2-PhC≡CPh){P(OMe)$_3$}$_2$(η-C_5H_5)]$^+$[MeOB(C_6F_5)$_3$]$^-$ (91) (214 mg 74 %) as a red/brown powder.

^{1}H NMR: (CD_2Cl_2, 20 °C): δ 7.47-7.37 (m, 10H, C_6H_5), 5.67 (s, 5H, C_5H_5), 3.52 [vt, {*J*(HP) +*J*(HP')} = 10.99, 18H, PO*Me*], 3.08 (br s, 3H, BO*Me*].

^{13}C-{^{1}H} NMR: (CD_2Cl_2, 20 °C): δ 223.6 [t, *J*(CP) = 13.5, ≡*C*C_6H_5], 148.0 [d, *J*(CF) = 241.5, *o*-$B(C_6F_5)_3$], 139.5 [d, *J*(CF) = 246.9, *p*-$B(C_6F_5)_3$], 138.6 (s, *ipso*-C_6H_5), 136.9 [d, *J*(CF) = 241.4, *m*-$B(C_6F_5)_3$], 129.7 (s, C_6H_5), 128.7 (s,C_6H_5), 127.5 (s, C_6H_5), 127.3 (s, C_6H_5), 126.3 (s, C_6H_5), 123.1 [s br, *ipso*-$B(C_6F_5)_3$], 95.1 (s, C_5H_5), 54.7 (s, BO*Me*).

^{31}P-{^{1}H} NMR: (CD_2Cl_2, 20 °C): δ 175.6 [s, *P*$OMe)_3$].

^{11}B-{^{1}H} NMR: (CD_2Cl_2, 20 °C): δ -5.4 (s, 1B, *B*OMe).

^{19}F NMR: (CD_2Cl_2, 20 °C): δ -134.7 [d, *J*(FF) = 20.8, 1F, *o*-F, $MeOB(C_6F_5)_3$], -134.9 [d, *J*(FF) = 15.2, 1F, *o*-F, $MeOB(C_6F_5)_3$], -135.4 [d, *J*(FF) = 19.7, 2F, *o*-F, $MeOB(C_6F_5)_3$], -136.3 [d, *J*(FF) = 19.6, 2F, *o*-F, $MeOB(C_6F_5)_3$], -161.0 [t, *J*(FF) = 20.8, 2F, *p*-F, $MeOB(C_6F_5)_3$], -161.1 [t, *J*(FF) = 16.1, 1F *p*-F, $MeOB(C_6F_5)_3$], -166.2 [t, *J*(FF) = 19.7, 3F, *m*-F, $MeOB(C_6F_5)_3$], -166.6 [t, *J*(FF) = 18.5, 2F, *m*-F $MeOB(C_6F_5)_3$], -167.1 [t, *J*(FF) = 20.2, 1F, *m*-F $MeOB(C_6F_5)_3$].

FAB Mass Spectrum: (+) FAB in NBA: 589, $[M]^+$; 481, $[M\text{-}3OMe_3\text{-}Me]^+$ and 427, $[M\text{-}P(OMe)_3\text{ -}OMe]^+$.

6.13 Reaction of [Mo{=C(Ph)CHPh}{P(OMe)$_3$}$_2$(η-C$_5$H$_5$)] (8) with B(C$_6$F$_5$)$_3$

In the absence of a trapping reagent, B(C$_6$F$_5$)$_3$ (87 mg, 0.17 mmol) was added to a solution of (8) (100 mg, 0.17 mmol) in CD_2Cl_2 at -78 °C. There was an instantaneous colour change (green → red) and the mixture was monitored by a temperature dependent NMR study. An EPR study was also carried out.

^{1}H NMR: (CD_2Cl_2, -78 °C): δ 7.52-7.26 (m, 10H, C$_6$*H*$_5$), 4.83 (s, 5H, C$_5$H$_5$), 3.62 [d, *J*(PH) = 9.04, 18H, PO*Me*].

(CD_2Cl_2, -50 °C): δ 7.58-7.31 (m, 10H, C$_6$*H*$_5$), 5.01 (s, 5H, C$_5$H$_5$), 3.63 [d, *J*(PH) = 11.06, 18H, PO*Me*], 3.33 (br s, 1H, B-O*H*).

(CD_2Cl_2, +25 °C): δ 7.43-7.23 (m, 10H, C$_6$*H*$_5$), 5.17 (s, 5H, C$_5$H$_5$), 3.42 [dd, *J*(PH) = 9.05, *J*(PH) = 2.01, 18H, PO*Me*], 3.23 (br s, 1H, B-O*H*).

^{31}P-{^{1}H} NMR: (CD_2Cl_2, -78 °C): δ 171.0 [dd, *J*(PP) = 351.8, *J*(PP) = 70.3, *thermodynamic* product], 169.1 [dd, *J*(PP) = 70.3, *kinetic* product].

(CD_2Cl_2, -50 °C): δ 170.9 [dd, *J*(PP) = 301.6, *J*(PP) = 60.3, *thermodynamic* product], 168.8 [dd, *J*(PP) = 120.6, *J*(PP) = 60.3, *kinetic* product].

(CD_2Cl_2, -25 °C): δ 170.6 [dd, *J*(PP) = 372.0, *J*(PP) = 70.3, *thermodynamic* product], 168.7 [dd, *J*(PP) = 120.6, *J*(PP) = 60.3, *kinetic* product].

(CD_2Cl_2, 0 °C): δ 170.7 [dd, *J*(PP) = 221.2, *J*(PP) = 70.4, *thermodynamic* product], 168.3 [dd, *J*(PP) = 251.3, *J*(PP) = 60.3, *kinetic* product].

(CD_2Cl_2, +25 °C): δ 170.5 [dd, *J*(PP) = 181.0, *J*(PP) = 70.4, *thermodynamic* product], 168.3 [dd, *J*(PP) = 301.6, *J*(PP) 50.2, *kinetic* product].

^{11}B-{^1H} NMR: (CD_2Cl_2, -78 °C): δ -5.0 (s br, 1B, HO*B*).
(CD_2Cl_2, -50 °C): δ -3.8 (s br, 1B, HO*B*).
(CD_2Cl_2, +25 °C): δ -2.5 (s br, 1B, HO*B*).

^{19}F NMR: (CD_2Cl_2, -78 °C): δ -136.5 [s, 6F, *o*-F, $HOB(C_6F_5)_3$], -160.9 [d, *J*(FF) = 221.2, 3F, *p*-F, $HOB(C_6F_5)_3$], -165.8 [d, *J*(FF) = 110.6, 6F, *m*-F, $HOB(C_6F_5)_3$].
(CD_2Cl_2, -50 °C): δ -136.4 [d, *J*(FF) = 20.1, 6F, *o*-F, $HOB(C_6F_5)_3$], -161.1 [s, 3F, *p*-F, $HOB(C_6F_5)_3$], -166.0 [s, 6F, *m*-F, $HOB(C_6F_5)_3$].
(CD_2Cl_2, +25 °C): δ -136.3 [d *J*(FF) = 10.1, 6F, *o*-F, $HOB(C_6F_5)_3$], -160.5 [s, 3F, *p*-F, $HOB(C_6F_5)_3$], -165.8 [s, 6F, *m*-F, $HOB(C_6F_5)_3$].

EPR (Chapter 4 Figure 4.4) [260 K, CH_2Cl_2: CH_3CHCl_2 (ratio 1:1)]
observable hyperfine coupling constants were detectable at:
g_{iso} = 2.011, ddd[A(^{1}H) 8.0 G, A(^{31}P) 23.9 G, A(^{31}P1) 37.9 G],
Mo satellites [A(^{95,97}Mo) 16.9 G].
g_{iso} = 1.976, t[A(^{31}P) 27.7 G],
triplet satellites not resolved.

6.14 EPR study of the reaction of $[Mo\{=C(Ph)CDPh\}\{P(OMe)_3\}_2(\eta\text{-}C_5H_5)]$ (8D) with $B(C_6F_5)_3$

EPR (Chapter 4 Figure 4.5) [260 K, CH_2Cl_2]
observable hyperfine coupling constants were detectable at:
g_{iso} = 2.011, dd[A(^{31}P) 24.0 G, A(^{31}P1) 37.9 G],
Mo satellites [A(^{95,97}Mo) 21.3 G].
g_{iso} = 1.975, t[(^{31}P) 27.7 G],

Mo satellites [A(^{95,97}Mo) 22.0 G].

6.15 Preparation of [Mo(η^2-PhC≡CPh){P(OMe)$_3$}$_2$(η-C$_5$H$_5$)]$^+$[PF$_6$]$^-$ (7)$^+$PF$_6^-$

[Fe(η-C$_5$H$_5$)$_2$][PF$_6$] (73 mg, 0.22 mmol) was dissolved in CH_2Cl_2 (5 cm^3) and was added to a solution of the η^2(3e)-vinyl complex [Mo{=C(Ph)CHPh}{P(OMe)$_3$}$_2$(η-C$_5$H$_5$)] (8) (130 mg, 0.22 mmol) in CH_2Cl_2 (15 cm^3) at -78 °C. The mixture was allowed to warm to ambient temperature and after 1 hr the solvent was removed *in vacuo* and the residue was washed with hexane (60 cm^3). The hexane washings were yellow and were found to contain [Fe(η-C$_5$H$_5$)$_2$]. The remaining residue was recrystallised from CH_2Cl_2/hexane to afford [Mo(η^2-PhC≡CPh){P(OMe)$_3$}$_2$(η-C$_5$H$_5$)]$^+$[PF$_6$]$^-$ (7)$^+$PF$_6^-$ (123 mg 76 %) as a red/brown powder.

^{1}H NMR: (CD_2Cl_2, 20 °C): δ 7.56-7.15 (m, 10H, C_6H_5), 5.70 (s, 5H, C_5H_5), 3.53 [vt, {*J*(HP) +*J*(HP')} = 11.36, 18H, PO*Me*].

^{13}C-{^{1}H} NMR: (CD_2Cl_2, 20 °C): δ 223.2 [t, *J*(CP) = 12.4, ≡*C*C_6H_5], 137.3 (s, *ipso*-C_6H_5), 128.8 (s, C_6H_5), 128.7 (s,C_6H_5), 127.4 (s, C_6H_5), 127.2 (s, C_6H_5), 126.5 (s, C_6H_5), 95.5 (d, *J*(CP) = 16.3, C_5H_5).

^{31}P-{^{1}H} NMR: (CD_2Cl_2, 20 °C): δ 175.6 [s, POMe)$_3$], -143.6 [q, *J*(PF) = 711, PF_6].

EPR (Chapter 4 Figure 4.2) [240 K, CH_2Cl_2:thf (ratio1:2)]
observable hyperfine coupling constants were detectable at:
g_{iso} = 2.011, ddd[A(^{1}H) 8.0 G, A(^{31}P) 23.7 G, A(^{31}P1) 37.8 G],
Mo satellites [A(^{95,97}Mo) 17.0 G].

6.16 EPR study of the reaction of [Mo{=C(Ph)CDPh}{P(OMe)$_3$}$_2$(η-C$_5$H$_5$)] (8D) with [Fe(η-C$_5$H$_5$)$_2$][PF$_6$]

EPR (Chapter 4 Figure 4.3) [260 K, CH_2Cl_2]

observable hyperfine coupling constants were detectable at:

g_{iso} = 2.011, dd[A(^{31}P) 24.4 G, A(^{31}P1) 37.2 G],

Mo satellites [A(^{95,97}Mo) 19.9 G].

6.17 EPR study of the reaction of [Mo{=C(Ph)CHPh}{P(OMe)$_3$}$_2$(η-C$_5$H$_5$)] (8) with [CPh$_3$][BF$_4$]

EPR (Chapter 4 Figure 4.6 and 4.7) [240 K, CH_2Cl_2]

observable hyperfine coupling constants were detectable at:

g_{iso} = 2.011, ddd[A(^{1}H) 8.1 G, A(^{31}P) 23.4 G, A(^{31}P1) 37.7 G],

Mo satellites [A(^{95,97}Mo) 17.0 G].

6.18 EPR study of the reaction of *cis*-[Cr(dppe)$_2$(CO)$_2$] with B(C$_6$F$_5$)$_3$

EPR (Chapter 4 Figure 4.9) [240 K, CH_2Cl_2]

observable hyperfine coupling constants were detectable at:

g_{iso} = 2.012, q[A(^{31}P) 28.7 G].

6.19 Preparation of [Mo{η^4-P$_2$C$_2$(*t*Bu)$_2$}{P(OMe)$_3$}$_2$(η^5-C$_9$H$_7$)]$^+$HOB(C$_6$F$_5$)$_3$]$^-$ /[(C$_6$F$_5$)$_3$B(μ-OH)B(C$_6$F$_5$)$_3$]$^-$ (95)

A solution of the η^2(3e)-vinyl complex [Mo{=C(Me)CPhH}{P(OMe)$_3$}$_2$(η^5-C$_9$H$_7$)] (94) (100 mg, 0.15 mmol) in CH_2Cl_2 (15 cm^3) was cooled to -78 °C and treated with *t*BuC≡P (24 μl, 0.15 mmol). B(C$_6$F$_5$)$_3$ (78 mg, 0.15 mmol) was then dissolved in CH_2Cl_2 (5 cm^3) and added to the mixture *via* cannula. The mixture was allowed to warm to ambient temperature and stirred for 1 hr. The solvent was removed *in vacuo* which afforded [Mo{η^4-P$_2$C$_2$(*t*Bu)$_2$}{P(OMe)$_3$}$_2$(η^5-C$_9$H$_7$)]$^+$[HOB(C$_6$F$_5$)$_3$]$^-$

/$[(C_6F_5)_3B(\mu\text{-}OH)B(C_6F_5)_3]^-$ (95) (71 mg, 42 %) as a brown oil. Yield was calculated by assuming the $[HOB(C_6F_5)_3]^-$ anion was produced in 100 % yield.

^1H NMR: (C_6D_6, 20 °C): δ 7.61-7.53 (m, 4H, C_9H_7), 7.44-7.21 (m, 10H, C_5H_5), 6.28-6.03 (m, 2H, C_9H_7), 5.25 (m, 1H, C_9H_7), (3.62 [d, *J*(PH) = 9.04, 18H, PO*Me*], 0.92 (s, 18 H, *t*Bu).

^{13}C-{^1H} NMR: (CD_2Cl_2, 20 °C): δ 147.3 [d, *J*(CF) = 238.7, *o*-$B(C_6F_5)_3$], 138.7 [d, *J*(CF) = 252.3, *p*-$B(C_6F_5)_3$] 136.1 [d, *J*(CF) = 246.9, *m*-$B(C_6F_5)_3$], 137.4 (s, *ipso*-C_5H_5), 125.9 (s, C_9H_7), 125.3 (s, C_9H_7), 125.3 (s, C_9H_7), 119.9 [br s, *ipso*-$B(C_6F_5)_3$], 114.8 9 (s, C_9H_7), 109.6 (s, C_9H_7), 97.7 [at, *J*(PC) = 54.3, *C*=P], 82.4 (s, CH, C_9H_7), 77.2 (s, C_9H_7), 53.7 (s, POMe), 35.7 (s, C*Me*$_3$), 31.9 (s, *C*Me$_3$).

^{31}P-{^1H} NMR: (CD_2Cl_2, 20 °C): δ 160.0 (s, *P*OMe), 67.0 (s, *P*=C), 65.6 (s, *P*=C).

^{11}B-{^1H} NMR: (CD_2Cl_2, 20 °C): δ -4.3 (s, 1B, HO*B*), -5.5 [s, 2B, *B*(μ-OH)*B*].

^{19}F NMR: (CD_2Cl_2, 20 °C): δ -134.8 [br s, 6F, *o*-F, $HOB(C_6F_5)_3$], -136.3 [br s, 12F, *o*-F, $(C_6F_5)_3B(\mu\text{-}OH)B(C_6F_5)_3$], -161.0 [t, *J*(FF) = 20.2, 3F, *p*-F, $HOB(C_6F_5)_3$], -163.0 [t, *J*(FF) = 20.2, 6F, *p*-F, $(C_6F_5)_3B(\mu\text{-}OH)B(C_6F_5)_3$], -166.6 [t, *J*(FF) = 18.0, 6F, *m*-F, $HOB(C_6F_5)_3$], -167.1 [t, *J*(FF) = 12F, 18.5, *m*-F, $(C_6F_5)_3B(\mu\text{-}OH)B(C_6F_5)_3$].

6.20 Reaction of $[Mo(\eta^2\text{-}P{\equiv}CtBu)\{P(OMe)_3\}_2(\eta\text{-}C_5H_5)]^+[HOB(C_6F_5)_3]^-$/ $[(C_6F_5)_3B(\mu\text{-}OH)B(C_6F_5)_3]^-$ (87) with MeC≡CMe.

An excess of MeC≡CMe was added to a solution of $[Mo(\eta^2\text{-}P{\equiv}CtBu)\{P(OMe)_3\}_2(\eta\text{-}C_5H_5)]^+[HOB(C_6F_5)_3]^-$/ $[(C_6F_5)_3B(\mu\text{-}OH)B(C_6F_5)_3]^-$ (87) CD_2Cl_2 (4 cm^3) in an NMR tube and the mixture was continually monitored over a period of two weeks by NMR spectroscopy.

^1H NMR: (C_6D_6, 20 °C): δ 7.55-7.15 (m, 10H, C_6H_5), 5.58 (s, 5H, C_5H_5), 3.73 [d, *J*(PH) = 10.99, 18H, PO*Me*], 1.26 [s, 6H, CH_3], 0.91 [s, 9H, *t*Bu].

$^{13}C\text{-}\{^1H\}$ NMR: (CD_2Cl_2, 20 °C): δ 224.6 [t, *J*(CP) = 13.6, Mo=*C*], 175.0 [s, Mo=*C*], 148.1 [d, *J*(CF) = 238.7, *o*-$B(C_6F_5)_3$], 143.0 [dd, *J*(CP) = 67.9, *J*(CP) = 20.4, *C*=P], 137.4 [d, *J*(CF) = 252.3, *p*-$B(C_6F_5)_3$], 137.4 (s, *ipso*-C_6H_5), 136.8 [d, *J*(CF) = 249.5, *m*-$B(C_6F_5)_3$], 129.3 (s, C_6H_5), 128.8 (s,C_6H_5), 128.6 (s, C_6H_5), 127.7 (s, C_6H_5), 126.5 (s, C_6H_5), 121.7 [s br, *ipso*-$B(C_6F_5)_3$], 95.1 (s, C_5H_5), 33.2 (s, CMe_3) and 31.0 (s, *C*Me_3).

$^{31}P\text{-}\{^1H\}$ NMR: (CD_2Cl_2, 20 °C): δ 181.0 (s), 159.8 (s), 134.8 (s).

6.21 Preparation of $[Pt{=}C(tBuC)P(OH)(O){=}O(PPh_3)_2]$ (107)

$[Pt(\eta^2\text{-}P{\equiv}CtBu)(PPh_3)_2]$ (86) (200 mg, 0.24 mmol) was suspended in $(CH_3)_2CO$ (20 cm^3) at -78 °C. Dimethyldioxirane (8.0 cm^3 of 0.04 M solution in acetone, 0.32 mmol) was added to the solution and the resulting suspension was allowed to warm to ambient temperature. The volatiles were then removed *in vacuo* and the solid was extracted with CH_2Cl_2 (10 cm^3) and filtered through a Celite pad. The volume of the solution was reduced to 3 cm^3 and hexane (40 cm^3) was added to

precipitate a very pale yellow powder. The supernatant liquid was removed and the powder washed with hexane (2 x 10 cm^3) and dried *in vacuo* to yield [Pt{=C(*t*BuC)P(OH)(O)=O}(PPh_3)$_2$] (107) (154 mg, 73 %).

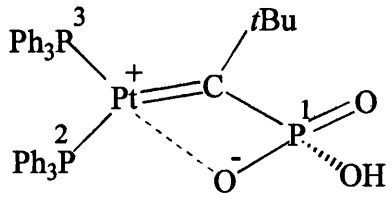

^1H NMR: (CD_2Cl_2, 20 ^oC): δ 7.75-7.13 (m, 30H, Ph), 0.91 (s, 9H, Me_3).

^{13}C-{^1H} NMR: (CD_2Cl_2, 20 ^oC): δ 135.6-128.2 (m, 36 C, Ph), 68.1 [s, Pt=*C*], , 35.2 (s, C*Me*$_3$), 32.3 (*s*, *C*Me$_3$).

^{31}P-{^1H} NMR: (CD_2Cl_2, 20 ^oC): δ 38.8 [br s, *J*(PtP) = 322.0, P^1], 22.9 [d, *J*(PP) = 13.4, *J*(PtP) = 1998.7, P^2], 14.0 [dd. *J*(PP) = 13.3, *J*(PP) = 6.7, *J*(PtP) = 4748.7, P^3].

IR: ν_{PO}/cm^{-1} (CH_2Cl_2) at 1090 (s).

FAB Mass Spectrum: (+) FAB in NBA: 869, $[M]^+$; 719, $[M\text{-}C(tBu)P(OH)(O)O]^+$; 456, $[M\text{-}C(tBu)P(OH)(O)O\text{-}PPh_3]^+$; 377, $[M\text{-}C(tBu)P(OH)(O)O\text{-}PPh_3\text{-}Ph]^+$.

Microanalysis	$C_{41}H_{38}PtO_3P_3$	requires:	C = 56.8, H = 4.41 %
		found:	C = 52.5, H = 4.25 %

Possibly crystallises with 1 mole of CH_2Cl_2 :

$C_{42}H_{40}PtO_3P_3Cl_2$	requires:	C = 53.0, H = 4.23 %

6.22 Preparation of [Pt(*t*BuC≡P)(dppf)] (99)

A solution of [Pt(η^2-C_2H_4)(dppf)] (200 mg, 0.26 mmol) in CH_2Cl_2 (15 cm^3) was cooled to -78 °C and treated with *t*BuC≡P (41 μl, 0.26 mmol). The mixture was allowed to warm to room temperature and was stirred for 30 min. After this period, the solvent was removed *in vacuo* and the product extracted with CH_2Cl_2 (30 cm^3) and filtered through a pad of Celite. Removal of solvent and recrystallisation from CH_2Cl_2/hexane afforded [Pt(*t*BuC≡P)(dppf)] (99) as a bright yellow powder (174 mg, 79 %).

^1H NMR: (CD_2Cl_2, 20 °C): δ 7.88-7.66 (m, 8H, Ph), 7.43-7.32 (m 12H Ph), 4.36 (s, 4H, C_5H_4), 4.09 (s, 2H, C_5H_4), 3.89 (s, 2H, C_5H_4), 0.91 (s, 9H, Me_3).

^{13}C-{^1H} NMR: (CD_2Cl_2, 20 °C): δ 134.4 [dd, *J*(CP) = 57.0, *J*(CP) = 13.6, P≡*C*], 130.0 (s, C_6H_5), 129.5 (s, C_6H_5), 127.9 (s, C_6H_5), 127.8 (s, C_6H_5), 127.6 (s, C_6H_5), 33.4 [d, *J*(CP) = 10.8, C*Me*$_3$], 31.2 [d, *J*(CP) = 5.4, *C*Me$_3$].

^{31}P-{^1H} NMR: (CD_2Cl_2, 20 °C): δ 82.7 [dd, *J*(PP) = 26.8, *J*(PP) = 16.8, *J*(PtP) = 104.0, *P*≡C], 23.1 [at, *J*(PP) = 26.9, *J*(PtP) = 3642.0], 23.1 [at, *J*(PP) = 16.8, *J*(PtP) = 3192.6].

FAB Mass Spectrum: (+) FAB in NBA: 850, $[M]^+$; 749 $[M-t\text{BuC}{\equiv}P]^+$.

Microanalysis	$C_{39}H_{37}PtFeP_3$	requires:	C = 55.1, H = 4.39 %
		found:	C = 53.7, H = 4.19 %

6.23 Preparation of [Pt{=C(*t*BuC)P(OH)(O)=O}(dppf)] (108)

[Pt(η^2-P≡C*t*Bu)(dppf] (99) (110 mg, 0.13 mmol) was suspended in $(CH_3)_2CO$ (12 cm^3) at -78 °C. Dimethyldioxirane (4.8 cm^3 of 0.04 M solution in acetone, 0.19 mmol) was added to the solution and the resulting suspension was allowed to warm to ambient temperature. The volatiles were then removed *in vacuo* and the solid was extracted with CH_2Cl_2 (10 cm^3) and filtered through a Celite pad. The volume of the solution was reduced to 3 cm^3 and hexane (40 cm^3) was added to precipitate a very pale yellow powder. The supernatant liquid was removed and the powder washed with hexane (2 x 10 cm^3) and dried *in vacuo* to yield [Pt{=C(*t*BuC)P(OH)(O)=O}(dppf)] (108) (84 mg, 72 %).

^{31}P-{^1H} NMR: (CD_2Cl_2, 20 °C): δ 39.6 [br s, *J*(PtP) = 311.9, P^1], 21.0 [d, *J*(PP) = 16.8, *J*(PtP) = 2107.7, P^2], 12.5 [dd. *J*(PP) = 16.7, *J*(PP) = 6.7, *J*(PtP) = 4732.7, P^3].

IR: ν_{PO}/cm^{-1} (CH_2Cl_2) at 1090 (s).

FAB Mass Spectrum: (+) FAB in NBA: 900, $[M]^+$; 749, $[M\text{-}C(t\text{Bu})P(OH)(O)O]^+$.

6.24 Preparation of [Pt{C(*t*Bu)=PH}$(PPh_3)_2$]$^+$[HOB$(C_6F_5)_3$]$^-$(109)

A solution of $B(C_6F_5)_3$ (86 mg, 0.16 mmol) in CH_2Cl_2 was added dropwise to a solution of the yellow complex [Pt(η^2-P≡C*t*Bu)$(PPh_3)_2$] (86) (139 mg, 0.16 mmol) in CH_2Cl_2 (15 cm^3) at -78 °C. The mixture was allowed to warm to ambient temperature and stirred for a further 1 hr. The solvents were removed *in vacuo* to afford the purple oil [Pt{C(*t*Bu)=PH}$(PPh_3)_2$]$^+$[HOB$(C_6F_5)_3$]$^-$ (109) in good yield (183 mg, 81 %).

^{1}H NMR: (CD_2Cl_2, 20 °C): δ 7.01-7.64 (m, 30 H, C_6H_5), 0.91 (s, 9H, *t*Bu).

^{13}C-{^{1}H} NMR: (CD_2Cl_2, 20 °C): δ 148.1 [d, *J*(CF) = 240.8, *o*-$B(C_6F_5)_3$], 139.6 [d, *J*(CF) = 261.1, *p*-$B(C_6F_5)_3$], 137.2 [d, *J*(CF) = 235.3, *m*-$B(C_6F_5)_3$], 135.9-128.0 (m, C_6H_5), 120.8 [s br, *ipso*-$B(C_6F_5)_3$], 66.6 (s, *C*=P), 33.9 (s, C*Me*$_3$) and 31.0 (s, *C*Me$_3$).

^{31}P-{^{1}H} NMR: (CD_2Cl_2, -78 °C): δ 130.0 [br d, *J*(PB) = 324.0, *J*(PPt) = 3236.6, *P*→B], 26.3-15.4 (m, *P*Ph_3).
(CD_2Cl_2, -50 °C): δ 185.7. [s br,C=*P*,*thermodynamic* isomer] , 168.3 [s br, C=*P*, *kinetic* isomer], 130.0 [br d, *J*(PB) = 324.0, *J*(PPt) = 3236.6, *P*→B], 26.3-15.4 (m, *P*Ph_3).
(CD_2Cl_2, -25 °C): δ 185.7.6 [dd, *J*(PP) = 24.1, *J*(PP) = 13.9, C=*P*, *thermodynamic* isomer], 168.3 [s br C=*P*, kinetic isomer], 20.9-17.3 (m, *P*Ph_3).
(CD_2Cl_2, +25 °C): δ 185.7 [dd, *J*(PP) = 24.1, *J*(PP) = 13.9, *J*(PPt) = 134.8, C=*P*, *thermodynamic* isomer], 22.8 [at, *J*(PP) = 16.5, *J*(PPt) = 3440.9, *P*Ph_3], 22.5 [at, *J*(PP) = 20.3, *J*(PPt) = 2998.4, *P*Ph_3].

^{11}B-{^{1}H} NMR: (CD_2Cl_2, 20 °C): δ -4.3 (s, 1B, HO*B*).

^{19}F NMR: (CD_2Cl_2, 20 °C): δ -136.1 [s, 6F, *o*-F, $HOB(C_6F_5)_3$], -161.3 [s, 3F, *p*-F, $HOB(C_6F_5)_3$], -165.4 [s, 6F, *m*-F, $[HOB(C_6F_5)_3]$].

CHAPTER SEVEN

REFERENCES

7.1 References

1. M. J. S. Dewar, *Bull. Soc. Chim.*, 1951, **18**, C79.

2. J. Chatt and L. A. Duncanson, *J. Chem. Soc.* B, 1953, 2939.

3. J. P. Collman and L. S. Hegedus, *Principles and Applications of Organotransition Metal Chemistry*, University Science Books, 1987.

4. J. M. Augl and D. P. Tate, *J. Am. Chem. Soc.*, 1963, **85**, 2174.

5. J. M. Augl, J. G. Grasselli, W. M. Ritchey, B. L. Ross and D. P. Tate, *J. Am. Chem. Soc.*, 1964, **86**, 3261.

6. R. M. Laine, R. F. Moriaty and R. Bau, *J. Am. Chem. Soc.*, 1972, **94**, 1402.

7. R. B. King, *Inorg. Chem.*, 1968, **6**, 1044.

8. J. L. Templeton and B. C. Ward, *J. Am. Chem. Soc.*, 1980, **102**, 3288.

9. K. Sünkel, U. Nagel and W. Beck, *J. Organomet. Chem.*, 1981, **222**, 251.

10. K. R. Birdwhistell, T. L. Tonker and J. L. Templeton, *J. Am. Chem. Soc.*, 1987, **109**, 1401.

11. J. L. Templeton, *Adv. Organomet. Chem.*, 1989, **29**, 1.

12. P. W. R. Corfield, L. M. Baltusis and S. J. Lippard, *Inorg. Chem.*, 1981, **20**, 2883.

13. J. L. Davidson, M. Green, F. G. A. Stone and A. J. Welch, *J. Chem Soc., Dalton Trans.*, 1976, 738.

14. J. A. K. Howard, R. F. D. Stansfield and P. Woodward, *J. Chem. Soc., Dalton Trans.*, 1976, 246.

15. M. Green, N. C. Norman and A. G. Orpen, *J. Am. Chem. Soc.*, 1981, **103**, 1267.

16. S. R. Allen, R. G. Beevor, M. Green, N. C. Norman, A. G. Orpen and I. D. Williams, *J. Chem. Soc., Dalton Trans.*, 1985, 435.

17. C. Carfagna, N. Carr, R. J. Deeth, S. J. Dossett, M. Green, M. F. Mahon and C. Vaughan, *J. Chem. Soc., Dalton Trans.*, 1996, 415.

18. J. L. Davidson, I. E. P. Murray, P. N. Preston, M. V. Russo, Lj. Manojlovic-Muir and K. W. Muir, *J. Chem. Soc., Chem. Commun.*, 1981, 1059.

19. J. L. Davidson, W. Wilson, Lj. Manojlovic-Muir and K. W. Muir, *J. Organomet. Chem.*, 1983, **254**, C6.

20. N. M. Agh-Atabay (in part), L. J. Canoira, L. Carlton and J. L. Davidson, *J. Chem. Soc., Dalton Trans.*, 1991, 1175.

21. D. L. Reger and P. J. McElligott, *J. Am. Chem. Soc.*, 1980, **102**, 5923.

22. M. Bottrill and M. Green, *J. Am. Chem. Soc.*, 1977, **99**, 5795.

23. F. R. Kreissl, P. Friedrich and G. Huttner, *Angew. Chem., Int. Ed. Engl.*, 1977, **16**, 162.

24. J. L. Davidson, G. Vasapollo, Lj. Manojlovic-Muir and K. W. Muir, *J. Chem. Soc., Chem. Commun.*, 1982, 1025.

25 J. L. Kiplinger and T. G. Richmond, *Polyhedron*, 1997, **16**, 409.

26. L. Carlton, J. L. Davidson, P. Ewing, Lj. Manojlovic-Muir and K. W. Muir, *J. Chem. Soc., Chem. Commun.*, 1985, 1474.

27. R. G. Harrison and T. G. Richmond, *J. Am. Chem. Soc.*, 1993, **115**, 5303.

28. W. Clegg, M. Green, C. A. Hall, D. C. R. Hockless, N. C. Norman and C. M. Woolhouse, *J. Chem. Soc., Chem. Commun.*, 1990, 1330.

29. C. P. Casey, J. T. Brady, T. M. Boller, F. Weinhold and R. K. Hayashi, *J. Am. Chem. Soc.*, 1998, **120**, 12500.

30. A. Fries, M. Green, M. F. Mahon, T. D. McGrath, C. B. M. Nation, A. P. Walker and C. M. Woolhouse, *J. Chem. Soc., Daton Trans.*, 1996, 4517.

31. A. G. Massey and A. J. Park, *J. Organomet. Chem.*, 1964, **2**, 245.

32. W. E. Piers and T. Chivers, *Chem. Soc. Rev.*, 1997, **26**, 345.

33. X. Yang, C. L. Stern and T. J. Marks, *J. Am. Chem. Soc.*, 1994, **116**, 10015.

34. D. J. Parks, R. E .v. H. Spence and W. E. Piers, *Angew Chem., Int. Ed. Engl.*, 1995, **34**, 809.

35. X. Yang, C. L. Stern and T. J. Marks, *Organometallics*, 1991, **10**, 840.

36. V. C. Williams, W. E. Piers, W. Clegg, M. R. J. Elsegood, S. Collins and T. B. Marder, *J. Am. Chem. Soc.*, 1999, **121**, 3244.

37. R. D. Chambers and T. Chivers, *Organomet. Rev.*, 1966, **1**, 279.

38. S. C. Cohen and A. G. Massey, *Adv. Fluorine Chem.*, 1970, **6**, 149.

39. H. H. Brintzinger, D. Fischer, R. Milhaupt, B. Rieger and R. M. Waymouth, *Angew. Chem., Int. Ed. Engl.*, 1995, **34**, 1143.

40. M. Bochmann, *J. Chem. Soc., Dalton Trans.*, 1996, **3**,255.

41. T. J. Marks, *Acc. Chem. Res.*, 1992, **25**, 57.

42. R. F. Jordan, *Adv. Organomet. Chem.*, 1991, **32**, 325.

43. A. M. Thayer, *Chem. Eng. News*, 1995, **73**, 15.

44. R. G. Harvar, *Chem. Ind.*, 1997, 212.

45. H. Sinn and W. Kaminsky, *Adv. Organomet. Chem.*, 1980, **18**, 99.

46. E. W. Abel, F. G. A. Stone and G. Wilkinson, *Eds Pergman*, 1995, **4**, 589.

47. R. F. Jordan and A. S. Guram, *Comprehensive Organometallic Chemistry.*

48. N. Piccolrovazzi, P. Pino, G. Consiglio, A. Sirone and M. Moert, *Organometallics*, 1990, **9**, 3098.

49. I. K. Lee, W. J. Gauthier, J. M. Ball, B. Iyengary and S. Collins, *Organometallics*, 1992, **11**, 2115.

50. S. Collins, W. J. Gauthier, D. A. Holden, B. A. Kuntz, N. J. Taylor and D. G. Ward, *Organometallics*, 1991, **10**, 2061.

51. T. A. Herzog, D. L. Zubris and J. E. Bercaw, *J. Am. Chem. Soc.*, 1996, **118**, 11988.

52. J. H. Gilchrist and J. E. Bercaw, *J. Am. Chem. Soc.*, 1996, **118**, 12021.

53. J. Karl, M. Dahlmann, G. Erker and K. Bergander, *J. Am. Chem. Soc.,* 1998, **120**, 5463.

54. W. Kaminsky and M. Arndt, *Adv. Polym. Sci.*, 1997, **127**, 143.

55. P. C. Möhring and N. J. Coville, *J. Organomet. Chem.*, 1994, **479**, 1.

56. K. B. Sinclair and R. B. Wilson, *Chem. Ind.*, 1994, **21**, 857.

57. X. Yang, C. L. Stern, and T. J. Marks, *J. Am. Chem. Soc.*, 1991, **113**, 3623.

58. J. A. Ewen and M. J. Edler, CA-A, 1991, **2**, 027.

59. M. Bochmann, S. J. Lancaster, M. B. Hursthouse and K. M. A. Malik, *Organometallics*, 1994, **13**, 2235.

60. G. S. Hill, L. M. Rendina and R. J. Puddephatt, *J. Chem. Soc., Dalton Trans.*, 1996, 1809.

61. B. Temme, G. Erker, J. Karl, H. Luftmann, R. Fröhlich and S. Kotila, *Angew. Chem., Int. Ed. Engl.*, 1995, **34**, 16.

62. J. Ruwwe, G. Erker and R. Fröhlich, *Angew. Chem., Int. Ed. Engl.*, 1996, **35**, 1.

63. J. Karl, G. Erker, R. Fröhlich, F. Zippel, F. Bickelhaupt, M. S. Goedheijt, O. S. Akkerman, P. Binger and J. Stannek, *Angew. Chem., Int. Ed. Engl.*, 1997, **36**, 24.

64. M. Bochmann, S. J. Lancaster and O. B. Robinson, *J. Chem. Soc., Chem. Commun.*, 1995, **20**, 2081.

65. G. J. Pindado, M. Thornton-Pett, M. Bouwkamp, A. Meetsma, B. Hessen and M. Bochmann, *Angew. Chem., Int. Ed. Engl.*, 1997, **36**, 21.

66. H.vd. H, B. Hessen and G. Orpen, *J. Am. Chem. Soc.*, 1998, **120**, 1112.

67. R. E. vH. Spence and W. E. Piers, *Organometallics*, 1995, **14**, 4617.

68. Y. Sun, R. E.vH. Spence, W. E, Piers, M. Parvez and G. P. A. Yap, *J. Am. Chem. Soc.*, 1997, **119**, 5132.

69. B. Temme, J. Karl and G. Erker, *Chem. Eur. J.*, 1996, **2**, 919.

70. B. Temme, G. Erker, R. Fröhlich and M. Grehl, *Angew. Chem., Int. Ed. Engl.*, 1994, **33**, 1480.

71. W. Ahlers, B. Temme, G. Erker, R. Fröhlich and T. Fox, *J. Organomet. Chem.*, 1997, **527**, 191.

72. B. Temme, G. Erker, R. Fröhlich and M. Grehl, *J. Chem. Soc., Chem. Commun.*, 1994, **14**, 1713.

73. G. G. Hlatky, H. W. Turner and R. R. Eckman, *J. Am. Chem. Soc.*, 1989, **111**, 2728.

74. W. Ahlers, G. Erker and R. Fröhlich, *Eur. J. Inorg. Chem.*, 1998, **7**, 889.

75. Y. M. Sun, W. E. Piers and S. J. Rettig, *J. Chem. Soc., Chem. Commun.*, 1998, **1**, 127.

76. A. D. Horton, *Organometallics*, 1996, **15**, 2675.

77. K. Ishihara, N. Hanaki, M. Funahashi, M. Miyata and H. Yamamoto, *Bull. Chem. Soc. Jpn.*, 1995, **68**, 1721.

78. D. J. Parks and W. E. Piers, *J. Am. Chem. Soc.*, 1996, **118**, 9440.

79. G. P. Mitchell and T. D. Tilley, *Angew. Chem., Int. Ed. Engl.*, 1998, **37**, 18.

80. G. Barrado, L. Doerrer, M. L. H. Green and M. A. Leech, *J. Chem. Soc., Dalton Trans.*, 1999, 1061.

81. L. H. Doerrer, J. R. Galsworthy, M. L. H. Green and M. A. Leech, *J. Chem. Soc., Dalton Trans.*, 1998, 2483.

82. L. H. Doerrer, J. R. Galsworthy, M. L. H. Green, M. A. Leech and M. Müller, *J. Chem. Soc., Dalton Trans.*, 1998, 3191.

83. J. R. Galsworthy, M. L. H. Green, N. Maxted and M. Müller, *J. Chem. Soc., Dalton Trans.*, 1998, 387.

84. A. A. Danopoulous, J. R. Galsworthy, M. L. H. Green, S. Cafferkey, L. H. Doerrer and M. B. Hursthouse, *J. Chem. Soc., Chem. Commun.*, 1998, **22**, 2529.

85. A. R. Siedle, R. A. Newmark, W. M. Lamanna and J. C. Huffman, *Organometallics*, 1993, **12**, 1491.

86. H. E. Katz, *J. Am. Chem. Soc.*, 1985, **107**, 1420.

87. H. E. Katz, *J. Org. Chem.*, 1985, **50**, 2575.

88. H. E. Katz, *Organometallics*, 1987, **6**, 1134.

89. G. E. Herberich, U. Englert, A. Fischer and D. Wiebelhaus, *Organometallics*, 1998, **17**, 4769.

90. M. Fontani, F. Peters, W. Scherer, W. Wachter, M. Wagner and P. Zanello, *Eur. J. Inorg. Chem.*, 1998, **12**, 1453.

91. D. J. Parks, R. E. v. H. Spence and W. E. Piers, *Angew. Chem., Int. Ed. Engl.*, 1995, **34**, 809.

92. R. E. v. H. Spence, D. J. Parks, W. E. Piers, M. MacDonald, M. J. Zaworotko and S. J. Rettig, *Angew. Chem., Int. Ed. Engl.*, 1995, **34**, 1230.

93. R. E. v. H. Spence, W. E. Piers, Y. Sun, M. Parvez, L. R. MacGillivray and M. J. Zaworotko, *Organometallics*, 1998, **17**, 2459.

94. M. V. Galakhov, G.Heinz and P. Royo, *J. Chem. Soc., Chem. Commun.*, 1998, **1**, 17.

95. J. B. Lambert, L. Kania and S. Zhang, *Chem, Rev.*, 1995, **95**, 1191.

96. S. H. Strauss, *Chem. Rev.*, 1993, **93**, 927.

97. L. Jia, X. Yang, C. Stern and T. J. Marks, *Organometallics*, 1994, **13**, 3755.

98. K. Kohler, W. E. Piers, S. Xin, Y. Feng, A. M. Bravakis, A. P. Jarvis, S. Collins, W. Clegg, G. P. A. Yap and T. B. Marder, *Organometallics*, 1998, **17**, 3557.

99. EHMO calculation employed the CACAO2 program package developed by Mealli and Proserpio: C. Mealli and D. M. Proserpio, *J. Chem. Educ.*, 1990, **67**, 399.

100. A. J. Pearson, *Recent Developments in the Synthetic Applications of Organoiron and Organomolybdenum Chemistry*, in *Advances in Metal-Organic Chemistry*, ed. L. S. Liebeskind, JAI Press, London 1989, Vol. 1, p. 1.

101. A. J. Pearson, *Synlett*, 1991, 10.

102. A. J. Pearson, *Cyclohexadienes, in Second Supplements to the 2nd edition of Rodd's Chemistry of Carbon Compounds,* ed. M. Sainsbury, Elsevier Science Publishers, Amsterdam, 1992, vol. IIA and B, p.447.

103. W. J. Vong, S. M. Peng, S. H. Lin, W. J. Lin and R. S. Liu, *J Am. Chem. Soc.*, 1991, **113**, 573.

104. S. H. Lin, G. H. Lee, S. M. Peng, and R. S. Liu, *Organometallics* 1993, **12**, 2591.

105. S. A. Benyunes, A. Binelli, M. Green, and M. J. Grimshire, *J. Chem. Soc., Dalton Trans.*, 1991, 895.

106. C. J. Beddows, M. R. Box, C. Butters, N. Carr, M. Green, M. Kursawe, M. F. Mahon, *J. Organomet. Chem.*, 1998, **550**, 267.

107. C. Djerassi, *Organic Reactions*, 1951, **6**, 207.

108. A. J. Mancuso and D. Swern, *Synthesis*, 1981, **3**, 165.

109. W. P. Griffith, S. V. Ley, G. P. Whitcombe, and A. D. White, *J. Chem. Soc., Chem. Commun.*, 1987, **21**, 1625.

110. C. Butters, N. Carr, R. J. Deeth, M. Green, S, M. Green and M. F. Mahon, *J. Chem. Soc., Dalton Trans.*, 1996, 2299.

111. J. W. Faller, H. H. Murray, D. L. White and K. H. Chao, *Organometallics*, 1983, **2**, 400.

112. J. W. Faller, D. F. Chodosh and D. Katahira, *J. Organomet. Chem.*, 1980, **187**, 227.

113. *A Guidebook to mechanism in organic chemistry*, sixth edition, editor Peter sykes, 254.

114. W. D. Bannister, M. Green, and R. N. Haszeldine, *J. Chem. Soc.* (A), 1966, 194.

115. J. C. T. R. Burckett-St. Laurent, P. B. Hitchcock, H. W. Kroto and J. F. Nixon, *J. Chem. Soc., Chem. Commun.*, 1981, **21**, 1141.

116. P. B. Hitchcock, M. J. Maah, J. F. Nixon, J. A. Zora, G. J. Leigh and M. A. Bakar, *Angew. Chem., Int. Ed. Engl.,* 1987, **26**, 474.

117. M. F. Meidine, C. J. Meir, S. Morton and J. F. Nixon, *J. Organomet. Chem.*, 1985, **297**, 255.

118. G. Becker, W. A. Herrmann, W. Kalcher, G. W. Kriechbaum, C. Pahl, C. T. Wagner and M. L. Ziegler, *Angew. Chem., Int. Ed. Engl.,* 1983, **22**, 413.

119. P. B. Hitchcock, M. F. Meidine and J. F. Nixon, *J. Organomet. Chem.*, 1987, **333**, 337.

120. P. Binger, R. Milczarek, R. Mynott, E. Raabe, C. Kruger and M. Regitz, *Chem. Ber.*, 1988, **121**, 637.

121. P. Binger, R. Milczarek, R. Mynott, M. Regitz, and W. Rosch, *Angew. Chem., Int. Ed. Engl.,* 1986, **25**, 644.

122. P. B. Hitchcock, M. J. Maah, and J. F. Nixon, *J. Chem. Soc., Chem. Commun.*, 1986, **10**, 737.

123. P. Binger, B. Biedenbach, C. Kruger, and M. Regitz, *Angew. Chem., Int. Ed. Engl.,* 1987, **26**, 764.

124. T. Wettling, B. Geissler, R. Schneider, S. Barth, P. Binger, and M. Regitz, *Angew. Chem., Int. Ed. Engl.,* 1992, **31**, 758.

125. T. Wettling, J. Schneider, O. Wagner, C. G. Kreiter and M. Regitz, *Angew. Chem., Int. Ed. Engl.,* 1989, **28**, 1013.

126. B. Geissler, T. Wettling, S. Barth, P. Binger and M. Regitz, *Synthesis*, 1994, 1337.

127. R. Bartsch, P. B. Hitchcock, and J. F. Nixon, *J. Organomet. Chem.*, 1989, **375**, C31-C34.

128. D. Hu, H. Schaufele, H. Pritzkow, and U. Zenneck, *Angew. Chem., Int. Ed. Engl.*, 1989, **28**, 900.

129. F. G. N. Cloke, K. R. Flower, P. B. Hitchcock and J. F. Nixon, *J Chem. Soc., Chem. Commun.*, 1995, **16**, 1659.

130. F. G. N. Cloke, K. R. Flower, P. B. Hitchcock and J. F. Nixon, *J. Chem. Soc., Chem. Commun.*, 1994, **4**, 489.

131. J. F. Nixon, *Chem. Rev.*, 1988, **88**, 1327.

132. P. Binger, B. Biedenbach, A.T. Herrmann, F. Langhauser, P. Betz, R. Goddard and C. Kruger, *Chem. Ber.*, 1990, **123**, 1617.

133. G. Brauers, M. Green, C. Jones and J. F. Nixon, *J. Chem. Soc., Chem. Commun.*, 1995, **11**, 1125.

134. S. G. Feng, P. S. White and J. L. Templeton, *J. Am. Chem. Soc.*, 1992, **114**, 2951.

135. G. Brauers, F. J. Feher, M. Green, J. K. Hogg and G. A. Orpen, *J. Chem. Soc., Dalton Trans.*, 1996, 3387.

136. D. C. Brower, K. R. Birdwhistell and J. L. Templeton, *Organometallics*, 1986, **5**, 94.

137. K. K. Laali, B. Geissler, O. Wagner, J. Hoffmann, R. Armbrust, W. Eisfield and M. Regitz, *J. Am. Chem. Soc.*, 1994, **116**, 9407.

138. B. Breit, U. Bergsträsser, G. Maas and M. Regitz, *Angew. Chem., Int. Ed. Engl.*, 1992, **31**, 1055.

139. G. Brauers, Ph.D. Thesis, University of Bath, 1995.

140. J. R. Bleeke, P. V. Hinkle and N. P. Rath, *J. Am. Chem. Soc.*, 1999, **121**, 595.

141. A. D. Burrows, M. Green, J. C. Jeffrey, J. M. Lynam and M. F. Mahon, *Angew. Chem., Int. Ed. Engl.,* 1999, in press.

142. J. C. Hayes and N. J. Cooper, *J. Am. Chem Soc.,* 1982, **104**, 5570.

143. A. M. Bond, R. Colton and J. J. Jackauski, *Inorg. Chem.*, 1975, **14**, 2526.

144. J. Lynam unpublished data.

145. O. Eisenstein and R. Hoffmann, *J. Am. Chem Soc.,* 1981, **103**, 4308.

146. K. Jonas, *Angew. Chem.*, 1985, **97**, 292.

147. K. P. C. Volhardt, *Angew. Chem.*, 1984, **96**, 525.

148. S. Creve, T. Nguyen and L. G. Vanquickenborne, *Eur. J. Inorg. Chem., 1999, 1281.*

149. M. E. Rerek, L. -N. Ji, F. Basolo, *J. Chem. Soc., Chem Commun.*, 1983, 1208.

150. P. Binger, R. Milczarek, R. Mynott, C. Kruger, Y.-H. Tsay, E. Raabe and M. Regitz, *Chem Ber.*, 1988, **121**, 637.

151. P. Binger, J. Haas, A. T. Herrmann, F. Langhauser and C. Krüger, *Angew. Chem. Int. Ed. Engl.,* 1991, **3**, 310.

152. C. J. Harlan, T. Hascall, E. Fujita and J. R. Norton, *J. Am. Chem. Soc.*, 1999, **121**, 7274.

153. S. I. Al-Resayes, P. B. Hitchcock, J. F. Nixon, D. M. P. Mingos, *J. Chem. Soc., Chem. Commun.,* 1985, 365.

154. N. Carr, M. Green, M. F. Mahon, C. Jones and J. F. Nixon, *J. Chem. Soc., Chem. Commun.*, 1995, 2191.

155. C. Carfagna, N. Carr, R. J. Deeth, S. J. Dosset, M. Green, M. F. Mahon and C. Vaughn, *J. Chem. Soc., Dalton Trans.*, 1996, 415.

156. W. A. Schenk, J. Frisch, W. Adam and F. Prechtl, *Angew. Chem., Int. Ed. Engl.*, 1994, **33**, 1609.

157. S. G. Davies and J. I. Seeman, *J. Chem. Soc., Chem. Commun.*, 1984, 1019.

158. S. G. Davies and J. I. Seeman, *Tetrahedron Lett.*, 1984 **25**, 1845.

159. J. I. Seeman, *Pure Appl. Chem.*, 1987, **59**, 1661.

160. A. Messeguer, *Acros Organics Acta*, 1995, **1,2,** 71.

161. H. C. Clark and C. R. Milne, *Can J. Chem.*, 1979, **57**, 958.

162. L. B. Quin and A. Szewczyk, *Multiple Bonds and Low Coordination in Phosphorus Chemistry*,1990, 352. (Edited by M. Regitz and O. J. Scherer).

163. R. Withnall and J. Andrews, *J. Phys. Chem.*, 1987, **91**, 784.

164. *The Chemistry of Organophosphorus Compounds, pimary, secondary and tertiary phosphines and heterocyclic organophosphorus (III) compounds volume 1, 16.* (Edited by Hartley).

165. N. S. Imyonitov, *Sov. J. Coord. Chem.*, 1985, **11**, 597.

166. L. Weber and K. Reizig, *Angew. Chem., Int. Ed. Engl*, 1985, **24**, 53.

APPENDICES

A1 Crystal Data for (76)

Empirical formula	$C_{23}H_{18}MoO_3$
Crystal System	orthorhombic
Space Group	$P2_12_12_1$
Unit Cell Dimensions (Å): a	8.198 (4)
b	14.899 (2)
c	15.546 (2)
β	90.000 (10)°
Volume (Å^3)	1901.0 (10)
D_{calcd}	1.531 gcm^{-3}
Z	4
F(000)	888
T	293 K

Table A1.1 *Fractional atomic coordinates (*10^4)*

Atom	x	y	z
Mo(1)	8081(1)	15(1)	2356(1)
O(1)	4352(7)	-245(5)	2373(5)
O(2)	7221(9)	-235(5)	4279(4)
O(3)	5522(8)	2170(4)	2480(4)
C(1)	5713(9)	-112(6)	2356(5)
C(2)	7557(10)	-128(6)	3579(6)
C(3)	8366(15)	-1308(11)	1620(17)
C(4)	9294(17)	-1379(6)	2308(11)
C(5)	10521(11)	-800(7)	2287(8)
C(6)	10421(19)	-349(8)	1583(10)
C(7)	9114(27)	-633(12)	1129(7)
C(8)	8733(10)	1393(5)	3124(5)
C(9)	8815(11)	1446(6)	2233(7)
C(10)	7476(10)	1363(6)	1680(5)
C(11)	10110(10)	1423(5)	3729(6)
C(12)	11727(11)	1321(6)	3462(6)
C(13)	12932(11)	1395(6)	4076(8)
C(14)	12620(15)	1558(8)	4917(9)
C(15)	11028(17)	1629(7)	5174(7)
C(16)	9782(12)	1575(5)	4571(6)
C(17)	5853(10)	1739(5)	1837(6)
C(18)	4613(10)	1633(5)	1150(5)
C(19)	3338(10)	2248(6)	1097(5)
C(20)	2166(12)	2179(7)	469(6)
C(21)	2209(17)	1494(8)	-108(7)
C(22)	3438(13)	888(6)	-87(6)
C(23)	4641(11)	948(5)	536(5)

Table A1.2 *Bond lengths (Å) and angles (°)*

Mo(1)-C(1)	1.950(7)	C(3)-Mo(1)-C(5)	56.2(4)
Mo(1)-C(2)	1.963(9)	C(7)-Mo(1)-C(5)	55.3(4)
Mo(1)-C(9)	2.224(9)	C(4)-Mo(1)-C(5)	33.1(4)
Mo(1)-C(3)	2.292(12)	C(10)-Mo(1)-C(5)	127.6(4)
Mo(1)-C(7)	2.300(11)	C(6)-Mo(1)-C(5)	32.0(4)
Mo(1)-C(4)	2.303(9)	C(1)-Mo(1)-C(8)	107.4(3)
Mo(1)-C(10)	2.321(8)	C(2)-Mo(1)-C(8)	70.3(3)
Mo(1)-C(6)	2.328(10)	C(9)-Mo(1)-C(8)	34.4(3)
Mo(1)-C(5)	2.343(9)	C(3)-Mo(1)-C(8)	161.5(4)
Mo(1)-C(8)	2.436(8)	C(7)-Mo(1)-C(8)	132.9(7)
O(1)-C(1)	1.134(9)	C(4)-Mo(1)-C(8)	132.9(5)
O(2)-C(2)	1.135(9)	C(10)-Mo(1)-C(8)	62.6(3)
O(3)-C(17)	1.221(10)	C(6)-Mo(1)-C(8)	105.6(4)
C(3)-C(4)	1.32(2)	C(5)-Mo(1)-C(8)	105.8(3)
C(3)-C(7)	1.40(2)	O(1)-C(1)-Mo(1)	175.2(8)
C(4)-C(5)	1.325(14)	O(2)-C(2)-Mo(1)	177.7(8)
C(5)-C(6)	1.29(2)	C(4)-C(3)-C(7)	104.3(12)
C(6)-C(7)	1.35(2)	C(4)-C(3)-Mo(1)	73.8(7)
C(8)-C(9)	1.391(12)	C(7)-C(3)-Mo(1)	72.5(7)
C(8)-C(11)	1.470(11)	C(5)-C(4)-C(3)	111.5(14)
C(9)-C(10)	1.401(11)	C(5)-C(4)-Mo(1)	75.1(5)
C(10)-C(17)	1.464(11)	C(3)-C(4)-Mo(1)	72.9(7)
C(11)-C(16)	1.357(13)	C(6)-C(5)-C(4)	108.2(13)
C(11)-C(12)	1.398(12)	C(6)-C(5)-Mo(1)	73.4(6)
C(12)-C(13)	1.379(12)	C(4)-C(5)-Mo(1)	71.8(5)
C(13)-C(14)	1.36(2)	C(5)-C(6)-C(7)	109.4(14)
C(14)-C(15)	1.37(2)	C(5)-C(6)-Mo(1)	74.6(6)
C(15)-C(16)	1.389(14)	C(7)-C(6)-Mo(1)	71.9(8)
C(17)-C(18)	1.483(12)	C(6)-C(7)-C(3)	106.6(12)
C(18)-C(19)	1.393(11)	C(6)-C(7)-Mo(1)	74.1(6)
C(18)-C(23)	1.398(11)	C(3)-C(7)-Mo(1)	71.9(8)
C(19)-C(20)	1.375(12)	C(9)-C(8)-C(11)	126.8(9)
C(20)-C(21)	1.36(2)	C(9)-C(8)-Mo(1)	64.5(5)
C(21)-C(22)	1.35(2)	C(11)-C(8)-Mo(1)	120.6(5)
C(22)-C(23)	1.386(12)	C(10)-C(9)-C(8)	124.7(9)
		C(10)-C(9)-Mo(1)	75.9(5)
C(1)-Mo(1)-C(2)	76.8(3)	C(8)-C(9)-Mo(1)	81.2(6)
C(1)-Mo(1)-C(9)	111.2(4)	C(9)-C(10)-C(17)	125.2(8)
C(2)-Mo(1)-C(9)	104.3(4)	C(9)-C(10)-Mo(1)	68.3(5)
C(1)-Mo(1)-C(3)	91.1(4)	C(1)-Mo(1)-C(7)	109.0(6)
C(2)-Mo(1)-C(3)	114.4(8)	C(2)-Mo(1)-C(7)	147.1(5)
C(9)-Mo(1)-C(3)	139.0(7)	C(9)-Mo(1)-C(7)	103.4(6)
C(1)-Mo(1)-C(5)	143.1(4)	C(3)-Mo(1)-C(7)	35.6(6)
C(2)-Mo(1)-C(5)	100.1(4)	C(1)-Mo(1)-C(4)	110.1(4)
C(9)-Mo(1)-C(5)	105.2(4)	C(2)-Mo(1)-C(4)	91.6(5)
C(9)-Mo(1)-C(4)	138.1(4)	C(16)-Mo(11)-C(8)	118.1(8)

C(3)-Mo(1)-C(4)	33.3(5)	C(12)-Mo(11)-C(8)	122.3(8)
C(7)-Mo(1)-C(4)	55.7(5)	C(13)-Mo(12)-C(11)	117.7(9)
C(1)-Mo(1)-C(10)	82.6(3)	C(14)-Mo(13)-C(12)	123.3(11)
C(2)-Mo(1)-C(10)	119.1(3)	C(13)-Mo(14)-C(15)	118.4(11)
C(9)-Mo(1)-C(10)	35.8(3)	C(14)-Mo(15)-C(16)	120.0(11)
C(3)-Mo(1)-C(10)	122.7(7)	C(11)-Mo(16)-C(15)	121.1(10)
C(7)-Mo(1)-C(10)	93.8(4)	O(3)-C(17)-O(10)	122.7(8)
C(4)-Mo(1)-C(10)	149.1(4)	O(3)-C(17)-O(18)	119.6(8)
C(1)-Mo(1)-C(6)	142.9(5)	C(10)-C(17)-C(18)	117.6(7)
C(2)-Mo(1)-C(6)	131.0(5)	C(19)-C(18)-C(23)	116.9(8)
C(9)-Mo(1)-C(6)	87.5(4)	C(19)-C(18)-C(17)	119.2(8)
C(3)-Mo(1)-C(6)	57.2(5)	C(23)-C(18)-C(17)	124.0(7)
C(7)-Mo(1)-C(6)	34.0(5)	C(20)-C(19)-C(18)	121.2(9)
C(4)-Mo(1)-C(6)	54.4(4)	C(21)-C(20)-C(19)	120.5(10)
C(10)-Mo(1)-C(6)	98.3(4)	C(22)-C(217)-C(20)	120.2(11)
C(17)-Mo(10)-C(1)	116.7(5)	C(21)-C(22)-C(23)	120.3(10)
C(16)-Mo(11)-C(12)	119.6(8)	C(22)-C(23)-C(18)	120.9(8)

A2 Crystal Data for (55)

Empirical formula	$C_{16}H_{20}MoO_3$
Crystal System	monoclinic
Space Group	$P2_1/n$
Unit Cell Dimensions (Å): a	10.919 (2)
b	10.578 (2)
c	13.724 (2)
β	90.18 (2)°
Volume (Å^3)	1585.1
D_{calcd}	1.49 gcm^{-3}
Z	4
F(000)	728
T	293 K

Table A2.1 *Fractional atomic coordinates (*10^4)*

Atom	x	y	z
Mo(1)	-56(1)	1486(1)	2564
O(1)	-2452(11)	2000(12)	1466(9)
O(2)	-1912(11)	1227(13)	4251(8)
O(3)	-1799(15)	-668(16)	631(9)
C(1)	898(7)	3136(8)	3411(6)
C(2)	284(8)	3651(8)	2563(6)
C(3)	852(8)	3145(8)	1727(6)
C(4)	1841(7)	2335(8)	2050(6)
C(5)	1853(8)	2340(9)	3070(6)
C(6)	652(10)	3467(11)	4468(7)
C(7)	-697(9)	4605(10)	2574(8)
C(8)	600(10)	3469(10)	699(7)
C(9)	2804(11)	1744(11)	1430(10)
C(10)	2765(10)	1652(11)	3729(8)
C(11)	-1566(14)	1746(14)	1880(11)
C(12)	-1215(12)	1265(15)	3649(11)
C(13)	211(12)	-413(12)	3357(10)
C(14)	785(11)	-372(11)	2446(13)
C(15)	132(12)	-220(13)	1541(11)
C(16)	-1183(16)	-754(16)	1394(13)
O(1')	-1808(26)	1022(26)	784(19)
O(2')	-2536(27)	2081(28)	3522(21)
O(3')	-1801(33)	-662(32)	4361(24)
C(11')	-1120(36)	1141(41)	1378(30)
C(12')	-1576(42)	1684(42)	3172(32)
C(16')	-1116(46)	-770(70)	3638(54)

Table A2.2 *Bond lengths (Å) and angles (°)*

C(1)-Mo(1)	2.339(10)	C(2)-Mo(1)	2.319(11)
C(3)-Mo(1)	2.322(10)	C(4)-Mo(1)	2.366(10)
C(5)-Mo(1)	2.373(10)	C(11)-Mo(1)	1.915(17)
C(11')-Mo(1)	2.030(44)	C(12)-Mo(1)	1.971(16)
C(12')-Mo(1)	1.872(45)	C(13)-Mo(1)	2.303(14)
C(14)-Mo(1)	2.176(13)	C(15)-Mo(1)	2.297(13)
O(1')-O(1)	1.563(31)	C(11)-O(1)	1.153(17)
C(11')-O(1)	1.720(45)	O(1)-O(1')	1.563(31)
O(3)-O(1')	1.800(32)	C(11)-O(1')	1.707(32)
C(11')-O(1')	1.114(41)	C(16)-O(1')	2.166(36)
O(2')-O(2)	1.509(32)	O(3')-O(2)	2.007(37)
C(12)-O(2)	1.126(15)	C(12')-O(2)	1.601(45)
O(2)-O(2')	1.509(32)	C(12)-O(2')	1.690(34)
C(12')-O(2')	1.228(46)	O(1')-O(3)	1.800(32)
C(16)-O(3)	1.246(23)	O(2)-O(3')	2.007(37)
C(16')-O(3')	1.250(61)	Mo(1)-C(1)	2.339(10)
C(2)-C(1)	1.448(12)	C(4)-C(1)	2.298(13)
C(5)-C(1)	1.420(13)	C(6)-C(1)	1.518(14)
Mo(1)-C(2)	2.319(11)	C(1)-C(2)	1.448(12)
C(3)-C(2)	1.412(12)	C(7)-C(2)	1.472(13)
Mo(1)-C(3)	2.322(10)	C(2)-C(3)	1.412(12)
C(4)-C(3)	1.447(13)	C(8)-C(3)	1.476(12)
Mo(1)-C(4)	2.366(10)	C(1)-C(4)	2.298(13)
C(3)-C(4)	1.447(13)	C(5)-C(4)	1.401(12)
C(9)-C(4)	1.479(13)	Mo(1)-C(5)	2.373(10)
C(1)-C(5)	1.420(13)	C(4)-C(5)	1.401(12)
C(10)-C(5)	1.527(14)	C(1)-C(6)	1.518(14)
C(2)-C(7)	1.472(13)	C(3)-C(8)	1.476(12)
C(4)-C(9)	1.479(13)	C(5)-C(10)	1.527(14)
Mo(1)-C(11)	1.915(17)	O(1)-C(11)	1.153(17)
O(1')-C(11)	1.708(32)	C(11')-C(11)	1.060(40)
C(12')-C(11)	1.775(47)	Mo(1)-C(11')	2.030(44)
O(1)-C(11)	1.720(45)	O(1')-C(11')	1.114(41)
C(11)-C(11')	1.060(40)	C(15)-C(11')	1.997(45)
C(16)-C(11')	2.006(46)	Mo(1)-C(12)	1.971(16)
O(2)-C(12)	1.126(15)	O(2')-C(12)	1.690(34)
C(12')-C(12)	0.882(41)	C(16')-C(12)	2.155(76)
Mo(1)-C(12')	1.872(45)	O(2)-C(12')	1.601(45)
O(2')-C(12')	1.228(46)	C(11)-C(12')	1.775(47)
C(12)-C(12')	0.882(41)	Mo(1)-C(13)	2.303(14)
C(14)-C(13)	1.401(18)	C(16')-C(13)	1.547(45)
Mo(1)-C(14)	2.176(13)	C(13)-C(14)	1.401(18)
C(15)-C(14)	1.439(20)	Mo(1)-C(15)	2.297(13)
C(11')-C(15)	1.997(45)	C(14)-C(15)	1.439(20)
C(16)-C(15)	1.555(21)	O(1')-C(16)	2.166(36)
O(3)-C(16)	1.246(23)	C(11')-C(16)	2.006(46)

C(15)-C(16)	1.555(21)	O(3')-C(16')	1.250(61)
C(12)-C(16')	2.155(76)	C(13)-C(16')	1.547(45)
C(2)-Mo(1)-C(1)	36.2(3)	C(3)-Mo(1)-C(1)	59.5(4)
C(3)-Mo(1)-C(2)	35.4(3)	C(4)-Mo(1)-C(1)	58.5(4)
C(4)-Mo(1)-C(2)	59.0(4)	C(4)-Mo(1)-C(3)	36.0(3)
C(5)-Mo(1)-C(1)	35.1(3)	C(5)-Mo(1)-C(2)	59.0(4)
C(5)-Mo(1)-C(3)	58.8(4)	C(5)-Mo(1)-C(4)	34.4(3)
C(11)-Mo(1)-C(1)	121.2(6)	C(11)-Mo(1)-C(2)	89.7(6)
C(11)-Mo(1)-C(3)	91.0(5)	C(11)-Mo(1)-C(4)	123.5(6)
C(11)-Mo(1)-C(5)	147.5(5)	C(11')-Mo(1)-C(1)	141.8(12)
C(11')-Mo(1)-C(2)	105.6(13)	C(11')-Mo(1)-C(3)	89.0(12)
C(11')-Mo(1)-C(4)	109.2(12)	C(11')-Mo(1)-C(5)	143.4(11)
C(11')-Mo(1)-C(11)	31.0(11)	C(12)-Mo(1)-C(1)	90.0(5)
C(12)-Mo(1)-C(2)	102.7(6)	C(12)-Mo(1)-C(3)	137.7(5)
C(12)-Mo(1)-C(4)	146.6(4)	C(12)-Mo(1)-C(5)	112.9(5)
C(12)-Mo(1)-C(11)	80.4(7)	C(12)-Mo(1)-C(11')	102.5(13)
C(12')-Mo(1)-C(1)	95.1(14)	C(12')-Mo(1)-C(2)	91.8(15)
C(12')-Mo(1)-C(3)	121.1(15)	C(12')-Mo(1)-C(4)	150.3(14)
C(12')-Mo(1)-C(5)	127.3(15)	C(12')-Mo(1)-C(11)	55.9(16)
C(12')-Mo(1)-C(11')	82.6(19)	C(12')-Mo(1)-C(12)	26.4(12)
C(13)-Mo(1)-C(1)	111.1(5)	C(13)-Mo(1)-C(2)	147.3(4)
C(13)-Mo(1)-C(3)	147.2(4)	C(13)-Mo(1)-C(4)	111.3(5)
C(13)-Mo(1)-C(5)	94.8(5)	C(13)-Mo(1)-C(11)	117.6(6)
C(13)-Mo(1)-C(11')	107.0(13)	C(13)-Mo(1)-C(12)	67.6(7)
C(13)-Mo(1)-C(12')	89.9(15)	C(14)-Mo(1)-C(1)	121.6(5)
C(14)-Mo(1)-C(2)	145.6(4)	C(14)-Mo(1)-C(3)	117.7(6)
C(14)-Mo(1)-C(4)	87.2(5)	C(14)-Mo(1)-C(5)	89.8(5)
C(14)-Mo(1)-C(11)	117.1(7)	C(14)-Mo(1)-C(11')	91.0(14)
C(14)-Mo(1)-C(12)	102.7(7)	C(14)-Mo(1)-C(12')	120.6(15)
C(14)-Mo(1)-C(13)	36.3(5)	C(15)-Mo(1)-C(1)	148.2(4)
C(15)-Mo(1)-C(2)	139.6(4)	C(15)-Mo(1)-C(3)	104.6(5)
C(15)-Mo(1)-C(4)	92.1(4)	C(15)-Mo(1)-C(5)	113.5(5)
C(15)-Mo(1)-C(11)	83.7(7)	C(15)-Mo(1)-C(11')	54.6(13)
C(15)-Mo(1)-C(12)	115.3(6)	C(15)-Mo(1)-C(12')	116.2(15)
C(15)-Mo(1)-C(13)	65.9(7)	C(15)-Mo(1)-C(14)	37.4(5)
C(11)-O(1)-C(1')	76.2(16)	C(11')-O(1)-C(1')	39.3(15)
C(11')-O(1)-C(11)	37.1(15)	O(3)-O(1')-O(1)	136.8(18)
C(11)-O(1')-O(1)	41.0(9)	C(11)-O(1')-O(3)	123.2(18)
C(11')-O(1')-O(1)	77.9(29)	C(11')-O(1')-O(3)	101.2(32)
C(11')-O(1')-C(11)	37.1(23)	C(16)-O(1')-O(1)	119.0(16)
C(16)-O(1')-O(3)	35.1(8)	C(16)-O(1')-C(11)	90.1(15)
C(16)-O(1')-C(11')	66.7(28)	O(3')-O(2)-O(2')	132.3(16)
C(12)-O(2)-O(2')	78.3(16)	C(12)-O(2)-O(3')	92.8(16)
C(12')-O(2)-O(2')	46.4(17)	C(12')-O(2)-O(3')	110.8(21)
C(12')-O(2)-C(12)	32.1(17)	C(12)-O(2')-O(2)	40.7(9)
C(12')-O(2')-O(2)	70.8(26)	C(12')-O(2')-C(12)	30.3(21)
C(16)-O(3)-O(1')	88.7(14)	C(16')-O(3')-O(1)	93.9(43)

C(2)-C(1)-Mo(1)	71.1(6)	C(4)-C(1)-Mo(1)	61.4(4)
C(4)-C(1)-C(2)	72.1(6)	C(5)-C(1)-Mo(1)	73.8(6)
C(5)-C(1)-C(2)	107.3(8)	C(5)-C(1)-C(4)	35.2(4)
C(6)-C(1)-Mo(1)	124.6(7)	C(6)-C(1)-C(2)	126.8(9)
C(6)-C(1)-C(4)	160.7(7)	C(5)-C(1)-C(5)	125.7(9)
C(1)-C(2)-Mo(1)	72.6(6)	C(3)-C(2)-Mo(1)	72.4(6)
C(3)-C(2)-C(1)	107.9(8)	C(7)-C(2)-Mo(1)	124.1(8)
C(7)-C(2)-C(1)	125.8(9)	C(7)-C(2)-C(3)	126.1(9)
C(2)-C(3)-Mo(1)	72.2(6)	C(4)-C(3)-Mo(1)	73.7(6)
C(4)-C(3)-C(2)	107.7(8)	C(8)-C(3)-Mo(1)	124.8(7)
C(8)-C(3)-C(2)	127.5(10)	C(8)-C(3)-C(4)	124.5(10)
C(1)-C(4)-Mo(1)	60.2(4)	C(3)-C(4)-Mo(1)	70.3(5)
C(3)-C(4)-C(1)	72.2(6)	C(5)-C(4)-Mo(1)	73.1(6)
C(5)-C(4)-C(1)	35.7(5)	C(5)-C(4)-C(3)	108.0(8)
C(9)-C(4)-Mo(1)	130.1(7)	C(9)-C(4)-C(1)	159.5(8)
C(9)-C(4)-C(3)	126.3(10)	C(9)-C(4)-C(5)	124.9(10)
C(1)-C(5)-Mo(1)	71.1(6)	C(4)-C(5)-Mo(1)	72.5(6)
C(4)-C(5)-C(1)	109.1(9)	C(10)-C(5)-Mo(1)	124.2(8)
C(10)-C(5)-C(1)	124.5(10)	C(10)-C(5)-C(4)	126.4(10)
O(1)-C(11)-Mo(1)	174.7(13)	O(1')-C(11)-Mo(1)	119.9(16)
O(1')-C(11)-O(1)	62.8(14)	C(11')-C(11)-Mo(1)	80.5(26)
C(11')-C(11)-O(1)	101.9(28)	C(11')-C(11)-O(1')	39.4(23)
C(12')-C(11)-Mo(1)	60.8(17)	C(12')-C(11)-O(1)	119.6(22)
C(12')-C(11)-O(1')	149.6(19)	C(12')-C(11)-C(11')	129.2(31)
O(1)-C(11')-Mo(1)	109.3(24)	O(1')-C(11')-Mo(1)	171.9(39)
O(1')-C(11')-O(1)	62.8(26)	C(11)-C(11')-Mo(1)	68.5(25)
C(11)-C(11')-O(1)	41.0(18)	C(11)-C(11')-O(1')	103.5(40)
C(15)-C(11')-Mo(1)	69.5(14)	C(15)-C(11')-O(1)	162.1(24)
C(15)-C(11')-O(1')	117.4(38)	C(15)-C(11')-C(11)	132.7(33)
C(16)-C(11')-Mo(1)	101.0(20)	C(16)-C(11')-O(1)	119.9(23)
C(16)-C(11')-O(1')	82.7(32)	C(16)-C(11')-C(11)	125.5(31)
C(16)-C(11')-C(15)	45.7(11)	O(2)-C(12)-Mo(1)	174.7(16)
O(2')-C(12)-Mo(1)	114.3(16)	O(2')-C(12)-O(2)	61.0(14)
C(12')-C(12)-Mo(1)	70.5(32)	C(12')-C(12)-O(2)	105.1(35)
C(12')-C(12)-O(2')	44.5(30)	C(16')-C(12)-Mo(1)	94.7(18)
C(16')-C(12)-O(2)	90.2(21)	C(16')-C(12)-O(2')	123.5(19)
C(16')-C(12)-C(12')	121.2(39)	O(2)-C(12')-Mo(1)	125.8(31)
O(2')-C(12')-Mo(1)	166.3(37)	O(2')-C(12')-O(2)	62.9(24)
C(11)-C(12')-Mo(1)	63.3(16)	C(11)-C(12')-O(2)	159.6(30)
C(11)-C(12')-O(2')	112.7(38)	C(12)-C(12')-Mo(1)	83.1(36)
C(12)-C(12')-O(2)	42.8(22)	C(12)-C(12')-O(2')	105.2(43)
C(12)-C(12')-C(11)	139.1(44)	C(14)-C(13)-Mo(1)	66.9(8)
C(16')-C(13)-Mo(1)	102.3(29)	C(16')-C(13)-C(14)	130.7(30)
C(13)-C(14)-Mo(1)	76.8(8)	C(15)-C(14)-Mo(1)	75.8(8)
C(15)-C(14)-C(13)	123.5(12)	C(11')-C(15)-Mo(1)	55.9(14)
C(14)-C(15)-Mo(1)	66.7(7)	C(14)-C(15)-C(11')	120.9(16)
C(16)-C(15)-Mo(1)	106.3(9)	C(16)-C(15)-C(11')	67.4(15)
C(16)-C(15)-C(14)	121.7(14)	O(3)-C(16)-O(1')	56.2(14)

C(11')-C(16)-O(1')	30.7(12)	C(11')-C(16)-O(3)	86.4(19)
C(15)-C(16)-O(1')	91.4(13)	C(15)-C(16)-O(3)	125.4(16)
C(15)-C(16)-C(11')	66.9(15)	C(12)-C(16')-O(3')	82.7(44)
C(13)-C(16')-O(3')	137.6(60)	C(13)-C(16')-C(12)	78.7(29)